UNIVERSITÉ MONTPELLIER 2

Ecole Doctorale : Systémes intégrés en Biologie, Agronomie, Géosciences, Hydrosciences et Environnement Spécialité

THÈSE

Pour obtenir le grade de

DOCTEUR DE L'UNIVERSITÉ MONTPELLIER 2

Discipline : Biologie Intégrative des Plantes

Présentée et soutenue publiquement par

Peerapat ROONGSATTHAM

le 16 Décembre 2011

Cell separation processes that underlie fruit abscission and shedding in oil palm (*Elaeis guineensis* Jacq.)

Equipe Biologie du Développement des Palmiers, UMR DIADE
BP 64501, 911 avenue Agropolis, F-34394 Montpellier Cedex 5, France

Jury :

Professor Paul Knox	**University of Leeds, UK**	**Rapporteur**
Dr. Shimon Meir	**Agricultural Research Organization, Israel**	**Rapporteur**
Professor Jeremy Roberts	**University of Nottingham, UK**	**Examinateur**
Dr. Serge Hamon	**IRD, France**	**Examinateur**
Dr. Jean-Luc VERDEIL	**CIRAD, France**	**Directeur de Thèse**
Dr. Timothy J. TRANBARGER	**IRD, France**	**Co-directeur de Thèse**
Dr. Fabienne Morcillo	**CIRAD, France**	**Invité**
Dr. Chatchawan_Jantasuriyarat	**Kasetsart University, Thailand**	**Invité**

Cell separation processes that underlie fruit abscission and shedding in oil palm (*Elaeis guineensis* Jacq.)

Etude moléculaire et développementale sur le processus d'abscission des fruits chez le palmier à huile (*Elaeis guineensis* Jacq.)

Acknowledgement

I would like to acknowledge the "Réseau Thématique de Recherche Avancée (RTRA)" for the financial support from "Agropolis Fondation" which provided a scholarship during my doctoral degree program at Université Montpellier 2 and Institut de Recherche pour le Développement (IRD). I also would like to acknowledge PHC Thailande projects 2007-2010 (codes 16589YK and 16589YK) to TJT and ST, and PalmElit SAS/IRD/CIRAD for the financial support for this project.

First of all, I would like to thank my thesis director, Dr. Jean-Luc Verdeil for his excellent guidance and training on histology research. I am also grateful for his critical discussions and comments on my laboratory work and thesis.

I also would like to thank my co-thesis directors, Dr. Timothy J. Tranbarger and Dr. Fabienne Morcillo for the time and all types of support they had given to me while I was working at IRD. I am impressed by their words that they came to help me to graduate not to take me down.

I appreciate my thesis committee, Professor Jeremy Roberts, University of Nottingham, Professor Bruno Touraine, UM2, and Dr. Bruno Nouy from PalmElit for their kind suggestions and comments on my thesis.

I thank Dr. Chatchawan Jantasuriyarat who suggested me to this program. I also thank Dr. Apichart Vanavichit, Dr. Somvong Tragoonrung, and the members of Rice Science Center & Rice Gene Discovery Unit for their supports while I performed research in Thailand. I also would like to thank Anek Limsriwilai, Golden Tenera Plantation, Thailand for the materials used in this study.

I appreciate Dr. James W. Tregear, Dr. Stefan Jouannic, Dr. Hélène Adam, and the members of oil palm group for their very kind of support.

I thank Myriam Collin, Chloé Guerin, Maxime Pizot, Amandine Crabos, Steven Moussu, Chonlada Borisut, Nusaneesa Jaedo, Pornpiroon Pleankong, Stéphanie Loubet and Marc Lartaud for their help on my research.

I would like to thank Nattawut Leelakanok and Ken Chuaphalakit for their spiritual support along my study.

I truly appreciate for everyone who passed me their regards when I had a health problem and had a depression. I thank Pornapat Surasombatpattana, Sirilaksana Patramool, Panupat Patramool and Dr. Potjaman Suraninpong for their supports during the illness. I would like to thank especially Dr. Timothy J. Tranbarger for his concern, understanding, and supports.

Finally, I dedicate all the success to my family who always have faith and always believe in me. Thank you for the supports and strength given to me. Without them, I could not come this far. Thank you very much.

Peerapat Roongsattham

November 2011

Abstract

The current thesis provides new insights into the molecular and cellular mechanisms underlying fruit abscission in the oil palm (*Elaeis guineensis* Jacq). Molecular and cellular approaches were used to examine the events during abscission zone (AZ) development and function. First, a field experimental system was setup and used to define the precise timing of cell separation, and to examine the response of oil palm fruit at different stages of development to ethylene. The results indicate the response to ethylene is developmentally regulated, with the ripest fruit beginning to separate first within 9 h. The search for polygalacturonase (PG) genes expressed in the fruit base containing the AZ led to the identification of fourteen transcripts that encode PGs. One PG transcript (*EgPG4*) increases 700-5000 fold during the ethylene treatment time course with the confirmation by *in situ* hybridization indicating a preferential increase in the AZ cell layers in the base of the fruit in response to ethylene prior to cell separation. Histological analysis of the oil palm fruit base reveals that AZ cells undergo periclinal cell divisions, while the adjacent mesocarp and pedicel cells divide anticlinally resulting in 10-12 AZ cell layers with aligned centrally localized nuclei during fruit development. The AZ cells accumulate large amounts of pectic substances during development, which is lost from the cells after separation suggesting a possible relation to the capacity for AZ function. Ultrastructural analysis indicates a polarized vesicle accumulation at the tip of AZ cells occurs during development, while immunohisto-analysis indicates an increase in the JIM5 epitope in the AZ layers during ethylene treatments prior to separation is observed, followed by a polarized increase in both JIM5 and JIM7 on the separated cell surfaces. The results obtained from diverse approaches allow an integrated view of the fruit abscission process in oil palm and a schematic model of AZ development and function during shedding has been developed.

Key Words: abscission, shedding, cell separation, *Elaeis guineensis*, oil palm, ethylene, polygalacturonase, pectin, methyl-esterification, fruit development, monocot

Résumé

Les travaux présentés dans ce mémoire apportent un éclairage nouveau sur les mécanismes moléculaires et cellulaires impliqués dans l'abscission du fruit chez le palmier à huile (*/Elaeis guineensis/* Jacq.). Des approches moléculaires et cellulaires ont été utilisées pour examiner les événements qui accompagnent la mise en place et le fonctionnement de la zone d'abscission (AZ). Tout d'abord, un protocole expérimental au champ a été mis en place pour définir avec précision, la cinétique d'abscission des fruits et examiner la réponse à l'éthylène en fonction de leur stade de développement. Les résultats indiquent que la réponse à l'éthylène est régulée au cours du développement et que l'abscission des fruits matures commencent après 9 h de traitement. La recherche des gènes codants des polygalacturonases (PG), exprimés à la base de fruit contenant l'AZ a permis l'identification de quatorze transcrits qui codent des PGs. L'un de ces transcrits EgPG4 augmente de 700 à 5000 fois au cours du temps, après traitement à d'éthylène. Sa localisation par hybridation */in situ/* a permis de montrer qu'il s'accumule préférentiellement dans les assises cellulaires qui composent la zone d'abscission, avant même que la séparation des cellules qui conduira à l'abscision du fruit soit initiée. L'analyse histologique de la base de fruits de palmier à huile montre la présence de mitoses essentiellement périclines. Il en résulte une organisation de la zone d'abscission en assises cellulaires (10 à 12 assises) dont les noyaux en position centrale sont alignés. Les cellules de l'AZ accumulent au cours du développement de grandes quantités de composés pectiques. Ces composés pectiques ne sont plus détectés dans les cellules de l'AZ lorsqu'elles se sont séparées, ce qui suggère une relation possible avec le fonctionnement de cette zone conduisant à la chute des fruits. L'analyse ultrastructurale par microscopie électronique à transmission a mis en évidence au cours du développement, une accumulation polarisée de vésicules à l'extrémité des cellules de l'AZ. L'analyse par immunohistochimie indique une augmentation de l'épitope JIM5 dans les assises cellulaires

de l'AZ, après traitement à l'éthylène et avant la séparation des cellules . Elle est suivie d'une l'accumulation considérable des deux épitopes JIM5 et JIM7 sur le pourtour des cellules après leur séparation.

Mots cles: abscission, séparation cellulaire, *Elaeis guineensis*, palmier à huile, éthylène, polygalacturonase, pectine, methyl-estérification, développement du fruit, monocotylédone

Table of Contents

Chapter 1. Introduction

Organ Abscission

Abscission in plants is the separation of an organ from the plant body at an abscission zone (AZ) located at the base of the organ where cell separation leads to organ shedding. It is a tissue process with the differentiation of the AZ and a cellular process with cell separation (Roberts *et al.* 2002). The shedding of plant organs is a highly coordinated developmentally programmed event that can occur in different contexts throughout the plant life cycle (Addicott 1982; Sexton and Roberts 1982; Roberts *et al.* 2002; Leslie *et al.* 2007). Organ abscission (from the Latin words, *ab* means away and *scindere* means to cut) is important for plant reproduction (shedding of flowers, fruits, and seeds), recycling of nutrients (senescence and subsequent leaf shedding), plant architecture (branch shedding), defence (branch and bark shedding) and assimilate partitioning (floral organ shedding for optimized reproduction) (Figure 1.1). The separation events that underlie organ abscission must be under a strict temporal regulation to avoid organ loss at inappropriate times. For example, the premature shedding of stamens before pollination, or a delay or inhibition of fruit or seed shedding would all have a negative effect on plant reproduction. Separation events must also be under tight spatial regulation to maintain adjacent tissue integrity and/or to avoid improper shedding of organs.

While the examples of organ shedding in plants are diverse, a common mechanism and model can be defined (Figure 1.2). Firstly, the differentiation of the AZ takes place at the base of the organ to be shed. Once the AZ develops, it must be activated to become competent for cell separation events that must take place at the base of the subtending organ to be shed. Secondly, the AZ is commonly characterized as one or more layers of generally small isodiametrically shaped cells with dense cytoplasms (Addicott 1982; Sexton and Roberts 1982; Roberts *et al.* 2002). For example, the AZs localized at the base of *Arabidopsis* floral organs consist of 1-2 layers, in the tomato flower/fruit pedicel AZ there are 5-10 layers,

while the AZ in the leaflet rachis of *Sambucus nigra* (common elder) consists of 30-40 layers. Differentiation of the AZ cell layers develops prior to cell separation and once developed, responds differently from adjacent tissues to the signals that induce cell separation (Taylor and Whitelaw 2001). Cells at the AZ are easily recognized prior to cell separation because they are typically smaller than adjacent cells, have dense cytoplasm, relatively small intercellular spaces, contain large deposits of starch, and have highly branched plasmodesmada (Sexton and Roberts 1982). As separation proceeds, the expansion of the golgi vesicles and the activation of the endomembrane system are observed. Finally, degradation of the middle lamella and dissociation of cellulose microfibrils occur. As cells separate, they may become rounded and that is thought to provide a hydraulic mechanism to separate the vascular traces, given that the walls of which do not break down (Brown 1997; Roberts *et al.* 2002).

Abscission can be induced by various factors including temperature, hormones, light, water and nutrient availability, photoperiod, wounding, pathogen attack and ozone (Addicott 1982; Taylor and Whitelaw 2001; Roberts *et al.* 2002). The two hormones that have the greatest influence on abscission are ethylene and auxin (Addicott 1982; Henderson and Osborne 1994; Taylor and Whitelaw 2001; Roberts *et al.* 2002). Ethylene is an abscission stimulator while auxin acts as abscission inhibitor. AZ cells are especially sensitive to ethylene and respond preferentially by changes in gene expression, in particular those encoding hydrolytic enzymes that are required to remodel and/or dismantle the cell wall (Brown 1997). Auxin is thought to delay abscission by decreasing the sensitivity of the AZ cells to ethylene, and thereby inhibits changes in gene expression necessary for abscission to occur (Roberts *et al.* 2002) .

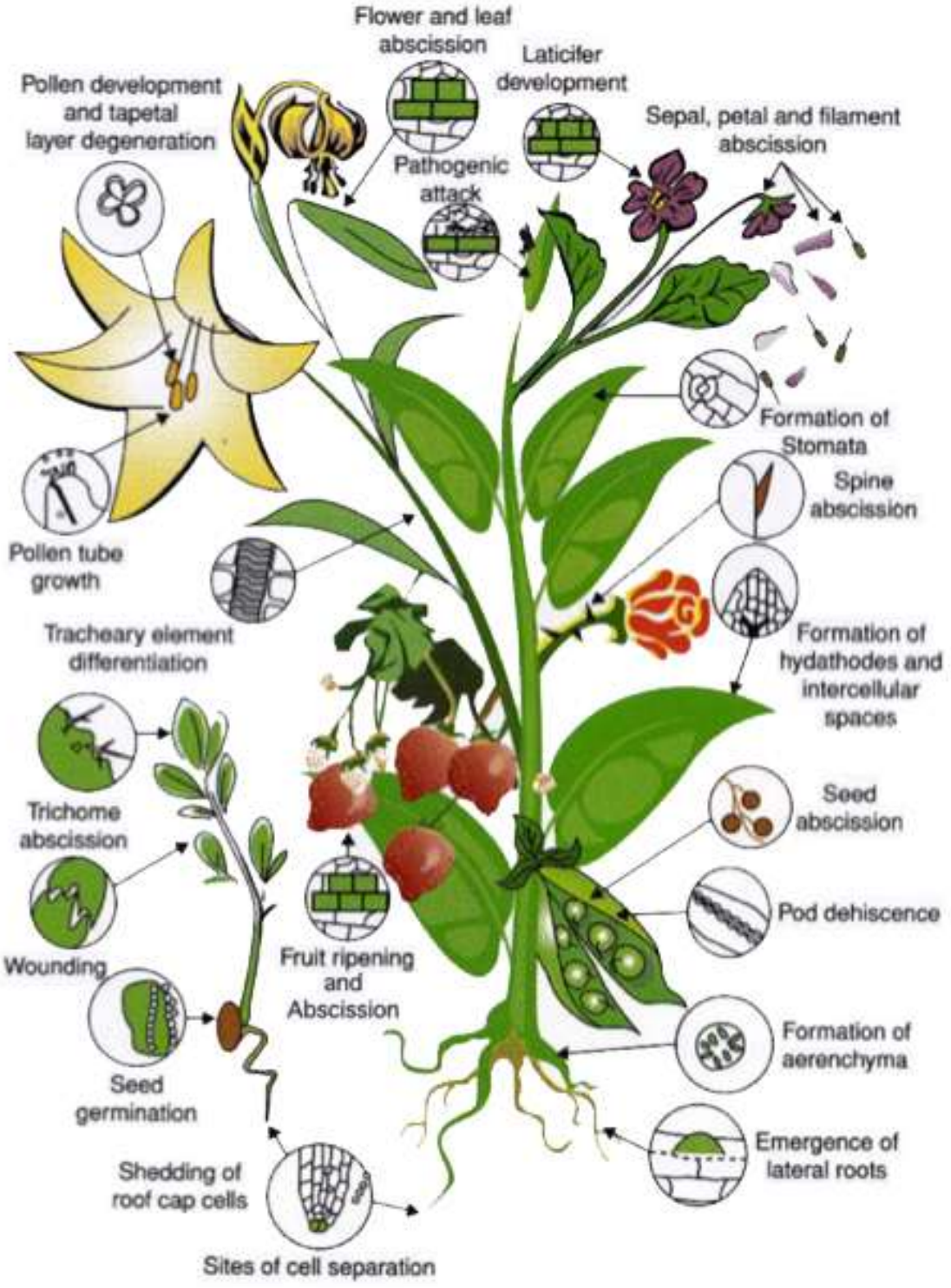

Figure 1.1. Possible cell separation sites during the plant lifecycle (Østergaard *et al.* 2007).

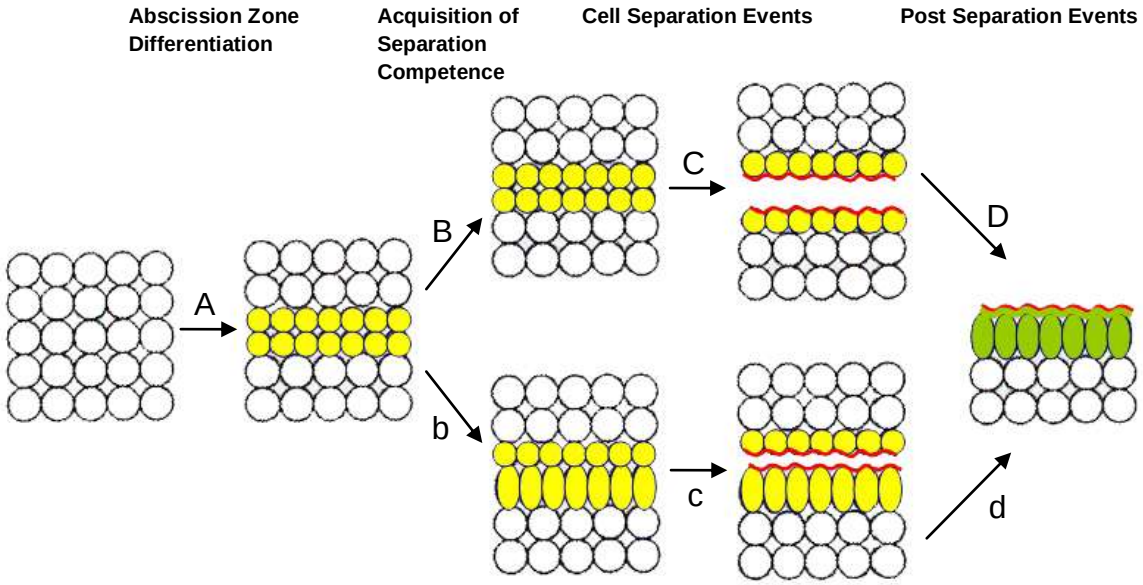

Figure 1.2. A generalized model that describes steps common to the organ abscission processes of plants. A, Cell differentiation takes place at the base of the organ to form the AZ layers (yellow circles). The AZ becomes competent to respond to signals and for cell separation to occur in specific AZ layers, which may (b) or may not (B) involve or result in cell elongation. C and c, a combination of environmental, developmental and hormonal signals induce cell wall modifying enzymes to be secreted between certain AZ cell layers, that results in reduced cell adhesion and cell separation to occur on opposing faces (indicated in red). After abscission, further cellular and or cell wall events may take place in the AZ at the site of organ detachment, and that can also include cell elongation and the defense related responses to protect the plant from pathogen attack. Despite evidence that supports this model, much less is known about the differences that exist between different species and or in different tissues at the molecular level and how to explain the temporal and spatial precision. Adapted from Leslie *et al.* (2007).

While ethylene has been studied extensively in the relation to abscission, both ethylene dependent and independent pathways control floral organ abscission in *Arabidopsis*. The analysis of the *dab* (delayed floral organ abscission) mutants compared to the ethylene-insensitive mutants *etr1-1* (*ETHYLENE RESPONSE1* ethylene receptor mutant) and *ein2-1* (*ETHYLENE-INSENSITIVE2* ethylene signal transduction mutant) indicate both ethylene dependent and independent processes control *Arabidopsis* floral abscission (Patterson 2001; Patterson and Bleecker 2004). While both the *dab* and the ethylene signalling mutants all displayed delayed floral organ abscission, ethylene treatment accelerated the process only in the *dab* mutants. Together the data indicate that ethylene may not be essential for abscission induction, but acts to stimulate or accelerate the process. The isolation of the abscission mutant *ida* (mutant of the *INFLORESCENCE DEFICIENT IN ABSCISSION* gene) and the characterization of the leucine-rich repeat receptor kinase HAESE validates the central importance of the ethylene independent pathways (Jinn *et al.* 2000; Butenko *et al.* 2003). The *ida* mutant is blocked in abscission, while *HAESA* reduced function plants display delayed floral abscission. Both signalling components are independent of ethylene given that the *ida* mutant remains sensitive to ethylene, and *HAESA* expression is independent of ethylene signal transduction. Furthermore, IDA and IDA-like proteins are thought to be ligands that act through HAESA to regulate abscission apparently in an ethylene independent manner (Stenvik *et al.* 2008). However, in the ethylene insensitive tomato mutant *Nr* (*Never-ripe*), flower abscission was completely blocked and wildtype plants with overexpression of ethylene production led to premature floral abscission (Lanahan *et al.* 1994). The results indicate differences may exist between species and or organ types and support an important role of ethylene for the organ abscission process in certain cases.

A central concept about the mechanism for organ abscission is the requirement for cell wall remodelling and or degradation, in particular within the pectin portion of the middle

lamella and possibly the primary cell wall (Addicott 1982; Brown 1997; Roberts and Gonzalez-Carranza 2007). Cell separation during organ abscission depends on the activity of at least two major families of hydrolytic enzymes that modify the cell wall including endo-β-1,4-glucanases (cellulase) and pectinases (PG, pectate lyase (polygalacturonate lyase) (PL)) and also one pectin modification enzyme, pectin methylesterase (PME) (Figure 1.3) (Addicott 1982). The common model includes the induction of the genes encoding cell wall hydrolytic enzymes that are secreted to the apoplast where they participate in modifications to the cell wall that allow separation to occur. Furthermore, the expression of these genes are often induced by ethylene and inhibited by auxin, features that correlate with the positive and negative effects of these hormones on the abscission process respectively (Addicott 1982; Brown 1997; Roberts *et al.* 2002; Roberts and Gonzalez-Carranza 2007).

PG gene expression and activity are common features of organ abscission (Addicott 1982; Roberts and Gonzalez-Carranza 2007). As with EGases, PG transcripts and activity increase in various species during the abscission process, and can be induced by ethylene or inhibited by auxin (Taylor *et al.* 1990; Bonghi *et al.* 1992; Taylor *et al.* 1993; Kalaitzis *et al.* 1995; Kalaitzis *et al.* 1997; Burns *et al.* 1998). PGs are thought to be a part of pectin disassembly occurring in many stages of plant development, especially those that require cell separation, and may be involved in cell expansion due to activity found in rapidly growing tissues (Hadfield and Bennett 1998). There are many reports indicating PG gene expression in fruits for example, banana (Mbéguié-A-Mbéguié *et al.* 2009), peach (Bonghi *et al.* 1992; Trainotti *et al.* 1993), apple (Pandita and Jindal 1991) and citrus (Greenberg *et al.* 1975). In tomato, there is a single PG transcript, pTOM6, expressed during fruit ripening (Grierson *et al.* 1986; Sheehy *et al.* 1988; Smith *et al.* 1988), while four other PGs (TAPG1, TAPG2, TAPG4, and TAPG5) are expressed in the flower and leaf AZ (Kalaitzis *et al.* 1995; Kalaitzis *et al.* 1997; Hong and Tucker 1998). Interestingly, the down-regulation or knockout of the

PG expressed in the fruit during ripening PG resulted in a decrease in soluble polyuronide and depolymerization during ripening, but surprisingly no change in fruit softening (Sheehy *et al.* 1988; Smith *et al.* 1988; Cooley and Yoder 1998). Overall, these experiments suggest that while PGs may indeed be important for cell separation during both ripening and abscission, there are other factors involved. By contrast, silencing of polygalacturonase (*TAPG1*) expression delayed abscission and increased break strength of the AZ (Jiang *et al.* 2008).

There may also be functional redundancy within the PG gene family. Indeed, there are at least 66 PG genes known in *Arabidopsis* and 59 for rice, all phylogenetically grouped within three distinct clades (clade A, B, and C), and all with glycosyl hydrolase 28 (GH28) domains. Four members of clade A (At2g41850, At2g43880, At2g43890, and At3g07970) are implicated in *Arabidopsis* floral abscission (Kim *et al.* 2006). Hadfield and Bennett (1998) have also classified PGs in three different clades based on full length cDNAs that encode PGs (clade A, B and C). Members of clade A relate to fruit and/or AZ, of which clade B relate to fruit or dehiscence zone while clade C are involved in pollen and anther development. Three PGs (ADPG1, ADPG2, and QRT2) from *Arabidopsis* have overlapping functions (Ogawa *et al.* 2009). ADPG1 and ADPG2 are essential for silique dehiscence, while ADPG2 and QRT2 contribute to floral organ abscission, and all three genes contribute to anther dehiscence (Ogawa *et al.* 2009). Furthermore, jasmonic acid (JA) and ethylene act together with abscisic acid to promote *QRT2* expression and hence regulate floral organ abscission. Together these results reveal the underlying complexity of the abscission process and the key role of PGs in different abscission and cell separation processes. Finally, although the biochemical process of cell separation in each organ has similar sequence of events, our knowledge of the specific molecular basis of the different cell separation events in

different developmental contexts and different species including those with high commercial value is limited (Roberts *et al.* 2002; Swain *et al.* 2011).

Cellulase (Endo-1,4-β-D-glucanase, EGase) is a large family of enzymes thought to hydrolyze β-1,4 linkages whereas their, *in planta*, substrates are still undetermined (Ferrarese *et al.* 1998; Loopstra *et al.* 1998; del Campillo 1999). There are three EGase subfamilies α-, β- and γ- in *Arabidopsis*, comprised of at least 25 sequences (Libertini *et al.* 2004). Two of the subfamilies (α and β) are secreted EGases with members implicated in abscission. The increase of activity of cellulase during the abscission process appears to be under transcriptional regulation induced by ethylene and inhibited by auxin (Tucker *et al.* 1988; Tucker *et al.* 2002). Furthermore, when the function of the tomato *Cel2* gene encoding an endo-1,4-β-glucanase (EGase) is reduced, an increase in the force required for separation to occur in the fruit AZ was observed, which provides evidence that *Cel2* contributes to cell wall disassembly during fruit abscission (Brummell *et al.* 1999). The exact substrate for EGases in the context of abscission is unknown but is thought to be the hemicellulose portion, possibly within the primary cell wall (Addicott 1982; Gonzalez-Bosch *et al.* 1997; Trainotti *et al.* 1997; Henderson *et al.* 2001b; Roberts and Gonzalez-Carranza 2007).

PLL cleaves α-1,4-linked galacturonic acid through transelimination reaction (Pedrolli *et al.* 2009; Sun and van Nocker 2010). In *Arabidopsis*, there are 26 genes (*AtPLLs*) which encode pectate lyase-like proteins (Palusa *et al.* 2007). It has been found that *PLLs* express in several *Arabidopsis* organs programmed for abscission – the perianth floral organ AZ, the DZ of the fruit, and the seed AZ. The activity is also seen in cell layers in the region of initiating lateral roots, flowers, and pollens. *PLL* genes are also involved in several aspects of growth and development both dependent and independent of cell separation (Palusa *et al.* 2007; Sun and van Nocker 2010)

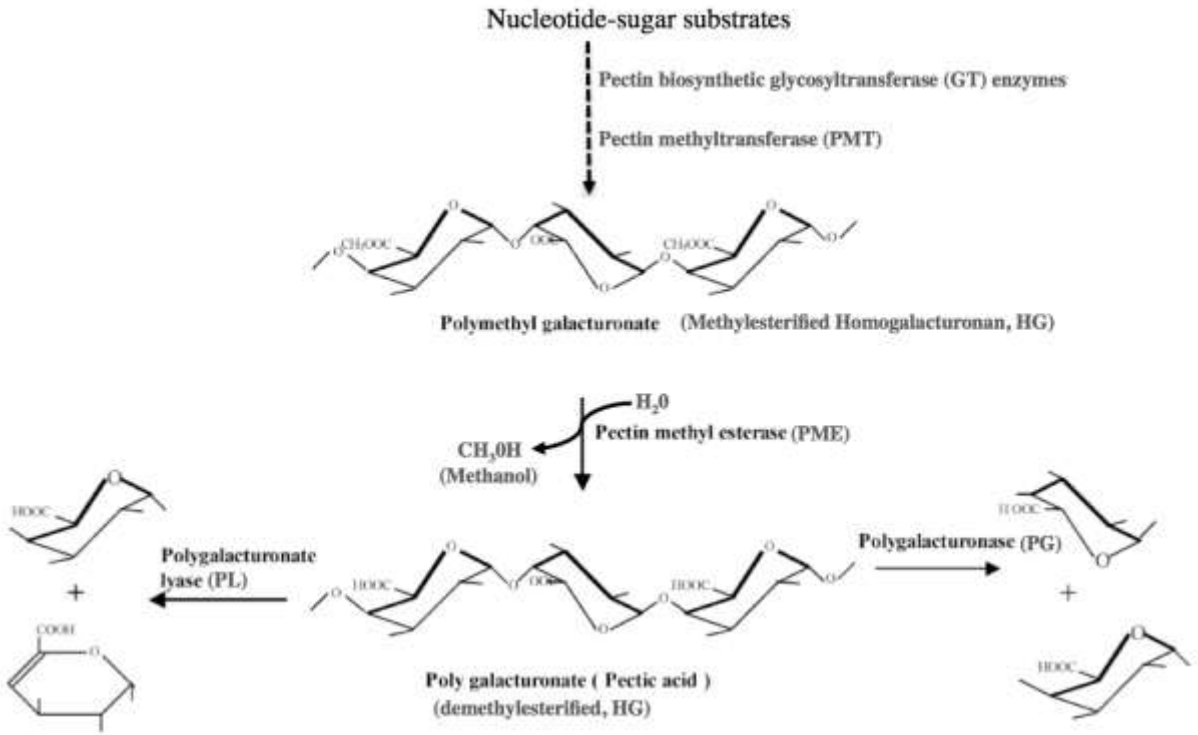

Figure 1.3. Overview of pectin biosynthesis and modification pathways and associated enzymes. Figure adapted from Prasanna *et al.* (2007) and Caffall and Mohnen (2009). Enzyme nomanclature is according to http://pec.biodbs.info/PectinaseClassification.html.

PME activity is thought to modulate the cell wall pectin methyl-esterification status and to play important roles during plant vegetative and reproductive development (Micheli 2001; Pelloux *et al.* 2007; Wolf *et al.* 2009). There are up to 66 PME-related proteins in the *Arabidopsis* genome. Twenty-three of them contain only catalytic PME domain while 43 of them also contain a PME inhibitor (PMEI) domain (Tian *et al.* 2006). PME activity was first shown to decrease during abscission, but in some cases did not change (Osborne 1958; Lamotte *et al.* 1969; Ratner *et al.* 1969; Moline *et al.* 1972). In the AZ of cotton petioles, there is an increase in methyl-esterified pectin, and the process is inhibited by auxin (Valdovinos and Muir 1965). During strawberry fruit ripening, PME gene expression is induced by auxin, inhibited by ethylene and associated with textural changes during ripening (Castillejo *et al.* 2004). PMEs are also implicated in cell separation events during pollen formation and root cap border cell shedding, (Wen *et al.* 1999; Francis *et al.* 2006; Wolf *et al.* 2009; Sun and van Nocker 2010). The mutation of *QUARTET1* (*QRT1*), a PME expressed in *Arabidopsis* pollen, and anthers leads to impaired pollen tetrad separation during flower development (Francis *et al.* 2006). A decrease in PME function in pea plants prevented normal separation of root border cells from the root tip (Wen *et al.* 1999). The expression of PME genes is observed in the *Arabidopsis* sepal, petal, stamen, and seed AZs, the fruit dehiscence zone, and in other separation sites including the flower styles, and the root endodermal and cortical layers during lateral root emergence (Sun and van Nocker 2010). During fruit ripening, PME activity is thought to prepare HG as substrate for PG hydrolysis by random de-methyl-esterification (Koch and Nevins 1989; Wakabayashi *et al.* 2000; Micheli 2001; Wakabayashi *et al.* 2003). Indeed, in *Arabidopsis*, QRT1 may act in tandem with QUARTET3 (QRT3), a polygalacturonase, to degrade de-methyl-esterified HG in the pollen mother cell primary walls (Rhee *et al.* 2003; Francis *et al.* 2006). Whether a similar relation between PMEs and PG exists in the context of organ abscission is yet to be

determined. Finally, several studies have used monoclonal antibodies to reveal dynamic changes in pectin methyl-esterification occurring prior to and during abscission (Uheda and Nakamura 2000; Lee *et al.* 2008). For example using the JIM5 and JIM7 monoclonal antibodies, which detect epitopes of different degrees of pectin methyl-esterification, revealed the presence of both JIM5 and JIM7 epitopes in the wall between AZ cells of branches of *Azolla* before abscission occurred, whereas the JIM5 epitope disappeared and only the JIM7 epitopes were observed in the middle lamella remaining after ethylene-induced abscission (Uheda and Nakamura 2000). A comparable result was observed during Impatiens leaf abscission, during which only the highly de-esterified HG epitope detected by JIM5 was observed to be reduced in the middle lamellae post-abscission and only at the plane of separation (Bowling and Vaughn 2011). In contrast to these first two studies, an AZ-associated de-esterification of HG was revealed by a reduction in the JIM5 epitope only in the AZ and distal area on day 7 after AZ induction, but no reduction after separation (Lee *et al.* 2008). It is not clear whether the differences observed are due to examining abscission processes in different subtending organs, or because the studies were done with different species. In any case, the studies suggest changes in the pectic methyl-esterification status are common to cell separation during organ abscission.

Cell Wall, Pectin and Cell Separation

Plant cells are surrounded by cell walls composed of structural proteins and complex polysaccharides including cellulose, hemicelluloses, and pectin. The cell wall is a dynamic structure that undergoes modifications during development and its composition depends on the tissue, developmental stage and relates to its functional specificity (Knox 2008). Indeed, the cell wall not only functions as a structure and protective layer against pathogenic attack, but also plays a central role in plant development and response to environmental changes. For

example, the cell wall contributes to a plant cell's rigidity and strength, however, in order for a plant to develop, the cell wall must undergo modifications to allow cell expansion and elongation (Cosgrove 2005). Furthermore, separation between adjacent cells is an essential part of developmental processes that occur throughout the life cycle of the plant (Figure 1.1) (Roberts *et al.* 2002; Driouich *et al.* 2007; Chervin *et al.* 2008). Despite the importance of cell separation in plants, our knowledge about the cell wall structural dynamics and molecular mechanisms that underlie the spatial and temporal precision of cell separation in different species, plant tissues and developmental contexts remains limited.

Pectin is the most structurally complex family of cell wall polysaccharides and is also a major component of primary walls of both monocots and dicots (Mohnen 2008). Pectic polysaccharides have roles in plant growth and development, provide mechanical strength and physical properties of primary walls, are involved in intercellular signalling that controls plant morphogenesis and plant defence against pathogens (Mohnen 2008; Caffall and Mohnen 2009). Pectin is abundantly found in walls of expanding and dividing cells, walls of cells in the soft parts of the plant, and most abundantly in the middle lamella and cell corners. In addition, pectin as the cement between two adjacent cells is of paramount importance for cell adhesion and during cell separation (Jarvis *et al.* 2003). Not only does it form the matrix in which the cellulose microfibers of the primary cell wall are embedded, but also is the main component of the middle lamella that adjoins adjacent cells (Figure 1.4) (Willats *et al.* 2001a; O'Neill *et al.* 2004). The structural characteristics and the role of how pectin participates towards cell separation to occur in a temporally and spatially precise manner are not completely understood despite a central importance during plant vegetative and reproductive development.

Pectin is comprised of the most complex naturally occurring polysaccharides known. Pectin is mainly composed of four major complex polysaccharides namely homogalacturan

(HG), rhamnogalacturonan I (RG-I), rhamnogalacturonan II (RG-II) and xylogalacturonan (XGA) (Figure 1.5) (Mohnen 2008; Caffall and Mohnen 2009). Pectic content is variable both between species and different organs, but in general more than 60% of pectin consists of HG, a linear homopolymer of α-1,4-linked galacturonic acid (GalA) (Figure 1.5). All the complex pectin polysaccharides contain O-1 to O-4 linked GalA as a component of their backbones, whereas only RG-I consists of 1,4-α-D-GalA-1,2-α-L-Rha disaccharide repeats. HG polymers can be 100-200 GalA residues in length and the GalA residues can be modified by methyl-esterification at the C-6 carboxyl and O-acetylated at O-2 or O-3 (Figure 1.6A) (Francis *et al.* 2006; Mohnen 2008). In particular, the methyl-esterification status of the HG has been shown to be important to maintain cell adhesion and implicated in mechanisms underlying separation as described below (Orfila *et al.* 2001; Willats *et al.* 2001a; Willats *et al.* 2001b; Jarvis *et al.* 2003; O'Neill *et al.* 2004; Caffall and Mohnen 2009). RG-II is the most complex structure of pectin, accounts for approximately 10% of total composition, and is fairly conserved across plant species (Mohnen 2008; Caffall and Mohnen 2009). RG-II form dimers that cross link with HG domains important for the overall macromolecular pectin network necessary for normal plant growth and development and cellular adhesion. RG-I represents 20-35% of the composition of pectin and with its repeating 1-4-α-D-GalA-1,2-α-L-Rha disaccharide backbone presents a large diversity that depends on developmental stage or cell type. The large variation in the RG-I structure observed in plants suggests diverse functional roles yet to be determined (Mohnen 2008; Caffall and Mohnen 2009). Finally, XGA is comprised of HG substituted at the O-3 with a β-linked xylose, and occasionally, further substituted at O-4 (Mohnen 2008). While XGA is most prevalent in reproductive tissues, it has also been detected in *Arabidopsis* stems and leaves. Furthermore, XGA functions during cell detachment (Willats *et al.* 2004) and resistance to pathogen attack (Jensen *et al.* 2008).

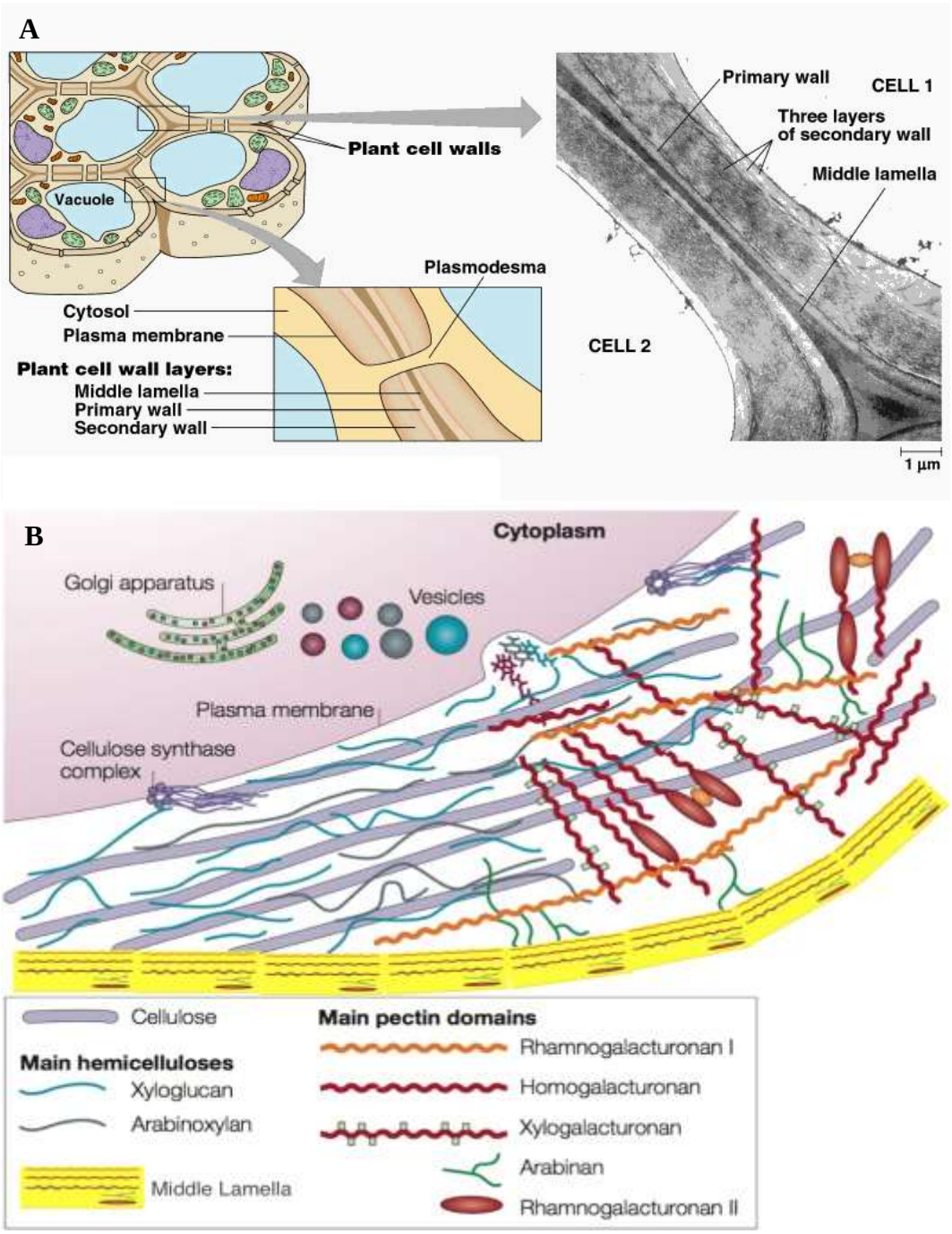

Figure 1.4. Schematic non-proportional representation of (A) the plant cell wall (Campbell and Reece 2002), (B) the pectin rich primary cell wall and middle lamella that joins together adjacent cells. Modified from Cosgrove (2005).

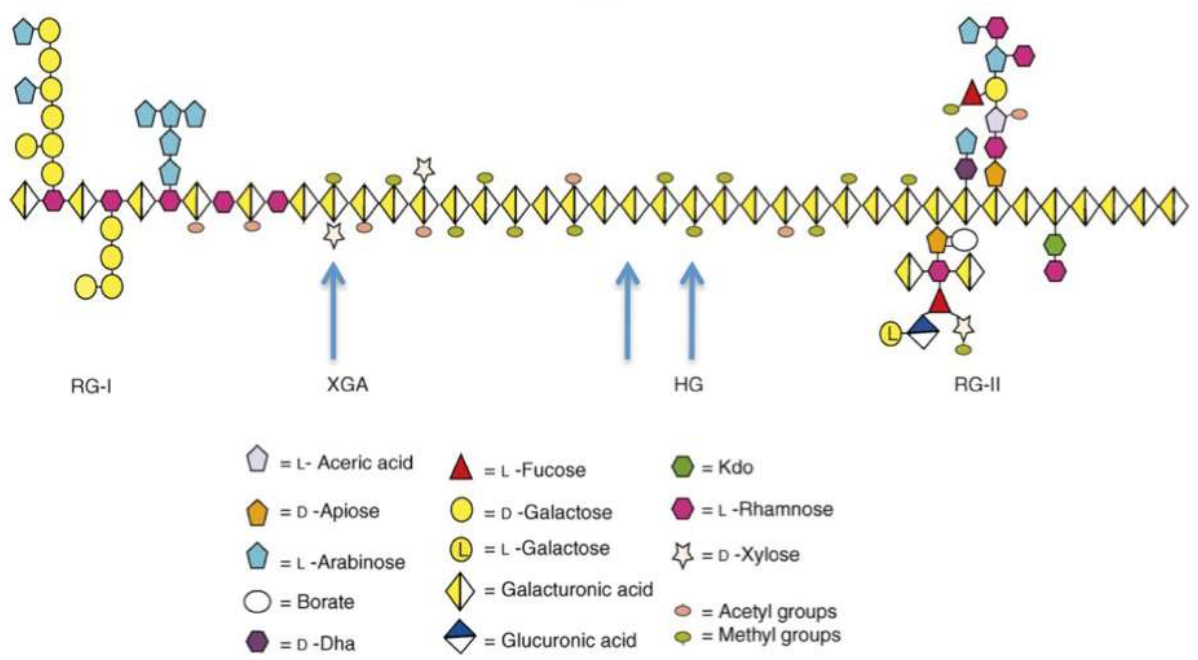

Figure 1.5. Schematic representation of pectin showing the four complex pectic polysaccharides homogalacturonan (HG), xylogalacturonan (XGA), rhamnogalacturonan I (RG-I) and rhamnogalacturonan II (RG-II) linked to each other. Blue arrows indicate pectin modifications implicated in cell separation. Figure adapted from Mohnen (2008).

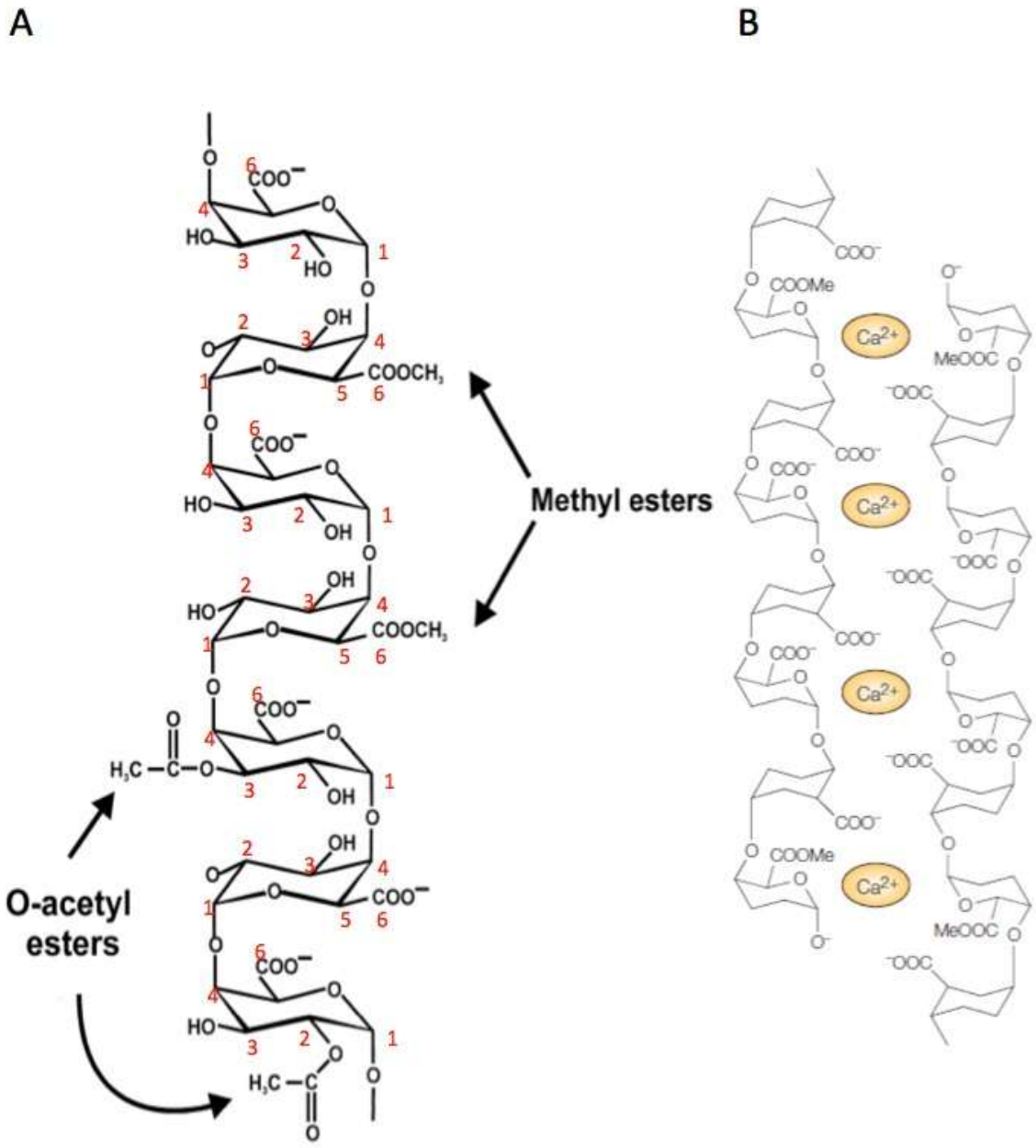

Figure 1.6. A, The primary structure of homogalacturonan indicating possible sites of methyl-esterification at the C-6 carboxyl and O-acetylation at the O-2 or O3 of linked GalA residues. B, Schematic model "egg-box" of ionic calcium bridge crosslinks between unmethyl-esterified carboxyl groups in antiparallel homogalacturonan that results in stiff gels. Adapted from Caffall and Mohnen (2009) and Cosgrove (2005).

The biosynthesis of pectin presumably involves many enzymes and the details have not fully been elucidated (Caffall and Mohnen 2009). In general, HG is thought to be synthesized in the golgi complex and modified by pectin methyltransferases (PMTs). PMTs add methyl groups at the C-6 carboxyl group (Caffall and Mohnen 2009). Then, modified pectin is targeted through vesicles *via* the *plasmodesmata* (PM) to the apoplast and finally inserted into the cell wall in a highly methylated form (Figures 1.3-1.6) (Kauss and Hassid 1967; Zhang and Staehelin 1992; Lennon and Lord 2000). The substrate for pectin polysaccharide synthesis including HG comes from nucleotide sugars and involves the activity of glycosyltransferase enzymes that have been localized within the golgi lumen (Sterling *et al.* 2001) (Figure 1.3). The current model of pectin biosynthesis pathway postulates that the HG backbone is initiated in the *cis cisternae* while extension and methyl-esterification of the HG GalA residues occurs in *medial cisternae*. Once new highly methylated pectin is inserted into the cell wall, PMEs are thought to remove the methyl groups in either a blockwise fashion resulting in domains of contiguous de-esterified GalA residues, or in a non-blockwise fashion that results in domains of non-contiguous de-esterified GalA residues (Willats *et al.* 2001b; Pelloux *et al.* 2007).

The methyl-esterification of HG plays an important role during plant development, as the methylation status can modulate the functionality of the pectin, in particular for cell adhesion and separation to occur (Jarvis *et al.* 2003). For example, during pollen tube tip growth, de-methyl-esterification of HG following tip expansion results in a more rigid pectin that contributes to the construction of the pollen tube wall, while the tip remains pliable to allow the burst of pollen necessary for fertilization (Hasegawa *et al.* 2000) (Li *et al.* 1994). Cells in other tissues also undergo de-esterification during development, as observed when intercellular spaces are formed (Willats *et al.* 2001b). Intercellular spaces arise during development and begin to form after cell division. When a cell divides, portions of the old

primary cell wall must be dismantled in order to link up adjacent middle lamellae to maintain apoplastic continuity between cells. Part of this process is characterized by the de-esterification of HG in specific locations of the primary wall that separate and lead to intracellular space formation. It is thought that de-esterification allows the formation of calcium (Ca^{2+}) cross links that results in the so-called "egg-box" pectin configuration between adjacent polymers (Figure 1.6 B) (Grant *et al.* 1973; Cosgrove 2005). As mentioned above, the de-methyl-esterification of HG is catalyzed by PME (EC 3.1.1.11), cell wall targeted proteins that modulate the methylation status of pectin HG (Micheli 2001; Pelloux *et al.* 2007). Furthermore, de-esterification related crosslinking increases pectin rigidity and may also allow targeting of cell wall modifying or pectin-degrading enzymes such as polygalacturonase (PG, EC 3.2.1.15) that further effect the texture and rigidity of the cell wall and may have roles during cell separation events such as those underlying organ abscission (Figure 1.3) (Hadfield and Bennett 1998). Pectate lyase or polygalacturonate lyase or pectate transeliminase (PL, EC 4.2.2.2) (Andro *et al.* 1984; Palusa *et al.* 2007) have been studied extensively in *Erwinia sp.*, a plant pathogen (Andro *et al.* 1984; Keen and Tamaki 1986). In the plant, there are proteins similar to PL called pectate lyase-like (PLL) proteins. The role of PLL is to depolymerise pectin by catalyzing the eliminative cleavage of α-1,4-linked galacturonic acid (Sun and van Nocker 2010) (Figure 1.3).

Oil Palm Fruit Abscission

Oil palm's botanical name is *Elaeis guineensis,* (Jacq.) which is derived from the Greek word *elaion* (oil) and the *guineensis* describes its origin from the Guinea coast (Henderson and Osborne 2000). Oil palm (Figure 1.7) is a tropical perennial monocotyledonous species in the Arecaceae family. It is one of the most important tropical crops due to the fleshly mesocarp from which edible oils are derived and recently became the number one source of

edible vegetable oil worldwide (Rival 2007). In addition, the oil from the mesocarp and kernel are used as major components of soaps, emulsifiers and pharmaceuticals (Henderson and Osborne 2000; Edem 2002; Rodrigues *et al.* 2004). Recently, due to depletion and the increased cost of fossil fuels, palm oil is considered a potential source of renewable energy usable as a biodiesel (Kalam and Masjuki 2002; Yusoff 2006; Tan *et al.* 2009). An increase in the use of palm oil as a source of biofuel is predicted to cause constraints on the worldwide supply of edible palm oil and increase the pressure for higher yields and an expansion of cultivatable areas. Conventional breeding schemes have allowed an increase in yield of palm oil up to 1 % per year (Rival 2007). However, while increases in yields are clearly possible with oil palm, one factor that limits overall yield gains is the loss due to non-synchronized ripening and subsequent shedding of the ripest fruit before harvest. In this context, our main goal is to examine the cellular and molecular mechanisms that occur during the cell separation process that leads to the abscission and shedding of the oil palm fruit.

The oil palm is monoecious; however, it is considered temporally dioecious given that separate male and female inflorescences occur on the same palm in an alternating cycle that depends on genetic factors, age and environmental (Cruden 1988; Adam *et al.* 2005). The oil palm fruit anatomy is as follows (Figure 1.8): i) the fleshy lipid rich mesocarp surrounds ii) the lignified shell containing the kernel with a distinct lipid composition, all situated on iii) the pedicel that is the fibrous stalk connection between the fruit base and the spikelet; iv) the rudimentary androecium refers to the aborted staminoid that forms a ring at the fruit base, while v) the tepals are the perianth located adjacent to rudimentary androecium, vi) the bracteoles are the outer perianth extensions of the spikelets, and finally vii) at the junction of the mesocarp and the pedicel is the primary AZ visible with the naked eye (Figure 1.8, position 1,). There are also four additional AZs around the outer perimeter of the fruit that originate at the perimeter of the primary AZ and terminate in four possible locations: between

the mesocarp and the rudimentary androecium (position 2), between the rudimentary androecium and the first tepal (position 3), between the tepals (position 4), and at the base of the tepals towards the bracteole (position 5). (Figure 1.8) (Henderson and Osborne 1990; Osborne *et al.* 1992).

The AZs are where cell separation occurs that leads to the complete abscission of individual ripe oil palm fruits from the fruit bunch. The adjacent AZs give the process of oil palm fruit abscission - one of its prominent characteristics described as a bi-phasic cell separation process (Henderson and Osborne 1990; Henderson and Osborne 1994). Cell separation occurs first within the primary AZ but the fruit remains firmly attached within the surrounding cup of rudimentary androecial ring, the tepals, bracteoles, and spiny floral bracts (Figure 1.8). After separation in the primary AZ occurs, separation in one of the four adjacent AZs will occur between 1 to 3 days later (Henderson and Osborne 1990). Furthermore, cell separation in the adjacent zones is developmentally regulated given that it takes place generally at the inside of rudimentary androecium (position 2) only with ripe fruit, while it can occur at one of the other adjacent AZs in less mature fruit (Henderson and Osborne 1990).

In the field, it is common that fruit shed at positions 1 and 2 cause most of the fruit to be shed completely without the rudimentary androecium (Henderson and Osborne 1990). However, a few shed fruit can be found with partial rudimentary androecium and some fruits can be found with complete rudimentary androecium. Separation at the adjacent zones is not induced by applied ethylene, ACC nor ABA and separation only occurs once the primary AZ is fully separated (Henderson and Osborne 1994). Furthermore, separation in the adjacent AZs of ripe or almost ripe fruit can occur when subjected to light pressure that results with fruit shed with the staminode ring and with some or all of the tepals. In contrast, bracteoles and the floral bract always remain attached to the spikelet. Unripe fruit do not undergo cell

separation either at position 1 or at other positions and fruit are not shed (Henderson and Osborne 1990). Finally, it was proposed that a signal other than ethylene may be released from the primary AZ to induce separation in the adjacent zones (Henderson and Osborne 1994).

Ethylene or its precursor 1-aminocyclopropane-l-carboxylic acid (ACC) initiates while auxin inhibits cell separation in the primary AZ of the oil palm fruit, This suggests both these hormones function to regulate abscission in oil palm as during the abscission processes with other species (Henderson and Osborne 1994; Brown 1997; Taylor and Whitelaw 2001; Roberts *et al.* 2002). Ethylene production is initiated at the ripe fruit stage and the progression of synthesis starts from the apex to base of the mesocarp in a positive correlation to the percentage of separation that occurs in the primary AZ. While the primary AZ, tepals and rudimentary androecium also increase in ethylene production during ripening, the amount is low which suggests the main source of ethylene production is in the mesocarp cells.

Transmission electron microscopy confirmed that cell separation at the AZ occurs at the middle lamella but attachment remains at the plasmodesmatal connections that may be last to separate. The cytoplasmic organelles of separating abscission cells include expanded mitochondria with multiple *cristae*, multiple polyribosomal clusters, expanded golgi stacks with associated vesicles, and evidence of vesicular traffic from the cytoplasm to the cell wall *via* the plasmalema (Henderson *et al.* 2001a). Phloroglucinol staining, which stains for the presence of lignin, indicated that intact AZ of ripe fruits shows continuous vascular tissue from pedicel traversing across the whole abscission region. However, the proportion of phloroglucinol-stained lignified vascular tissue with the intact AZ of ripe fruit is very low comparing to the adjacent mesocarp and pedicel tissues suggesting lignin synthesis is inhibited within the AZ layers (Henderson *et al.* 2001a).

Another interesting feature of the oil palm fruit abscission is that the abscinded AZ cells have higher pectin content when compared to the adjacent mesocarp and pedicel tissues that do not separate, based on uronic acid analysis (Henderson *et al.* 2001a). Furthermore, ^{13}C CP/MAS NMR spectra analysis revealed fewer methoxyl groups that was interpreted to reflect a lower level of pectin esterification exists in the abscinded AZ cells (Henderson *et al.* 2001a). Finally, an inducible polygalacturonase activity in abscinded AZ that is at least 35 fold compared with the value of intact AZ and adjoining zones (Henderson *et al.* 2001a). Together, these results were proposed as part of the basis for the localized precision of cell separation events in the base of the oil palm fruit. Together, these features and observations provide a basis towards understanding the cellular and molecular basis of abscission in the oil palm fruit and the context of this thesis.

Objectives of the Thesis

The objectives of this thesis are as follows:

1. Identify the PG genes responsible for the activity induced during separation; provide a global analysis of PG gene expression in the oil palm fruit tissues.

2. Identify characteristic features related to the development of the primary AZ in the oil palm fruit. To reach this goal we conducted a detailed histological examination of the development of the primary AZ compared to the adjacent pedicel and mesocarp tissue during oil palm fruit development.

3. Identify characteristic features of the primary AZ during cell separation induced by ethylene; microscopic and histological examination of the cellular changes that take place before, during, and after cell separation and abscission.

4. Identify characteristic features of the pectin within the primary AZ during development and cell separation induced by ethylene. To reach this goal, I conducted a histo-

immuno characterization of the primary AZ pectin using antibodies raised against pectin with different methyl-esterification patterns, in addition to one antibody for xylogalacturonan associated with cell separation. Develop an integrated model as a basis to explain the mechanisms underlying cell separation and fruit shedding in the oil palm.

Figure 1.7. Oil palm tree (*Elaeis guineensis*)

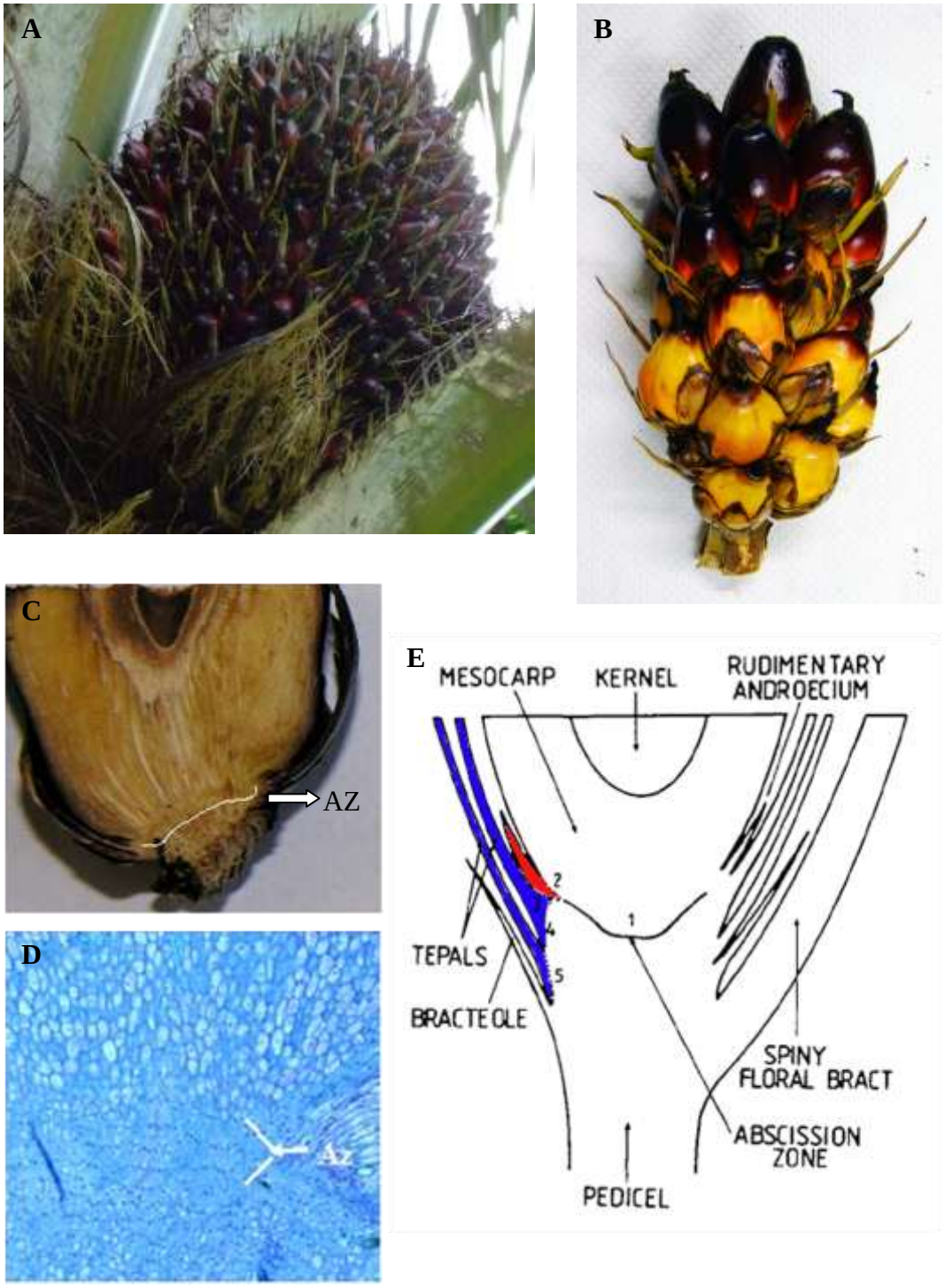

Figure 1.8. The oil palm fruit bunch, spikelet, and fruit including different tissues of oil palm fruit and AZ classical histology. (A) Oil palm bunch, (B) oil palm spikelet, (C) oil palm fruit base showing AZ, (D) longitudinal histological section of the fruit base showing the AZ, and (E) different tissues of oil palm fruit adapted from Henderson and Osborne (1994).

Literature Cited

Adam, H., S. Jouannic, J. Escoute, Y. Duval, J.-L. Verdeil and J. W. Tregear (2005). "Reproductive developmental complexity in the African oil palm (Elaeis guineensis, Arecaceae)." Am J Bot **92**(11): 1836-1852.

Addicott, F. (1982). Abscission, University of California Press, Ltd. London.

Andro, T., J. P. Chambost, A. Kotoujansky, J. Cattaneo, Y. Bertheau, F. Barras, F. Van Gijsegem and A. Coleno (1984). "Mutants of Erwinia chrysanthemi defective in secretion of pectinase and cellulase." J Bacteriol **160**(3): 1199-1203.

Bonghi, C., N. Rascio, A. Ramina and G. Casadoro (1992). "Cellulase and polygalacturonase involvement in the abscission of leaf and fruit explants of peach." Plant Mol Biol **20**(5): 839-848.

Bowling, A. J. and K. C. Vaughn (2011). "Leaf abscission in Impatiens (Balsaminaceae) is due to loss of highly de-esterified homogalacturonans in the middle lamellae." Am J Bot **98**(4): 619-629.

Brown, K. M. (1997). "Ethylene and abscission." Physiol Plant **100**(3): 567-576.

Brummell, D., B. Hall and A. Bennett (1999). "Antisense suppression of tomato endo-1,4-β-glucanase Cel2 mRNA accumulation increases the force required to break fruit abscission zones but does not affect fruit softening." Plant Mol Biol **40**(4): 615-622.

Burns, J. K., D. J. Lewandowski, C. J. Nairn and G. E. Brown (1998). "Endo-1,4-β-glucanase gene expression and cell wall hydrolase activities during abscission in Valencia orange." Physiol Plant **102**(2): 217-225.

Butenko, M. A., S. E. Patterson, P. E. Grini, G.-E. Stenvik, S. S. Amundsen, A. Mandal and R. B. Aalen (2003). "INFLORESCENCE DEFICIENT IN ABSCISSION Controls Floral Organ Abscission in Arabidopsis and Identifies a Novel Family of Putative Ligands in Plants." Plant Cell **15**(10): 2296-2307.

Caffall, K. H. and D. Mohnen (2009). "The structure, function, and biosynthesis of plant cell wall pectic polysaccharides." Carbohydr Res **344**(14): 1879-1900.

Campbell, N. A. and J. B. Reece (2002). Biology, Benjamin Cummings.

Castillejo, C., J. I. de la Fuente, P. Iannetta, M. Á. Botella and V. Valpuesta (2004). "Pectin esterase gene family in strawberry fruit: study of FaPE1, a ripening-specific isoform*." J Exp Bot **55**(398): 909-918.

Chervin, C., A. Tira-umphon, N. Terrier, M. Zouine, D. Severac and J.-P. Roustan (2008). "Stimulation of the grape berry expansion by ethylene and effects on related gene transcripts, over the ripening phase." Physiol Plant **134**(3): 534-546.

Cooley, M. B. and J. I. Yoder (1998). "Insertional inactivation of the tomato polygalacturonase gene." Plant Mol Biol **38**(4): 521-530.

Cosgrove, D. J. (2005). "Growth of the plant cell wall." Nat Rev Mol Cell Biol **6**(11): 850-861.

Cruden, R. W. (1988). "Temporal Dioecism: Systematic Breadth, Associated Traits, and Temporal Patterns." Bot Gaz **149**(1): 1-15.

del Campillo, E. (1999). 2 Multiple Endo-1, 4-β-D-glucanase (Cellulase) Genes in Arabidopsis. Current Topics in Developmental Biology. A. P. Roger and P. S. Gerald, Academic Press. **Volume 46:** 39-61.

Driouich, A., C. Durand and M. Vicre-Gibouin (2007). "Formation and separation of root border cells." Trends Plant Sci **12**(1): 14-19.

Edem, D. O. (2002). "Palm oil: Biochemical, physiological, nutritional, hematological and toxicological aspects: A review." Plant Food Hum Nutr **57**(3): 319-341.

Ferrarese, L., L. Trainotti, S. Gattolin and G. Casadoro (1998). "Secretion, purification and activity of two recombinant pepper endo-β-1,4-glucanases expressed in the yeast Pichia pastoris." FEBS Lett **422**(1): 23-26.

Francis, K. E., S. Y. Lam and G. P. Copenhaver (2006). "Separation of Arabidopsis Pollen Tetrads Is Regulated by QUARTET1, a Pectin Methylesterase Gene." Plant Physiol **142**(3): 1004-1013.

Gonzalez-Bosch, C., E. del Campillo and A. B. Bennett (1997). "Immunodetection and Characterization of Tomato Endo-[beta]-1,4-Glucanase Cel1 Protein in Flower Abscission Zones." Plant Physiol **114**(4): 1541-1546.

Grant, G. T., E. R. Morris, D. A. Rees, P. J. C. Smith and D. Thom (1973). "Biological interactions between polysaccharides and divalent cations: The egg-box model." FEBS Lett **32**(1): 195-198.

Greenberg, J., R. Goren and J. Riov (1975). "The Role of Cellulase and Polygalacturonase in Abscission of Young and Mature Shamouti Orange Fruits." Physiol Plant **34**(1): 1-7.

Grierson, D., M. J. Maunders, A. Slater, J. Ray, C. R. Bird, W. Schuch, M. J. Holdsworth, G. A. Tucker and J. E. Knapp (1986). "Gene Expression During Tomato Ripening." Philosophical Transactions of the Royal Society of London Series B, Biological Sciences **314**(1166): 399-410.

Hadfield, K. A. and A. B. Bennett (1998). "Polygalacturonases: Many Genes in Search of a Function." Plant Physiol **117**(2): 337-343.

Hasegawa, Y., S. Nakamura, E. Uheda and N. Nakamura (2000). "Immunolocalization and possible roles of pectins during pollen growth and callose plug formation in angiosperms." Grana **39**(1): 46-55.

Henderson, J., H. A. Davies, S. J. Heyes and D. J. Osborne (2001a). "The study of a monocotyledon abscission zone using microscopic, chemical, enzymatic and solid state 13C CP/MAS NMR analyses." Phytochemistry **56**(2): 131-139.

Henderson, J., L. Lyne and D. J. Osborne (2001b). "Failed expression of an endo-β-1,4-glucanhydrolase (cellulase) in a non-abscinding mutant of Lupinus angustifolius cv Danja." Phytochemistry **58**(7): 1025-1034.

Henderson, J. and D. J. Osborne (1990). "Cell Separation and Anatomy of Abscission in the Oil Palm, Elaeis guineensis Jacq." J Exp Bot **41**(2): 203-210.

Henderson, J. and D. J. Osborne (1994). "Inter-tissue signalling during the two-phase abscission in oil palm fruit." J Exp Bot **45**(7): 943-951.

Henderson, J. and D. J. Osborne (2000). "The oil palm in all our lives: how this came about." Endeavour **24**(2): 63-68.

Hong, S. B. and M. L. Tucker (1998). "Genomic organization of six tomato polygalacturonases and 5 ' upstream sequence identity with tap1 and win2 genes." Mol Gen Genet **258**(5): 479-487.

Jarvis, M. C., S. P. H. Briggs and J. P. Knox (2003). "Intercellular adhesion and cell separation in plants." Plant, Cell Environ **26**(7): 977-989.

Jensen, J. K., S. O. Sørensen, J. Harholt, N. Geshi, Y. Sakuragi, I. Møller, J. Zandleven, A. J. Bernal, N. B. Jensen, C. Sørensen, M. Pauly, G. Beldman, W. G. T. Willats and H. V. Scheller (2008). "Identification of a Xylogalacturonan Xylosyltransferase Involved in Pectin Biosynthesis in Arabidopsis." Plant Cell **20**(5): 1289-1302.

Jiang, C. Z., F. Lu, W. Imsabai, S. Meir and M. S. Reid (2008). "Silencing polygalacturonase expression inhibits tomato petiole abscission." J Exp Bot **59**(4): 973-979.

Jinn, T.-L., J. M. Stone and J. C. Walker (2000). "HAESA, an Arabidopsis leucine-rich repeat receptor kinase, controls floral organ abscission." Genes Dev **14**(1): 108-117.

Kalaitzis, P., S. M. Koehler and M. L. Tucker (1995). "Cloning of a tomato polygalacturonase expressed in abscission." Plant Mol Biol **28**(4): 647-656.

Kalaitzis, P., T. Solomos and M. L. Tucker (1997). "Three Different Polygalacturonases Are Expressed in Tomato Leaf and Flower Abscission, Each with a Different Temporal Expression Pattern." Plant Physiol **113**(4): 1303-1308.

Kalam, M. A. and H. H. Masjuki (2002). "Biodiesel from palmoil--an analysis of its properties and potential." Biomass Bioenerg **23**(6): 471-479.

Kauss, H. and W. Z. Hassid (1967). "Enzymic Introduction of the Methyl Ester Groups of Pectin." J Biol Chem **242**(15): 3449-3453.

Keen, N. T. and S. Tamaki (1986). "Structure of two pectate lyase genes from Erwinia chrysanthemi EC16 and their high-level expression in Escherichia coli." J Bacteriol **168**(2): 595-606.

Kim, J., S.-H. Shiu, S. Thoma, W.-H. Li and S. Patterson (2006). "Patterns of expansion and expression divergence in the plant polygalacturonase gene family." Genome Biol **7**(9): R87.

Knox, J. P. (2008). "Revealing the structural and functional diversity of plant cell walls." Curr Opin Plant Biol **11**(3): 308-313.

Koch, J. L. and D. J. Nevins (1989). "Tomato Fruit Cell Wall : I. Use of Purified Tomato Polygalacturonase and Pectinmethylesterase to Identify Developmental Changes in Pectins." Plant Physiol **91**(3): 816-822.

Lamotte, C. E., C. Gochnauer, L. R. Lamotte, J. R. Mathur and L. L. R. Davies (1969). "Pectin Esterase in Relation to Leaf Abscission in Coleus and Phaseolus." Plant Physiol **44**(1): 21-26.

Lanahan, M. B., H. C. Yen, J. J. Giovannoni and H. J. Klee (1994). "The Never Ripe Mutation Blocks Ethylene Perception in Tomato." Plant Cell **6**(4): 521-530.

Lee, Y., P. Derbyshire, J. P. Knox and A. K. Hvoslef-Eide (2008). "Sequential cell wall transformations in response to the induction of a pedicel abscission event in Euphorbia pulcherrima (poinsettia)." Plant J **54**(6): 993-1003.

Lennon, K. and E. Lord (2000). "In vivo pollen tube cell of *Arabidopsis thaliana*; I. Tube cell cytoplasm and wall." Protoplasma **214**(1): 45-56.

Leslie, M. E., M. W. Lewis and S. J. Liljegren (2007). Organ Abscission. Annual Plant Reviews Volume 25: Plant Cell Separation and Adhesion, Blackwell Publishing Ltd**:** 106-136.

Li, Y., F. Chen, H. Linskens and M. Cresti (1994). "Distribution of unesterified and esterified pectins in cell walls of pollen tubes of flowering plants." Sex Plant Reprod **7**(3): 145-152.

Libertini, E., Y. Li and S. McQueen-Mason (2004). "Phylogenetic Analysis of the Plant Endo-ß-1,4-Glucanase Gene Family." J Mol Evol **58**(5): 506-515.

Loopstra, C. A., A. Mouradov, A. Vivian-Smith, T. V. Glassick, B. V. Gale, S. G. Southerton, H. Marshall and R. D. Teasdale (1998). "Two Pine Endo-β-1,4-Glucanases Are Associated with Rapidly Growing Reproductive Structures." Plant Physiol **116**(3): 959-967.

Mbéguié-A-Mbéguié, D., O. Hubert, F. C. Baurens, T. Matsumoto, M. Chillet, B. Fils-Lycaon and S. Sidibé-Bocs (2009). "Expression patterns of cell wall-modifying genes from banana during fruit ripening and in relationship with finger drop." J Exp Bot **60**(7): 2021-2034.

Micheli, F. (2001). "Pectin methylesterases: cell wall enzymes with important roles in plant physiology." Trends Plant Sci **6**(9): 414-419.

Mohnen, D. (2008). "Pectin structure and biosynthesis." Curr Opin Plant Biol **11**(3): 266-277.

Moline, H. E., C. E. LaMotte, C. Gochnauer and A. McNamer (1972). "Further Comparative Studies of Pectin Esterase in Relation to Leaf and Flower Abscission." Plant Physiol **50**(6): 655-659.

O'Neill, M. A., T. Ishii, P. Albersheim and A. G. Darvill (2004). "RHAMNOGALACTURONAN II: Structure and Function of a Borate Cross-Linked Cell Wall Pectic Polysaccharide." Annu Rev Plant Biol **55**(1): 109-139.

Orfila, C., G. B. Seymour, W. G. T. Willats, I. M. Huxham, M. C. Jarvis, C. J. Dover, A. J. Thompson and J. P. Knox (2001). "Altered Middle Lamella Homogalacturonan and Disrupted Deposition of (1→5)-α-l-Arabinan in the Pericarp ofCnr, a Ripening Mutant of Tomato." Plant Physiol **126**(1): 210-221.

Osborne, D. J. (1958). "Changes in the Distribution of Pectin Methylesterase across Leaf Abscission Zones of Phaseolus vulgaris." J Exp Bot **9**(3): 446-457.

Osborne, D. J., J. Henderson and R. H. V. Corley (1992). "Controlling fruit-shedding in the oil palm." Endeavour **16**(4): 173-177.

Østergaard, L., B. Borkhardt and P. Ulvskov (2007). Dehiscence. Annual Plant Reviews Volume 25: Plant Cell Separation and Adhesion, Blackwell Publishing Ltd**:** 137-163.

Palusa, S. G., M. Golovkin, S. B. Shin, D. N. Richardson and A. S. Reddy (2007). "Organ-specific, developmental, hormonal and stress regulation of expression of putative pectate lyase genes in Arabidopsis." New Phytol **174**(3): 537-550.

Pandita, V. and K. Jindal (1991). "Enzymatic and anatomical changes in abscission zone cells of apple fruits induced by Ethephon." Biol Plant **33**(1): 20-25.

Patterson, S. E. (2001). "Cutting Loose. Abscission and Dehiscence in Arabidopsis." Plant Physiol **126**(2): 494-500.

Patterson, S. E. and A. B. Bleecker (2004). "Ethylene-Dependent and -Independent Processes Associated with Floral Organ Abscission in Arabidopsis." Plant Physiol **134**(1): 194-203.

Pedrolli, D. B., A. C. Monteiro, E. Gomes and E. C. Carmona (2009). "Pectin and Pectinases: Production, Characterization and Industrial Application of Microbial Pectinolytic Enzymes." The Open Biotechnology Journal **3**: 9-18.

Pelloux, J., C. Rustérucci and E. J. Mellerowicz (2007). "New insights into pectin methylesterase structure and function." Trends Plant Sci **12**(6): 267-277.

Prasanna, V., T. N. Prabha and R. N. Tharanathan (2007). "Fruit Ripening Phenomena–An Overview." Crit Rev Food Sci Nutr **47**(1): 1-19.

Ratner, A., R. Goren and S. P. Monselise (1969). "Activity of Pectin Esterase and Cellulase in the Abscission Zone of Citrus Leaf Explants." Plant Physiol **44**(12): 1717-1723.

Rhee, S. Y., E. Osborne, P. D. Poindexter and C. R. Somerville (2003). "Microspore Separation in the quartet 3 Mutants of Arabidopsis Is Impaired by a Defect in a Developmentally Regulated Polygalacturonase Required for Pollen Mother Cell Wall Degradation." Plant Physiol **133**(3): 1170-1180.

Rival, A. (2007). Oil Palm. Biotechnology in Agriculture and Forestry, Springer-Verlag Berlin Heidelberg. **61:** 59-80.

Roberts, J. and Z. Gonzalez-Carranza (2007). Cell Separation and Adhesion Processes in Plants. Annual Plant Reviews Volume 25: Plant Cell Separation and Adhesion, Blackwell Publishing Ltd**:** 1-7.

Roberts, J. A., K. A. Elliott and Z. H. Gonzalez-Carranza (2002). "Abscission, Dehiscence, and Other Cell Separation Processes." Annu Rev Plant Biol **53**(1): 131-158.

Rodrigues, M., N. Peiriço, H. Matos, E. Gomes de Azevedo, M. R. Lobato and A. J. Almeida (2004). "Microcomposites theophylline/hydrogenated palm oil from a PGSS process for controlled drug delivery systems." J Supercrit Fluids **29**(1-2): 175-184.

Sexton, R. and J. A. Roberts (1982). "Cell Biology of Abscission." Ann Rev Plant Physio **33**(1): 133-162.

Sheehy, R. E., M. Kramer and W. R. Hiatt (1988). "Reduction of polygalacturonase activity in tomato fruit by antisense RNA." Proc Natl Acad Sci USA **85**(23): 8805-8809.

Smith, C. J. S., C. F. Watson, J. Ray, C. R. Bird, P. C. Morris, W. Schuch and D. Grierson (1988). "Antisense RNA inhibition of polygalacturonase gene expression in transgenic tomatoes." Nature **334**(6184): 724-726.

Stenvik, G.-E., N. M. Tandstad, Y. Guo, C.-L. Shi, W. Kristiansen, A. Holmgren, S. E. Clark, R. B. Aalen and M. A. Butenko (2008). "The EPIP Peptide of INFLORESCENCE DEFICIENT IN ABSCISSION Is Sufficient to Induce Abscission in Arabidopsis through the Receptor-Like Kinases HAESA and HAESA-LIKE2." Plant Cell **20**(7): 1805-1817.

Sterling, J. D., H. F. Quigley, A. Orellana and D. Mohnen (2001). "The Catalytic Site of the Pectin Biosynthetic Enzyme α-1,4-Galacturonosyltransferase Is Located in the Lumen of the Golgi." Plant Physiol **127**(1): 360-371.

Sun, L. and S. van Nocker (2010). "Analysis of promoter activity of members of the PECTATE LYASE-LIKE (PLL) gene family in cell separation in Arabidopsis." BMC Plant Biol **10**(1): 152.

Swain, S., P. Kay and M. Ogawa (2011). "Preventing unwanted breakups: using polygalacturonases to regulate cell separation." Plant Signal Behav **6**(1): 93-97.

Tan, K. T., K. T. Lee, A. R. Mohamed and S. Bhatia (2009). "Palm oil: Addressing issues and towards sustainable development." Renew Sust Energ Rev **13**(2): 420-427.

Taylor, J. E., G. A. Tucker, Y. Lasslett, C. J. S. Smith, C. M. Arnold, C. F. Watson, W. Schuch, D. Grierson and J. A. Roberts (1990). "Polygalacturonase expression during leaf abscission of normal and transgenic tomato plants." Planta **183**(1): 133-138.

Taylor, J. E., S. T. J. Webb, S. A. Coupe, G. A. Tucker and J. A. Roberts (1993). "Changes in Polygalacturonase Activity and Solubility of Polyuronides during Ethylene-stimulated Leaf Abscission in Sambucus nigra." J Exp Bot **44**(1): 93-98.

Taylor, J. E. and C. A. Whitelaw (2001). "Signals in abscission." New Phytol **151**(2): 323-340.

Tian, G.-W., M.-H. Chen, A. Zaltsman and V. Citovsky (2006). "Pollen-specific pectin methylesterase involved in pollen tube growth." Dev Biol **294**(1): 83-91.

Trainotti, L., N. Rascio and G. Casadoro (1993). "Expression of an endopolygalacturonase gene during growth and abscission of peach fruits." Hereditas **119**(3): 301-304.

Trainotti, L., S. Spolaore, L. Ferrarese and G. Casadoro (1997). "Characterization of ppEG1, a member of a multigene family which encodes endo-β-1,4-glucanase in peach." Plant Mol Biol **34**(5): 791-802.

Tucker, M. L., R. Sexton, E. del Campillo and L. N. Lewis (1988). "Bean Abscission Cellulase : Characterization of a cDNA Clone and Regulation of Gene Expression by Ethylene and Auxin." Plant Physiol **88**(4): 1257-1262.

Tucker, M. L., C. A. Whitelaw, N. N. Lyssenko and P. Nath (2002). "Functional Analysis of Regulatory Elements in the Gene Promoter for an Abscission-Specific Cellulase from Bean and Isolation, Expression, and Binding Affinity of Three TGA-Type Basic Leucine Zipper Transcription Factors." Plant Physiol **130**(3): 1487-1496.

Uheda, E. and S. Nakamura (2000). "Abscission of Azolla Branches Induced by Ethylene and Sodium Azide." Plant Cell Physiol **41**(12): 1365-1372.

Valdovinos, J. G. and R. M. Muir (1965). "Effects of D and L Amino Acids on Foliar Abscission." Plant Physiol **40**(2): 335-340.

Wakabayashi, K., J.-P. Chun and D. J. Huber (2000). "Extensive solubilization and depolymerization of cell wall polysaccharides during avocado (Perseaamericana) ripening involves concerted action of polygalacturonase and pectinmethylesterase." Physiol Plant **108**(4): 345-352.

Wakabayashi, K., T. Hoson and D. J. Huber (2003). "Methyl de-esterification as a major factor regulating the extent of pectin depolymerization during fruit ripening: a comparison of the action of avocado (Persea americana) and tomato (Lycopersicon esculentum) polygalacturonases." J Plant Physiol **160**(6): 667-673.

Wen, F., Y. Zhu and M. C. Hawes (1999). "Effect of Pectin Methylesterase Gene Expression on Pea Root Development." Plant Cell **11**(6): 1129-1140.

Willats, W. G. T., L. McCartney, W. Mackie and J. P. Knox (2001a). "Pectin: cell biology and prospects for functional analysis." Plant Mol Biol **47**(1): 9-27.

Willats, W. G. T., C. Orfila, G. Limberg, H. C. Buchholt, G.-J. W. M. van Alebeek, A. G. J. Voragen, S. E. Marcus, T. M. I. E. Christensen, J. D. Mikkelsen, B. S. Murray and J. P. Knox (2001b). "Modulation of the Degree and Pattern of Methyl-esterification of Pectic Homogalacturonan in Plant Cell Walls." J Biol Chem **276**(22): 19404-19413.

Willats, W. T., L. McCartney, C. Steele-King, S. Marcus, A. Mort, M. Huisman, G.-J. Alebeek, H. Schols, A. J. Voragen, A. Goff, E. Bonnin, J.-F. Thibault and J. P. Knox (2004). "A xylogalacturonan epitope is specifically associated with plant cell detachment." Planta **218**(4): 673-681.

Wolf, S., G. Mouille and J. Pelloux (2009). "Homogalacturonan Methyl-Esterification and Plant Development." Mol Plant **2**(5): 851-860.

Yusoff, S. (2006). "Renewable energy from palm oil - innovation on effective utilization of waste." J Clean Prod **14**(1): 87-93.

Zhang, G. F. and L. A. Staehelin (1992). "Functional Compartmentation of the Golgi Apparatus of Plant Cells : Immunocytochemical Analysis of High-Pressure Frozen- and Freeze-Substituted Sycamore Maple Suspension Culture Cells." Plant Physiol **99**(3): 1070-1083.

Chapter 2. Temporal and Spatial Expression of Polygalacturonase Gene Family Members Reveals Complex Regulation During Fleshy Fruit Ripening and Abscission of the Monocot Oil Palm*

*This chapter was submitted for publication to the Journal of Experimental Botany on November 1, 2011 and is currently under review.

Introduction

The shedding of plant organs is a highly coordinated developmentally programmed event that can occur in different contexts throughout the plant life cycle (Addicott 1982; Sexton and Roberts 1982; Roberts *et al.* 2002; Leslie *et al.* 2007). Organ shedding is important for both plant vegetative and reproductive development, including abscission of leaves, branches, whole flowers, floral parts, seeds and immaturely aborted or ripe fruit. In particular, cell separation that occurs during fleshy fruit abscission and dry fruit dehiscence facilitate seed dispersal, the final stage of reproductive development, and are important characters to control the abscission for many crop species. For fruit to be shed, cell separation must occur in a precise location timed for optimize dispersal under the most favourable conditions. For crop species, if fruit are shed too early or too late, economic consequences can be significant. Whereas our understanding of the evolutionary context for these phenomenon are mainly limited to model systems such as tomato and *Arabidopsis*, less is known about the mechanisms underlying fruit abscission in non-model crop species in general and, monocot species in particular.

Oil palm is a tropical perennial monocotyledonous species in the Arecaceae family with an extraordinarily oil-rich fleshly mesocarp, which is the number one source of edible vegetable oil worldwide. In addition, potential use of palm oil as a biofuel is predicted to cause constraints on the worldwide supply of edible palm oil and increase the pressure for higher yields and an expansion of cultivatable areas. While conventional breeding schemes have allowed increases in yield of palm oil up to 1% per year, non-synchronized ripening and subsequent shedding of the ripest fruit before harvest limit yield gains (Osborne *et al.* 1992; Rival 2007). In addition, the difficulty to schedule regular harvests due to non-synchronized fruit shedding results in a labour intensive logistics that increases overall production costs. Furthermore, several original characters of oil palm fruit shedding warrant further detailed

investigations. Namely, a two-stage process involving primary and adjacent abscission zones (AZs), the extraordinary low amount of methylated pectin and high levels of polygalacturonase (PG) activity suggest that divergent mechanisms may underlie the cell separation that leads to fruit shedding in this monocotyledonous species (Henderson and Osborne 1990; Henderson and Osborne 1994; Henderson *et al.* 2001a). Finally, the only organ observed to shed in this palm species is the ripe fruit. Notably, flowers and immature fruitlets from many species are naturally thinned by organ abscission in response to nutritional status to optimized reproductive success, whereas this phenomenon is not observed to any extent in oil palm. Indeed, the oil palm maintains all fruit on a bunch until ripening related signalling takes place to induce ripe fruit abscission.

While examples of organ shedding in plants are diverse, the common model proposed is mainly based on studies with dicotyledons (Roberts *et al.* 2002; Leslie *et al.* 2007). Firstly, the development of the AZ takes place at the base of subtending organ to be shed. Secondly, as the AZ develops, it must become competent for cell separation events required for organ abscission. Indeed, once the AZ develops, it responds differently from adjacent tissues to the signals that induce cell separation (Taylor and Whitelaw 2001). After the AZ becomes competent for separation to be induced, cellular activity, in particular the expansion of the golgi vesicles and activation of the endomembrane system with the release of hydrolytic enzymes to the apoplast leads to the degradation of the middle lamella that leads to cell separation. An important feature of the model is the induction of the genes encoding cell wall hydrolytic enzymes targeted to modify and degrade cell wall components for separation to occur. The expression of these genes are often induced by ethylene and inhibited by auxin, characteristics that correlate with the positive and negative effects of these hormones on the abscission process respectively (Addicott 1982; Roberts *et al.* 2002; Leslie *et al.* 2007). Despite the central importance of the mechanisms that allow changes in adhesion of adjacent

cells to take place with such temporal and spatial precision, our understanding of these events even in model organisms is limited.

PG gene expression and activity are common features of organ abscission, observed in bean, tomato, peach and *Sambucus nigra* (Berger and Reid 1979; Tucker *et al.* 1984; Bonghi *et al.* 1992; Taylor *et al.* 1993). PG activity depolymerises the homogalacturonan backbone of pectin and while PG transcripts and activity increase in various species during the abscission process, they can also be induced by ethylene or inhibited by auxin (Giovannoni *et al.* 1989; Taylor *et al.* 1990; Bonghi *et al.* 1992; Taylor *et al.* 1993; Kalaitzis *et al.* 1995; Kalaitzis *et al.* 1997; Hadfield and Bennett 1998; Hadfield *et al.* 1998). In tomato, there is a single PG transcript (*pTOM6,* also known as *TFPG*) expressed during fruit ripening, while up to four other PGs (*TAPG1*, *TAPG2*, *TAPG4* and *TAPG5*) are expressed in the flower/fruit pedicel AZ associated with abscission (Dellapenna *et al.* 1986; Sheehy *et al.* 1988; Smith *et al.* 1988; Dellapenna *et al.* 1989; Kalaitzis *et al.* 1995; Kalaitzis *et al.* 1997; Hong and Tucker 1998; Sitrit and Bennett 1998). Interestingly, the down-regulation or knockout of *TFPG* resulted in a decrease in pectin depolymerization, but surprisingly no change in fruit softening which suggests other components are involved (Sheehy *et al.* 1988; Smith *et al.* 1988; Smith *et al.* 1990; Cooley and Yoder 1998). Furthermore, down regulation of fruit *TFPG* has no effect on the timing or rate of leaf abscission, indicating a specific function of this enzyme during fruit ripening but not organ abscission (Taylor *et al.* 1990). In contrast, silencing of the abscission *TAPG1* expression delayed abscission and increased break strength of the AZ (Jiang *et al.* 2008). Overall, these experiments suggest that while PGs are important for processes during both ripening and abscission, the same genes may not be responsible and there are other factors involved in abscission. Indeed, there are up to 69 and 59 PG genes in *Arabidopsis* and rice respectively, many with overlapping expression domains (Kim and Patterson 2006; Gonzalez-Carranza *et al.* 2007). At least four of the

Arabidopsis PG genes have expression profiles correlated to cell wall loosening and cell wall dissolution events during floral organ abscission (Kim and Patterson 2006). Furthermore, *ADPG1*, *ADPG2* and *QRT2* were shown to have overlapping functions during different cell separation processes. *ADPG1* and *ADPG2* are essential for silique dehiscence, while *ADPG2* and *QRT2* contribute to floral organ abscission, and all three genes contribute to anther dehiscence, suggesting precise combinations of PG activities may be necessary during the cell separation events underlying these different processes.

A previous study revealed a large increase in PG activity in the oil palm AZ in the base of the fruit during cell separation events that lead to fruit abscission (Henderson *et al.* 2001a). Our main objective in the present study was to identify PG genes that could be responsible for this activity observed during fruit shedding. We have performed a detailed expression analysis of 14 genes that encode PGs from diverse phyologenetic clades, and that are expressed in the base of the oil palm fruit. PG diversity in the fruit tissues and there profiles of expression during ripening and during ethylene induced abscission contrasts with that observed in tomato suggesting some functional divergence underlying these processes in this monocotyledon fruit species. The results of a phylogenetic analysis of EgPG4 with PGs with known functions from various species will also be discussed with relation to divergence that may have occurred between eudicots and monocots, in particular between fleshy and dry fruit species.

Results

Ethylene induced oil palm fruit shedding experimental system

Previous studies published on oil palm fruit shedding were done with material transported by airfreight from plantations in Malaysia to a laboratory in the United Kingdom where the experiments were performed (Henderson and Osborne 1990; Henderson and Osborne 1994; Henderson *et al.* 2001a). In order to determine precisely the timing of events that occur during abscission, our first objective was to set up an experimental system that could be used in a local field setting to eliminate problems that could arise due to the time and conditions required for storage and long distance shipment of the fruit. Based on the results of earlier studies with oil palm, ethylene was implicated as the main signal that induces cell separation in the primary AZ of the oil palm fruit (Henderson and Osborne 1994). Therefore, to synchronize fruit shedding, we treated spikelet explants with ethylene in airtight boxes (see Material and Methods for details; Figure 2.1A). The first experiment examined the ethylene dose effect on the induction of cell separation in the primary AZ of ripe fruit (150 days after pollination, DAP) treated for 12 h (Figure 2.1B). An increase in the number of fruit shed (13%) was observed in spikelets treated with 0.1 µl l^{-1} ethylene, while at 10 µl l^{-1}, 100% of the fruit underwent cell separation in the primary AZ. This experiment confirmed the use of 10 µl l^{-1} as an effective concentration for our studies as used previously (Henderson and Osborne 1994). In addition, the experiment also confirmed the two-stage separation process (data not shown) during which separation first occurs within the predetermined primary AZ, followed later by separation events in adjacent AZs (Henderson and Osborne 1990; Henderson and Osborne 1994). Further experiments used the concentration of 10 µl l^{-1} to compare separation in fruit at different stages of development (Figure 2.1C). Spikelets of fruit at 30, 120 and 180 DAP were treated and shedding was quantified at time intervals up to 24 h after of treatment. No fruit were observed to shed at 3

and 6 h. Fruit at 30 DAP were only observed to shed after 24 hours of treatment, while 120 DAP fruit and 180 DAP fruit began to separate after 12 h and 9 h of treatment respectively. In air controls, only the 180 DAP fruit were observed to shed at 12 h (1%) and 24 h (100%). These experiments define the time frame during which cell separation must occur for oil palm fruit shedding to take place, and suggest importance of developmental factors that influence the response to ethylene.

Polygalacturonase gene family expression in the oil palm fruit tissues and the identification of the *EgPG4* transcript induced in the abscission zone prior to fruit shedding

A 35-fold increase in PG activity was reported to occur in the AZ during fruit shedding (Henderson *et al.* 2001a). Furthermore, PGs are implicated in cell separation underlying organ separation in many species. In this context, our next objective was to identify PG candidate genes responsible for this large PG activity observed during cell separation events in the AZ. Briefly, our approach involved searches of available databases for sequences similar to known PGs, including local 454 derived transcriptome data; then followed by designing specific primers for each sequence identified to test, along with degenerate primers, for amplification from a mixture of cDNAs derived from fruit tissues treated or not with ethylene, or from genomic DNA (see Materials and Methods for details). Overall, our searches resulted in the identification of 35 putative non-redundant PG sequences, 28 of which contained either a partial or complete GH28 PG signature domain and were retained for further studies (see Supplementary Table S2.3 for nucleotide sequences). From the 28 sequences, RT-PCR analysis revealed that 14 non-redundant PG transcripts were expressed in the AZ of oil palm fruit and a detailed analysis of their expression in fruit tissues during ethylene induced abscission was performed. The 14 transcripts are *EgPG1*, *EgPG3*,

EgPG4, *EgPG7*, *EgPG8*, *EgPG9*, *EgPG10*, *EgPG11*, *EgPG16*, *EgPG17*, *EgPG18*, *EgPG19*, *EgPG22* and *EgPG26*.

To analyze expression, qPCR analysis was performed with tissue samples from the ethylene experiments described above (Figure 2.1C). The results confirmed the RT-PCR analysis in that each of the 14 primer pairs successfully amplified a PG sequence from the oil palm fruit AZ, and also from the adjacent pedicel or mesocarp tissues before and after ethylene treatment (Figure 2.2A-N). The profiles of transcript abundance can be grouped into the following three main categories: I) five transcripts increase significantly (more than two fold; Figure 2.2A-E), II) four transcripts decrease significantly (less than 0.5 fold; Figure 2.2F-I) and, III) five transcripts have no significant change in abundance in the AZ during ethylene treatments (Figure 2.2J-N) respectively. By far the most abundant PG transcript detected with the most dramatic increase in abundance in the AZ is that of *EgPG4* (Fig 2B and Figure 2.3). *EgPG4* transcript increases approximately 700, 2000, 4000 and 5000 fold in the AZ after 3, 6, 9 and 12 h of ethylene treatment respectively. In contrast, *EgPG4* is also highly expressed in the mesocarp sampled from the upper portion of the untreated fruit, but only increases 10, 5, 36 and 13 fold after 3, 6, 9 and 12 h of ethylene treatment respectively (Figure 2.2B and Figure 2.3). Finally, *EgPG4* is faintly detectable in pedicel tissue before ethylene treatment, and increases at a lower magnitude during the ethylene treatments compared to that observed in the AZ.

An overview of PG gene expression reveals that the three adjacent fruit tissues respond differently to the ethylene treatments (Figure 2.3). In the upper portion of the mesocarp of untreated 180 DAP fruit, the *EgPG4* transcript represents 95% of the total PG transcript detected, while increases to 99% after 6h of ethylene treatment (Figure 2.3). In contrast, in the AZ of fruit prior to ethylene treatment, *EgPG11* is the most abundant (43%) followed by *EgPG10* (15%) and *EgPG8* (10%) and *EgPG18* (10%), whereas *EgPG4*,

represented only 4% of the total PG transcript detected. By contrast, *EgPG4* accounts for 99% of the PG transcript in the AZ after 6 h of ethylene treatment. In the pedicel, *EgPG10* (62%) *and EgPG11* (19%) are the most abundant PG transcripts after 6 h ethylene treatment, while the *EgPG4* transcript accounts for only 7% and 4% total transcript in untreated and ethylene treated fruit respectively.

Our findings indicate that *EgPG4*, the most abundant PG transcript detected, is spatially and temporally differentially regulated in the three adjacent fruit tissues examined. Indeed, *EgPG4* accounts for the majority of the total PG transcript detected in the mesocarp, and more notably undergoes a dramatic increase in abundance preferentially in the AZ, that correlates with the onset of separation observed by 9 h of ethylene treatment (Figure 2.1C). During our ethylene experiments, we observed that 30 and 120 DAP fruit do not separate without treatment with ethylene (control treatments in air in the presence of ethylene absorbing material), while in the presence of ethylene first separate after 12 h and 24 h respectively, and only after 24 h of ethylene treatment are the majority of the fruit shed (Figure 2.1C). By contrast, the 180 DAP fruit treated with air in the presence of ethylene absorbing material (control treatments) will begin to undergo cell separation after 12 h and will completely separate after 24 h (Figure 2.1C). To determine whether *EgPG* transcript accumulation correlates with these observations, we examined the expression of *EgPG4* in 30, 120 and 180 DAP fruit in the presence or absence of ethylene (Figure 2.1 C and Figure 2.4). The results reveal a close correlation to the expression of *EgPG4* with the timing of shedding of 30, 120 and 180 DAP fruit. Indeed, EgPG4 has very low relative expression in untreated 30 and 120 DAP fruit compared to 180 DAP, and after 3 h of ethylene treatment, the increase is 2,400 fold in the 180 DAP fruit compared to only 2.5 fold and 17 fold in the 30 and 120 DAP fruit, respectively. After 6 h, *EgPG4* transcript increases 0.70, 260 and 6,803 fold in 30, 120 and 180 DAP fruit, respectively, while after 9 h of ethylene treatment,

the *EgPG4* transcript is increased 143, 350 and 14,200 in 30, 120 and 180 DAP fruit, respectively.

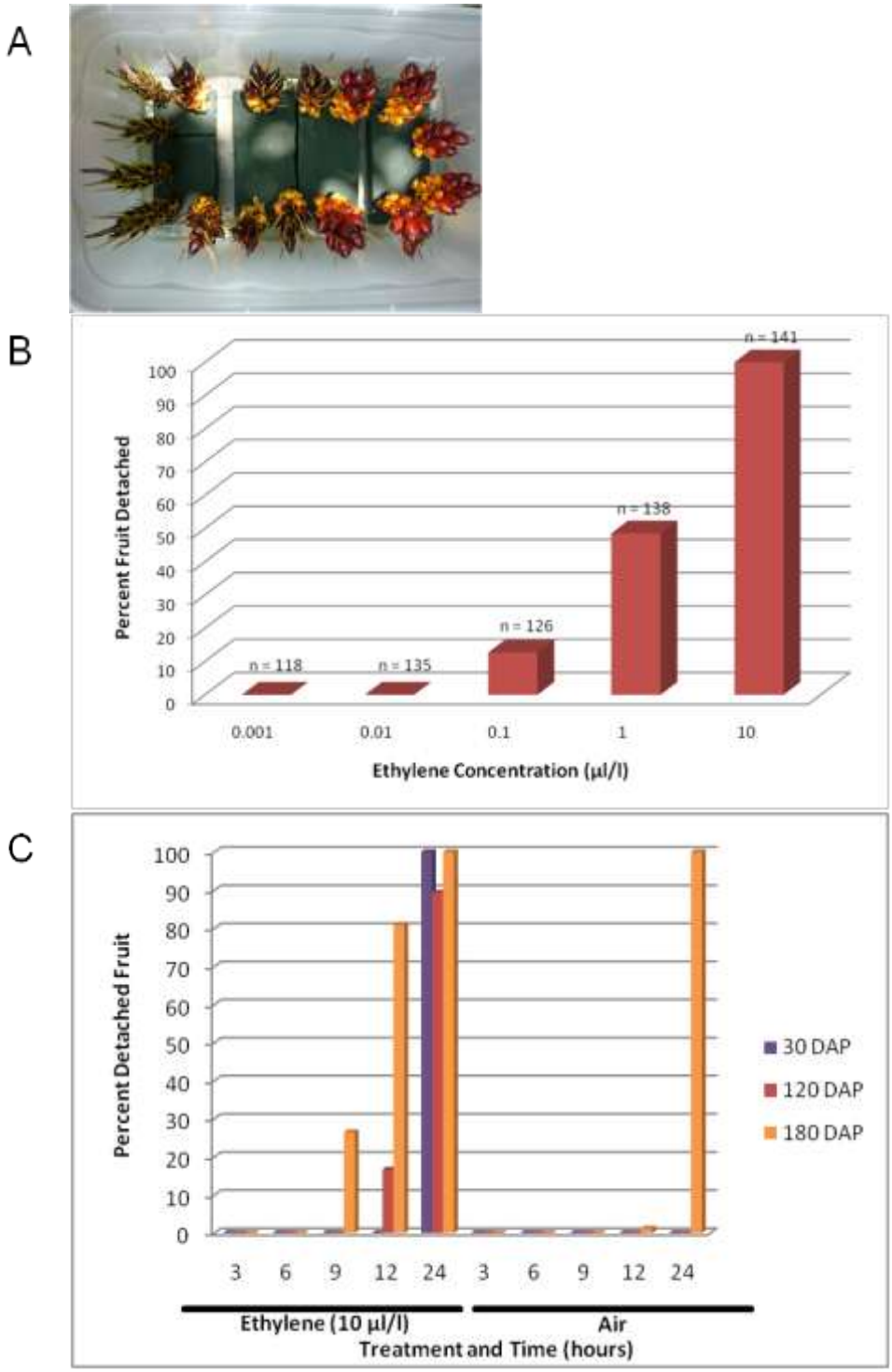

Figure 2.1. (A) Experimental system used for ethylene-induced fruit shedding experiments. (B) Dose response of ripening fruit (150 days after pollination, DAP) treated with a selected concentration range of ethylene for 12 h. C, Ethylene time course treatment of oil palm fruit spikelets at contrasting stages of development (DAP 30, 120, and 180). To test for separation, fruits were subjected to light pressure and separation in the primary zone was recorded. For 30 DAP samples, n = > 200, for 120 DAP samples n = > 90 and for 150 DAP samples n = > 80 per time point/treatment respectively. Experiments were performed twice during 2010 and once during 2011 for three biological repetitions with comparable results.

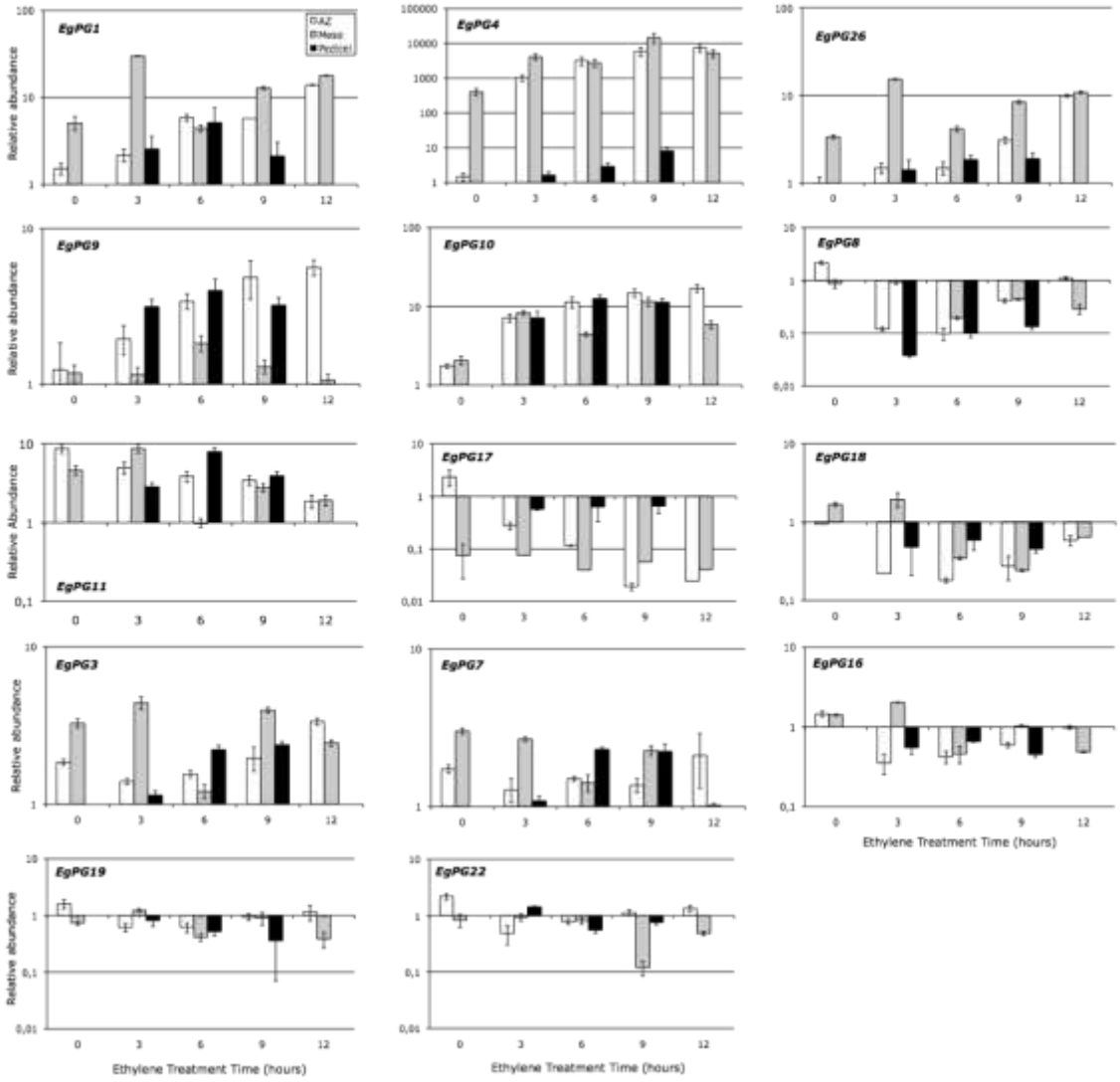

Figure 2.2. qPCR analysis of PG transcript abundance in oil palm fruit tissues and during ethylene treatment time course. (A-E) PG transcripts that increase during ethylene treatment in one or all tissues examined; (F-I) PG transcripts that decrease during ethylene treatment in one or all tissues examined; (J-N) PG transcripts with no significant change and/or with low abundance. Standard deviation (error bars) was calculated from three experiments.

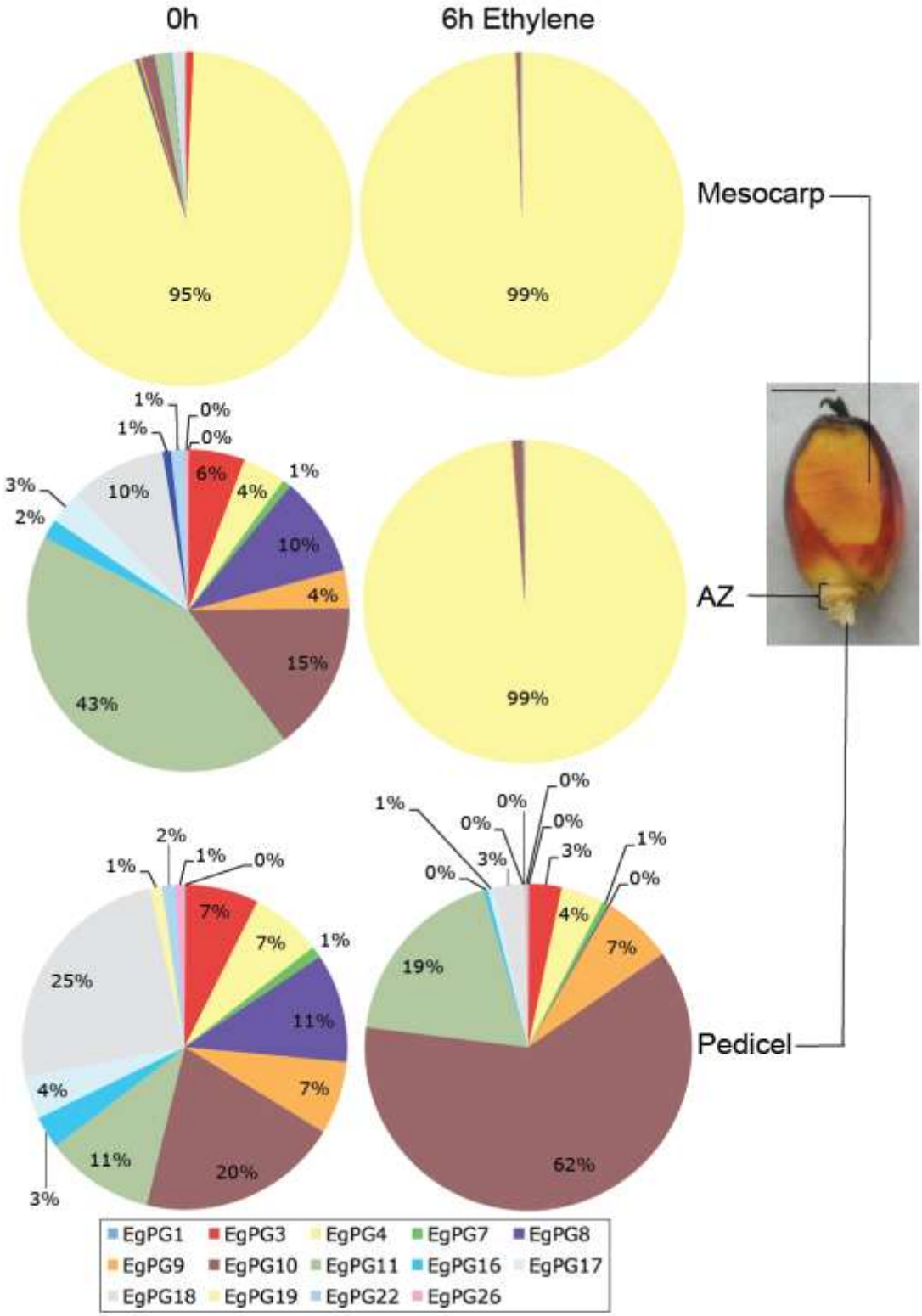

Figure 2.3. The percentage contribution of individual PG family members to total expression in the AZ, mesocarp and pedicel of the oil palm fruit in untreated and six-hour ethylene treated fruit. Data were calculated from the expression values shown in Figure 2.2. Standard error is in Supplementary Table S2.4. Scale bar 1 cm.

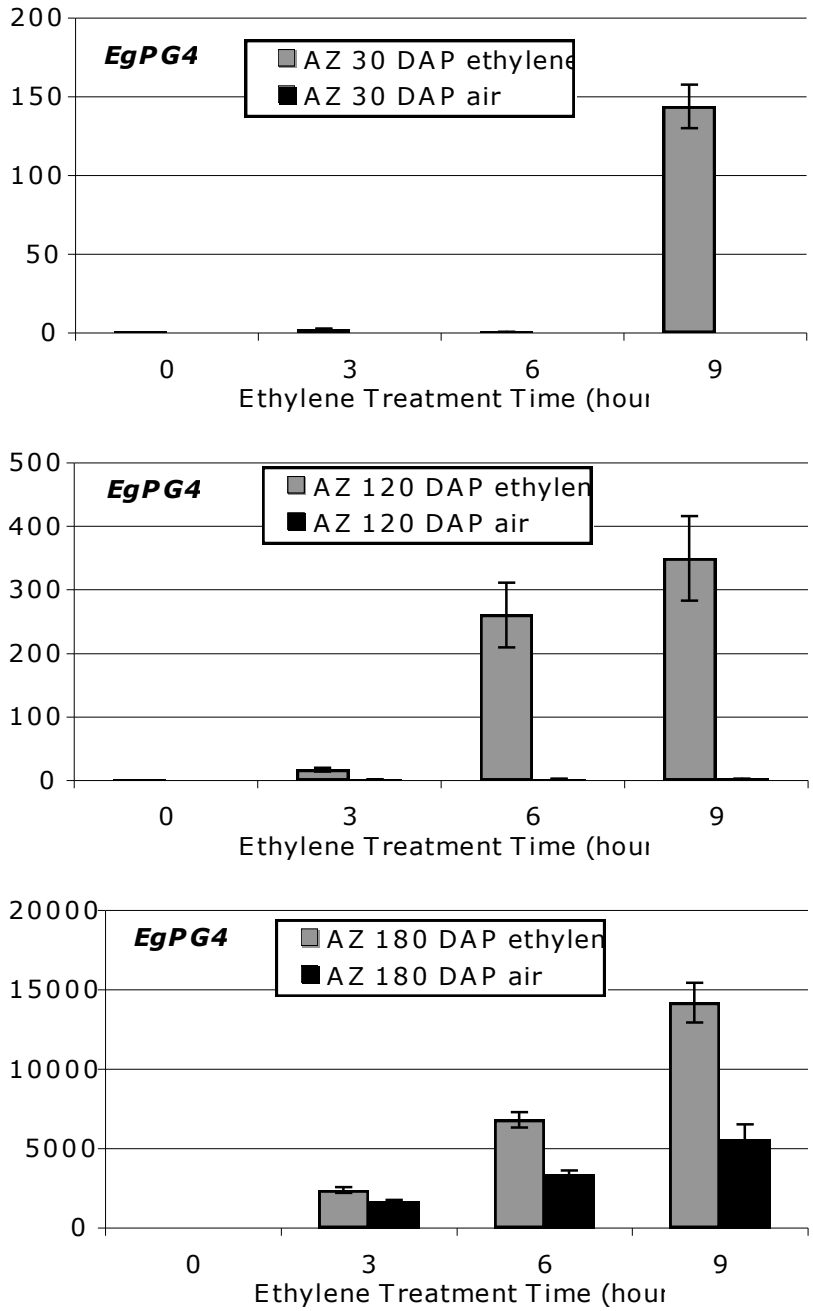

Figure 2.4. qPCR analysis of EgPG4 transcript abundance in the AZ of fruit treated for different time periods with ethylene (10 µl l^{-1}) or air. Standard deviation (error bars) was calculated from three experiments.

***In situ* analysis of the spatial and temporal expression of EgPG4 during ethylene induced fruit shedding**

Whereas the qPCR analysis of *EgPG4* transcript accumulation correlates well with the timing of cell separation events that occur in the base of the oil palm fruit, the AZ samples that were used for the gene analysis include a mixture of all three tissues including the AZ and the margins of the adjacent pedicel and mesocarp tissues (Figure 2.5). To examine whether both the temporal and spatial expression of *EgPG4* correlates with the cell separation events in the AZ that lead to fruit shedding, *in situ* hybridization analysis was performed. Firstly, we used a combination of bright field, polarized light and epifluorescence microscopy to clearly distinguish the localization of the *EgPG4* transcript within the AZ cells, compared to the adjacent mesocarp and pedicel tissues (Figure 2.5A-J). With polarized light, the AZ cell layers are well defined in addition to the lignified vasculature in all the tissues (Figure 2.5E-G). In contrast, epifluorescence microscopy mainly detected the lignified vasculature, predominantly in the pedicel and the mesocarp and only at the lower magnifications (Figure 2.5H-J). In the base of ripe fruit before ethylene treatment, *EgPG4* transcript was neither detected in the AZ, nor the lower margin of the mesocarp or upper margin of the pedicel tissues (Figure 2.5A, E, H). By 6 h after ethylene treatment, the *EgPG4* transcript increased in abundance preferentially in the AZ cell layers, including the parenchyma cells and the undifferentiated xylem cells of the vascular bundles (Figure 2.5B, F, I). By contrast, no *EgPG4* transcript was detected or was only present in relatively lower amounts in the adjacent pedicel and mesocarp tissues, or in the central cells of the vascular strands within the AZ. At higher magnification of the boundary region between the pedicel and the AZ, the *EgPG4* transcript clearly accumulates in the AZ cells while remains at very low or undetectable amounts in the adjacent pedicel cells (Figure 2.5C, G, J, G). In contrast, the control hybridizations with ribosomal RNA (rRNA) revealed an even distribution of

rRNA throughout the pedicel, AZ and mesocarp tissues (Figure 2.5D). As a comparison, *in situ* hybridization experiments were also performed with *EgPG10* and *EgPG8*, the former of which is shown by qPCR analysis to increase similarly in all three tissues, while the later decreases during the ethylene treatments (Figure 2.2E and F). For *EgPG10*, the results showed an even distribution of transcript present in the three tissues after ethylene treatment, while *EgPG8* was not detected (data not shown). Together, these results corroborate the correlation between the spatial and temporal expression profile of the *EgPG4* transcript in relation to ethylene and cell separation observed by qPCR, and provides further evidence for an important function for this transcript during fruit abscission.

Phylogenetic analysis of EgPG4 with relation to polygalacturonases with known functions

To examine the relationship of EgPG4 and plant PGs, a phylogenetic comparison of its amino acid sequence with those from *Arabidopsis* and rice was performed. Firstly, EgPG4 groups within the PG clade A3 formed with members from both rice and *Arabidopsis* previously defined (Kim and Patterson 2006) (see supplementary data Figure S2.1). Notably, *EgPG4* does not group with the PGs from *Arabidopsis* in clade A15 shown to function during floral organ abscission, silique or anther dehiscence including At2g41850 (PGAZAT/ADPG2), At3g07970 (QUARTET2), and At3g57510 (PGDZAT/ADPG1) (Kim and Patterson 2006; Gonzalez-Carranza *et al.* 2007; Ogawa *et al.* 2009). However, EgPG4 is grouped in the A3 clade with two other *Arabidopsis* PGs (At2g43880 and At2g43890) that are expressed during floral organ abscission (Kim and Patterson 2006).

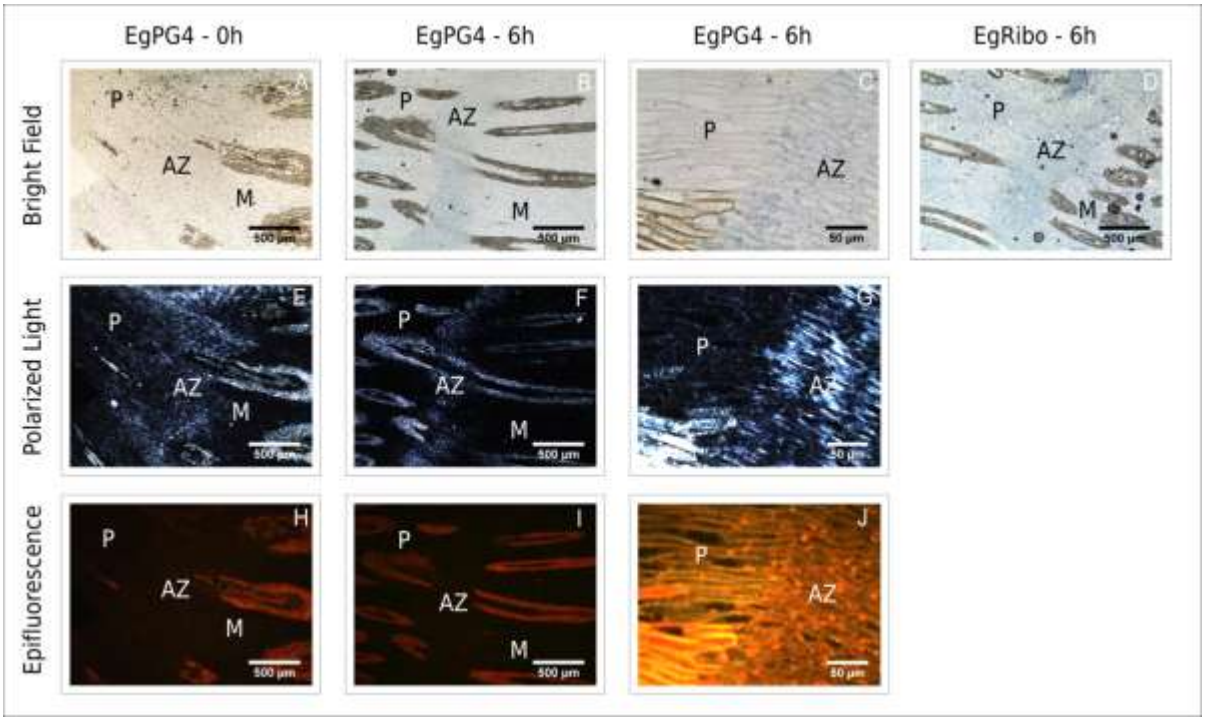

Figure 2.5. *In situ* localization of *EgPG4* transcripts in the fruit base containing the AZ. (A-C) Longitudinal sections of the fruit base were hybridized with digoxigenin-labelled antisense RNA fragments of *EgPG3* and (D) the 18S ribosome and expression is observed as a blue coloring using bright field microscopy. Sections were made from fruit prior to ethylene treatment (A, E, H) and after 6 h of ethylene treatments (B-D, F, G, I, J). (E-G) Sections were also observed using polarized light and (H-J) epiflourescence microscopy to distinguish the AZ from the adjacent pedicel (P) and mesocarp (M) tissues.

To examine possible structure function relationships of the *EgPG4* amino acid sequence with those of known PGs from a variety of species, including those from fleshy fruit (apple, plum, peach, tomato, kiwi, grape, papaya), and dry fruit (soybean, *B. napus*, *Arabidopsis*), a phylogenetic analysis was performed with selected plant PGs with expression associated with or shown to function during germination, root or pollen development, fruit ripening, organ abscission, and anther and pod dehiscence (Dellapenna *et al.* 1986; Sheehy *et al.* 1988; Smith *et al.* 1988; Atkinson 1994; Lester *et al.* 1994; Tebbutt *et al.* 1994; Kalaitzis *et al.* 1995; Jenkins *et al.* 1996; Petersen *et al.* 1996; Kalaitzis *et al.* 1997; Hadfield *et al.* 1998; Hong and Tucker 1998; Sitrit and Bennett 1998; Jenkins *et al.* 1999; Sitrit *et al.* 1999; Wang *et al.* 2000; Degan *et al.* 2001; Sander *et al.* 2001; Gonzalez-Carranza *et al.* 2002; Hayama *et al.* 2006; Kim *et al.* 2006; Murayama *et al.* 2006; Sekine *et al.* 2006; Gonzalez-Carranza *et al.* 2007; Tucker *et al.* 2007; Deytieux-Belleau *et al.* 2008; Fabi *et al.* 2009; Huang *et al.* 2009a; Huang *et al.* 2009b; Ogawa *et al.* 2009; Tacken *et al.* 2010). Firstly, the reconstructed tree and bootstrap values confirm earlier analyses that PGs can be separated into three major subclades, two that consist of PGs involved in fruit ripening and abscission and one with PGs involved in pollen development (Hadfield and Bennett 1998; Hadfield *et al.* 1998) (Figure 2.6). The presence of a fourth clade containing soybean (GmPG6_DQ382356) and grape (VvPG2_EU078975) PGs supports more recent studies that indicate this gene family consists of more than three subclades (Torki *et al.* 2000; Deytieux-Belleau *et al.* 2008). In addition, the bootstrap analysis confirms a close phylogenetic relationship between EgPG4 and two *Arabidopsis* PGs expressed during floral organ abscission (Kim and Patterson 2006). Notably, in the same subclade there are also four abscission related tomato PGs (TAPG1, TAPG2, TAPG4 and TAPG5) in addition to two PGs associated with ripening and abscission of melon (CmPG1 and CmPG2), and PGs expressed during ripening of papaya (CpPG), pear (PcPG3) and peach (PpPRF5). An additional

Arabidopsis PG (At2g43860) that functions in cell separation between endosperm cells when the radicle emerges during germination was also found within this subclade. The analysis also revealed that the *Arabidopsis* PGs involved in abscission or dehiscence including PGDZAT, PGAZAT, and QTR2, are grouped within a distinct subclade with other PGs that function during fruit ripening, floral organ abscission and pod dehiscence. Notably, no PG involved in abscission of a fleshy fruit is found in this clade, only those from species with dry fruit such as *Arabidopsis*, *B. napus* and soybean.

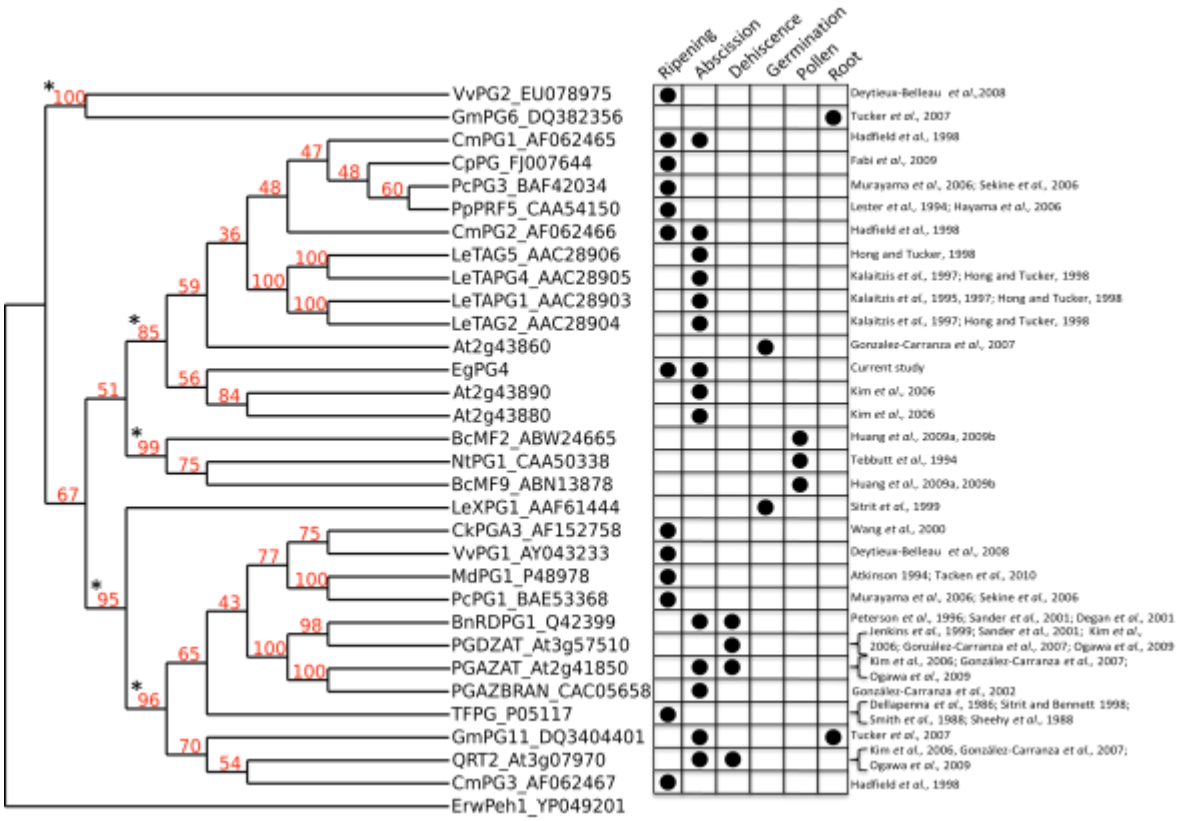

Figure 2.6. Phylogenetic analysis of EgPG4 and selected plant PGs from clade A with known functions using the neighbor-joining method based on multiple alignment of the sequences containing the GH28 domain. The endo-PG ErPeh1 from *Erwinia carotovora* was used as a root. Numbers on the branches are bootstrap values for 100 replicates. The black asterisks at bootstrap values indicate branch points of the four PG subclades.

Discussion

The sequence and expression analysis of *EgPG4* suggest functional conservation and divergence between monocots and eudicots

PGs are thought to play a central role in the disassembly of pectin in the middle lamella or primary cell wall during cell separation and cell elongation (Hadfield and Bennett 1998). In particular, PGs have been extensively studied during fruit ripening, organ abscission and pollen development, yet how divergence has occurred between species and to fulfil different roles in these various tissues is still not completely understood. In particular, very little data is available from monocot species to compare the ripening and abscission processes with those of eudicots.

The phylogenetic and bootstrap analysis confirmed several previous phylogenetic analysis that showed PGs involved in organ abscission and fruit ripening are found mainly in two distinct subclades, with a third subclade containing only pollen related PGs (Hadfield and Bennett 1998; Hadfield *et al.* 1998; Kim and Patterson 2006; Gonzalez-Carranza *et al.* 2007). A fourth minor subclade that contained a PG from ripening grape skin was also observed as previously (Deytieux-Belleau *et al.* 2008). While the current phylogenetic analysis was done with the complete GH28 domain, not including the prosequences characteristic of some PGs, the results support a previous conclusion that the presence or lack of prosequences are not the basis for the divergence of these sequences into distinct clades (Hadfield and Bennett 1998). The first notable observation is that all the tomato abscission PGs known group closely within a subclade that also contains the two closely related *Arabidopsis* floral organ abscission associated PGs (At2g43890 and At2g43880), in addition to an *Arabidopsis* PG (At2g43860) implicated in radicle emergence (Kim and Patterson 2006; Gonzalez-Carranza *et al.* 2007). The presence of At2g43860 that functions during separation of endosperm cells when the radicle emerges during germination, suggests structural relationships between PGs

with functions beyond fruit ripening and organ abscission. Notably, EgPG4 groups closest with these *Arabidopsis* abscission PGs, which suggests functional conservation, and that these sequences are derived from a common ancestral PG prior to the separation of monocots and eudicots. A second notable observation is that the tomato fruit PG (TFPG) is more closely associated with the abscission and dehiscence PGs than the tomato PGs involved in organ abscission. This contrasts with sequences from melon that are in the same subclade with the tomato abscission PGs, and have expression profiles associated with both fruit ripening and abscission (Hadfield *et al.* 1998). Similarly, the *EgPG4* transcript does not only increase in the AZ in relation to abscission, but also is highly expressed in the portion of the ripening mesocarp. Together, it appears that some PGs may function both in ripening fruit tissues, in addition to during cell separation in the AZ that leads to fruit organ abscission in monocots and eudicots. Our data also indicate that the regulation of *EgPG4* is closely associated with the capacity for cells to respond to ethylene, related to the developmental stage of ripening, and may be an important mechanism to control the spatial and temporal functionality of *EgPG4* during mesocarp ripening and cell separation in the AZ. Indeed, the mesocarp produces an increasing amount of ethylene as development progresses, was found to progress from the apex to the fruit base, and was proposed that an increase just above the AZ provides the signal for the initiation of the separation events (Henderson and Osborne 1994; Tranbarger *et al.* 2011).

The sequence and expression of *EgPG4* suggest functional divergence between dry and fleshy fruit

Another notable observation is that PGs related to fleshy fruit abscission are not found within the clade containing the well-characterized abscission and/or dehiscent related PGs including QRT2, PGAZAT, PGDZAT, BnRDPG1 and PGAZBRAN (Gonzalez-Carranza *et*

al. 2002; Ogawa *et al.* 2009). By contrast, PGs involved in fleshy fruit ripening, such as the tomato (TFPG), grape (VvPG1), apple (MdPG1), kiwi (CkPGA3) and pear (PcPG1) are also found within this clade (Dellapenna *et al.* 1986; Sheehy *et al.* 1988; Smith *et al.* 1988; Atkinson 1994; Sitrit and Bennett 1998; Wang *et al.* 2000; Murayama *et al.* 2006; Sekine *et al.* 2006; Deytieux-Belleau *et al.* 2008; Tacken *et al.* 2010). In addition, only the melon PG (CmPG3) that has a profile related to ripening is found in the same subclade as the dry fruit dehiscence and abscission PGs, while the other two melon PGs (CmPG1 and CmPG2) associated with organ abscission and ripening are in the same subclade as EgPG4 (Hadfield *et al.* 1998). While there is no current data that suggests that the fleshy fruit PGs within this subclade are involved in fruit or other organ abscission processes, it is possible their involvement in cell separation during organ abscission has not but sufficiently investigated. Indeed, the analysis and results discussed here are based on the two best-characterized organ abscission model systems available, including tomato and *Arabidopsis*, and indicate a limitation of our current status to evaluate the functional diversity of plant PGs. Nevertheless, the results suggest that dry fruit species appear to have PGs from at least two distinct subclades involved in cell separation for dehiscence, while fleshy fruit may have PGs specialized in ripening or abscission, or, that may function in both contexts. Overall, the results suggest that divergence may have occurred between PGs involved in dry fruit dehiscence and fleshy fruit abscission, which merits further investigations.

The high expression and induction of *EgPG4* by ethylene suggests functions during both fruit ripening and abscission

Studies on fruit ripening and floral pedicel abscission of tomato provide examples of how individual members of this gene family may have distinct functions in adjacent tissues undergoing cell separation processes in a fleshy fruit species, and highlight the central

importance of tissue specific transcriptional regulation of PGs during these developmental processes. Indeed, the tomato fruit *TFPG* is the only PG gene expressed in the ripening fruit tissues, its transcription is positively regulated by ethylene, and the encoded protein is responsible for the PG activity required for pectin depolymerization that occurs during ripening (Dellapenna *et al.* 1986; Sheehy *et al.* 1988; Smith *et al.* 1988; Dellapenna *et al.* 1989; Sitrit and Bennett 1998). Notably, the *TFPG* mRNA accounts for up to 2.3% of the total RNA in ripening tomato fruit, and down regulation of *TFPG* has no effect on the timing or rate of leaf abscission, indicating a specific function of this enzyme during fruit ripening but not organ abscission (Dellapenna *et al.* 1987; Taylor *et al.* 1990). In contrast, in the pedicel where the AZ is located at the base of the tomato floral organs, there are at least four abscission-related PG genes (*TAPG1*, *TAPG2*, *TAPG4* and *TAPG5*) expressed, three of which are induced by ethylene and correlate well with the cell separation that occurs in the flower and leaf AZs (Kalaitzis *et al.* 1995; Kalaitzis *et al.* 1997; Hong and Tucker 1998). Furthermore, silencing of the tomato abscission-related PGs using a *TAPG1* fragment, delayed abscission and increased break strength of the leaf petiole AZs in explants treated with ethylene. These studies suggest a combination of tissue specific transcriptional regulation and/or localized cellular differences in response to ethylene are important factors that determine the spatial and temporal precision for their functional roles during fruit ripening and organ abscission.

Oil palm fruit shedding has some similarities but also notable differences from that seen with tomato. Firstly, the timing of separation induced by ethylene in oil palm is comparable to that in tomato. In the presence of ethylene, cell separation begins to occur by 9 h, while 80-100% of ripe fruit are shed by 12 h, whereas in tomato, flower shedding begins at 6 h and is complete by 12 h (Roberts *et al.* 1984). This result is striking given the surface area of the primary AZ of ripe oil palm, up to 10 mm (Figure 2.3) is approximately 20 times larger

than the tomato pedicel AZ, up to 0.55 mm (Roberts *et al.* 1984). Secondly, we observe a greater diversity of *PGs* expressed in the oil palm fruit tissues than that of tomato during ripening or abscission. Notably, at least 14 transcripts that encode distinct PGs with either partial or complete GH28 domains are expressed in the base of the fruit containing the AZ, five of which appear to be regulated positively, while four others negatively in response to ethylene. In addition, five PGs revealed no significant change in abundance during the ethylene treatments. A previous study with banana fruit reported at least four PG genes are expressed during ripening (Asif and Nath 2005). However, none of the PGs identified in that study contained the full-length GH28 domain and thus we were not able to compare their phylogenetic relationship with the oil palm PGs and other PGs presented in Figure 2.6. The expression of the banana PG genes was also analyzed during finger drop, a process that also involves pectin breakdown disassembly (Asif and Nath 2005; Mbéguié-A-Mbéguié *et al.* 2009). The results indicated that the four banana PGs were also expressed in the finger drop zone where cell separation takes place, while *MaPG4* was the most highly expressed with a profile of accumulation correlated to the decrease in the pedicel rupture force observed. Together with the present results, the mechanisms of pectin disassembly during banana and oil palm fruit ripening may involve a larger number of PGs than with dicotyledonous species examined thus far. The current study allows a more complete view of PG expression in relation to ethylene in a monocot fruit, given that the earlier studies with banana included fewer and shorter PG sequences (Asif and Nath 2005; Mbéguié-A-Mbéguié *et al.* 2009). In addition, whereas both are monocots, the banana is a parthenocarpic berry-type fruit that accumulates large amounts of starch, while the oil palm is a drupe with the high oil content, which may also implicate different ripening regulatory mechanisms between these two species. Future work awaits molecular resources for more complete comparative studies on

ripening and abscission of these two diverse monocots, in addition to the well-characterized dicot tomato model.

In comparison to tomato, the diversity and complexity of PG expression in the oil palm fruit tissues are far greater than that observed in the AZs or during ripening. In the oil palm, all 14 *EgPG* transcripts are detected to some extent in the ripening mesocarp tissue in contrast to the single *TFPG* expressed during tomato fruit ripening. Notable, none of the *EgPGs* identified appear to be completely tissue specific as observed with the tomato PGs involved in abscission and ripening. However, the data presented here suggests that differences in their tissue and developmental stage dependent response to the ethylene may be important for spatial and temporal control. The most notable example is that of *EgPG4*, which is not only the most abundant PG transcript in the mesocarp of untreated ripe fruit, but also undergoes the most dramatic increase in abundance in the base of the fruit containing the AZ in response to ethylene. The high abundance of *EgPG4* in the mesocarp and the massive increase in response to ethylene is similar to PG expression in tomato, however, *EgPG4* is highly expressed in both the ripening mesocarp and the AZ after ethylene treatment. Furthermore, our *in situ* hybridization experiments indicate the increase in *EgPG4* transcript abundance in the base of the fruit occurs preferentially in the AZ compared with the adjacent mesocarp and pedicel tissues. Importantly, a delayed and less significant increase in *EgPG4* transcript is also observed in the AZ of untreated fruit, as well as in 30 and 120 DAP fruit treated with ethylene, which corresponds to the delay in shedding observed at these stages of ripening. Together, these results provide evidence that *EgPG4* integrates cell wall pectin modifications during both mesocarp ripening and in the AZ cells during fruit shedding, in close relation to a developmentally regulated cell sensitivity or competence to respond to ethylene. Future work has the objective to identify the regulatory factors that control the ripening and abscission related expression of *EgPG4*, to provide a basis to compare these

processes not only between monocots and eudicots, but in particular between fleshy and dry fruit species. Finally, the identification of genes involved in oil palm fruit shedding will be helpful for oil palm improvement selection strategies.

Materials and Methods

Plant material, ethylene treatment and RNA extraction

Oil palm (*Elaeis guineensis* Jacq) fruits were harvested at Krabi Golden Tenera plantation, from a *tenera* clone (clone C) produced in Thailand. For each stage of development studied, independent bunches were collected on distinct individuals of the same genotype. Spikelets were then collected in the centre of each bunch and sets of 6 spikelets were randomly sampled from them and put in individual hermetically sealed 50 l volume boxes. Spikelets with fruits at 150 days after pollination (DAP) were treated with different concentrations of ethylene (0, 0.001, 0.01, 0.1, 1, 10 µl l^{-1}). In absence of ethylene treatment, ethylene absorber (ETHYL-GONE, http://www.biosafer.com/ethyl-gone.php) was added in the box. All the boxes were kept at ambient temperature (approximately 30 °C), and after 24 h of treatment the number of fruit separating from the spikelets were counted. Using the concentration of ethylene (10 µl l^{-1}) that induced and synchronized the highest amount shed fruit, a time course analysis was then conducted that used the same process with fruit from 30, 120 and 180 DAP. Spikelets were treated with or without ethylene, and every 3 h, for each stage of development, treated or untreated spikelets were collected and shedding was quantified. For each time point, the mesocarp, pedicel and the base of the fruit containing the primary and adjacent AZs were isolated and frozen immediately in liquid nitrogen. Samples from two independent experimentations were collected immediately after bunches were harvested.

Total RNA from mesocarp, pedicel and the base of the fruit enriched in AZs, treated or not with ethylene was extracted as previously described (Morcillo *et al.* 2006). Total RNA (1µg) was used to synthesis cDNA using the first-strand cDNA synthesis kit (ImProm-II™ Reverse Transcription System, Promega).

Identification of oil palm non-redundant polygalacturonase nucleotide sequences from fruit

To identify oil palm PG cDNA sequences a number of molecular resources were used. First, the tblastn program was used to search available databases that contain *Elaeis guineensis* sequences, including NCBI (http://www.ncbi.nlm.nih.gov), local 454 pyrosequencing derived oil palm mesocarp contigs (Tranbarger *et al.* 2011) and contigs derived from tissues enriched in the AZ (Jantasuriyarat *et al.*, unpublished), for sequences with high similarity to PGs from *Arabidopsis* and rice previously described (Kim and Patterson 2006). Additional sequences were also kindly contributed by Dr. Arondel (Bourgis *et al.* 2011). A complementary approach utilized degenerate primers (Gonzalez-Carranza *et al.* 2002) to amplify cDNA from AZ tissues treated with or without ethylene at different development stages and from oil palm genomic DNA. Primers from the oil palm PEST643 (accession number N° AY291341) were designed in the most conserved regions of PGs and also used to amplify PGs from fruit tissues. For sequences lacking the 3' regions, RACE (Clontech) amplification was performed and from sequences obtained, sequence specific primer pairs were designed and used to amplify non-redundant PGs from the oil palm fruit tissues. A total of 35 putative non-redundant PG sequences were identified from these complementary approaches and were compared to confirm similarity to plant PGs, in particular the presence of a partial or complete glycoside hydrolase 28 (GH28) domain that covers approximately 75% of each PG coding sequence (Kim *et al.* 2006).

Quantitative Real-Time RT-PCR

qPCR was conducted on a LightCycler 480 (Roche) in 96 well plates in a volume of 10 µl containing 2 µl of cDNA diluted 1/100, 1.5 µl of primer forward (2 µM), 1.5 µl of reverse primer (2 µM) and 5 µl SYBR® Green Mastermix (Roche). Supplemental Table S2.1

lists the primers used. PCR was initiated by denaturation at 95 °C for 10 min, followed by 45 cycles of 95°C for 15 s, 60°C for 15 s, and a final extension at 70 °C for 1 min. All expression was normalized to the *EgEfα1* (accession number: AY550990) mRNA from *Elaeis guineensis*, and relative mRNA abundance was determined with the formula as described previously (Pfaffl 2001). No change of *EgEfα1* transcript accumulation was found in the fruit tissues treated or not treated with ethylene. Control using RNA matrices were also conducted to validate the absence of DNA in each sample. Each time point was replicated three times from 2 independent biological samples, and all amplified cDNA fragments were sequenced by Beckman-Cogenics to check the specificity of the amplification products. Gene abundance is expressed as mean and standard error bars are calculated from the technical replicates of one of the biological repetitions.

Phylogenetic Analysis

Phylogenetic trees were constructed based on similarity searches performed with BLASTp programs with default parameters in protein sequence databases provided by the NCBI server (http://www.ncbi.nlm.nih.gov). Phylogenetic analyses were performed on the Phylogeny.fr platform (http://www.phylogeny.fr) (Dereeper *et al.* 2008). Amino acid sequences from the GH28 domain were aligned with ClustalW (v2.0.3) (Thompson *et al.* 1994). After alignment, ambiguous regions (i.e. containing gaps and/or poorly aligned) were removed with Gblocks (v0.91b). The phylogenetic tree was constructed using the neighbor joining method implemented in Neighbor from the PHYLIP package (v3.66) (Saitou and Nei 1987). Distances were calculated using ProtDist. The Jones-Taylor-Thornton substitution model was selected for the analysis (Jones *et al.* 1992). The robustness of the nodes was assessed by bootstrap proportion analysis computed from 100 replicates (Felsenstein 1985).

Graphical representation and edition of the phylogenetic tree were performed with TreeDyn (v198.3) and Inkskape, respectively.

RNA *in situ* hybridization

To obtain DNA templates for the RNA probe synthesis, PCR amplifications were performed with gene-specific antisense primers tailed with a T7 RNA polymerase binding site. PCRs were performed with the EgPG4qS1–EgPG4qAS1T7 and EgPGq4S1T7–EgPG4qAS1, and the EgRiboS-EgRiboAST7 and EgRiboST7–EgRiboAS primer pairs for EgPG4, and EgRibo-specific probes, respectively (Supplementary Table S2.2). The resulting DNA fragments were used directly as templates to synthesize antisense probes, with the incorporation of UTP–digoxigenin (Roche) as the label with using the MAXIscript® T7 Kit (Ambion). Each amplification product was sequenced to check the specificity of the amplification products. *In situ* hybridization experiments were carried out as described previously (Jabnoune *et al.* 2009) with some modifications. The fruit bases were fixed overnight in the dark at 4°C in fixation buffer (4% paraformaldehyde, 0.1 M phosphate buffer pH 7). After 16h, they were washed two times in 0.1 M phosphate buffer with 2% glycine, then two times in 0.1 M phosphate buffer before dehydration through a increasing series of ethanol and butanol concentrations. After 15 days in butanol to soften the tissues, the samples were embedded in Paraplast plus (Paraplast X-Tra, Oxford Labware) and sectioned to 12 µm with a microtome. Tissue sections were deparaffinised with Safesol (LaboNord, France), rehydrated through an ethanol series of decreasing concentrations, and then pre-treated with proteinase K (100 U μl^{-1}, Roche) in TRIS-HCl (100 mM, pH 7.5), EDTA (50 mM) at 37 °C for 35 min. Digestion was stopped by washing twice for 5 min each with TRIS-HCL (20 mM, pH 7.5, $CaCl_2$ (2mM) and $MgCl_2$ (50 mM), then phosphate-buffered saline (0.1 M PBS) with 0.2% glycine for 2 min, and then twice with 0.1 M PBS. After ethanol baths, hybridization

was performed at 45 °C overnight with 200 ng of the digoxigenin-labelled RNA probe in 100 µl of hybridization solution (50 µl formamide, 10 µl 20X SSC, 1 µl Denhardt 100X, 20 µl dextran sulphate 50%, 1 µl tRNA at 100 mg/ml). After hybridization, slides were washed in 2X SSC at 25 °C for 5 min, in 2X SSC at 50 °C for 45 min and in 1X NTE (TRIS-HCl 10 mM, NaCl 0.5 M, EDTA 1 mM, pH 7.5) at 25 °C then 37 °C for 5 min each. An RNase A digestion (20 µg/ml) was carried out for 30 min at 37 °C and stopped by washing with 1X NTE at 37 °C. Final washes were conducted twice in 1X SSC for 30 min each at 55 °C. Detection was performed using the Vector Blue Alkaline Phosphatase Substrate Kit III (Vector Laboratories). Control without probe was conducted to valid the absence of endogenous alkaline phosphate activity. Samples were incubated in blocking reagent [Roche; 10% (w/v) in PBS] for 1 h and afterwards for 45 min at 37 °C containing antidigoxigenin alkaline phosphatase-conjugated Fab fragment antibody (Roche) diluted at 1:500 in blocking reagent. After three washes for 10 min in 0.1 M PBS, tissues were equilibrated in detection buffer (100 mM TRIS-HCl pH 8.2) then several batches of 3 h at 37 °C with Blue vector. Finally the detection was amplified by ethanol vapour for 20 min and samples were mounted on slides with Mowiol and observed with a bright-field microscope (Leica DM6000) using the 40X/0.75 numeric aperture. To visualize the AZ, tissue sections were also observed under polarized light and epifluorescence with a TXR filter. Photographs were taken with a Retiga 2000R camera (Qimaging). *In situ* hybridization and microscopy analysis were conducted at the "Plate-Forme d'Histocytologie et Imagerie Cellulaire Végétale" (PHIV platform; http://phiv.cirad.fr/).

Appendix

Name of genes	Name and sequence of primers	
EgPG1	EGPG1qS1	ACAAACAGAGCTAAAGACCC
	EGPG1qAS1	GGTGCACAAATATACTGAAACTAC
EgPG3	EGPG3qS1	GTTACCCAGCTAATCATTTGAAAC
	EGPG3qAS1	CAAACATTTCGGACAAATGAAGA
EgPG4	EGPG4qS1	ACCTACGGAAACAAGCC
	EGPG4qAS1	AATCCTACATCACCCATTTCA
EgPG7	EGPG7qS1	CTCATCCAAGCTCCAATATTAGT
	EGPG7qAS1	TTTATTCTGATACCATGCTTTGAGTTA
EgPG8	EGPG8qS1	AGCTACATTTCTTCATTCAAACTGTAA
	EGPG8qAS1	CTCCTATCCCATTCCCAGATAA
EgPG9	EGPG9qS1	AATACTGATGGCATTGATCCAGA
	EGPG9qAS1	GAGACCCTGCGAACAAC
EgPG10	EGPG10qS1	CACAAGATACTATGATCCTTCGT
	EGPG10qAS1	TTTCTAAGAAGTCCACCACCG
EgPG11	EGPG11qS1	AATCTCCGAGGTTGCATTC
	EGPG11qAS1	AACCTTCAAGGCTTTAACATTT
EgPG16	EGPG16qS1	CATGTCAGAATCTCGACCTTT
	EGPG16qAS1	ACTGCCACGGAATAACC
EgPG17	EGPG17qS2	TGTGGATGTTGTGAAGTCGAA
	EGPG17qAS2	ATGGGTAAAGAACCTGTTGG
EgPG18	EGPG18qS2	GTTGTCACATCAAACACTCTGGTA
	EGPG18qAS2	CCTCTGCTCCGTTCAAT
EgPG19	EGPG19S1	TGAGCTATTGAAGCAGACAC
	EGPG19AS1	ATTTATGAAGCATGGACAAATACG
EgPG22	EGPG22qS1	CATTGTGAATGCTAGCTCAATTAT
	EGPG22qAS1	CATTGGTAGTGCCTGTAAGT
EgPG26	EGPG26qS2	AAAGGATGTCTCATACATGAACATAAA
	EGPG26qAS2	GGGTCATCCACCAACTC
EgEF1	EGEF1S4	TATCAAAGGATGGGCAGACC
	EGEF1AS4	TCATCATACCTTGCCTTGGA

Table S2.1. List of primers for the expression analysis of oil palm PG genes by qPCR.

Name of genes	Name and sequence of primers	
EgPG4	EGPG4qS1	ACCTACGGAAACAAGCC
	EGPG4qS1T7	GAAATTAATACGACTCACTATAGGGAGAACCTACGGAAACAAGCC
	EGPG4qAS1	AATCCTACATCACCCATTTCA
	EGPG4qAS1T7	GAAATTAATACGACTCACTATAGGGAGAAATCCTACATCACCCATTTCA
EgRIB	EGRiboS	GCCGACCCTGATCTTCTG
	EGRiboST7	GAAATTAATACGACTCACTATAGGGAGAGCCGACCCTGATCTTCTG
	EGRiboAS	TCTTTCGCCCCTATACCCAA
	EGRiboAST7	GAAATTAATACGACTCACTATAGGGAGATCTTTCGCCCCTATACCCAA

Table S2.2. List of primers used for the synthesis of *in situ* hybridization probes.

Table S2.3. List of the 28 sequences contained either a partial or complete GH28 PG signature domain.

Name of genes	sequence
EgPG1	>Contig_223666S6AS7 AGGCATCAGCATTGGGAGCCTCGGCGTGCACAACTCGCAGGCTTGCGTTTCGAACATTAGGGTCA AGAATGCAGTGATCAGGAACTCTGACAATGGGGTCAGGATCAAGACATGGCAGGGTGGGATGGGC TCAGTAACAAGCATTAGCTTCGAGAACATCATCATGGAGAATGTTAAAAACTGCATCATTATAGA CCAGTACTATTGCCTAAGCAAGCAGTGTATGAATCAAACGTCGGCGGTCTACGTAAAGGATGTCT CATACATGAACATAAAGGGGACGTATGATGTCAGGAGCCCACCGATACACTTTGCTTGCAGTGAT GCCGTGCCATGCACCAACATCACCATGTCTGATGTGGAGCTGCTCCCATTTGATGGAGAGTTGGT GGATGACCCCTTTTGTTGGAATGCCTATGGGAGCATGGAGACACTAACAATTCCACCCATCTCTT GCTTGCAGGATGGGGAGCCTCAGTCCATCAAAGAGAACCTTAGATTAGGTTGCTGAACTTGTTAG TGCTTCAGGTACCGCAATTTAGAGACACAATAACACAAACAGAGCTAAAGACCCATATGGTCAAA CCTTTATTTTTTCCAATATGTGGCTGTTGTGGGGATTTAGTCATGCTTGGGGGGCCCTCATGGAG CTTGTTTTCATGTATTGATCGGAACATATTATGCATGGGCTTATTTCAAAGTGTCAAAAGTTCAG GTAGTTTGAGTATATTTGTGCACCTGTGGAAGGAACAATGTTTGGCTCTGTTTAACTTCTGTAGC TGGTTCACTAGAAGAAACGGATAGTGACGAGAATTTTTCTGTAAAAAAAAAAAAAAAAAAAAAA
EgPG3	>CL1Contig7023 TTGTTACATCAGCACTGGTGGATGATCTAAATTGCAGTCAAAAGCGGACTGGGAGTGAATATGGC ATTCCTTTGCTCATCCAAGCTCCAATATTAGTATCCGCCGCATCACTGGAGAAACAAAATTAGGT GCTGGCATTGCGTTTGGAAGTGAGATGTCTGGTGGTGTATCAGAAGTTTGGGCAGAGGACATCCA CCTCTTTAACTCAAAGCATGGTATCAGAATAAAACATCTCCAGGGCGAGGTGGCTATATTCGAAA TATCTACATCTCTGATGTGATCATGAAGAATGTGGACATAGCGATCAGGATCCAAGGTCAATATG GCGAGCATCCAGATGAAAAGTATGACCCAAATGCACTTCCAATCATAAACAGGATAACCATAAAA AATGTTGCGGGAGCAAATATCAGACTTGCAGGTCTTTTAGAGGGTATTCACGGAGATAATTTCAG CAACATATGCCTATCTAATATCATCCTTAACGTAACATCCCCTCATCCTTGGAATTGTTCATATG TTGAAGGTTATTCCAATATGGTGTCTCCAGAGTCCTGTGAGCCTCTTAAAGAAATACCTGAAGAT TCTTCTATTTGTTACCCAGCTAATCATTTGAAACCACAACAATCCAGTGCAATTCGTTTGATTAG TCCCTTCATTAAGTTCATAGCAATGTAACCAAAGTCTGGCGCTGTATATAAGTTGGAACTTCTGT CAAGGGATCTTCATTTGTCCGAAATGTTTGGTTTTGTATGGTTTTTCAACAATAAAGTGTATAGA GTTTTGGGGTTTCCGTCATGTAAGTAATTGTATGGTGAACAGCTATATGAAATTGATTTTTTTTT TTTTCCTTGTAACATTTTTGGCAAGCAATTTATTTGAGATGAGGATCTTGC
EgPG4	>CL1Contig5616 GATGCATCCATCGAAGACGCTCTGCAGCATCACGTGAGCTGCTTCAGCGGCCATCGGAGCACTGG AATCGGAAGAAGAAGGCTTTTTGGCTCCCCCCGCGTACTCTGCGTTGATACCACTGCTTAAGCAG TGGTATCAACGCAGAGTACGCGGGGCATCCAAGTCCCTCCAAACCCACTCATACCTATATCTCAT AATCTCCTTCCTTTAAGACCTTCTATACTTTCATAAAAAAAAGGAGTCCAATGACTCAAATCATG TGCTCCTTCCGCCTCCTCCTCCTAGCAATTCTCATGATCCATTTCTCCTCATCAGTAAAAGCATC TTACGACGTTACTTCCTTTGGTGCCAAACCCAATGGTCGGACAGACTCGACCAAATCATTCATTA GTGCATGGACTGCCGCCTGTCACTCAACAAACCCTGCAACCATCCATGTACCCTCCGGCTTCTTC CTGATAGGTCCGGTCACCTTCAATGGTCCTTGTAGGAGCAGTAGGATCACCATCCAGATCGACGG AACCCTCGTCGCACCATCGAATTATGCTAATCTTCGCAATCTTGAACAGTGGATTTTGTTCGATC ATGTCGACGGCATCTCGGTGTACGGTGGGACCATCGACGGCCATGGCTCACCTCTATGGGCCTGC AAGGCTGCCGGCCGGAACTGCCCTGCCGGTGCAAGGTCGTTAGTGTTCAGGAACTCGAAGAACAT CTTGATCAGTGGACTGACGTCGATCAATAGCGAGAGGTTCCACATCGTGATCGATGGCTGCCAGG TGGTGACGGTGCACGGGGTCAGGATCACGGCCCCCGGCAACAGCCCCAACACCGATGGCATCCAC GTCCAGTCCTCCACCGACGTCACGATCACCGGAGCCGGCATCAAGACGGGCGACGACTGCATCTC GATCGGGCCCGGCACGACGAACCTATGGATCGAGAAGGTCACTTGTGGACCTGGCCATGGCATAA GCATTGGGAGCTTGGGGAATGAGTACGAGGAGAAGGGGGTGGAGAACGTAACGGTGAAGACGGCG GTGTTCACGGGAACGGAGAACGGGCTGAGGATAAAGACGTGGGGGAGGCCGAGCGAGGGGTTCGT GAAGGGAGTGGTGTTCGAGCACGCCATGATGCAGAATGTCCGAAATCCCATCATCATTGACCAAA ATTACTGCCCCCATGAGAAAAGATGCCCTGGCCAGAATTCTGGAGTGAAGATTAGTCAGGTGAAC TATATGGATGTCCAAGGGTCATCTGCATCACAAGTGGGGATAAACTTTGACTGTAGTGCCAGCAA CCCATGCACCGGAATTGGACTGCAAGACATCAAGCTTACCTACGGAAACAAGCCAGCAAAATCGT TTTGTGAGCATGTCCATGGTACTGCCTCTGGTTCTGTTGTGCCGAGTTGCTTCTGACTCTTCGAG TTGGAATAGTATGTATAGATCGTATGTCAGAGTATGCATGTGTTGATGAAATGGGTGATGTAGGA TTCGTAACTTTTCTTATCCTCCATGTCCAAGCGTTACTCTAGTAGACATGGAATGGAATAAATAT TTAATGGATTGATATGTGTTTTTTATTATAATAATTTCGGCCTAAACTAACGTTCTCATTCATGG TCCCCAATTAAAAAAAAAANAAAAAAAGTAACTCTGCGTTGATACTACTGCTTAAGCAGTGGTAT CAAC
EgPG6	>CL1Contig8210_RC CCTACGGGAACTGTTTGTGATATTTTAAGGAAGGCAGAATTATTTCAAGAAAGAACTTCGATTCG AGTTAATTAAAGGAAAAAAAAAGAAAAAAAANAAAAAAAAAAAGTAACTCTGCGTTGATACCACTG CTTAAGCAGTGGTATCAACGCAGAGTACGCGGGGGAACTGCCCTGCCGGTGCAAGGTCGTTAGTG TTCAGGAACTCGAAGAACATCTTGATCAGTGGACTGACGTCGATCAATAGCGAGAGGTTCCACAT CGTGATCGATGGCTGCCAGGTGGTGACGGTGCACGGGGTCAGGATCACGGCCCCCGGCAACAGCC CCAACACCGATGGCATCCACGTCCAGTCCTCCACCGACGTCACGATCACCGGAGCCGGCATCAAG ACGGGCGACGACTGCATCTCGATCGGGCCCGGCACGACGAACCTATGGATCGAGAAGGTCACTTG TGGACCTGGCCATGGCATAAGCATTGGGAGNTTGGGGAATGAGTA
EgPG7	>CL1Contig694_RC TTCAACGAGTCTATAGCCTTGGCCGACAGGCCCGGGTAATCTTCGAAAATTTCATCGTGATGGAG TGACACTTAACACTAAAGCATTTCAAAATGCTATCTTTTATCTACAGTCATTTGCTGATAAGGGT GGGGCACAGCTCTTTGTACCAGCAGGAAGGTGGTTGACGGGAAGTTTTAATCTTATCAGCCACCT CACATTATGCTTAGACAAGGATGCAGTAATTATTGGATCCACAGATTCGTCAAGCTGGCCAGTTA TCGATCCATTGCCTTCATATGGAAGAGGTAGAGAGCTACCTGGTGGGAGGCATAAAAGCCTCATT

Table S2.3. (Cont.) List of the 28 sequences contained either a partial or complete GH28 PG signature domain.

Name of genes	sequence
	CACGGTTCCAATCTGACAGATGTGATAATAACAGGTGACAATGGGACTATTGATGGCCAAGGCAG CATTTGGTGGGATTGGTTCCATAATAAAACGTTGAACTTTACTCGCCCCCATTTGGTTGAGCTCA TGTATTCAACCAAGGTGGTTATCTCAAATCTGACATTCATTAATTCCCCATTTTGGACCATTCAT CCTGTATATTGCAGCAATGTCCTTGTCCGGAATGTCACAATTCTCGCCCCTCTTGATTCACCAAA CACAGATGGAATTGATCCAGACTCAGCAAACAATGTCTGCATTGAAGATTGTTACATCAGCACTG GTGATGATCTAATTGCAGTCAAAAGCGGATGGGATGAATATGGCATTTCCTTTGCTCATCCAAGC TCCAATATTAGTATCCGCCGCATCACTGGAGAAACAAAATTAGGTGCTGGCATTGCGTTTGGAAG TGAGATGTCTGGTGGTGTATCAGAAGTTTGGGCAGAGGACATCCACCTCTTTAACTCAAAGCATG GTATCAGAATAAAAACATCTCCAGGGCGAGGTGGCTATATTCGAAATATCTACATCTCTGATGTG ATCATGAAGAATGTGGACATAGCGATCAGGATCCAAGGTCAATATGGCGAGCATCCAGATGAAAA GTATGACCCAAATGC
EgPG8	>CL1Contig4380 AACGCAGAGTACNCGGGGGACTTCTCCTCTGTATCTCATTCTTCCTCCATAATTCCACCCCGTCT CTCTCTTAATCTTCTTCATCTATTCATTCTCTTTGCCGGCTCTTCTGGTTGGAGCTTCTCCTTGT GCCTTGTCCTGCCCCTGGGCTTAAGGGGGCTCATGAGGAGGCTAGTAGTTGTGCTATTAGTTTTA GCAGTTGCTAATGCTGTAGGAGTCGATGGAGCCAGTTATGAGAATTGCAAATATGAGAGGAGTTT GAACCAAAGGCCGCACAGTGTTTCTATAACGGATTTTGGTGCTGTCGGAGATGGGGTGACACTAA ATACACTCGCCTTTCAGAATGCCATCTTCTATTTGCGGTCATTCGCCGACAAGGGCGGCGCTCAA CTTTATGTTCCTAAAGGAAGGTGGCTGACTGGAAGTTTCAACCTCACCAGCCACCTCACCCTCTT TTTGGACAAGGATGCTGTTATAATTGGCACTCAGGAATCATCTCAGTGGCCTATTGTTGAGCCGC TACCTTCATATGGCCAAGGCCAGGATCTTCCAGGTGGAAGGCATCGTAGCTTGATAAATGGGCAA AACTTGACAGATGTTGATAACAGGTGATAATGGAACCATTGATGGTCAGGGTTCAGTTTGGTGGG GGTGGCTCCGTTCTCACACATTAAACTTTAGCCGTCCTCACCTTGTGGAACTTGTGAGTTCCAAT GATATTGTGATTTCAAATCTGATATTTTTGAATTCCCCTGCTTGGAGCATTCATCCAGTATACTG TGGAAATGTGGAGGTCCGGAACATAACGATCCACACTTCATCCGATTCTTCATTTACAAGTGGTA TAGTTCCAGATTCATGCTCAAATGTATGCATTGAGGATTGCAGCATTAGTGTCTCACATGATGCC ATTTCTCTGAAAAGCGGTTGGGACAACTATGGAATCTCTTTTGGAAGACCTTCCTCCAACATTCA CATCGACAATGTCCATCTGCAGACTTCTCTTGGTTCTGCCCTTGCTTTTGGCAGTGAGATGTCTG GTGGAATATCTGACATACATGTTCAGCACCTACATGTCCATGATTCTTTCACCGGTATAAAATTC AAGACTATCCGAGGCCGAGGTGGGTTCATGGAAAACATAGTCATATCGGATGTGGAGATGGAAAA TGTTCAGGAGGCTTTTCAATTCACAGGACATTGTGGAAGCCACCCTGATGACCATTATGATCCTG ATGCTCTTCCAGTCATCAAGCGGATTACCCTTAAGAATGTGGTTGGTACAAACATTTCAATTGCT GGTGTCCTCTCTGGAATTGAAGATGATCCCTTCACTGCTATCTGCCTTTCAAATGTCAACTTTTC TGTCACCTCAGATCCTTCTGCTTCTTGGGTTTGTTCATATGTCTCCGGGTTCTCCGAATCAGTCT TCCCTCAACCATGTGCCGATCTCCAAATCCCATACTCAAATTCTTCTCTCGTGTGCTTCTCGCTT CCAAACTACAGTGCTCTTGCAGCAGCCAAATGAGATCTTTTTGCTATCTTATCATTTGCTTCAGT CCCTCTGTACGATTGAGAGACTTGAGCTTCCATTACCATCTTGCCAATTCTTTTGCCAATAAATC CCAAAAAAGTCGGACCAAAGATTTCCTTTCTATCACCATTCAATTCATGCTTCTTGGGACTCAAG CAATTAGTTATCTTGCACCTTCAAACAGGAAAAAAAAAAGGGTGGGGGGGCCATCCGAGATGACA ATGTGCTTGCCTGTACAGCTACATTTCTTCATTCAAACTGTAAGAAAAAGTTTTGGTAGTTGTTG GAATCCAGACATTGATTGACACTGTTGCATTTGCCATTAAACCATTAGAATTTGGTTGATATTTG TATATTCTATCCTGTGTGGACATGAAAATGAATTAAATTATCTGGGAATGGGATAGGAGTGGTTT GTGTATGCCACATGGCTTCATGTTATTAAAATAAATGGGTGGTTGGCTGTTAAAGTTATAAAACA GCTTGATCTAGAAAAAAAAAAAAAAAAAAAAAAAAANAAAAAAAGTACTCTAGCGTTGATACCA
EgPG9	>CL8640Contig1 TCATGGCTCCAGATGAGTCCGACGAGGCCGGTGGGGGTCGCAACCCCTCCGGCCTATGGAGACGC CGGTGCCGCGCCGGTGGAACACCCGAGCAGCAGCTGCTCGGGTTTCTACCGGCCCGGCGGGGGAG GAGGGTGGTTTGCTCGATAGAGGAATTTGGCGGCGTGGGGGACGGGACGACGTCGAACACCGACG CGTTTCGAAGGGCGGTGGAGCACCTGAAGGCCTTCGCCGATGAGGGCGGGTCGCAGCTGACCGTG CCTCGGGGAAGGTGGCTCACCGGCAGCTTCAACCTGACGAGCAACTTCACCCTCTACTTGGAGGA GGGTGCAATTATTTTGGGATCACAGGATCCAAAAGAGTGGCCTCTGATAGAGCCATTGCCAATCC TATGGGCGTGGAAGAGAGAGGTTAGGAGCACGCTACATTAGCCTCATCCATGGAGATGGCCTCAG TGATGTTGTCATCACGGGACAGAATGGGAGCATTGATGGACAAGGGAGGATGTGGTGGGAGCTGT GGTGGAATAGAACTCTGAAACACACTAGGGGACACCTTCTTGAGCTAATGAATTCACACAACATC CTCATATCCAACCTCACCTTCATCAACTCTCCATTTTGGACAATCCATCCAGTCTATTGCAGCAA CGTGGTGGTAAAAATGTAACCATACTGGCACCACTTAATGCTCCAAATACTGATGGCATTGATCC AGACTCGAGCTCAAATGTGTGCATTGAAGACTGTTACATTGAGAGCGGGGATGACCTGGTTGCCA TAAGAGTGGCTGGGACCAGTATGGGATCGCCATGGCCTATCCTAGCTCAAACNTTGTTGTTCGCA GGGTCTCCGGCACAACTCCGA
EgPG10	>CL4959Contig1 GTGCCGCCCCGCCTCGTGGGCTTCATCGACTCCAAGGACGTTCGGATCTGGGACATCACGCTCAA CCAGCCCGCCTACTGGTGTTTACATCTAGTCAGGTGCGATAACACATTGATTCACGATATATCCA TTTATGGAGATTTTGATTCCCCCAACAATGATGGCATCGACATCGAGGATTCAAACAACACAGTC ATCACAAGGTGTCATATTGACACTGGAGATGATGCAATATGTCCAAAATCTTCGACAGGGCCTGT ATATAACTTAACAGCAACAGACTGTTGGATTCGCACCAAATCTAGTGCAATTAAGCTTGGAAGCG CTAGCTGGTTTGATTTCAGAAGGTTCTTCTTCAACAATATTGACATTGTGGATTCACATAGAGGG CTTGGGATGCAGATACGAGATGGAGGAAATGTGAATGACATTGTCTTCTCTAACATCAGAATAAG CACAAGATACTATGATCCTTCGTGGTGGGGAAGAGCAGAGCCTATTTACATCACAACCTGCCCGA GGGATTCAAATTCAAAAGCTGGGTCTATCTCCAACGTTCTCTTTGTTAACATATCAGCAACTTCG GAAAATGGAGTGTTCCTATCGGGTTCCGGTGGTGGACTTCTTAGAAATCTAAGATTCGAAAATGT CCAATTAACTTATAGAAGAACAACCCGCTATCCAGGTGGGTTGTATGATTACAGGCCTGGATGTC AGGGCCTGGTTCCTCACAGAATGGGTGGAATCATGATGGAGCATGTTTCAGGTCTGGAGATAGAG AATGTGAAGATGAGGTGGATTAAGAGCAACTCAAGAGGCTGGAACAACCCTCTTGAGTTCACACC TTCCACTGTAAACAAGCTCTCTTTCCATGAATGGCTGTCAGATGTCTCTTAGCCAAAAGAAAAAA AGAAAAGATCAAAGGATTTCAATTTGAGTGAAGGCTCCCAGGTCATTCTTATGCAAAGTCAGAAT

Table S2.3. (Cont.) List of the 28 sequences contained either a partial or complete GH28 PG signature domain.

Name of genes	sequence
	AGATACTATGTCTCTATTTATTGTTATCATTTGCTCATGATTAAT
EgPG11	>M01000011018:1,1896 CCGTGCCAACCTGCTGCTTTCTCCGTCCTTCTTCACAAATGGCTTGGCGGAGGCACAGTAGCATC TCACTCCAAACCTTGGCGTTATGGATTTCACTAATGGCGGTATTCATCGGAACGGCGGAATGCGC CCGGCGGAGCATCCACCTCCCCGGCGGCAGCCGCGATGGCGGGGTGATGGGGGCGTTCCAGTACG CGGCGACGAGCTGCCGGGCCAACACGGCGTCGCTGAAGGACTTCGGCGGGGTTGGCGACGGCAAG ACCTCCAACACGAAGGCCTTCCAGGCGGCGGTGGCGCACCTGGCCCAGTTCGCCGGCGACGGCGG CGGTGGTATGCTGTACGTGCCGGCGGGGCGGTGGCTGACGGGCCCCTTCAACCTTACCAGCTCCT TCACCCTCTTCCTCCACCGCGACGCCGTCATCCTCGCCACCCAGGATATTAGTGAATGGCCTGTC ATCGATCCTCTGCCCTCGTATGGAAGAGGAAGAGATCATGCTGGTGGAAGATACAGCAGCCTCAT TGGAGGATCAAACCTCACTGATGTAATTATCACAGGGGACAATGGAACAATTGATGGGCAGGGGG CCTTCTGGTGGCAGCAATTCCATGGAGGCAAGCTTAAATACACACGCGGATATCTCATTGAACTA TTACACTCCGACCAGATATTTATATCCAATCTTACACTACTCAACTCTCCTGCATGGAACGTCCA TCCGGTCTACAGCAGCAACATTATAATTTCGGGCATCACTATACTCGCACCACTCCATTCTCCAA ACACAGATGGGATAAACCCAGACTCCTGCACCCATGTTCGAATTGAGGACTGCTACATAGTCTCT GGTGATGACTGCGTTGCCATCAAGAGCGGCTGGGATGAGTATGGCATTGCTTTCGGAATGCCGAG CCAGCACATCATTATCCGAAGGCTAACCTGCATCTCCCCGACCAGTGCCGTCATCGCTCTAGGGA GCGAGATGTCAGGTGGAATTCAAGATGTGAGGGCTGAGGATATCACCGCCATCGATTCCGAGTCC GGTGTCCGAATCAAGACTGCTATTGGGAGGGGAGCATATGTGAAGGATATCTTTGTCAGGGGGAT GAATCTCAACACCATGAAGTGGGTGTTCTGGATGACTGGAGCCTACAAGTCCCACCCTCGATAAC AAGTATGATCCCAATGCCATTCCGGTTGTCAAAGGGATCAGTTACAGTGATGTTGTTGCCACAGA TGTAACACAAGCAGCAAGGTTGGAGGGGATTTCAAACGCACCATTTACAGGCATTTGCATTTCTA ATGTCACAGTCCATTTAGCAGCAAAGGCAAAGAAGCAGTCATGGACCTGTACTGATGTTGAGGGT GTGTCTAGTGGAGTGAGTCCTACACCTTGTGCTTCACTACCAGATCGGGGTGCCGGTGCTGAGCC ATGCCCGTTCCCGACCGACAGACTACCTATTGATGATGTGGTGTTTGAGGAGTGCTCATACATGA GCTAATAATCTCCGAGGTTGCATTCGCATATGGTTCGTTCATATAGTGTTTATCAAGTCAATCCT CATGTACAATGGTGGCTGGTGGCAGAGCTTTTGTGTGCTTCTAGCTTCTTGATGCTTAAGGTTTG CTATAAAAATGTTAAAGCCTTGAAGGTTATGGAGTAATCCATTCCTCCTTTGTGTGCTAGATCTA TGTTCTTACATTTCAAAGTTCTATAATATTTCCACATAACTTGATTACAGAGGACTGTATACTAA AAATGCATGATGCCATGATGTTATTACTTGGACAGGGTCTTGCCTTCATTTTGATAGAAATGGTA CATGAAAATTGAACAAAGAAAGACTGCAATTGACAACAAGATTTTAGTGGAGCAATAAAATGTTG ATACAAATATT
EgPG12	>M01000058719:1,1373 TGAAGGGATACTTGAAGGGAACAACAGATTTGAGCCAGTATGTCACAGGTGATTGGGTGGATATG TTGATATTGACCGGAGGAGGGACCTTCGATGGCCAAGGAGCTGTATCATGGCCCTATAACAAGTG CCCTACAAATAAACATTGCAAAGTCCTCCCCACTTCGGTCAAGTTCGTTGTCACATCAAACACTC TGGTACAGAACATCAAATCAAGTTTTTCCACATAGCTCTGGTTGGCTGCAAGAACTTCTGGGGCA AAAATATCCAGATCACCGCCCCTTCAAACAGCCCCAACACCGACGGAATTCACATTGAACGGAGC AGAGGCGTAACTATATATAACTCGGTGATCGGAACTGGTGATGATTGTATCTCCATTGGACATGG TAACTCACAAGTATTACTGAGTGGCATCAGTTGTGGACCAGGGCATGGGATCAGGCAAGTCCTCT TGAAGTTCTCCTGCTACAATATTGTTATGTTCTGATTGAAATTTTTGATCCAATCCAAATGAGAA CAGATCCTTGGATTAATCCTGGGTTTAGACTGATGTCCGATGCACTTCTATTTGACCCTCACCAG ACCCCGCAATGCATTGGGAGTTTAGGAAGATATCATAATGAAGGGGACGTCCGAGGACTCGTCAT CAAAGATAGCACCCTTGCCGGGACTTCAAACGGTGTAAGGATCAAGACATGGGAGAACTCTCCAG GAACCAGTAAGGCTGTTAACATGACCTTTGAGAACATTGTCATGAACAGTGTTGCAAATCCCATC ATCATTGACCAGATGTACTGCCCCTACAGCTCTTGTGCATCAGATGCACCATCTGGGGTGATTCT GAGTGACATCTTCTTCCGGAACATAAGAGGGACGTCGACGACTCCGGTGGCGGTGACCCTCAGGT GCAGCAGAGGAGTGCCATGCAAGAACGTCAATCTCCAAGACGTCAACCTCAAGTACGTTGGCCAG CTTCCGGCCACTGCCTCGTGCATGAACGTCAAAGCAAGCTTCAGCGGGACCCAAATCCCCCCACC TTGCCGCTAGGCAAACCGACCCAAAACTTAGCTAATTGGCCCCCTTGGTGCTCGTGGAACTCATT GAAGCCATTCTTCCTGGCCTCCATCTAAGGCTGGGTTACATTCTTTCCTGTGGGTTGTAACCATC TTACCATCAAGCATGAGTAATTTGTTTTTGGATTATATTTACAGGCTGTGGAAATCCGGGGACTG AGTAATTTGTTTTTGGATGGATTATATTGAGAGGTGGCTCTGGTTGAACCGCCATTCTTTCTGTG GTTATCTTTCTTTCTTTGTATTTTTTGGGAACCAATGTTGTTATCTTTGTTTAGTTGTTGGGATT TTGATTTG
EgPG13	>M01000001841:1,1933 CTAAACATTCTTACGCTTTTTTTCTGTTTCCATCTTCACGGCTTGGCGGAGCTCCTCTGCTTCTC CCTGGGCCAAGAAAAATAAAAACTAAACAACTTCAGATGGCGTCAAGACCACCGATGGCGCTGGT ACTGGCAGCGTTCCTTCTCTTGGTGGAATGGGGCTCGGCGGCGGCGGCGGCGGCGGCAGGGG AGGAGACGTGCTCGGGGATAGTGCCGATGAAGGAGCGGGGAACGGCAATGTCGGTGGAGGATTTC GGCGGGGTGGGGGACGGCCGGACGCTCAACACGGCGGCTTTCGAGAAGGCCGTGGCGGAGATCGA ACGGCGAGGGGTGGCCGGTGGCACCCTCTACGTCCCGCCGGGGGTCTGGCTCACGGGGGCCTTCA ATCTCACCAGCCATATGACCCTTTTCCTCGCCAGGGGCGCCGTCATCAAGGCCACCCAGGATACA TCGAGCTGGCCTTTGATCGATGCTTTGCCATCATATGGGAGAGGTCGGGAGCTACCTGGTGGGAG ATATATGAGTCTGATTCATGGAAATGGAATTCATGATGTGATAATAACAGGTGAGAATGGAACAA TTGATGGGCAAGGCGAGGTCTGGTGGAATATGTGGAGGCAAAGAACCCTACCTTTCACAAGACCA AATATATTGGAGCTCATGCATTCTAAAGATATTATTATTTCTAATGTGGTCTTCCAAAACTCACC ATTTTGGAACATTCACCCTGTTTATTGCAGTAATGTGGTAGTAAGAAATGTGACCGTGTTGGCTC CATATGACTCTCCTAACACGGATGGAATCGATCCAGATTCCAGCTTAAATGTCTGCATAGAGGAC TGCTATATTTCAACAGGGGATGATCTAGTAGCTGTGAAAAGTGGGTGGGATGAGTATGGCATGGC CTATGCCCGCCCCAGCTCTGGCATCACCATTCGGCGGTTGACCGGCTCCTCTCCTTTTGCCGGAA TCGCAGTTGGAAGCGAAACCTCCGGTGGGGTGGAGAATGTCTTAGTGGAGAGCATACATATCTAT AACACTGGTATTGGGATACATATAAAAACCAATTCTGGTAGGGGTGGGTATATAAGAAACATAAC CGTCTCCGGTGTGAATCTGAGCAATGTTCGCAAGGCTCTGAGAATTGCAGGTGATGTTGGAGATC

Table S2.3. (Cont.) List of the 28 sequences contained either a partial or complete GH28 PG signature domain.

Name of genes	sequence
	ATCCTGACGACATGTATAATCCAAATGCTCTTCCAATTGTCAATGGTTTGACCATCAAGGATGTG TGGGGTGCGGATATCCAGCAGCCTGGGTCGATAGATGGCATCAAGAACTCACCCTTCACAGGGGT ATGTCTTTCTAATGTCAAGCTTAATGGTGATGGAACACGGGAAGTGCCATGGAAGTGTGCGGATG TGAGTGGTGGTGCCCTCGGGGTGCAGCCATCACCATGCACGGAGTTGACAAGTATTTCTGGGTTG AGCTTTTGTACGAATGCAATCTGATGTTCTATCATTTGTTGGATGCCGTTGTCACTAAGAAAATG CATGTCTTTGCCTATTTGGCTGATAGAAAAAAAATTTGAGCATAAAATTTGGTGCTATTATAAAG ATATGCAGCTTGTATATGAAAGAATCTATATCTCATGATTTTCAAAGCATGAAAATATTTGAAGT TATCGACCAAGTGCCGGAGGTATTGCCGATATAAGTATCAACCAGGCAGAAGATAAGCTCTGTTT CTGTGCAACTAACAAAAATGCGGGTTGATTTTTATTGAACTAGAGTGGCTATCATAGTACAGTTG CAGTGTTATGCTGGAAAGAGATCTAAGATATGGCATACTACAATTTGCAGTATTATGCTATCTAG TTAACAAGCAGCATTTGCAAACGGGCTTAAATTGTTATCTATTGTAATTTCATTGGATGCATATA CAGTTATTCTAGAGTATGGTTTAATATTTGATGGTCCTTGACTGGATG
EgPG16	>M01000013617_RC:1,1490 CCGGACAAGGCGGCGCCGAGGCTCCGTCCGTTTGCGTACAATATCACGGACTTTGGTGGGGTTGG CGATGGAGTGACGCTGAATACTGAGGCATTTGAGCGCGCGGTGGCGGCGATCGCGAGGCATAGGG GGAGGGGCGGCGGGCAGCTCAATGTGCCGCCTGGAGTCTGGTTGACGGCGCCGTTCAATCTTACG AGTCATATGACTCTATTTCTTGCAGAAGGTGCCGAGATTCGTGGAATTGAGGATGAGAGATATTG GCCATTAATGCCTCCAGTTCCATCATATGGATTTGGGAGGGAACATAAGGGACCTCGATATGGAA GTCTGATCCATGGCCAGAATCTGAAGGATTTGGTTATAACAGGACACAATGGAACCATAAATGGA CAAGGTCAAGCATGGTGGGCAAAATATCGCAAAAGGCTTCTCAACAACACTAGAGGACCTCTTGT GCAGATCATGTGGTCCAAAGACATAGTTATTTCCAACATAACTCTGCGCGATTCTCCTTTTTGGA CACTCCATCCTTTCGATTGCAAAAATGTTACTGTTACAAATGTTACCATCTTGGCTCCTGTTACT GGAGCTCCAAACACGGATGGGATAGATCCGGATTCATGTGAGGATGTGGTGATAGAGAACTGTTA CATATGCGTAGGTGATGATGGAGTGGCCATAAAGAGTGGTTGGGATCAGTATGGAATTGCGTATG GGCGCCCATCTACTAACATTTTAATCCGCAATCTCACTGTTCGCTCTGTGGTGAGTGCTGGAGTA TCAATAGGCAGTGAGATGTCTGGAGGAGTTTCAAATGTTACTGTGGAAGACCTTAATATCTGGGA GTCCAGGCGGGGCATTAGAATAAAGACTGCCCCTGGGAGAGGAGGCTACATTCGCAACATATCCT ACCACAATGTGACCCTTGATAATGTTCGTGTTGGCATTGTGATCAAGACCGACTACAACGAGCAC CCTGATGAAGGCTTCGATCCCAAGGCTGTTCCCCTCTTTGAGAACATATCCTTCAGTGGGATTCA TGGCCAGGGAGTCCGTGTCCCAGTTCGGATCCATGGCAGTGAGGACATCCCTGTTAAGGGTGTCA GCTTCCGTGACATGTCTGTGGGTATAACCTACAAGAAGAAGCACATATTCCAGTGTTCCTTTGTT CAAGGACGTGTGATTGGGTCCATCTTCCCTGCACCATGTCAGAATCTCGACCTTTATGATGAGCA GGGGCAGCTGGTGAGGCAATCAGCATCACAGAACAGCACCGACATTGACTATGATATTTGAAAAT TTTGTTCCCTCTCCATTGTCCAGATGGGAGGAGTGCCGGGTTATTCCGTGGCAGTGATGGTTCTG TCAAGCATCTGTTCCCAAGGTTTCAACCCCCCTGGCTTGTACATACAGAGCTTTCAATTTTTGAT TTTTTTTTTTTTTTTTGGTAATTATCTGGTGATATGCCTCACCACTTCATGATCTTGCAG
EgPG17	>M01000033226:1,1913 GTCTCTCTGTGGGACGGTTGCAGTCTTTCTAGCTAATAATGGCGTTGCTCGGAAGCAATCCCTCA AGAAACCTCTACGTACTAAAGTTGGTGATTTTATGGATGGTGGTGGCGGGACTTATGAGGGCGGC GGAGTGCACGAGGCTAAGGCACCACGGCCACCACCGCCGGAGGCCCGGCGGAGGCTTGCCCGCGG GGGCGGCGGCGGCGGGTGCCTTCGGCTGCCGAGCCTACAAGGCGAGCCTGACGGATTTCGGGGCG GTGGGTGACGGGACCACCTCCAACACCCACGCCTTCGCCGCGGCCGTCGCCAACCTCAGCCTCTA CGCCGCCCACGGCGGGGCGATGCTCTTCGTGCCCCCCGGCAAATGGCTCACTGGTCCTTTCAATC TCACCAGCCACTTCACCCTCTTCCTCCACCGCGACGCCGAAATCCTGGCCTCCCAGGACATTGAT GAATGGCCAATTATTGATCCCTTGCCCTCTTATGGGAGAGGAAGGGACTTACCTGGTGGAAGATA CAGCAACTTCATCATGGGATCTAACCTCACTGATGTGATCATCACAGGGGATAATGGAACAATCA ATGGGCAGGGGAAAGTCTGGTGGGATAAGTTTCATGATAACAAGCTGGAGTACACTCGTGGTTAC TTCGTTGAAATAATGTACTCAGACCACATCCTTATTTCCAACCTTATATTCAAAGATGCTCCTGC ATGGAACCTTCATCCGGTTTACAGCAGCAATGTTCTTGTGTTAAATGTGACAATTCTTGCACCGG TTACCTCTCCAAACACCGATGGAATTGATCCAGACTCCAGCTCCAACGTCCTCATCGAGGACTGC TTCATAGTCTCTGGTGATGATTGCATCGCCATCAAAAGTGGTTGGGATGAGTATGGAATTGCCTT CAACATGCCAACCCGACATGTAATTATTAGAAGGCTCACCTGCATTTCCCCCACCAGTGCCACCA TTGCCCTTGGAAGCGAGATGTCTGGTGGTATCGAAGACGTCAGGGCTGAAGATATCACGGCCATC AACACAGAATCTGGGGTCAGAATCAAGACGGCCATTGGTAGGGGAGGATATGTTAAGGATATTTT TGTGAGAAGAATGACCTTGAACACCATGAAGTATGTTTTTTGGATGGCTGGAAATTATGGGCAGC ACCCTGATGACAAGTATGACCCCAACGCAATCCCAATAATCCACAATATCAATTACAGAGATGTG GTTGCCGAGGATGTCACCATAGCTGGAAAGTTGGAGGGACTTCCTAAGGCACCCTTCACTGGGAT ATGCTTGTCTAATGTGACTGTGGATGTTGTGAAGTCGAAGAAGCTGAAGTGGAACTGCACTGATG TTGAGGGGGTCTCAAGTGCTGTGATGCCTACTCCTTGCGACTCACTCCGAGATCTAGGAGCTGAT GATGCTCCATGCCCTTTCCCAACAGGTTCTTTACCCATAGAAACTGTTGCATTCCAGGAATGTCA ATACGGAAGAGTTAAACTGTGAGTGTTGGTGTGAGCTTTGTTTTATTTTCCTTGGAGTCATTCCT CATGACCGATGTCTGCAAGGAGAAGAGCTCTTATGTGCTTCTGTCTCTTGATAATTGGAGGTTCG ATGAGGAAAACTAGTGTTGCAATAAGTCATTTGTTTCTCCTAGGTATTGGAGTTTTTTCCTTTTT AAAGTATATTATGTCATGTGAGTGCATGTATGTGAAGCTGGACCTAAATTTGTGACCAACAAGTG GTAGTTTAATGGCTACAGGGGCTACTGCAAGTGATTCTAAACCTTTTTGGATTGCTATGCTAGCT TCATCAGGTCAGCCTAAACCTTTTACTTCATTATGTAAATTAAACTTTATCATCTGAAAGTTTAT ATATATATATCTGGAATTTGTATCAAAA
EgPG18	>M01000001611:1,1662 AACAACAGATTTGAGCCAGTATGTCACAGGTGATTGGGTGGATATGTTGATATTGACCGGAGGAG GGACCTTCGATGGCCAAGGAGCTGTATCATGGCCCTATAACAAGTGCCCTACAAATAAACATTGC AAAGTCCTCCCCACTGTAAACTCTCAAGCCTCATTTATCCTTTATGCTCTCTACGGTAGATCTAA TACTTGCAACTCGAGTATATATAGTTACCACGTACACGTCCTTTCTAATTTGACAATTTTGCACA AAAGTAGAAATAATGTATGAAATCAAGCCAATCACATACTGGTGCATTTTAGAGCTTTAAAACTA GCTCACTGCATAAGGCAATTAGTATTTCCCAGCTAGTAGCTACTTCACCAAAAGTTTCACAGTGG AATAATGGCAGTGCCAGATTTTTTTTTGTCCGCATCAAGGAAGAATGAATAACTCTATATAGGCTT

Table S2.3. (Cont.) List of the 28 sequences contained either a partial or complete GH28 PG signature domain.

Name of genes	sequence
	AGATTAATGAATATTCTAGACTAGAGTAGTACTTTCATGTTGCTACCCAAACTGCAGTAGCAAAA TTTGTCCAACCGTTGTCTTTTAGATGTAACACTTGCCCTCTGCATTTTAGGGTGAAGTATTTTTC TAAGACAAGCATTGTAGCATGAAGTTATAGCAGCTAGCTATCAATACTCATAATTGCCAGCATCA TTAAGATCACAGATGTTAGTAAAAACTGTAGAAGCTCTATAGTCCAAATTTGCTATTCAGCTTAT CATCTAAACATGCTTAATTGTCATTTTGGTGATTATCTTGAGCATTTCAGTCGGTCAAGTTCGTT GTCACATCAAACACTCTGGTACAGAACATCAAATCAAGTTTTTCCACATAGCTCTGGTTGGCTGC AAGAACTTCTGGGGCAAAAATATCCAGATCACCGCCCCTTCAAACAGCCCCAACACCGACGGAAT TCACATTGAACGGAGCAGAGGCGTAACTATATATAACTCGGTGATCGGAACTGGTGATGATTGTA TCTCCATTGGACATGGTAACTCACAAGTATTACTGAGTGGCATCAGTTGTGGACCAGGGCATGGG ATCAGGCAAGTCCTCTTGAAGTTCTCCTGCTACAATATTGTTATGTTCTGATTGAAATTTTTGAT CCAATCCAAATGAGAACAGATCCTTGGATTAATCCTGGGTTTAGACTGATGTCCGATGCACTTCT ATTTGACCCTCACCAGACCCCGCAATGCATTGGGAGTTTAGGAAGATATCATAATGAAGGGGACG TCCGAGGACTCGTCATCAAAGATAGCACCCTTGCCGGGACTTCAAACGGTGTAAGGATCAAGACA TGGGAGAACTCTCCAGGAACCAGTAAGGCTGTTAACATGACCTTTGAGAACATTGTCATGAACAG TGTTGCAAATCCCATCATCATTGACCAGATGTACTGCCCCTACAGCTCTTGTGCATCAGATGTAA GCAAGCTAACACAATCATGTCATGCAAAAATATGAGGGGCTCATATAATATTTTTTCCGCATATA GTGCTTAGAGCTTGATAATGCATGCATTTAAACAACAAAACTTGGCCAGGGCTTGGAGGAGATGG TCCGCTGTGGTTTCTCCTGTGAATAGGCTCTACTTATCTTTCCCTGCTACAGAAGAAGGCATTAC TTAGTTTGACAATAAAATTGTGCAAAGTACTAAATCC
EgPG19	**>M01000015126:1,1043** GCAGTTGCATCCTATATCTCAGGAAGTGCCCAGCTGGATTGCTTTGTTTTTAGTTGTCTCAAGTA AAAAGACAACTGATAATATCATTTTTTTAATCTTAATTTTTGTATGGAATCAGCATAGGGAGCCT CGGGAAGGACAATGCGACTGCCATAGTTACAGCAATCGTCTTGGACACAGCAACACTTACAGGCA CTACCAATGGCCTTAGAATCAAAACCTGGCAAGGAGGATCAGGCTATGTTAAATCAGTGCGCTTT GAAAATGTGAAGATGGATGATGTTGAGAACCCAATCATCATCGACCAATTTTACTGTGATTCTCC AACCAGTTGCAAGAACCAGACATCGGCAGTGAAGATAAGCCAAGTCCTCTACAGGAACATAAGTG GGACCTCAAGGACTCCTAATGCCATGAAATTTGCTTGCAGTGACACAGTACCATGCAGCAACATT GTGTTGAACAACATAAATCTAGAGAGAGAAAATGGCATTGTAGAGACCTTCTGCAACTGTGCCAT GGGATTTGACTATGGGTTTGTGCGGCCAGCGGCAGATTGCCTTCGCAATGCTAAAAATTCCCGCT GTGATGGGACAAAGAATGACAACCAAAACCAAACTTATGATCCCGTGCATACAGAGCTATGATCT CTCTATATCATATCAAGGTATCATATTACAGACCACGATAGGTGGAGACCAACAAAAAACCGTAC TTACAAGTACGCCTACATGTTACTGAGTTCTGGCATATTGAATAGAAAGATTTAGTGGAAGAATT TGAGCTATTGAAGCAGACACAAGCTAGCGACTTTGACGCATATATCTTAGGCAATCAAAAATGGT ATAGAAGAAAGAAATCGATGTACTTGAACTCTAAAGATATCCTGTATGACTTTTAAGGAACAACC GTATTTGTCCATGCTTCATAAATGGAAACAGAAATCACAAGGACACTCTTTCTGGACTATTGGAT CCAGGGGATGTAAAACCCATACCACTACCATGTCAATTGTAGAAGCATTTATGCAGCAATTATTG TTC
EgPG20	**>M01000028952_RC:1,1051** TTTTCGGTATTGTATTTTAGTTGCATGACTTTTGTCTCATCTGTCTTTTCTATAGTTATTTTCTC GCAATATGTGCTTGGTAGATTCTTTTTTTTTTTTTGTTTTTTATTCTAATTGCTTTTTTTTTAGT TATGATTCGATCATGATCCATTGTTTTTTACTCTTTCTTTTCTTCTCCCTTCAACTCTTCTCTCA TTCCTTTTTTTTTTGAATAATAAAATTTAAATAACTAACGTTTAAGTTTTTCTTTTGCTTGATTC TTTTTGGAAGTATTTTGTTCTGCATGCCGGGAGGCCAATTTAAATTGAAGCTGAACCTTCCTTCA TGATCCAACATAACGAGAAGATAATGTGATCTCAGCCATCTATTGAATGGACTTCAGAAACTGAT CATCACATAGAAATCTATCTTCCAAATGTTACGGTTGTTGTCATTTATTTTTGTTTTAAAGACAT AATGGCTTTTTTAATAAACTACAATGCTTCAAAACTTTTTGTTTGGAGATAATATACTGTCCTTA ATTCTAAAGTGAGAAACATTGCATCAAAGGTAGTCTTAGAACATCAAAAGCAAGGTAGCAATGTT TAAATCTAGGATTTGTTCTTGCTGTGCTAATTGTTTCCTTGTTGGTGATGGGTAAGCTGGCTTTT AATCAATTAGCTAAGGCATTCATGGCCGCATGGAAGGCAGCATGCGCAGCAGTTGGTGTGGTCAA GCTTCAGATACCTGCAGGAACTTATCTTATTGGCCCTACTAAGTTTGCTGGTCCTTGCAAAAATG TTCACTCCCTTACAGTGAATATGAAGGGATACTTGAAGGGAACAACAGATTTGAGCCAGTATGTC ACAGGTGATTGGGTGGATATGTTGATATTGACCGGAGGAGGGGACCTTCGATGGCCAAGGAGCTG TATCATGGCCCTATAACAAGTGCCCTACCAAATAAACAATTGCAAAGTACCTCCCCACCTTCGGT TCAAGTTACGTTGTCACATCAAACACTCTGGTACAGAACAATCAAATACAAGTTTTTACCTACCA TAGCTCTGGTT
EgPG21	**>M01000034881:1,1267** GCGTTTCGAAGGGCGGTGGAGCACCTGAAGGCCTTCGCCGATGAGGGCGGGTCGCAGCTGACCGT GCCTCGGGGAAGGTGGCTCACCGGCAGCTTCAACCTGACGAGCAACTTCACCCTCTACTTGGAGG AGGGTGCAATTATTTTGGGATCACAGGATCCAAAAGAGTGGCCTCTGATAGAGCCATTGCCATCC TATGGGCGTGGAAGAGAGAGGTTAGGAGCACGCTACATTAGCCTCATCCATGGAGATGGCCTCAG TGATGTTGTCATCACGGACTCGAGCTCAAATGTGTGCATTGAAGACTGTTACATTGAGAGCGGGG ATGACCTGGTTGCCATAAAGAGTGGCTGGGACCAGTATGGGATCGCCATGGCCTATCCTAGCTCA AACATTGTTGTTCGCAGGGTCTCCGGCACAACTCCGACTTGCTCAGGGATTGGATTTGGAAGTGA AATGTCTGGTGGAATATCCAACGTCTTGGTGGAAGACCTGCATGTCTGGAATTCAGCAGCAGCAG TGAGACTGAAGACTGACAGAGGGAGGGGAGGATACATTTCCAACATCACAATTGCTAATGTGACC ATGGAAAGGGTTAAGATTCCCATAAGATTTAGCAGAGGCTCTAATGATCATGCCGATGAAGGTTA TGACCCAAAGGCCCTTCCTAGAATAAATGGTGTTTACATTAAAAATAGTAGCCGGCATCGACGTA GGGAAGGCGCCGGTTCTGGAAGGCATTGAGGGAACAATATATGAAAAGATATGCTTCAGAAATGT TAGCTTAGGGAGGTTAAGCCCTAAGGCCAGATGGCATTGTGAGTTTGTTGCTGGAGAAGCTTATG ATGTGTTCCCAACGCCATGTCAACAGCTTAAGAACAATGGTTCTTCATCTTGGTGCAGATACTCC TAGGCCATATAGACAGGAATCAAGGTTTTCAGCCTCAACTCTGCCTCAAAGATAATGAGGTGGAA TGATCCATAACAATCTTGAAGTAGTAGTCCAAATGGTATACATGAGGGTGTGGTATCTTGGAGAT GTTAGCTTTGGGATTAGTTCGTTTGTATTTTCTTTTATTTGGTAGGTTCAGATATAAACTAGAAA GTAGCATATAGGATTAACAAGATACATATTCCATTTATTTGTACTTATTAAAGAGAGTGACGTAG GTCTTTGTGATTCTTTTAGTCAAGGAAGTTTATTCTATAAATTTTTTTTTTATCAATAGTAGAGG

Table S2.3. (Cont.) List of the 28 sequences contained either a partial or complete GH28 PG signature domain.

Name of genes	sequence
	AAGACTGAAAGTTCCTTTTTCTTTAAAAGAAG
EgPG22	>M01000018577:1,1075 AGTCAGAGCAATCGACTTAGTAATAGAGGGCGAGAAGTATGTCGTGCTTCTCCCTGCTTCTTATG CTGATGTTAGTTGTACTGATGATGGGGGCCGTGTCCAAAGGTGATGACAATTTTGCCCCATCTGA GGATATCGGGCCCTGGACGGTCGGTACGGACGGCGAGGAAGAGCAAGAAGGAGACGAGTATGATG AATTGGACTCCCTACCGGCATGGGGAAGCGAGCGGGTTGGGAGGATCCCTGTCAATGTCGACAGC TTTGGTGCTGTAGGGGATGGAGTTGCAGACGATACCCAGGCATTTCTAGAGGCTTGGGAAACGGC GTGCTCCATAAAGAATGCAGTTTTCCTAGTGCCCGAGCGGCGCCGTTACAAAGTCAACGCAACCA GGCTACGAGGGCCGTGCGAAAGGAAGCTACTCATCCAGGTGAGCGGGACAATTGTAGCCCCTGAT GAGCCAAACGACTGGGACCCGAAGAACCCAAGGACATGGCTATCTTTCTCTATGCTGAAGGGCGT CAGGATCCAGGGCGGTGGGATTATCGACGGCTCAGGCAGCAAATGGTGGGCGTCATCCTGCAAAA TCAACAGGACCAGTCCATGCAGAGGAGCTCCAACGGCACTGACCATAGATTCAAGCTCAAAGGTA AGGGTGAAGGACCTCACCATCCAGAATGCACAGCAGATGCACTTCACCATCTCCCGATCTGATGC CATACGAGTGTCTGGGTTGCGTGTGAGAGCTCCACAAGACAGCCCTAACACAGATGGCATTCATA TCAGTGAATCCACCAATGTTGCCATCCAGAACTGCCACATTGGAACAGGGGACGACTGTATCTCC ATTGTGAATGCTAGCTCAATTATCAAGATGAAAAACATTGTGTGTGGGCCAGGGCATGGAATCAG CATAGGGAGCCTCGGGAAGGACAATGCGACTGCCATAGTTACAGCAATCGTCTTGGACACAGCAA CACTTACAGGCACTACCAATGGCCTTAGAATCAAAACCTGGCAAGGAGGATCAGGCTATGTTAAA ATCAAGTGCGCTTTGAAAATGTGAAGATGGATGAT
EgPG24	>M01000015281_RC:1,623 AAAAAAGATCCTTGTTACCCCACCTACTCCTTATACCAATCAAGGATAAGTACACTTCCTATCCA GTAGGCTTGATCTATTTTTTATGTTCAGTGTGTTCTCTGTATGTATGTATGATGAACAGAAGCAT TCATGGAGAAGTATTTTGCCAGGGGATTCTAAGAGTTGCTCTAAAGTTTTTTTTCTTTTTCCTCC TTGGATTTCATCTGATCTGAGGTCTCACTACTTAGTTTCTGAGGCATGGTTTTGTGAGCCAGGTC TATGGATGATGGGTGAATAGGGTTGTTTTTGAAAGCTTTATGTTTTCATTTTTTAATTTTTTATT GAATGGTGCAGGATACATCGAGCTGGCCTTTGATCGATGCTTTGCCATCATATGGGAGAGGTCGG GAGCTACCTGGTGGGAGATATATGAGTCTGATTCATGGAAATGGAATTCATGATGTGATAATAAC AGGTGAGAATGGAACAATTGATGGGCAAGGCGAGGTCTGGTGGAATATGTGGAGGCAAAGAACCC TACCTTTCACGAGACCAAATATATTGGAGCTCATGCATTCTAAAGATATTATTATTTCTAATGTG GTCTTCCAAAACTCACCATTTTGGAACATTCACCCTGT
EgPG25	>M01000031930_RC:1,710 CAAACTATGAGTACAACTTTGGAAAGCCTTATTAACCTAACTTCAAAGATGTCAAAACTGGTATT TTTATTTCAAAGATTGTTGTTACATAGGCAAGCCTTTCTGAGTAAGCTGGAAATTAATTAGCTTT GCAGATAATGGGAACTCATAGTTTTTCTTGTATTTTAATTGCATTGCCTTTATTTTCTCTGAATA ATAATTTTCGATAATAACTGGCCATCTTATCTTTAATCAGAACCTGATCATGAATTTGAGTGCAT TAGTATATGCACATATAATGACTGTAATATGTAGAATATCTTGTATGTTTATATATGTACGTAGG TATGTGTATATGTACGTATATATGTATGGCTGTATGCATTCATGTTATTTCGTTCTTTAATTTAT CTCATTGCATACTAGTATGATTCTATGAACTAATTAATATGGGCATTATCCTTAAAAACATTACG TTAAATTTCTTTTGTCCCACTTCTTGTTCCCAGGTGAGAATGGAACAATTGATGGGCAAGGCGAG GTCTGGTGGAATATGTGGAGGCAAAGAACCCTACCTTTCCCGAGACCAAATATATTGGAGCTCAT GCATTCTAAAGATATTATTATTTCTAATGTGGTCTTCCAAAACTCACCATTTTGGAACATTCACC CTGTTTATTGCAGTAATGTGGTAGTAAGAAATGTGACCGTGTTGGCTCCATATGACTCTC
EgPG26	>M01000039313:1,541 GGAGAATGTTAAAAACTGCATCATTATAGACCAGTACTATTGCCTAAGCAAGCAGTGTATGAATC AAACATCGGCGGTCTACGTAAAGGATGTCTCATACATGAACATAAAGGGGACGTATGATGTCAGG AGCCCACCAATACACTTTGCTTGCAGTGATGCCGTGCCATGCACCAACATCACCATGTCTGATGT GGAGCTGCTCCCATTTGATGGAGAGTTGGTGGATGACCCTTTTGTTGGAATGCCTATGGGAGCAT GGAGACACTAACAATTCCACCCATCTCTTGCTTGCAGGAAGGGGAGCCTCAGTCCATCAAAGAGA ACTCATACAGTCTCGGGCTGTGCTTTGTGGTGGCATTAGAAGAGATATATCTGTCAATCCTGTAA GTTCACGAGCTCTTGCAAAGAAGAGGACCTTAACCTCGATCCATGGACCCACTTCCCTTTCTTCC ATGTCACTTGTTTTCTGCATCTTGGTTACTCCACCCGCTTTATTAGCAGCACAAGTGTCTTCGGA TTCTTCCGCCATGGACGTAAC
EgPG27	>M01000041301_RC:1,603 TGATAAGGCACTCTGATAATGGTCTAAGGATCAAGACATGGCAGGGTGGTATGGGGACCGTATCG AGTATTAGCTTCGACACCGTATACCTGGAGAACGTAAGGAATTGTATCATCATAGACCAATACTA TTGCTTGGACAAGAAGTGTAGGAATCAAACATCGGCGGTCTACGTATCCGATGTCTCATACACTA ACATCAAAGGGACATACGATGTAAGGAGTGCCCCCATACACTTTGCATGCAGTGACACCGTGCCA TGCACCAATATTACCATGTCGGAGGTCGAGCTACTACCTTATGAAGGGGAGCTTGTGGATGATCC CTTCTGTTGGAATGCTTATGGGGTCACACAGACCCTCACAATCCCTCCTATCCTTTTTGTTTGCA GGACTGGGCAGCCTCAGAATCTCCAGGACAGCTCCAATTATAATTGCTAACACAACATAACATGC TTTGGCCATAGCAAATAGTAGCCACATATAGAACATAGAATAAAGTCCAAGACCCGTACAGCTGA TGAACAATTTAATTTTTCTTCGTTGTTCTGGCCATTGTGGGGCTTGCATGGTGTTTGTGAACCTT TTCTATATGTATTTGCTT
EgPG28	>M01000041909:1,534 CCTGCTACAATATTGTTATGTTCTGATTGAAATTTTTGATCCAATCCAAAATGAGAACAGATCCT TGGATTAATCCTGGGTTTAGACTGATGTCCGATGCACTTCTATTTGACCCTCACCAGACCCCGCA ATGGTAAGAGCCTCGTGTACTAGGGTACCTCCCTTTTTTTGGTTTCCGACTTTTTATGGGTTAGA TGTGGCCCAAGTAAGGTCTAGAACTGCTAAATGAGCTAAATTGTGCTGCCACAGCTGCTGCTAAT ATTGCTGATGCAGTTTCATTTTATATGGTCATTGCAGCATTGGGAGTTTAGGAAGATATCATAAT GAAGGGGACGTCCGAGGACTCGTCATCAAAGATAGCACCCTTGCCGGGACTTCAAACGGTGTAAG GATCAAGACATGGGAGAACTCTCCAGGAACCAGTAAGGCTGTTAACATGACCTTTGAGAACATTG

Table S2.3. (Cont.) List of the 28 sequences contained either a partial or complete GH28 PG signature domain.

Name of genes	sequence
	TCATGAACAGTGTTGCAAATCCCATCATCATTGACCAGATGTACTGCCCCTANAGCTCTTGTGCA TCAGATGCACCATC
EgPG29	>M01000051458:1,630 AAGGGTAGTTTAGTTCTCATAATCTTGGTGATATTAGTTTAATTTATCGTGTAGATGAAACTCAT AGGCAAGTTTTTGGTGCACACAATAATATGAGAAGCCCTCTGCCTGTGTTCCCTGATTCCTCTAT CCTGAATTAGGTGGGACTGGTTCTTAGGTCTCTGACAGAGCACAAAGTCATCATCAATGAATAAA CTTTACCAGTGAACTCTAACAAGAACATTCTGATGCAATCCTATTATGACATTGCCCTACTTTAG ATTTGGTGCTGTTTCCTATCTTAAGCCAGAAGAACATAAACTAATATGAGCAGTGAGTTTAGCTA AATCTTTCCTAACGTTCACCCTAAGAAAAATAAATTAAAATCAACACACAAAAACAATAGCAATG AGTGTATGTGATTGAATGCAGGCACCATCTGGGGTGATTCTGAGTGACATCTTCTTCCGGAACAT AAGAGGGACGTCGACGACTCCGGTGGCGGTGACCCTCAGGTGCAGCAGAGGAGTGCCATGCAAGA ACGTCAATCTCCAAGACGTCAACCTCAAGTACGTTGGCCAGCTTCCGGCCACTGCCTCGTGCATG AACGTCAAAGCAAGCTTCAGCGGGGACCCCAAAATCCCCCCNCCT
EgPG30	>M01000063855_RC:1,693 AGTTTACTCTGCTAAGAAAAAGAGCAAACAAAGCTACAATTCTGCTTCAAAGTTGCTAACGCTAC TTTCTCCAGTTCAGCATGGCGATCCTTCGATCGCTGTTCTGTGTCTGGATGTTGGTCACATTGCT GTCATTGGGTCCCCAGAGCTCACTCGGAAGATCTCATTTCCATAAGAAGCAAAAGAGTACTCCGA AAAACGGTAAAGGCCATAGCTCTGTGTCCCCCTGTAAATTCCCCAGCAAACGCACCAGGTACTAC CACTACCGATCCCTGCAATTCAAGCTCGGATCCATGTATCTTCGATGTGAGATCCTTCGGTGCGG TCGGTGATGGTTCCACCGATGACACCGAAGCATTCCGGTCGGCATGGAAGGAAGCCTGCTCCGTC GAGTCAGGTACGCTGCTCGTGCCGTCGGATGGCGTCTTCATGATCACTTCCACAATCTTCTCTGG CCCTTGCCAACCGGGGCTTGTGTTTCAAGTTGATGGAGTTTTGATGCCACCCAACGGCCCCGACT GCTGGCCAGAGTCCGACAGCAAGCTCCAGTGGCTCGTGTTTTATCGACTCGATGGGATGACTTTG AGAGGAGAAGGAACAATTGAAGGGAATGGAGAAGAGTGGTGGAACCTCCCCTGCAAACCCCACAG AGGGCCAAATGGATCCACATTGCCCGGACCTTGCAGCAGTCCT
EgPG32	>M01000031649_RC:1,535 GTACCGAGAATAGTTGTATAGGGCCTACAATAGACTGAAATAGGTCCCTCACTGCCAAGGAGGTG AGAAAGAAAGAAAGGAGGACCAAGAGAATCAGCCTCACAGTTCCACTTGGGCCATCTTTTAGCTT CCCCTCCTTTACCAAGTAGAGATGGATCTGCTACACTCCCTTGAGATTGAAACGAGGCATAAAAC ATCATCAAAGATTGTTTCTGTTCCTCACCTTTCCTTGTATAGATCCACTGTATAACACAACACAT ACTGCAGTGGTCAAACAAGTGTGAAAATCCCATATGTTTGCTGACATTAGAGTTTTGGCTTGTGT CATACAGGTGATGACTGCATCTCCATCCAAACAGGATGCTCAAATGTATACATACACAATGTGAA CTGTGGACCAGGCCATGGGATTAGCATAGGCGGACTTGGGAAGGACAACACCAAAGCATGCGTCT CCAATATAACAGTAAGGGATGTCAACATGCATAACACGATGACTGGTGTCCGAATCAAGACCTGG CAGGTAACAAACTTC
EgPG34	>M01000044771_RC:1,534 TAAATTTTCCAGTACAAGTCAGGCAATAAAGTAGGCCTTGGCTAATAGTCGGTCGAAGCTGCACA ACATGGCTAGACCAGCAAAGTTTCTGTCGCTGAAGAAAATAAAAACAATACTTATAGGCAATGCT GTCGAGGTGACAATCCACTGCCACCATCTTCACCATCACCGCCATTTTTTTGTGTAGGCACTGAC CATAGATTCAAGCTCAAAGGTAGGGTGAAGGACCTCACCATCCAGAATGCACAGCAGATGCACTT CACCATCTCCCGATCTGATGCCATACGAGTGTCTGGGTTGCGTGTGAGAGCTCCACAAGACAGCC CTAACACAGATGGCATTCATATCAGTGAATCCACCAATGTTGCCATCCAGAACTGCCACATTGGA ACAGGTACCTTGACATGCTTGTACATTGATCTACCATTCTGATATACCATACATGAAAGATTACC TGAAGGAAACGAGAAGAATAATAACAATAACAGTGATTATTCATTGACTTCACTATGACTGAAAC TGCAATTAACTTCC
EgPG35	>M01000046001:1,808 AGCATAGGAGGACTCGGGAAAGGCAATAGCCCTAGCCTGTGTCTCCAATGTCACTGTTGATACGC ATCAATGTTCAAAATGCTCTGTCTGGAGTAAGGATCAAAACATGGCAGGTAAATACTAAGAAGAC ATGTAAAAACCTTGATTTAGATGTACTGTAATACTAAATATGTGTCCACCAAAAAAGCCATGTAA TCTTACCTTGTGATTTAAGAGATGCTACAAAAATAGTTGATTTATAACTCCTAAACTTTCATCAC AGGGAGGTCTAGGATCTGTCAGGAATGTCATATTTTCCGATGTTCGAGTCTCCAATGTTGAGATC CCAGTTGTGATTGATCAGTATTACTGCAACAAGAAGGCATGCAAGAACAAGACTGATGCAGTGGC TGTTTCAGGAGTCATGTACAAAAGGATAACTGGGACATATTCATACCAACCAATGCATCTTGCTT GCAGTGACAGCAATCCATGCACGAGCATCAAATTGACTGATATCCGGCTATCACCAGTTAATGCA TCTCAATTTCAGCAGGACGCCTTCTGCTGGAAGTCATATGGAGAGTCACAAGGTCCTCTTGAGCC TTTAAGCATTGGTTGCTTGCAAAGGACCAGTAGGTCCATCAAGCCCCTAATAAAGTCATCCAATC ACACTTGCTAGGAAGTATGGCTATTCAATTTCTAGGGCTACTATATTGTTATCATGGCTTCCCCT TTCTGAACTTTGGACAGTAAGAAGGTGATGGTTTTTCTGATGCGTTGATAAGCAGGGAGTGATTC AAAGTTAATTCAGAGAAGAAGAGATTAT

Ethylene Treatment Time (hours)		Gene	Fruit tissue, expression values, percentages and standard deviations					
			AZ		M		P	
			Means	SD	**Means**	SD	**Means**	SD
	0	*EgPG1*	**0.01**	0.003	**0.06**	0.02	**0.10**	0.10
		EgPG3	**0.71**	0.03	**5.65**	0.27	**7.29**	0.38
		EgPG4	**94.32**	2.38	**4.37**	0.38	**7.11**	0.96
		EgPG7	**0.11**	0.01	**0.88**	0.22	**1.15**	0.11
		EgPG8	**0.27**	0.02	**9.95**	0.90	**10.84**	0.41
		EgPG9	**0.26**	0.01	**3.88**	0.53	**7.28**	0.90
		EgPG10	**1.26**	0.02	**15.04**	1.88	**20.01**	1.05
		EgPG11	**1.55**	0.12	**42.68**	2.56	**10.82**	1.03
		EgPG16	**0.13**	0.01	**1.96**	0.16	**3.23**	0.12
		EgPG17	**0.02**	0.002	**3.41**	0.53	**4.29**	0.43
		EgPG18	**1.21**	0.07	**9.58**	0.66	**24.46**	0.98
		EgPG19	**0.03**	0.004	**0.82**	0.15	**1.20**	0.12
		EgPG22	**0.03**	0.01	**1.35**	0.05	**1.32**	0.19
		EgPG26	**0.09**	0.01	**0.37**	0.06	**0.92**	0.21
		TOTAL	**100.00**	2.70	**100.00**	8.37	**100.00**	7.01
	6	*EgPG1*	**0.002**	0.0003	**0.002**	0.001	**0.11**	0.03
		EgPG3	**0.04**	0.003	**0.04**	0.002	**3.21**	0.10
		EgPG4	**99.33**	2.85	**98.64**	4.54	**4.23**	0.21
		EgPG7	**0.01**	0.001	**0.01**	0.0004	**0.58**	0.03
		EgPG8	**0.01**	0.002	**0.004**	0.0004	**0.20**	0.02
		EgPG9	**0.06**	0.003	**0.11**	0.01	**7.03**	0.32
		EgPG10	**0.43**	0.02	**0.99**	0.04	**61.60**	1.95
		EgPG11	**0.05**	0.002	**0.17**	0.01	**18.63**	0.38
		EgPG16	**0.01**	0.001	**0.01**	0.0005	**0.42**	0.01
		EgPG17	**0.002**	0.001	**0.003**	0.001	**0.57**	0.10
		EgPG18	**0.04**	0.003	**0.02**	0.001	**2.83**	0.27
		EgPG19	**0.002**	0.0001	**0.003**	0.0002	**0.12**	0.02
		EgPG22	**0.005**	0.001	**0.004**	0.001	**0.13**	0.04
		EgPG26	**0.02**	0.001	**0.01**	0.001	**0.33**	0.05
		TOTAL	**100.00**	2.70	**100.00**	4.60	**100.00**	3.54

Table S2.4. Percentages were calculated from gene expression data derived from qPCR analysis that included individual values (3 technical repetitions) compared to the average expression of the reference gene (*Eg*E*F1α* : elongation factor 1α), together with the standard deviation (SD) for the following three tissue regions of the fruit: AZ, Abscission Zone; M, Mesocarp; P, Pedicel.

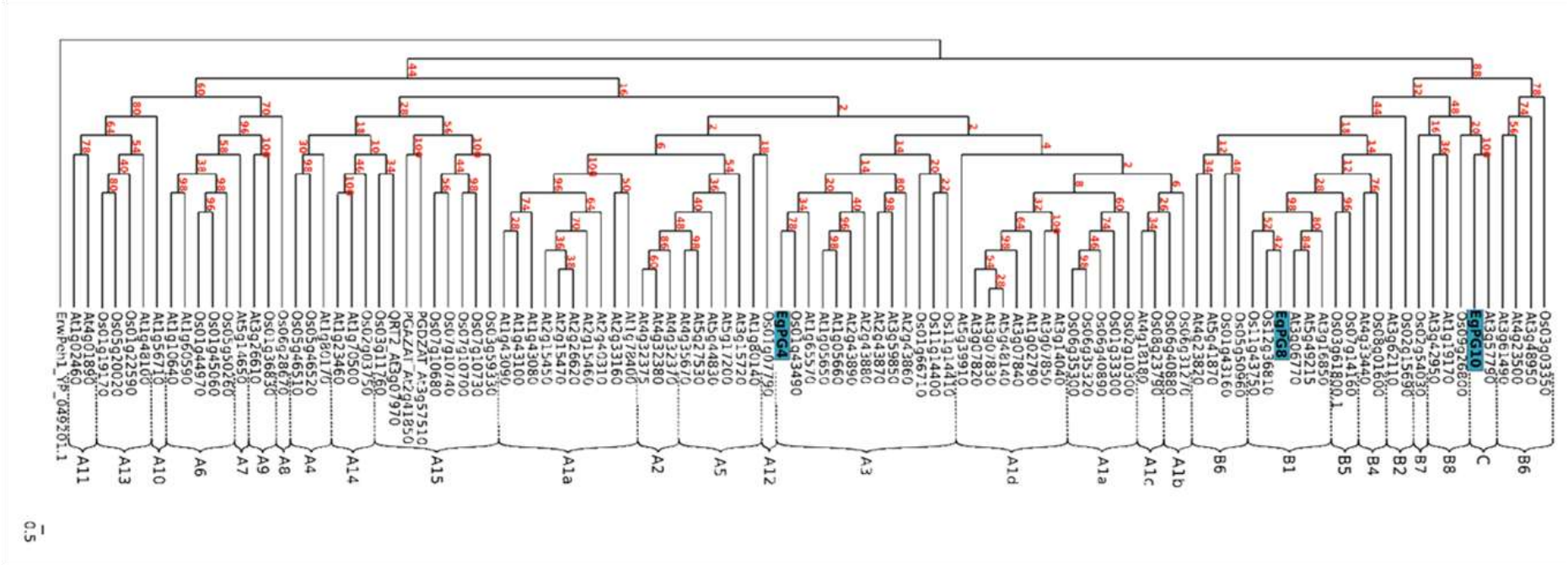

Figure S2.1. Phylogenetic analysis of EgPG4, EgPG8 and EgPG10 with sequences from *Arabidopsis* and rice.

Literature Cited

Addicott, F. (1982). Abscission, University of California Press, Ltd. London.

Asif, M. H. and P. Nath (2005). "Expression of multiple forms of polygalacturonase gene during ripening in banana fruit." Plant Physiol Biochem **43**(2): 177-184.

Atkinson, R. G. (1994). "A cDNA clone for endopolygalacturonase from apple." Plant Physiol **105**(4): 1437-1438.

Berger, R. K. and P. D. Reid (1979). "Role of polygalacturonase in bean leaf abscission." Plant Physiol **63**(6): 1133-1137.

Bonghi, C., N. Rascio, A. Ramina and G. Casadoro (1992). "Cellulase and polygalacturonase involvement in the abscission of leaf and fruit explants of peach." Plant Mol Biol **20**(5): 839-848.

Bourgis, F., A. Kilaru, X. Cao, G. F. Ngando-Ebongue, N. Drira, J. B. Ohlrogge and V. Arondel (2011). "Comparative transcriptome and metabolite analysis of oil palm and date palm mesocarp that differ dramatically in carbon partitioning." P Natl Acad Sci USA **108**(30): 12527-12532.

Cooley, M. B. and J. I. Yoder (1998). "Insertional inactivation of the tomato polygalacturonase gene." Plant Mol Biol **38**(4): 521-530.

Degan, F. D., R. Child, I. Svendsen and P. Ulvskov (2001). "The cleavable N-terminal domain of plant endopolygalacturonases from clade B may be involved in a regulated secretion mechanism." J Biol Chem **276**(38): 35297-35304.

Dellapenna, D., D. C. Alexander and A. B. Bennett (1986). "Molecular cloning of tomato fruit polygalacturonase: Analysis of polygalacturonase mRNA levels during ripening." Proc Natl Acad Sci U S A **83**(17): 6420-6424.

Dellapenna, D., D. S. Kates and A. B. Bennett (1987). "Polygalacturonase Gene Expression in Rutgers, rin, nor, and Nr Tomato Fruits." Plant Physiol **85**(2): 502-507.

Dellapenna, D., J. E. Lincoln, R. L. Fischer and A. B. Bennett (1989). "Transcriptional Analysis of Polygalacturonase and Other Ripening Associated Genes in Rutgers, rin, nor, and Nr Tomato Fruit." Plant Physiol **90**(4): 1372-1377.

Dereeper, A., V. Guignon, G. Blanc, S. Audic, S. Buffet, F. Chevenet, J. F. Dufayard, S. Guindon, V. Lefort, M. Lescot, J. M. Claverie and O. Gascuel (2008). "Phylogeny.fr: robust phylogenetic analysis for the non-specialist." Nucleic Acids Res **36**(Web Server issue): W465-469.

Deytieux-Belleau, C., A. Vallet, B. Doneche and L. Geny (2008). "Pectin methylesterase and polygalacturonase in the developing grape skin." Plant Physiol Biochem **46**(7): 638-646.

Fabi, J. P., B. R. Cordenunsi, G. B. Seymour, F. M. Lajolo and J. R. do Nascimento (2009). "Molecular cloning and characterization of a ripening-induced polygalacturonase related to papaya fruit softening." Plant Physiol Biochem **47**(11-12): 1075-1081.

Felsenstein (1985). "Confidence Limits on Phylogenies: An Approach Using the Bootstrap." Evolution **39**(4): 783-791

Giovannoni, J. J., D. DellaPenna, A. B. Bennett and R. L. Fischer (1989). "Expression of a chimeric polygalacturonase gene in transgenic rin (ripening inhibitor) tomato fruit results in polyuronide degradation but not fruit softening." Plant Cell **1**(1): 53-63.

Gonzalez-Carranza, Z. H., K. A. Elliott and J. A. Roberts (2007). "Expression of polygalacturonases and evidence to support their role during cell separation processes in Arabidopsis thaliana." J Exp Bot **58**(13): 3719-3730.

Gonzalez-Carranza, Z. H., C. A. Whitelaw, R. Swarup and J. A. Roberts (2002). "Temporal and spatial expression of a polygalacturonase during leaf and flower abscission in oilseed rape and Arabidopsis." Plant Physiol **128**(2): 534-543.

Hadfield, K. A. and A. B. Bennett (1998). "Polygalacturonases: Many Genes in Search of a Function." Plant Physiol **117**(2): 337-343.

Hadfield, K. A., J. K. C. Rose, D. S. Yaver, R. M. Berka and A. B. Bennett (1998). "Polygalacturonase gene expression in ripe melon fruit supports a role for polygalacturonase in ripening-associated pectin disassembly." Plant Physiol **117**(2): 363-373.

Hayama, H., T. Shimada, H. Fujii, A. Ito and Y. Kashimura (2006). "Ethylene-regulation of fruit softening and softening-related genes in peach." J Exp Bot **57**(15): 4071-4077.

Henderson, J., H. A. Davies, S. J. Heyes and D. J. Osborne (2001). "The study of a monocotyledon abscission zone using microscopic, chemical, enzymatic and solid state 13C CP/MAS NMR analyses." Phytochemistry **56**(2): 131-139.

Henderson, J. and D. J. Osborne (1990). "Cell Separation and Anatomy of Abscission in the Oil Palm, Elaeis guineensis Jacq." J Exp Bot **41**(2): 203-210.

Henderson, J. and D. J. Osborne (1994). "Inter-tissue signalling during the two-phase abscission in oil palm fruit." J Exp Bot **45**(7): 943-951.

Hong, S. B. and M. L. Tucker (1998). "Genomic organization of six tomato polygalacturonases and 5 ' upstream sequence identity with tap1 and win2 genes." Mol Gen Genet **258**(5): 479-487.

Huang, L., J. Cao, A. Zhang, Y. Ye, Y. Zhang and T. Liu (2009a). "The polygalacturonase gene BcMF2 from Brassica campestris is associated with intine development." J Exp Bot **60**(1): 301-313.

Huang, L., Y. Ye, Y. Zhang, A. Zhang, T. Liu and J. Cao (2009b). "BcMF9, a novel polygalacturonase gene, is required for both Brassica campestris intine and exine formation." Ann Bot **104**(7): 1339-1351.

Jabnoune, M., S. Espeout, D. Mieulet, C. Fizames, J. L. Verdeil, G. Conejero, A. Rodriguez-Navarro, H. Sentenac, E. Guiderdoni, C. Abdelly and A. A. Very (2009). "Diversity in expression patterns and functional properties in the rice HKT transporter family." Plant Physiol **150**(4): 1955-1971.

Jenkins, E. S., W. Paul, S. A. Coupe, S. J. Bell, E. C. Davies and J. A. Roberts (1996). "Characterization of an mRNA encoding a polygalacturonase expressed during pod development in oilseed rape (Brassica napus L)." J Exp Bot **47**(294): 111-115.

Jenkins, E. S., W. Paul, M. Craze, C. A. Whitelaw, A. Weigand and J. A. Roberts (1999). "Dehiscence-related expression of an Arabidopsis thaliana gene encoding a polygalacturonase in transgenic plants of Brassica napus." Plant Cell Environ **22**(2): 159-167.

Jiang, C. Z., F. Lu, W. Imsabai, S. Meir and M. S. Reid (2008). "Silencing polygalacturonase expression inhibits tomato petiole abscission." J Exp Bot **59**(4): 973-979.

Jones, D. T., W. R. Taylor and J. M. Thornton (1992). "The rapid generation of mutation data matrices from protein sequences." Comput Appl Biosci **8**(3): 275-282.

Kalaitzis, P., S. M. Koehler and M. L. Tucker (1995). "Cloning of a tomato polygalacturonase expressed in abscission." Plant Mol Biol **28**(4): 647-656.

Kalaitzis, P., T. Solomos and M. L. Tucker (1997). "Three Different Polygalacturonases Are Expressed in Tomato Leaf and Flower Abscission, Each with a Different Temporal Expression Pattern." Plant Physiol **113**(4): 1303-1308.

Kim, J. and S. E. Patterson (2006). "Expression divergence and functional redundancy of polygalacturonases in floral organ abscission." Plant Signal Behav **1**(6): 281-283.

Kim, J., S.-H. Shiu, S. Thoma, W.-H. Li and S. Patterson (2006). "Patterns of expansion and expression divergence in the plant polygalacturonase gene family." Genome Biol **7**(9): R87.

Leslie, M. E., M. W. Lewis and S. J. Liljegren (2007). Organ Abscission. Annual Plant Reviews Volume 25: Plant Cell Separation and Adhesion, Blackwell Publishing Ltd**:** 106-136.

Lester, D. R., J. Speirs, G. Orr and C. J. Brady (1994). "Peach (Prunus persica) endopolygalacturonase cDNA isolation and mRNA analysis in melting and nonmelting peach cultivars." Plant Physiol **105**(1): 225-231.

Mbéguié-A-Mbéguié, D., O. Hubert, F. C. Baurens, T. Matsumoto, M. Chillet, B. Fils-Lycaon and S. Sidibé-Bocs (2009). "Expression patterns of cell wall-modifying genes from banana during fruit ripening and in relationship with finger drop." J Exp Bot **60**(7): 2021-2034.

Morcillo, F., C. Gagneur, H. Adam, F. Richaud, R. Singh, S.-C. Cheah, A. Rival, Y. Duval and J. W. Tregear (2006). "Somaclonal variation in micropropagated oil palm. Characterization of two novel genes with enhanced expression in epigenetically abnormal cell lines and in response to auxin." Tree Physiol **26**(5): 585-594.

Murayama, H., D. Sekine, Y. Yamauchi, M. Gao, W. Mitsuhashi and T. Toyomasu (2006). "Effect of girdling above the abscission zone of fruit on 'Bartlett' pear ripening on the tree." J Exp Bot **57**(14): 3679-3686.

Ogawa, M., P. Kay, S. Wilson and S. M. Swain (2009). "ARABIDOPSIS DEHISCENCE ZONE POLYGALACTURONASE1 (ADPG1), ADPG2, and QUARTET2 Are Polygalacturonases Required for Cell Separation during Reproductive Development in Arabidopsis." Plant Cell **21**(1): 216-233.

Osborne, D. J., J. Henderson and R. H. V. Corley (1992). "Controlling fruit-shedding in the oil palm." Endeavour **16**(4): 173-177.

Petersen, M., L. Sander, R. Child, H. vanOnckelen, P. Ulvskov and B. Borkhardt (1996). "Isolation and characterisation of a pod dehiscence zone-specific polygalacturonase from Brassica napus." Plant Mol Biol **31**(3): 517-527.

Pfaffl, M. W. (2001). "A new mathematical model for relative quantification in real-time RT-PCR." Nucleic Acids Res **29**(9): e45.

Rival, A. (2007). Oil Palm. Biotechnology in Agriculture and Forestry, Springer-Verlag Berlin Heidelberg. **61:** 59-80.

Roberts, J. A., K. A. Elliott and Z. H. Gonzalez-Carranza (2002). "Abscission, Dehiscence, and Other Cell Separation Processes." Annu Rev Plant Biol **53**(1): 131-158.

Roberts, J. A., B. Schindler and G. A. Tucker (1984). "Ethylene-promoted tomato flower abscission and the possible involvement of an inhibitor." Planta **160**: 159-163.

Saitou, N. and M. Nei (1987). "The neighbor-joining method: a new method for reconstructing phylogenetic trees." Mol Biol Evol **4**(4): 406-425.

Sander, L., R. Child, P. Ulvskov, M. Albrechtsen and B. Borkhardt (2001). "Analysis of a dehiscence zone endo-polygalacturonase in oilseed rape (Brassica napus) and Arabidopsis thaliana: evidence for roles in cell separation in dehiscence and abscission zones, and in stylar tissues during pollen tube growth." Plant Mol Biol **46**(4): 469-479.

Sekine, D., I. Munemura, M. Gao, W. Mitsuhashi, T. Toyomasu and H. Murayama (2006). "Cloning of cDNAs encoding cell-wall hydrolases from pear (Pyrus communis) fruit and their involvement in fruit softening and development of melting texture." Physiol Plant **126**(2): 163-174.

Sexton, R. and J. A. Roberts (1982). "Cell Biology of Abscission." Ann Rev Plant Physio **33**(1): 133-162.

Sheehy, R. E., M. Kramer and W. R. Hiatt (1988). "Reduction of polygalacturonase activity in tomato fruit by antisense RNA." Proc Natl Acad Sci USA **85**(23): 8805-8809.

Sitrit, Y. and A. B. Bennett (1998). "Regulation of tomato fruit polygalacturonase mRNA accumulation by ethylene: A Re-examination." Plant Physiol **116**(3): 1145-1150.

Sitrit, Y., K. A. Hadfield, A. B. Bennett, K. J. Bradford and A. B. Downie (1999). "Expression of a polygalacturonase associated with tomato seed germination." Plant Physiol **121**(2): 419-428.

Smith, C. J., C. F. Watson, P. C. Morris, C. R. Bird, G. B. Seymour, J. E. Gray, C. Arnold, G. A. Tucker, W. Schuch, S. Harding and *et al.* (1990). "Inheritance and effect on ripening of antisense polygalacturonase genes in transgenic tomatoes." Plant Mol Biol **14**(3): 369-379.

Smith, C. J. S., C. F. Watson, J. Ray, C. R. Bird, P. C. Morris, W. Schuch and D. Grierson (1988). "Antisense RNA inhibition of polygalacturonase gene expression in transgenic tomatoes." Nature **334**(6184): 724-726.

Tacken, E., H. Ireland, K. Gunaseelan, S. Karunairetnam, D. Wang, K. Schultz, J. Bowen, R. G. Atkinson, J. W. Johnston, J. Putterill, R. P. Hellens and R. J. Schaffer (2010). "The role of ethylene and cold temperature in the regulation of the apple POLYGALACTURONASE1 gene and fruit softening." Plant Physiol **153**(1): 294-305.

Taylor, J. E., G. A. Tucker, Y. Lasslett, C. J. S. Smith, C. M. Arnold, C. F. Watson, W. Schuch, D. Grierson and J. A. Roberts (1990). "Polygalacturonase expression during leaf abscission of normal and transgenic tomato plants." Planta **183**(1): 133-138.

Taylor, J. E., S. T. J. Webb, S. A. Coupe, G. A. Tucker and J. A. Roberts (1993). "Changes in Polygalacturonase Activity and Solubility of Polyuronides during Ethylene-stimulated Leaf Abscission in Sambucus nigra." J Exp Bot **44**(1): 93-98.

Taylor, J. E. and C. A. Whitelaw (2001). "Signals in abscission." New Phytol **151**(2): 323-340.

Tebbutt, S. J., H. J. Rogers and D. M. Lonsdale (1994). "Characterization of a tobacco gene encoding a pollen-specific polygalacturonase." Plant Mol Biol **25**(2): 283-297.

Thompson, J. D., D. G. Higgins and T. J. Gibson (1994). "CLUSTAL W: improving the sensitivity of progressive multiple sequence alignment through sequence weighting, position-specific gap penalties and weight matrix choice." Nucleic Acids Res **22**(22): 4673-4680.

Torki, M., P. Mandaron, R. Mache and D. Falconet (2000). "Characterization of a ubiquitous expressed gene family encoding polygalacturonase in Arabidopsis thaliana." Gene **242**(1-2): 427-436.

Tranbarger, T. J., S. Dussert, T. Joët, X. Argout, M. Summo, A. Champion, D. Cros, A. Omore, B. Nouy and F. Morcillo (2011). "Regulatory mechanisms underlying oil palm fruit mesocarp maturation, ripening and functional specialization in lipid and carotenoid metabolism." Plant Physiol.

Tucker, G. A., B. Schindler and J. A. Roberts (1984). "Flower abscission in mutant tomato plants." Planta **160**: 164-167.

Tucker, M. L., A. Burke, C. A. Murphy, V. K. Thai and M. L. Ehrenfried (2007). "Gene expression profiles for cell wall-modifying proteins associated with soybean cyst nematode infection, petiole abscission, root tips, flowers, apical buds, and leaves." J Exp Bot **58**(12): 3395-3406.

Wang, Z. Y., E. A. MacRae, M. A. Wright, K. M. Bolitho, G. S. Ross and R. G. Atkinson (2000). "Polygalacturonase gene expression in kiwifruit: relationship to fruit softening and ethylene production." Plant Mol Biol **42**(2): 317-328.

Chapter 3. Abscission Zone Development and Acquisition of Competence for Cell Separation Functions and Response to Ethylene

Introduction

Abscission can also occur in various parts of plant such as leaf (Belfield *et al.* 2005), flower (Patterson and Bleecker 2004), and fruit (Cin *et al.* 2005). Ethylene-containing illuminating gas was first reported in defoliation between 1860 and 1870 (Burg 1968). Since ethylene is recognized as a plant organ shedding and separation substance, studies have been performed in many plant species such as *Arabidopsis* (Francis *et al.* 2006), apple (Li and Yuan 2008), tomato (Gonzalez-Bosch *et al.* 1997), and oil palm (Henderson and Osborne 1994).

Cell separation occurring during abscission is a tissue and cellular process involving the differentiation of a special zone located at the base of the organ called abscission zone (AZ). Generally, the plant AZ consists of one to several layers of cells. Cells in this zone have isodiametrically shape with dense cytoplasms (Addicott 1982; Sexton and Roberts 1982; Roberts *et al.* 2002). The oil palm AZ has distinct characteristics. It has two main AZs, called primary and adjacent zones. The primary zone is the first area to be separated while adjacent zones separate only after the primary zone has separated, that suggested an inducing signal arises from the primary zone (Henderson and Osborne 1994). Adjacent cell walls are joined together by the middle lamella composed primarily of pectin. Pectin, known as the most structurally complex family of cell wall polysaccharides, is a major component of primary walls of both monocots and dicots (Mohnen 2008). Pectin is also the main component of the middle lamella between adjacent cells (Willats *et al.* 2001a; O'Neill *et al.* 2004). It is of paramount importance for cell adhesion and during cell separation (Jarvis *et al.* 2003). However, the structural characteristics and the role of how pectin functions during cell separation are not completely understood.

The methyl-esterification of homogalacturonan (HG) plays an important role during plant development, can modulate the functionality of the pectin, and plays particular roles for

cell adhesion and for cell separation to occur (Jarvis *et al.* 2003). HG is thought to be synthesized in the golgi complex, targeted through vesicles via the PM to the apoplast and finally inserted into the cell wall in a highly methylated form (Kauss and Hassid 1967; Zhang and Staehelin 1992; Lennon and Lord 2000). However, the current model of pectin synthesis is limited to studies on only a few species and developmental contexts, and therefore may not be universal. In ripe oil palm fruit, high levels of unmethylated pectin shows in AZ (Henderson *et al.* 2001a). During development, cells undergo de-esterification and when intercellular spaces arise after cell division, modulation of the methyl-esterification status occurs at cell junctions for separation to take place (Willats *et al.* 2001b). It is believed that de-esterification allows the formation of calcium (Ca^{2+}) cross links resulting in the "egg-box" pectin configuration between adjacent polymers (Grant *et al.* 1973; Cosgrove 2005). The de-esterification of HG is catalyzed by enzymes called pectin methylesterases (PME, EC 3.1.1.11) which modulate the methylation status of pectin HG (Pelloux *et al.* 2007). Besides, de-esterification-related crosslinking increases pectin rigidity and may also allow targeting of other cell wall modifying or pectin-degrading enzymes such as polygalacturonase (PG, EC 3.2.1.15) that further modify the texture and rigidity of the cell wall and may have roles during cell separation processes such as those controlling organ abscission (Hadfield and Bennett 1998).

The objectives of this chapter are:

1. To determine the cellular characteristic changes associated to the development of the AZ during oil palm fruit development and after shedding to provide insight in to the mechanisms that underlie the acquisition of AZ function.

2. To examine changes in cellular characteristics related to cell separation to gain insight into the underlying mechanisms of AZ function.

In this chapter, classical histology stained with different dyes was used to examine cellular characteristics of the oil palm fruit AZ. Toluidine blue is a metachromasia compound that stains lignin and phenols to bluish-green with a pH-independent covalent bonding and non-lignin cell wall components to reddish-violet (acid) (e.g. pectin) and bluish-violet (neutral) (Conrad 2008). Ruthenium red is a specific dye to pectin, which selectively binds to the intramolecular spaces of carboxyl groups of pectin (Hou *et al.* 1999; Usadel *et al.* 2004; Leroux *et al.* 2007).

Due to the resolution limitation of low contrast microscopy, the electron microscope (EM) was used to allow a more detailed histological characterization. EM achieves resolution lower than 20 Å in micrographs (Watson 1958). Thus, the electron microscope was also used in this experiment in order to determine ultrastructure characteristics.

In the current study, the use of immunochemical techniques were employed to characterize the pectin in the cell walls of the AZ compared to the neighbouring mesocarp (M) and pedicel (P) tissues during development and cell separation that leads to fruit shedding. Advantages of immunochemical techniques over other methods such as chemical methods in structural analysis of pectin are the relatively small amounts of material required, possible to use for single cell wall localization, and no pectin property changes (Willats *et al.* 2000). Willats *et al.* (2000), found that JIM5 and JIM7 both bound preferentially to samples with a wide methyl-esterification pattern rather to fully de-esterified pectin. In order to understand the epitope structures recognized by JIM5, JIM7 and LM7, another pectin antibody, Clausen et al, 2003 used five methyl hexagalacturonates with varying occurrences of methyl-ester groups (Figure 3.1). Competitive-inhibition ELISAs were used by determining the effectiveness of the methyl hexagalacturonates in inhibiting the binding of the antibodies to model pectin (Figure 3.1). JIM5 was inhibited by compounds 1 and 2 and it was concluded that JIM5 requires at least four contiguous un-esterified residues between or

adjacent to a methyl-ester group to optimally bind. In contrast, JIM7 was inhibited by compounds 3, 4 and 5, which indicated that the important features of the JIM7 epitope are methyl-ester groups at every second residue and no preference for the esterification state of the intervening residue. LM7 was inhibited only by compound 1, indicating that LM7 requires four un-esterified GalA residues between methyl-ester groups. The epitope of LM8 is xylogalacturonan (XGA) associated with detached cells or supposed to be detached cells in pea and legume (Willats *et al.* 2004).

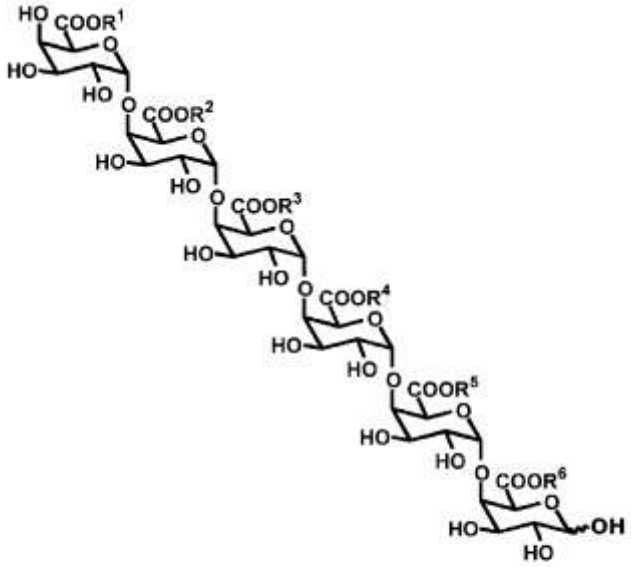

Cmp	R^1	R^2	R^3	R^4	R^5	R^6		Inhibited antibody
1	Me	H	H	H	H	Me		JIM5, LM7
2	Me	Me	H	H	H	Me		JIM5
3	H	H	Me	Me	Me	H	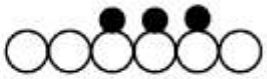	JIM7
4	H	Me	Me	Me	Me	H	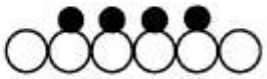	JIM7
5	Me	H	Me	H	Me	H		JIM7

Figure 3.1. Structure of methyl hexagalacturonates (compounds 1-5) used as potential haptens. The presence or absence of methyl-ester groups is shown for each residue (R^1 to R^6). The methyl-esterification pattern of each compound is shown schematically. The inhibited antibodies are shown for each compound. Adapted from (Clausen *et al.* 2003)

Results

Cellular studies of the oil palm fruit abscission zone

Cellular characteristics of the primary abscission zone of ripe fruit

At 30 DAP, cell division and expansion known to take place in the M at this stage (Tranbarger *et al.* (2011). The size of the fruit increases dramatically from 30 DAP to 60 DAP fruit. After that, 120 DAP is the beginning of maturation stage by an increase in M fresh mass and the beginning of lipid accumulation (Tranbarger *et al.* 2011). During maturation, the ripening stage starts at 140 DAP and continues until the fruit are shed. During the ripening process, the signal initiating cell separation starts and leads to the final step: fruit shedding at the AZ (Osborne *et al.* 1992). The ethylene treatment experimental data presented in Chapter Two clearly showed that fruits at 30, 120, and 180 DAP responded to ethylene differently. 30 DAP fruits abscised at 24 h with ethylene treatment, while 120 DAP and 180 DAP fruits started to abscised at 12 h and 9 h with ethylene treatment. The selected ages of fruit in this experiment are good stages to examine the developmental aspects but in relation to ethylene treatment.

At the ripe stage of development, around 180 DAP, the fruit AZ are fully functional to respond to the signals that start the process of cell separation and lead to fruit shedding. In the following section, I have performed a detailed description of the AZ at this precise stage of fruit development, just before cell separation process.

In the AZ there are two main types of tissues: parenchyma tissue and vascular bundles (phloem and xylem, vascular parenchyma). In addition, parenchyma tissue has two cell types: non-polyphenol containing parenchyma cells and polyphenol-containing parenchyma cells (Figure 3.2 B). Polyphenol-containing cells can be found throughout three fruit tissues (M, AZ, and P) with a high amount in the P and AZ tissues (Figure 3.2 A). Parenchyma cells in AZ appear smaller than those in adjoining tissues (M and P) (Figure 3.2) and they have a lot

of different shape particles accumulated inside them which are supposed to be acidic pectin because they are stained with toluidine blue in reddish-violet, and ruthenium red (Figure 3.2 B, 2.4 H, and Figure 3.10 C). One other interesting characteristic is the well aligned nuclei of the AZ cells which can easily be used to count the AZ cell layers after DAPI staining (Figure 3.2 C, and D). Generally, there are 8-10 cell layers in AZ and possibly more or less in some regions. Vascular tissues have another interesting characteristic of non-fully differentiated tissues which is unlignified when passing through the AZ and becoming lignified in non-AZ tissues (Figure 3.2 A, and B).

Ontogenesis and cellular characteristic evolution of primary AZ during fruit development

Because the previous data showed a difference in the response to ethylene depend on stage of fruit development and consequently affected the number of fruit separated (Figure 2.1), we decided to compare the AZ at the cellular level at 30, 120 and 180 DAP that represent different degrees of capacity for the AZ to function. An overview of the cellular characteristics of the M, AZ and P during these three stages of fruit development is shown in Figures 3.3, 3.4, and 3.7-3.9.

At 30 DAP, differences in the orientation of cell division between M, AZ and P are visible. In the AZ, cell division is periclinal while in the M and P, cell divisions are anticlinal (Figure 3.4 A-C, see arrows). The cell shape at this stage is quite isodiametric (Figure 3.7). Vascular parenchyma tissues have not been lignified yet but can be distinguished from parenchyma cells (longer thinner cells) (Figure 3.2 B). As mentioned before, polyphenol-containing cells are found among M, AZ and P parenchyma cells but are most evident in P and AZ (Figure 3.3 A). Nuclear alignment is starting to be visualized in vascular tissues. It is easily to define nucleus by conventional histological method. At 120 DAP, most of the cells have finished cell division, however, a few recent cell divisions can be observed (Figure 3.4

D-F) and the cell shape is elongated (Figure 3.8). Pectin appears to accumulate in AZ, which can be detected by toluidine blue staining (Figure 3.4 E) and confirmed by pectin-specific staining with ruthenium red (Figure 3.10 D). Xylem vessels are well differentiated and lignified except those in AZ (Figure 3.3 C). Polyphenol-containing cells appear larger by 120 DAP (Figure 3.3 C). Nuclear alignment and the layers of the AZ are easily detectable with DAPI in parenchyma cells (Figure 3.3 D). It is difficult to define, but the nucleus is visible by conventional histological method (Figure 3.4 E). At 180 DAP, cell division is finished and no dividing cells are observed (Figure 3.4 G-I). The cell shape is the most elongated (Figure 3.9). Pectin is highly accumulated in AZ (Figure 3.4 H, and Figure 3.10 C). Vascular tissues and polyphenol-containing cells have no change (Figure 3.3 E).

To complete these observations, we measured several quantitative parameters of the cells from the different fruit tissues. Figure 3.5 shows the way that measurements were performed on three majors parameters including: cell width, cell wall width and middle lamella width. The cell width measurement data from classical histology reveals that the width of the M cell average is about 28.29 µm at 30 DAP and significantly increases to about 36.67 µm at 120 DAP. Considering the AZ, the width of the cell average is about 16.05 µm at 30 DAP and significantly increases to about 17.84 µm at 120 DAP. At 180 DAP, the cell width gains maximum about 21.87 µm while in P, the width of the cell average is about 30.94 µm at 30 DAP and has no significantly increases to about 32.08 µm at 120 DAP. At 180 DAP, the cell width gains maximum about 34.19 µm. Interestingly, the AZ cell width at each developmental stages remains smaller than the other tissues (Figure 3.6 A).

In view of the M, the width of the cell wall average is about 0.59 µm at 30 DAP and significantly increases to about 1.25 µm at 120 DAP. At 180 DAP, the cell wall width gains maximum about 2.59 µm. Examining the AZ, the width of the cell wall average is about 0.91 µm at 30 DAP and significantly increases to about 2.12 µm at 120 DAP. At 180 DAP, the

cell wall width gains maximum about 2.58 µm. Considering the P, the width of the cell wall average is about 1.05 µm at 30 DAP and significantly increases to about 1.26 µm at 120 DAP. At 180 DAP, the cell wall width gains maximum about 2.61 µm. Interestingly, AZ cell wall width at 120 DAP dramatically increases more than the other tissues. At 180 DAP, all tissues gain the maximum width and have no statistically significant difference (Figure 3.6 B).

Looking at the middle lamella at 30 DAP, no data is available because it is impossible to measure the middle lamella width from confocal microscopy images. Examining the M, the width of the middle lamella average is about 0.58 µm at 120 DAP and significantly increases to about 0.93 µm at 180 DAP. Considering AZ, the width of the middle lamella average is about 0.59 µm at 120 DAP and significantly increases to about 0.94 µm at 180 DAP. Considering P, the width of the middle lamella average is about 0.65 µm at 120 DAP and significantly increases to about 0.99 µm at 180 DAP. Interestingly, the middle lamella width of all tissues has no significantly difference between 120 and 180 DAP (Figure 3.6 C).

Cellular characteristics of primary AZ during and after cell separation

To understand the tissue and cellular modifications in the AZ during fruit shedding, ethylene was used to induce cell separation of oil palm fruit at 180 DAP (Figure 2.1). During and after cell separation occurs, no cell rupture appears and no cell divisions occur. Cells separate in the middle region of AZ layers not at the outer layers towards the adjacent P or M tissues (Figure 3.12 A, and C). Finally, the observed prominent characteristic after cell separation is the change of toluidine blue staining from reddish-violet to bluish violet at the AZ which indicates a change of acidity in this region, possibly due to a change from acidic to more neutral pectin. In contrast, in the M, many cells can be found with a lot of acidic pectin

inside (Figure 3.12 B, Figure S3.3 C) as in P, where acidic pectin can be found in the cells as well (Figure 3.12 D, Figure S3.3 D).

The cell width measurement data from classical histology before and after separation reveals that the average width of the M cells and P cells do not significantly change at 180 DAP with ethylene treatment when separation occurs in the AZ. By contrast, the width of the AZ cell average is about 21.87 µm at 180 DAP and a slight but significant decrease to about 19.28 µm is observed at 180 DAP with ethylene treatment when separation occurs. Considering P, the width of the cell average is about 34.19 µm at 180 DAP and has no significantly decreases to about 34.12 µm at 180 DAP with ethylene treatment (separation occurs) (Figure 3.11 A). For additional staining, see supplementary data.

In view of the M, the width of the cell wall average is about 2.59 µm at 180 DAP with no significant increase at 180 DAP with ethylene treatment. Considering the AZ, the width of the cell wall average is about 2.58 µm at 180 DAP and significantly decreases to about 1.76 µm at 180 DAP with ethylene treatment at the separated layer and to about 1.84 µm at 180 DAP with ethylene treatment in unseparated AZ layers. Examining the P, the width of the cell wall average is about 2.61 µm at 30 DAP and slightly but significantly decreases to about 2.46 µm at µm at 180 DAP with ethylene treatment (Figure 3.11 B).

At 180 DAP in M, the width of the middle lamella average is about 0.93 µm and significantly decreases to about 0.52 µm after ethylene treatment (separation occurs in AZ). The same was observed for P, the width of the middle lamella average is about 0.99 µm at 180 DAP and significantly decreases to about 0.58 µm at 180 DAP with ethylene treatment (separation occurs in AZ) (Figure 3.11 C). Looking at AZ, the width of the middle lamella average is about 0.94 µm, and in contrast to M and P significantly increases after ethylene treatment to about 1.49 µm at level of separated layer and to about 1.10 µm at level of unseparated layers (Figure 3.11 C).

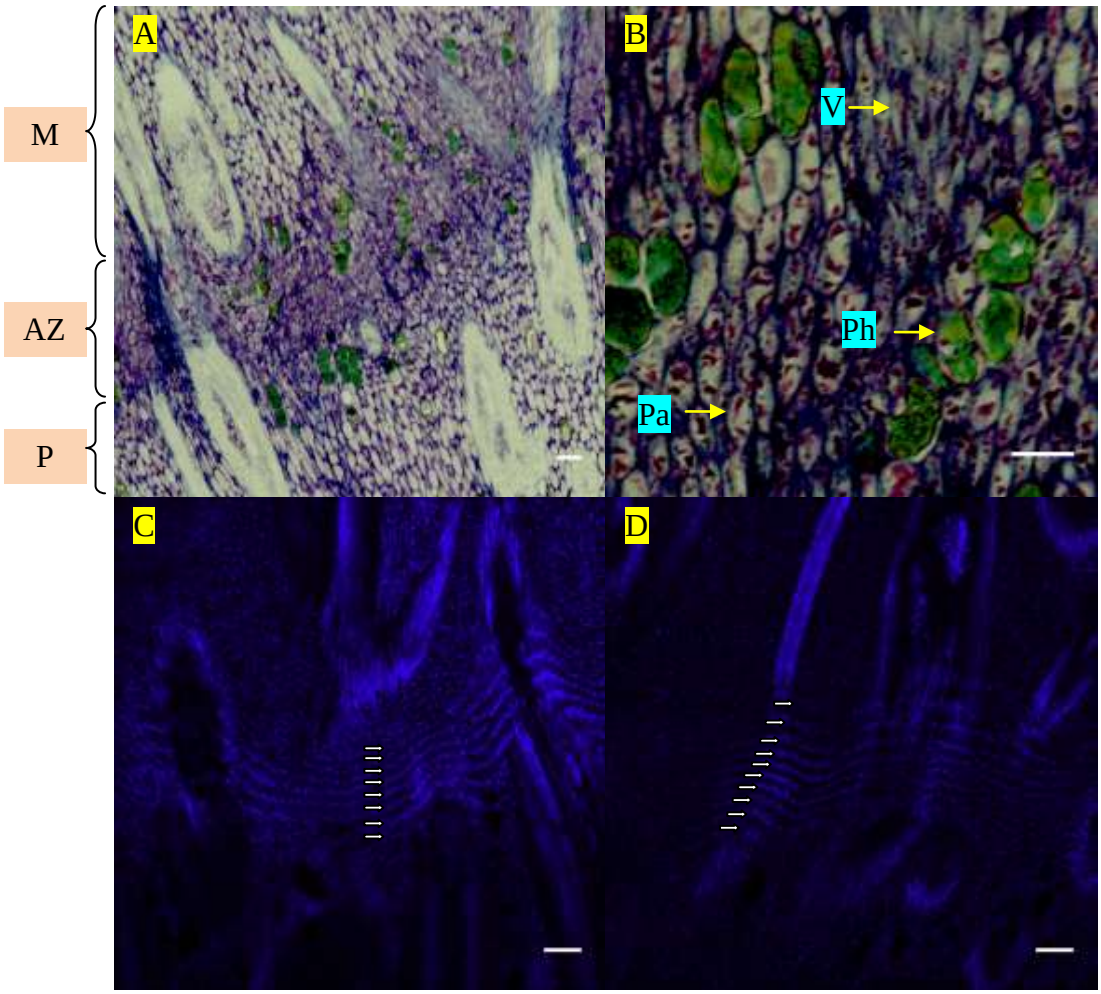

Figure 3.2. Classical histology stained with Toluidine blue show the overview of AZ and different cell types within AZ in ripe fruit. Fluorescence histology stained with DAPI show AZ cell layers. (A) 180 DAP fruit AZ classical histology overview including M (upper) and P (lower). (B) Classical histology of 180 DAP AZ tissues with different cell types. (C, D) fluorescence histology of AZ show well-aligned AZ nucleus different from M (upper) and P (lower) after DAPI staining. Pa = Parenchyma cell, Ph = Polyphenolic-containing parenchyma cell, V = vascular parenchyma tissues. Scale bar = 100 µm in A, C, and D, scale bar = 50 µm in B.

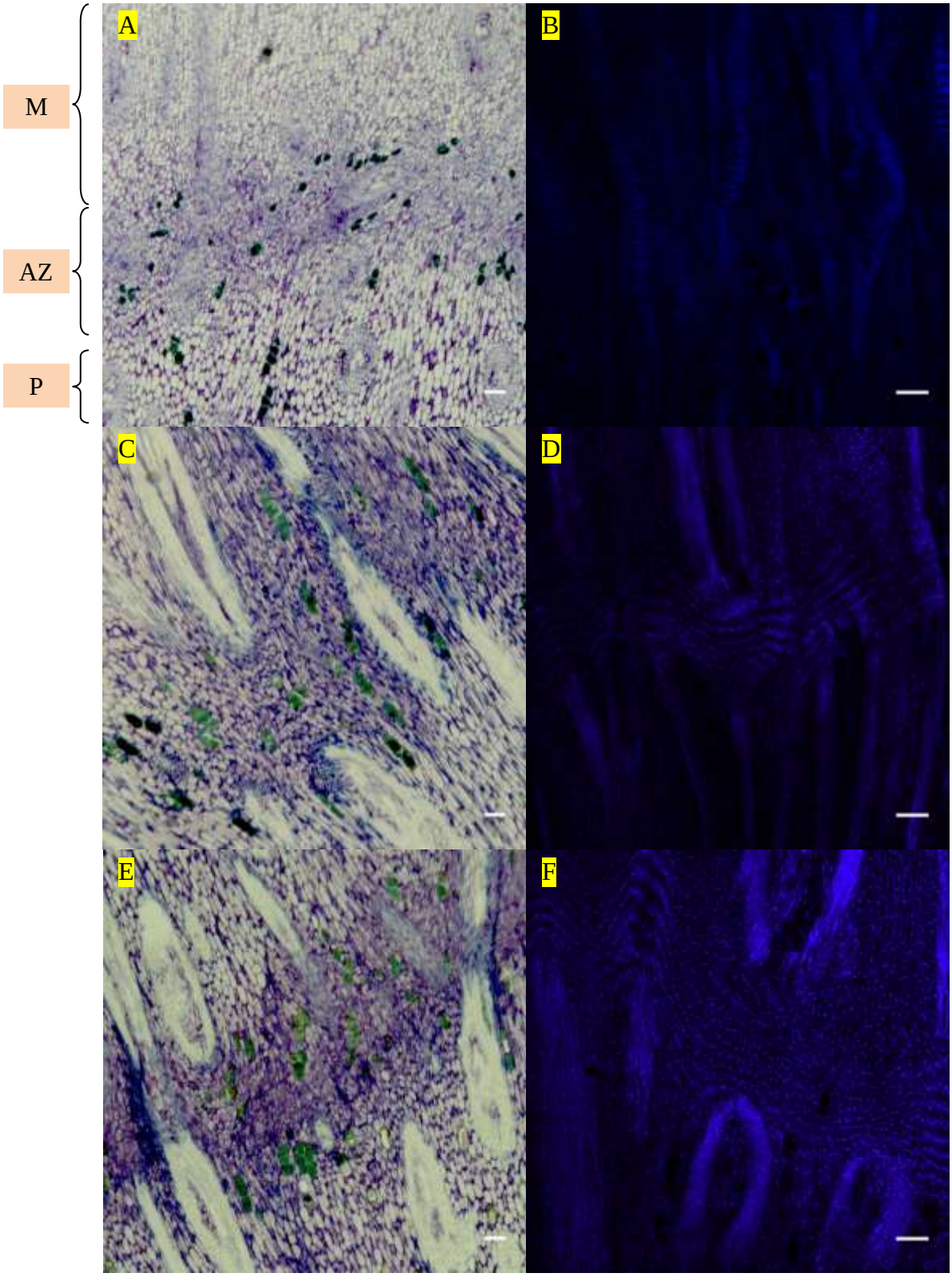

Figure 3.3. Comparison of AZ during developmental stages by classical histology and fluorescence histology after DAPI staining. (A, B) 30 DAP classical histology and fluorescence histology, respectively. (C, D) 120 DAP classical histology and fluorescence histology, respectively. (E, F) 180 DAP classical histology and fluorescence histology, respectively. Scale bar = 100 µm.

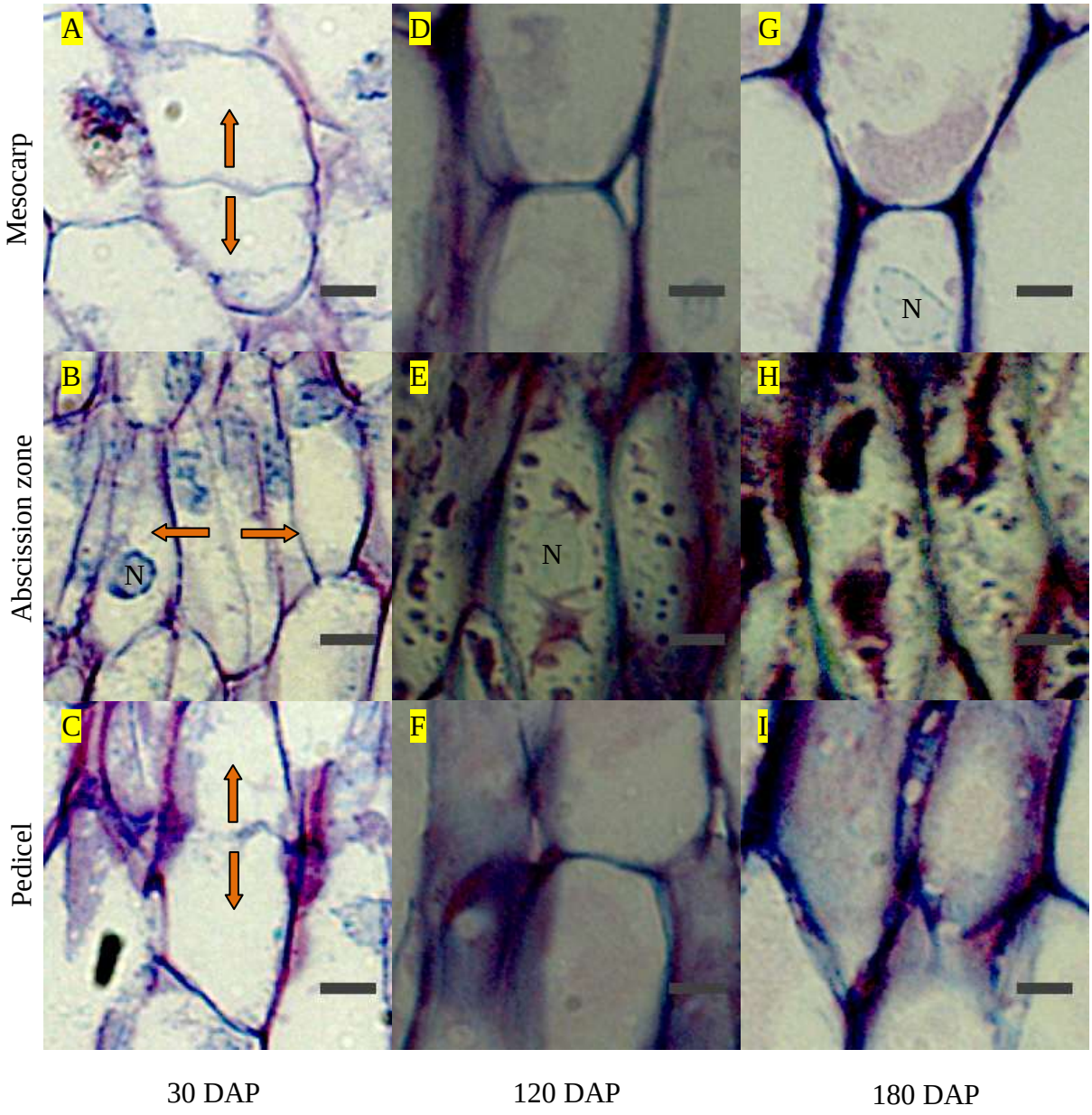

Figure 3.4. Classical histology stained with toluidine blue show M, AZ, and P cells during fruit development at 30, 120, and 180 DAP. (A) 30 DAP M shows cell division in anticlinal direction. (D), and (G) show 120, and 180 DAP M, respectively. (B) 30 DAP AZ shows cell division in periclinal direction. (E), and (H) show 120, and 180 DAP AZ accumulating pectic-supposed substances inside, respectively. (C) 30 DAP P shows cell division in anticlinal direction. (F), and (I) show 120, and 180 DAP P, respectively. N = Nucleus. Scalebar = 10 µm.

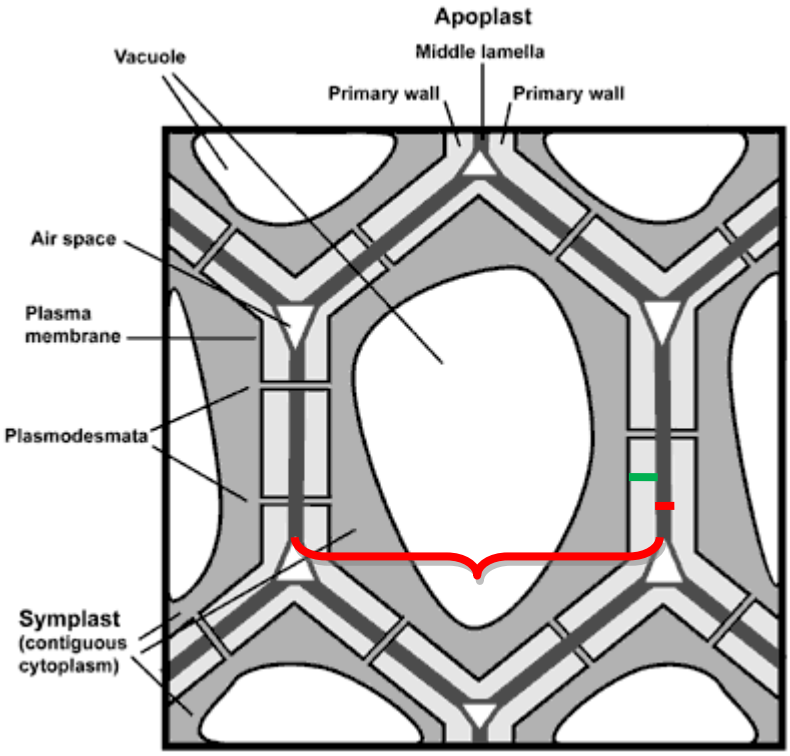

Figure 3.5. Adapted plant cell wall diagram (http://www.ccrc.uga.edu/~mao/intro/ouline.htm) shows measured region for cell width (measured under low contrast microscopy images), cell wall width (measured under confocal microscopy images), and middle lamella width (measured under confocal microscopy images). The red bracket represents the measured cell width. The green straight line represents the measured cell wall width. The red straight line represents the measured middle lamella.

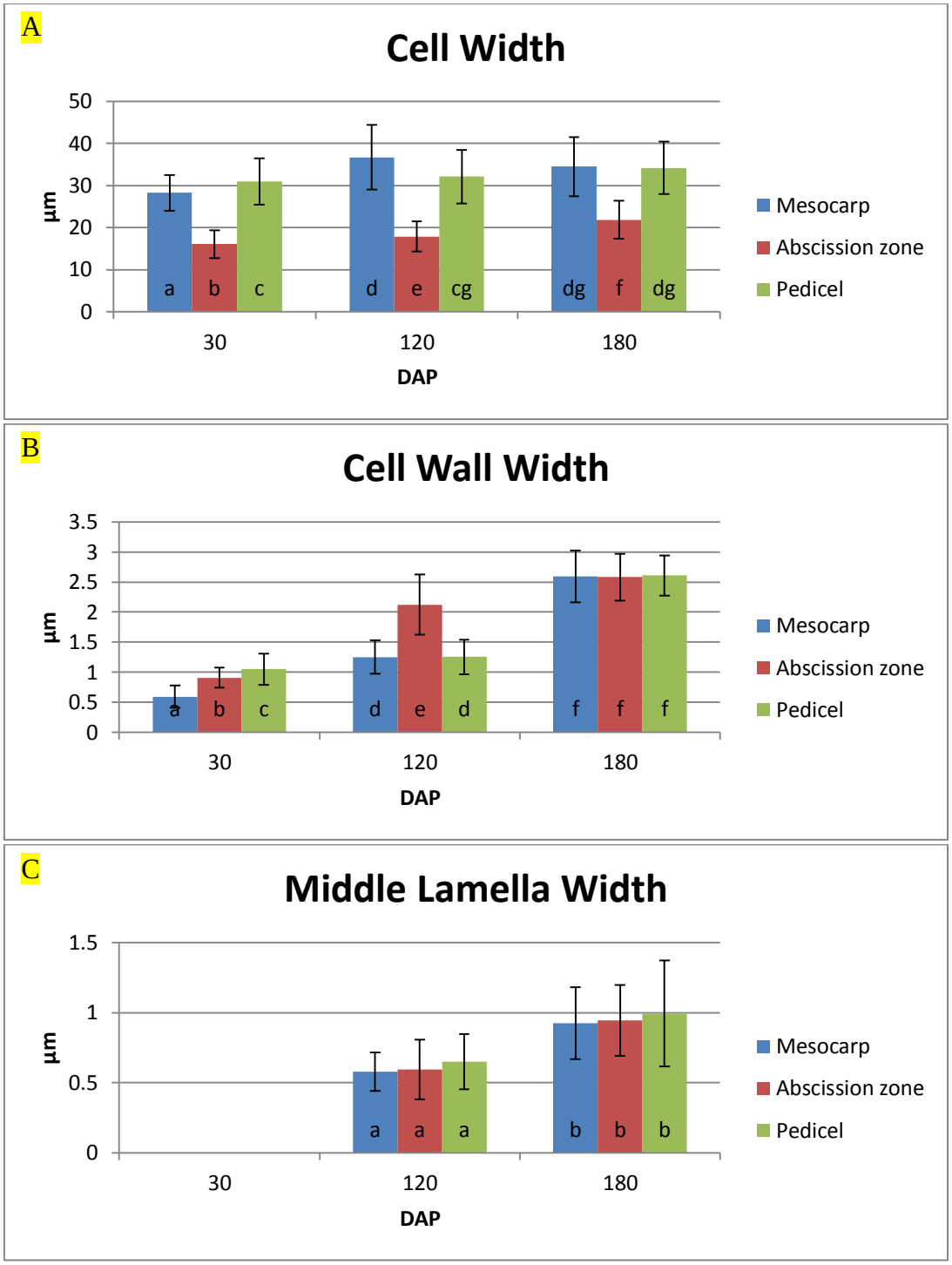

Figure 3.6. Characterization of the cells by measuring cell width, cell wall width, and middle lamella width. (A) cell width, (B) cell wall width, and (C) middle lamella width of different tissues during development. The same lower case alphabets represent non-statistical significance. The different lower case alphabets represent statistical significance. The two lower case alphabets represent non-statistical significance to the shared alphabet one. The error bars represents standard deviation.

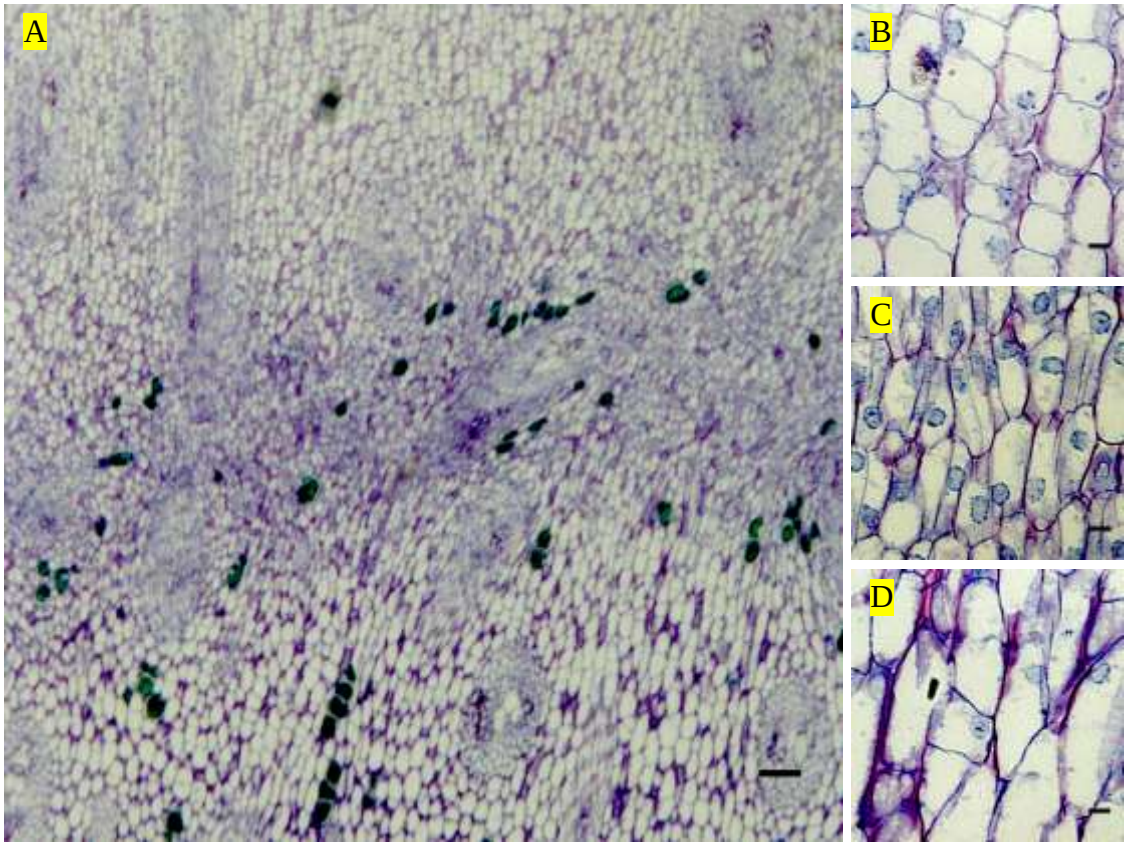

Figure 3.7. 30 DAP toluidine blue staining classical histological images show tissue overview and the details in each zones. (A) Tissue overview 5X including M, AZ, and P, (B) M 40X, (C) AZ 40X, and (D) P 40X. Scale bar = 100 µm in A, scale bar = 10 µm in B-D.

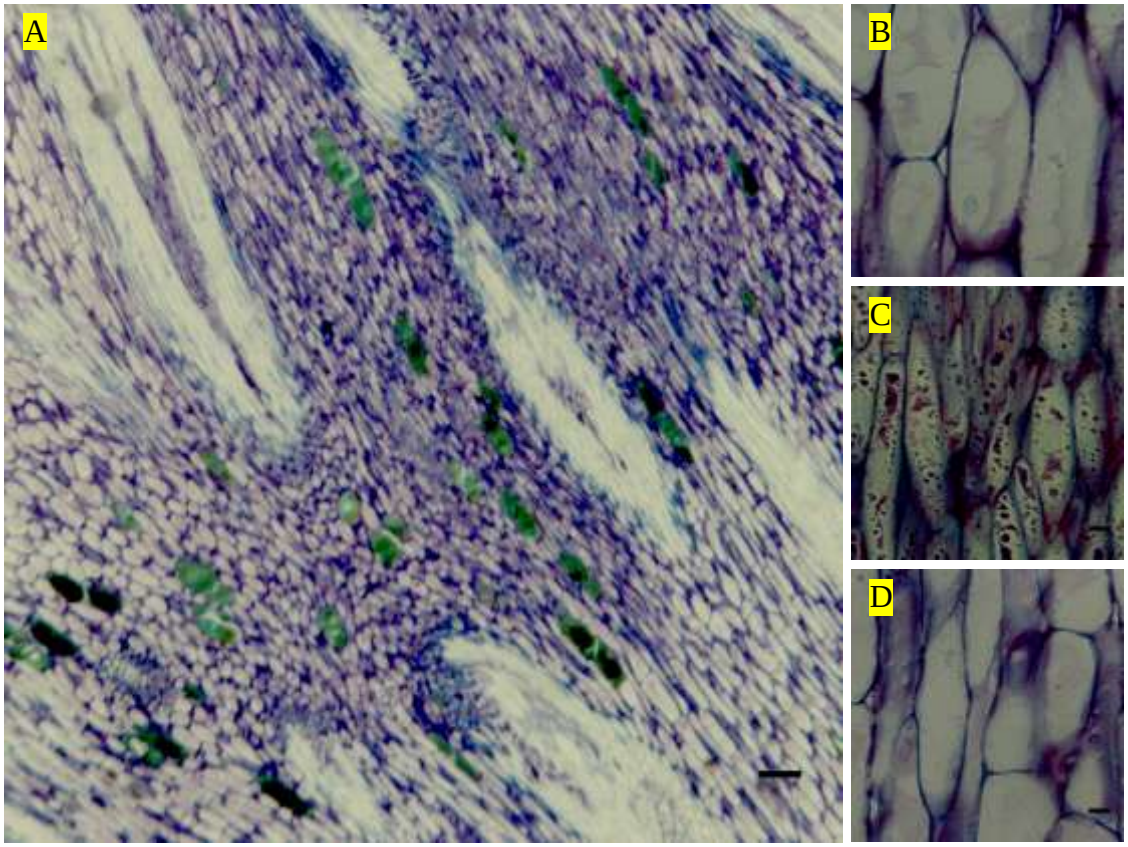

Figure 3.8. 120 DAP toluidine blue staining classical histological images show tissue overview and the details in each zones. (A) Tissue overview 5X including M, AZ, and P, (B) M 40X, (C) AZ 40X, and (D) P 40X. Scale bar = 100 µm in A, scale bar = 10 µm in B-D.

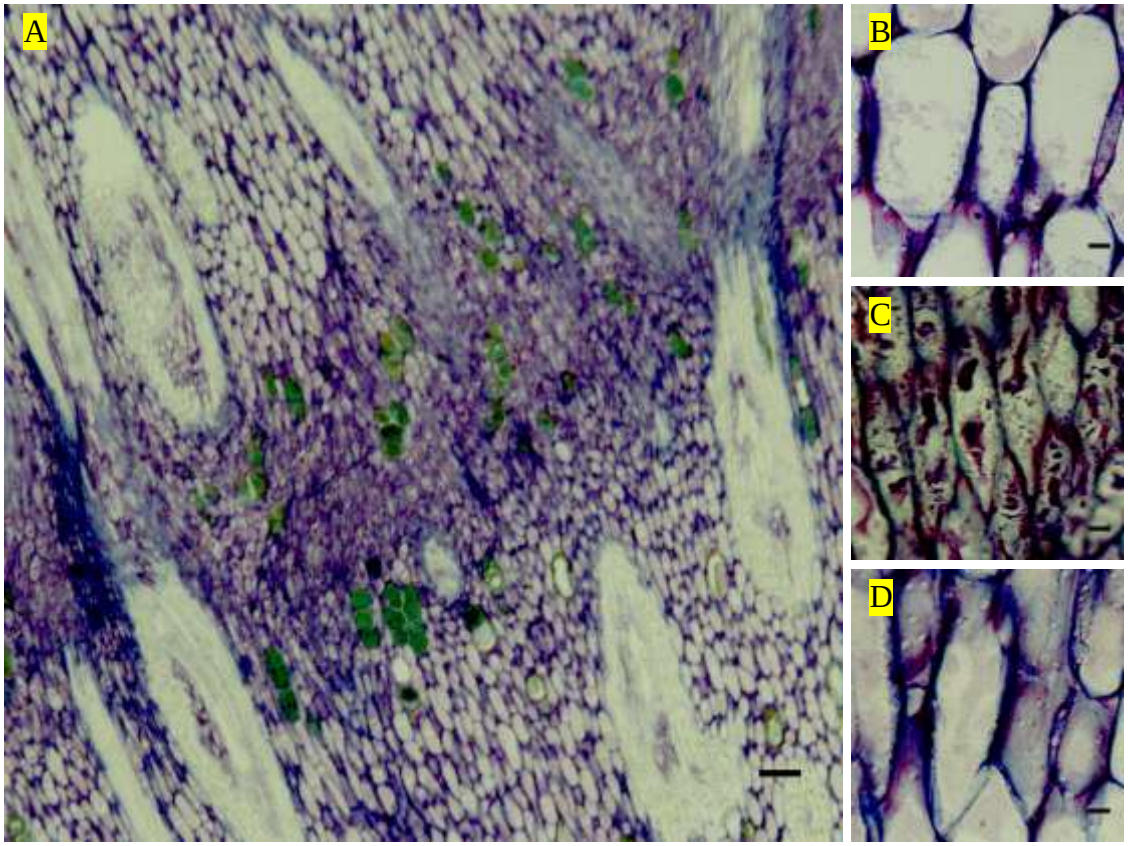

Figure 3.9. 180 DAP toluidine blue staining classical histological images show tissue overview and the details in each zones. (A) Tissue overview 5X including M, AZ, and P, (B) M 40X, (C) AZ 40X, and (D) P 40X. Scale bar = 100 µm in A, scale bar = 10 µm in B-D.

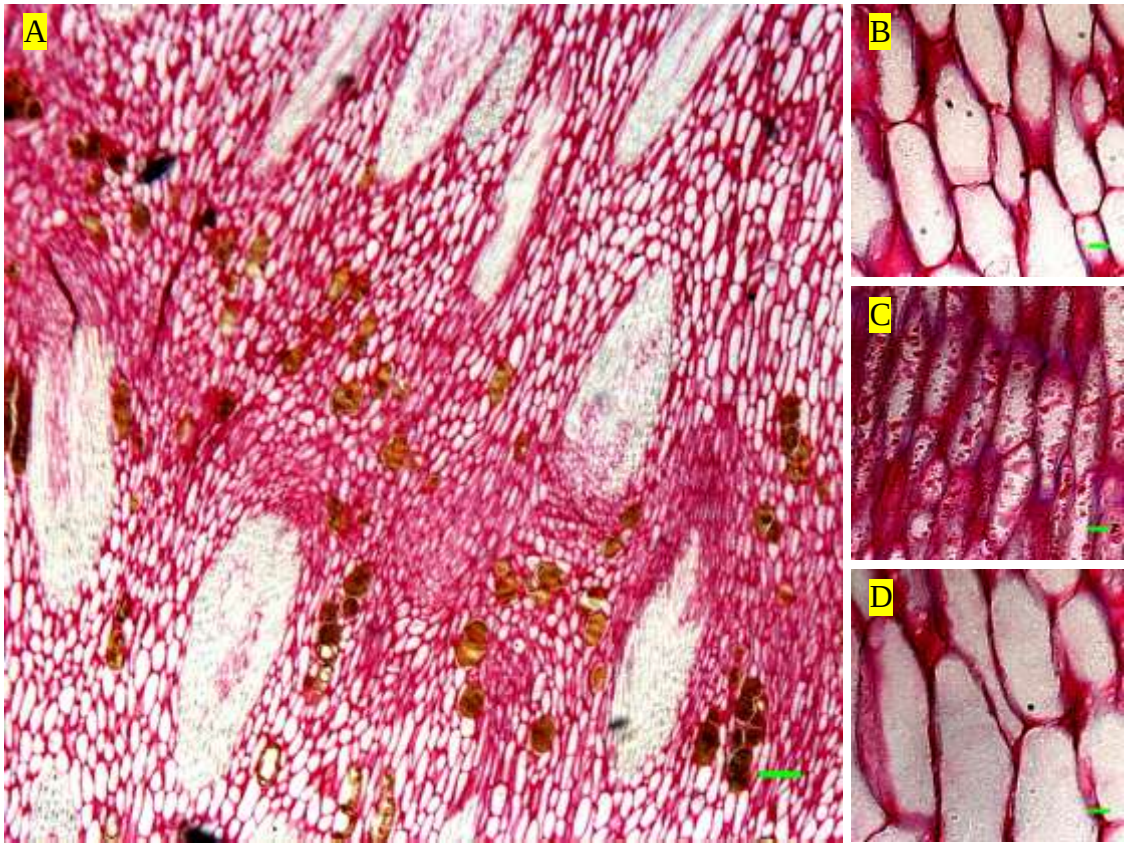

Figure 3.10. 180 DAP ruthenium red staining classical histological images show tissue overview and the details in each zones. (A) Tissue overview 5X including M, AZ, and P, (B) M 40X, (C) AZ 40X, and (D) P 40X. Scale bar = 100 µm in A, scale bar = 10 µm in B-D.

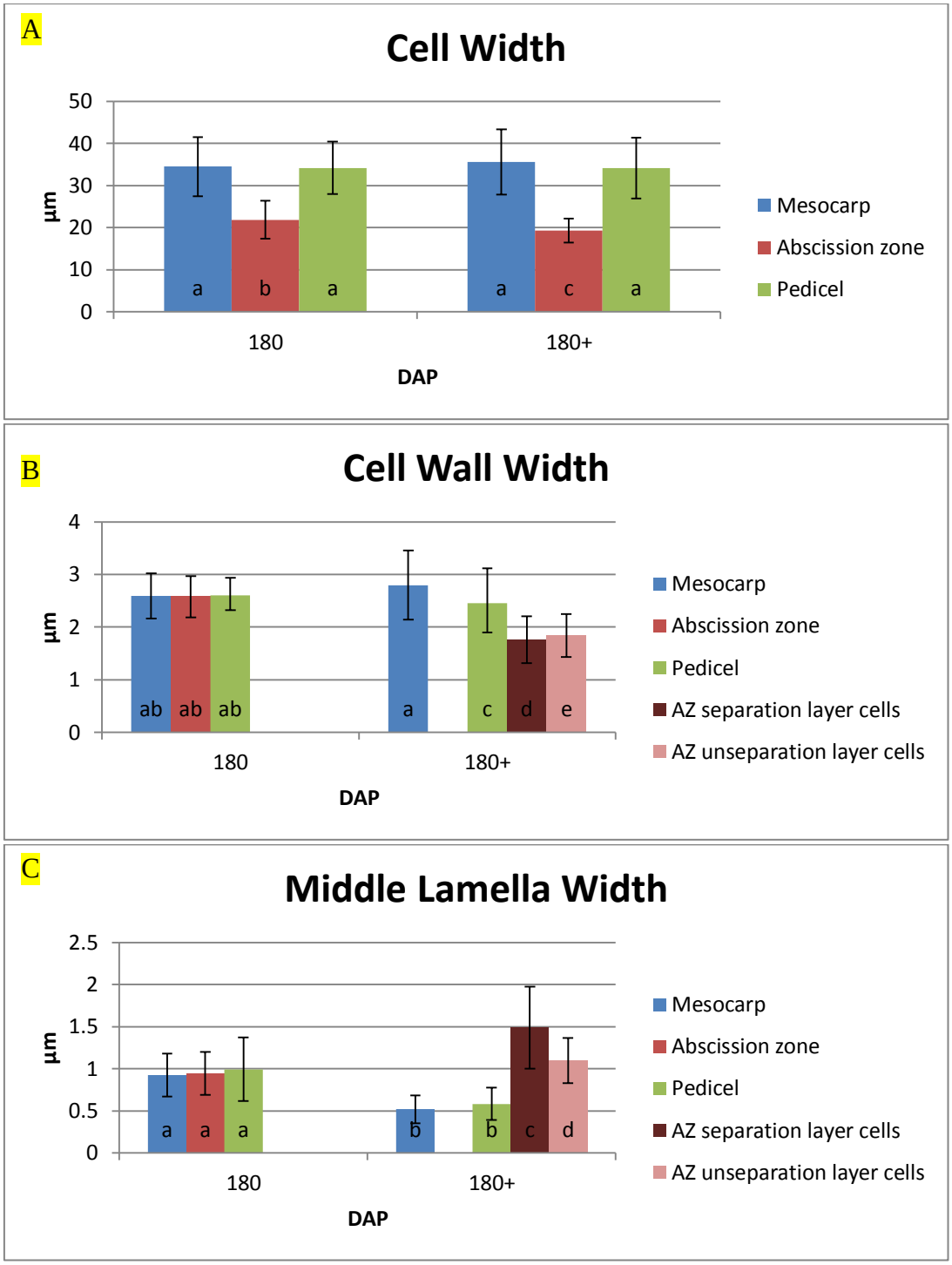

Figure 3.11. Characterization of the cells by measuring cell width, cell wall width, and middle lamella width. (A) cell width, (B) cell wall width, and (C) middle lamella width comparing separated and non-separated samples. The same lower case alphabets represent non-statistical significance. The different lower case alphabets represent statistical significance. The two lower case alphabets represent non-statistical significance to the shared alphabet one. 180+ represents 180 DAP with ethylene treatment at 9 h. The error bars represents standard deviation.

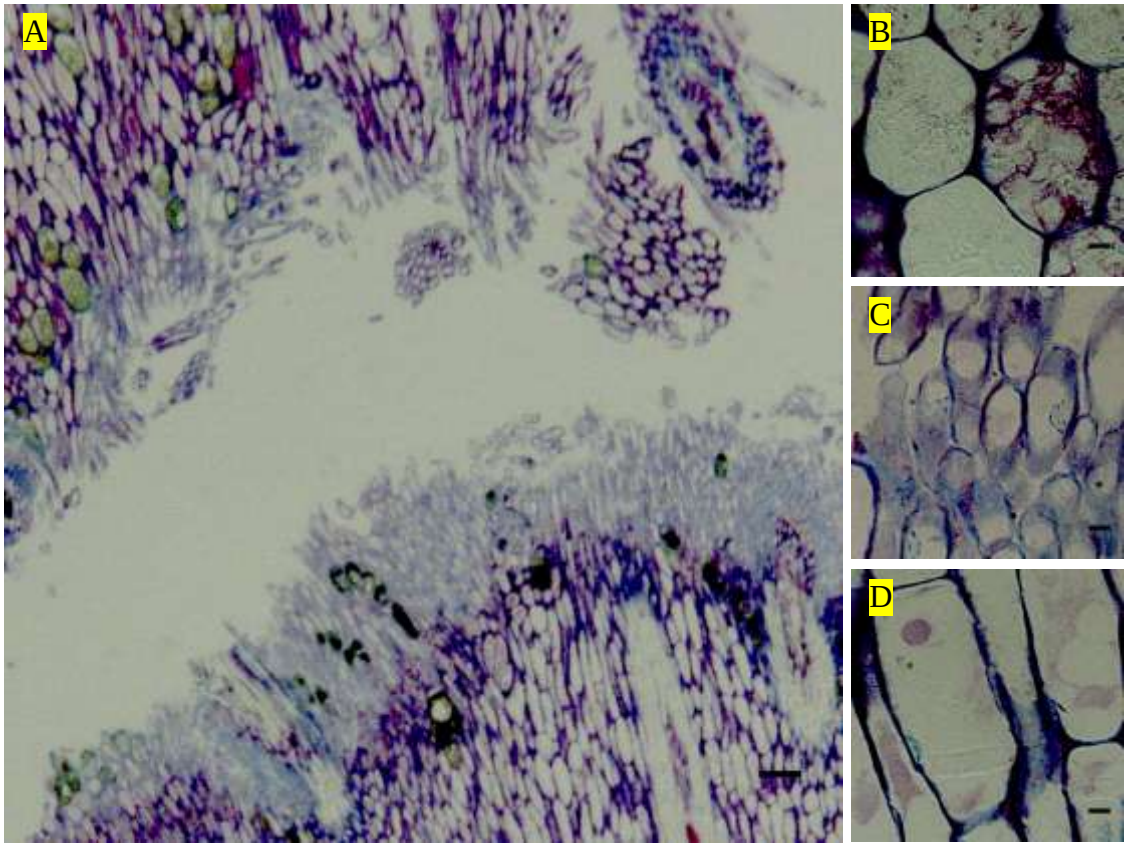

Figure 3.12. Classical histological images of 180 DAP with 9 h ethylene treatment and cell separation occurring with toluidine blue staining show tissue overview and the details in each zones. (A) Tissue overview 5X including M, AZ, and P, (B) M 40X, (C) AZ 40X, (D) P 40X. Scale bar = 100 µm in A, scale bar = 10 µm in B, C, and D.

Ultrastructure of oil palm fruit abscission zone during development analysis

Starting at the nucleus, AZ parenchyma cell nuclear shapes at 30 DAP are usually round or a little bit elongated like rugby shape while those at 120 DAP have angles (amoeboid shape) (Figure 3.13 A, and C). The nuclear membrane at 30 DAP is starting to disappear indicating that mitosis (prophase) is occurring (Figure 3.13 A). Nucleoli can be generally found in 30 DAP but rarely found in 120 DAP (Figure 3.13 A, and C). At 30 DAP, a lot of nucleus with highly condensed chromatin and without nuclear membrane (nucleus in the prophase stage of the mitosis) can be found (Figure 3.13 A). Nuclei in vascular bundle cell in AZ are distinguishable from parenchyma nuclei by their very elongated shape (Figure 3.13 B).

In the AZ, considering the plasmodesmata, there are several plasmodesmata on the cell walls at 30 DAP which are connected to other cells on the same layer but it is infrequent to find plasmodesmata connected the cells between different layers (Figure 3.14 A). The striations in the wall which are filled with dispersions of microfibrils are more distinct during development (Figure 3.14 C, and D) (Sexton *et al.* 1977). At 120 DAP, plasmodesmata are decreased in number but increased in width and located in the middle of the cell (Figure 3.14 B). The measurement of the width of plasmodesmata confirm these observations: at 30 DAP their width are about 0.70 µm while those at 120 DAP increase almost two times (Figure 3.14 A, and B). Moreover, the vesicle fusion to plasmamembrane can be observed (Figure 3.14 C).

Concerning the cell shape, at 30 DAP it is quite rectangular, while at 120 DAP it is more elongated (Figure 3.15 A, and B). Interestingly, at the tip of the elongated AZ parenchyma cells, the cell wall is thicken with the appearance of multiple layers within the primary cell wall (Figure 3.15 C). Indeed, these layers that result in the increase of cell wall thickness originate from the modification of the middle lamella (Figure 3.15 C). Finally, in

the cytoplasm, ribosome, mitochondria, and vesicles are accumulated at the border of cytoplasm and fibrous matrix can be found throughout the cell interior (Figure 3.15 C).

.

Alterations to methylated homogalacturonan and xylogalacturonan in the oil palm fruit abscission zone

Immunolocalization of the main pectin epitopes during abscission zone ontogenesis and after cell separation

The classical and electron microscopy results discovered that pectin accumulates during development and appears to be lost after separation (Figure 3.10 and Figure 3.12). JIM5, JIM7, and LM7 can be used to distinguish the cellular localization of partially methyl-estirified HG, while LM8 recognizes XGA. For each experiment, DAPI reveals well aligned nuclei to visualize the location of AZ easily. The immunohistological controls were performed with a combination of primary antibody and/or secondary antibody and/or none with the combinations with the different tissues examined (Figure 3.16).

The signal intensity corresponding to JIM5 epitope at 30 DAP shows the highest signal in all tissues (M, AZ, and P) by comparison with the later stages of development (Figure 3.17A-R). At this stage, each fruit tissue has diffuse signals in the cytoplasm and also signals throughout the cell periphery are clearly noticeable (Figure 3.17A-F). At 120 DAP, the signal intensity in all tissues is dramatically decreased (Figure 3.17G-L). M and P tissues show low signal throughout cell walls, and have a little bit higher signal on the inner side of primary cell wall (Figure 3.17G, H, K and L). AZ tissue shows no signal at the wall but maintains some signals on the inner side of primary cell wall. At 180 DAP, M and P show very low signal while AZ shows the signal mostly on the inner side of the primary cell wall (Figure 3.17). The localization of JIM5 in inner side of primary cell wall was confirmed by symplastic localization (Figure 3.21).

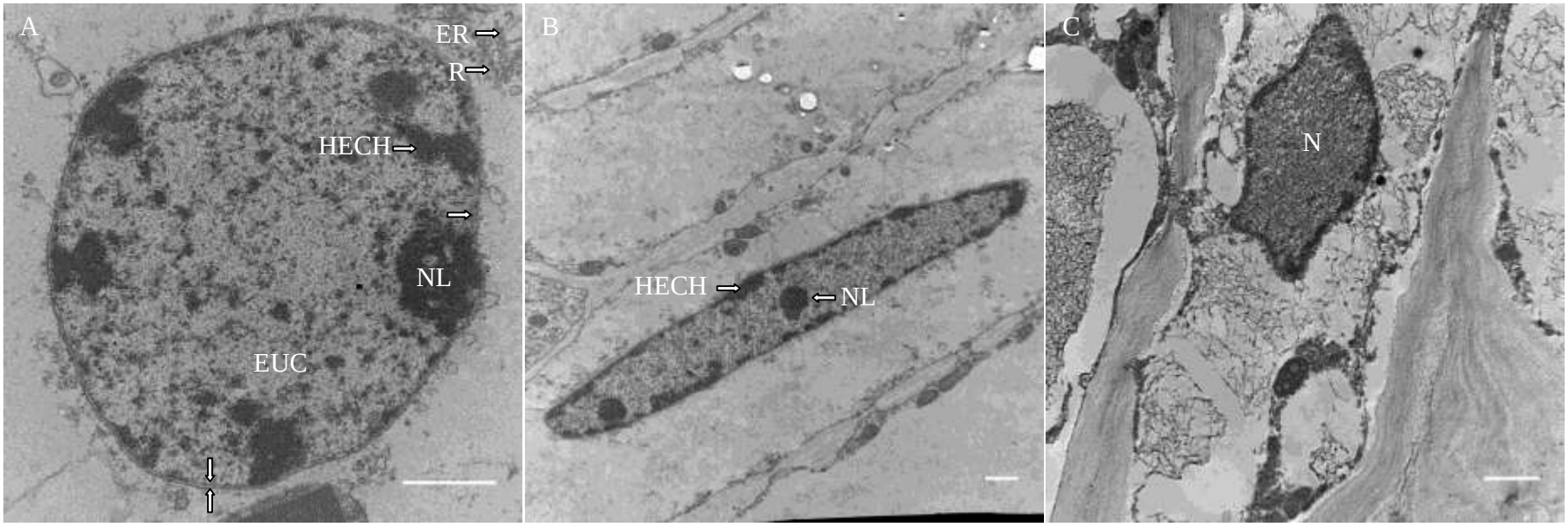

Figure 3.13. Scanning electron microscopy AZ nucleus comparison during developmental stages and comparison between parenchyma and vascular bundle nucleus. (A) 30 DAP parenchyma nucleus. (B) 30 DAP vascular parenchyma nucleus. (C) 120 DAP parenchyma nucleus. ER = Endoplasmic reticulum, EUCH = Euchromatin, HECH = Heterochromatin, NL = Nucleolus, and R = Ribosome. Scale bar = 1 µm.

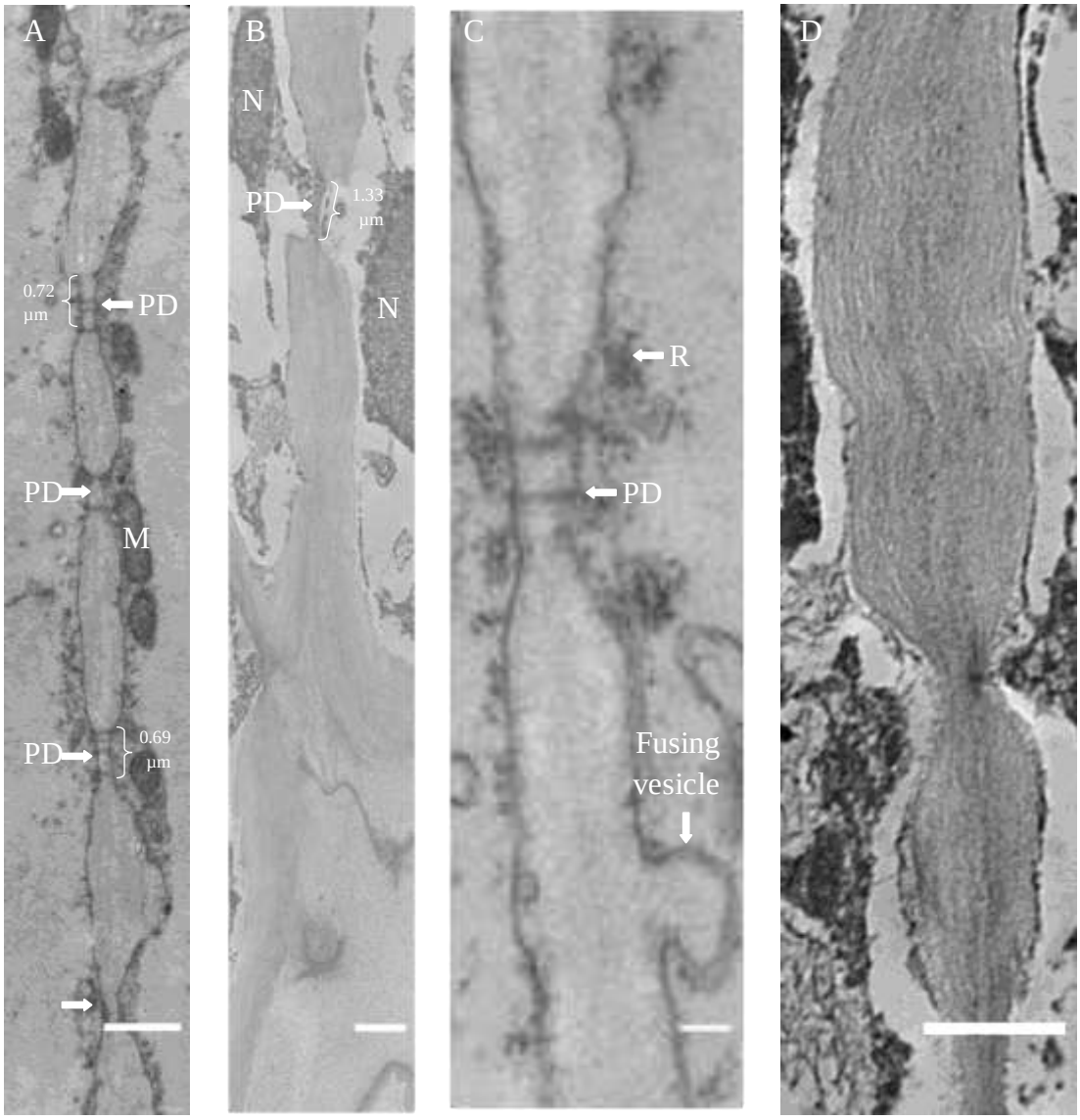

Figure 3.14. AZ cell wall shows different number of plasmodesmata and striation appearance during development. (A, C) Cell wall at 30 DAP. (B, D) Cell wall at 120 DAP. M = Mitochondria. N = Nucleus. PD = Plasmodesmata. R = Ribosome. Scale bar = 1 µm in A, B, and D. Scale bar = 0.1 µm in C.

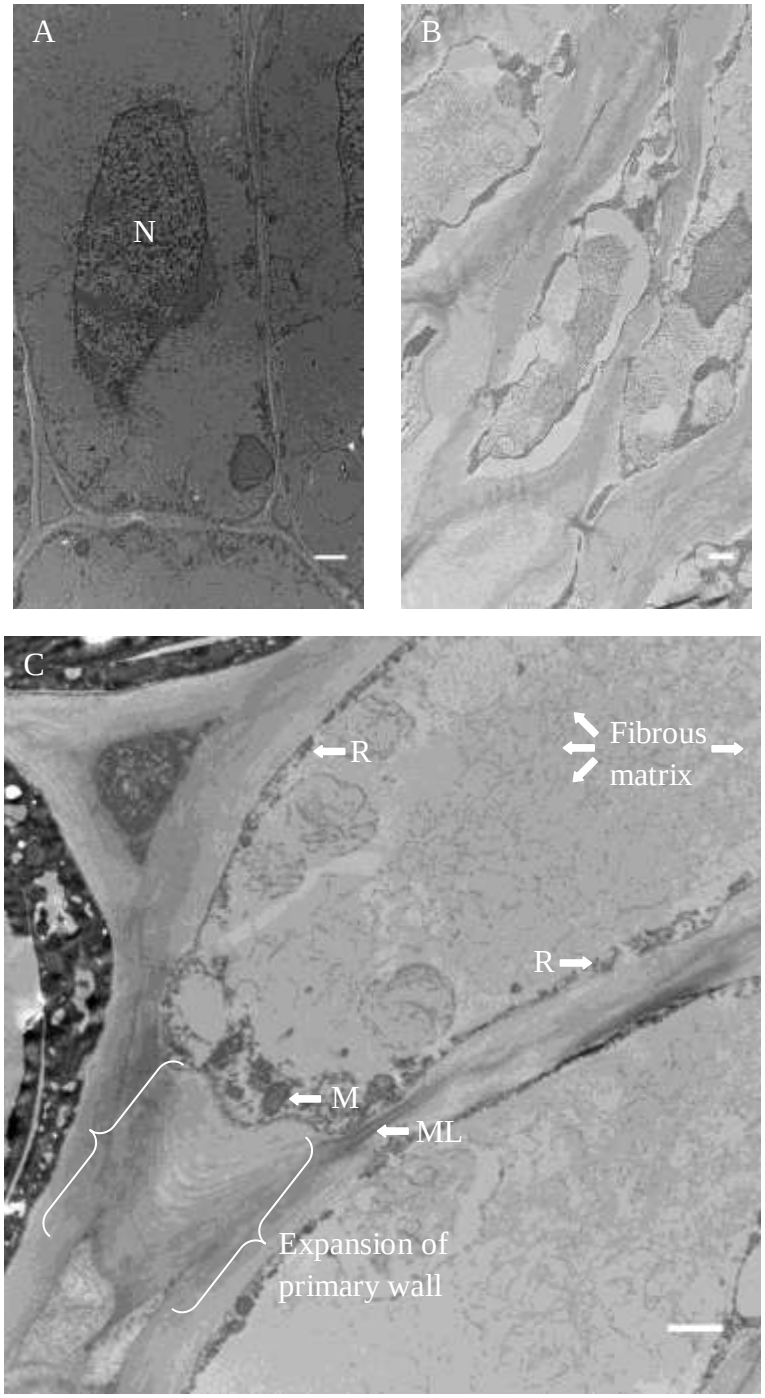

Figure 3.15. Cell change during development. (A) 30 DAP AZ cell. (B, C) 120 DAP AZ cell. ML = Middle lamella. M = Mitochondria. R = Ribosome. Scale bar = 1 μm.

As found with JIM5, the signal intensity corresponding to JIM7 epitope at 30 DAP shows the highest signal in all tissues (M, AZ, and P) by comparison with the later stages of development studied (Figure 3.18 A-R). At this immature stage, M tissue has a slightly higher signal intensity than that of the AZ and P (Figure 3.18 A-F). M, AZ, and P tissues have diffuse signal in the cytoplasm but signal throughout the cell periphery is also clearly noticeable. P tissue shows the highest signal within the inner sides of the primary cell wall and at the junction of intercellular spaces. At 120 DAP, the signal intensity in all tissues is dramatically decreased (Figure 3.18 G-L). AZ and P tissues show low signal throughout cell walls and have a little bit higher signal on the inner side of the primary cell wall (Figure 3.18 I-L). M tissue shows very low signal (Figure 3.18 G and H). Finally, at 180 DAP, M and P show no signal while AZ shows low signal on the inner side of the primary cell wall (Figure 3.18 M-R).

The signal intensity corresponding to the LM7 epitope at 30 DAP also shows the highest signal in all tissues (M, AZ, and P) as with the two previous antibodies (Figure 3.19 A-R). At this stage, M and AZ tissues have diffuse signals in the cytoplasm (Figure 3.19 A-F). Signal throughout the cell walls in all tissues is clearly noticeable. P tissue shows clear evidence of signal on the inner side of primary cell wall. At 120 DAP, the signal intensity in all tissue is dramatically decreased. M and P show only faint signal throughout the cell wall. AZ shows signal on the inner side of the primary cell wall. At the ripe stage, 180 DAP, all tissues show very low signal, mostly on the inner side of primary cell wall (Figure 3.19 M-R).

As with the three previous antibodies, the signal intensity corresponding to the LM8 epitope shows the highest signal in all tissues (M, AZ, and P) at 30 DAP (Figure 3.20 A-R). At this stage, M and AZ tissues have diffuse signals in cytoplasm and higher signal than P tissue. Signal throughout the cell walls in the three tissues are clearly noticeable. At 120

DAP, the signal intensity is dramatically decreased in fruit, and found mostly on the inner side of primary cell wall. At 180 DAP, the signal appears to increase slightly in all the tissues. Notably, there are unevenly spaced points of signal concentrations in that ring the cell on the inner side of the cell wall in all tissues, especially the AZ (Figure 3.20 O-P). A summary of the results described above is shown in Table 3.1.

Pectin biochemical modification mapping by immunolocalizaton after fruit shedding induced by ethylene

The signal intensity corresponding to the JIM5 epitope in the AZ from ripe fruit (180 DAP) after 3 h with air treatment only shows very low signal (Figure 3.22 A and B). In contrast by 3 h and 6 h after ethylene treatment, the signal obtained with JIM5 increases on the inner side of primary cell wall (Figure 3.22 C-F). By 9 h after ethylene treatment when separation has occurred, the signal increases dramatically at the separated primary cell wall of separation layer cells on both the M and P sides (Figure 3.22 G-J). Signals on the inner side of the primary cell wall and in cytoplasm can be detected, in addition to line like signals that arise from deeper within the AZ cells and/or cell layers. By 12 h after ethylene treatment, the signal at the separated primary cell wall of separation layer cells in both M and P side remains high, while the line like signals are lost from the M side (Figure 3.22 K-N). Finally, the "zipper" AZ samples (samples of the AZ where both separation has both occurred and not yet occurred) at 9 h with ethylene treatment show the signal gradually increases towards the site of separation (3.22 O and P). In addition, the signal intensity increases along the separated cell surface. Moreover, the signal at possible future separation sites within the non-separated zone can be detected (Figure 3.22, and Figure 3.26 A-D). This has been confirmed by analyzing grey level profile across the AZ (Figure 3.27).

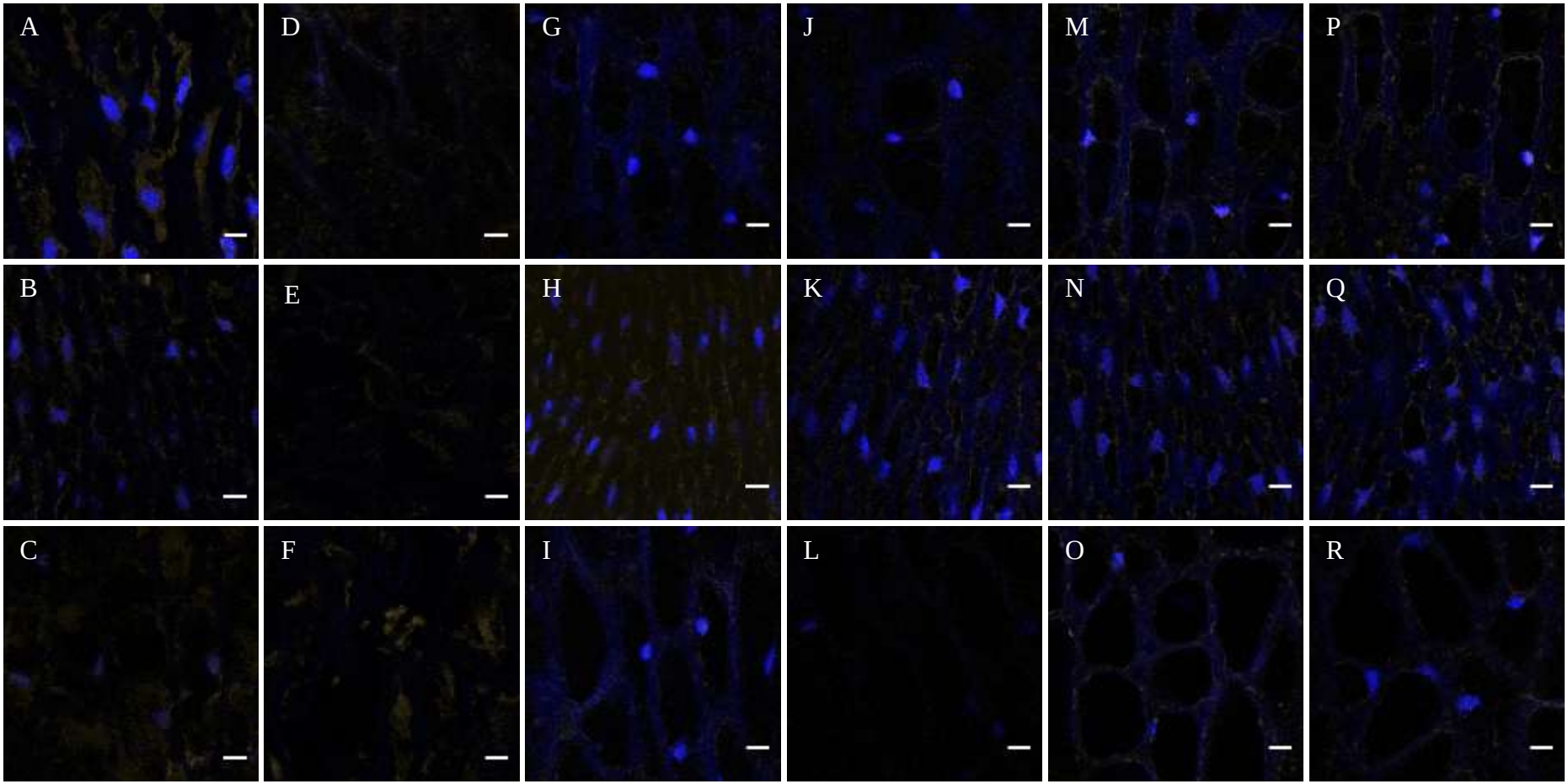

Figure 3.16. Immunohistological controls. (A) AZ 180 DAP with DAPI. (B) AZ 180 DAP with seconday antibody and DAPI. (C) M 180 DAP with secondary antibody and DAPI. (D) P 180 DAP with secondary antibody and DAPI. (E) AZ 180 DAP with JIM5 primary antibody without secondary antibody. (F) AZ 180 DAP with JIM7 primary antibody without secondary antibody. (G-I) 180 DAP with JIM5 with secondary antibody and with DAPI M, AZ, and P, respectively, (J-L) with JIM7 with secondary antibody and with DAPI M, AZ, and P, respectively. (M-O) with LM7 with secondary antibody and with DAPI M, AZ, and P, respectively. (P-R) 180 DAP with LM8 with secondary antibody and with DAPI M, AZ, and P, respectively. Scale bar = 10 μm.

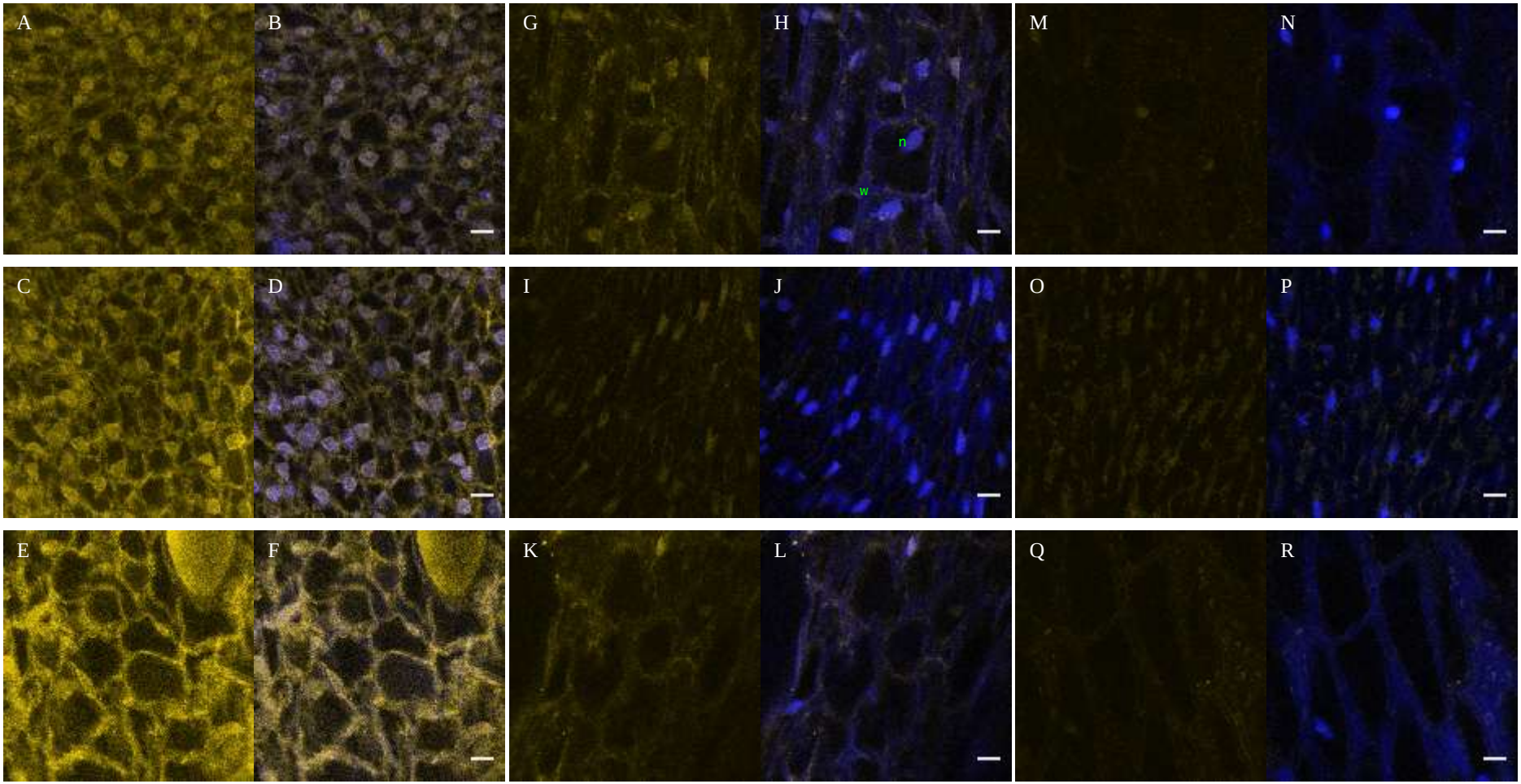

Figure 3.17. JIM5 immunohistological images show decreased signal during developmental stages. (A) 30 DAP M JIM5, and (B) 30 DAP M JIM5 and DAPI. (C) 30 DAP AZ JIM5, and (D) 30 DAP AZ JIM5 and DAPI. (E) 30 DAP P JIM5, and (F) 30 DAP P JIM5 and DAPI. (G) 120 DAP M JIM5, and (H) 120 DAP M JIM5 and DAPI. (I) 120 DAP AZ JIM5, and (J) 120 DAP AZ JIM5 and DAPI. (K) 120 DAP P JIM5, and (L) 120 DAP P JIM5 and DAPI. (M) 180 DAP M JIM5, and (N) 180 DAP M JIM5 and DAPI. (O) 180 DAP AZ JIM5, and (P) 180 DAP AZ JIM5 and DAPI. (Q) 180 DAP P JIM5, and (R) 180 DAP P JIM5 and DAPI. n = nucleus, w = cell wall. Scale bar = 10 µm.

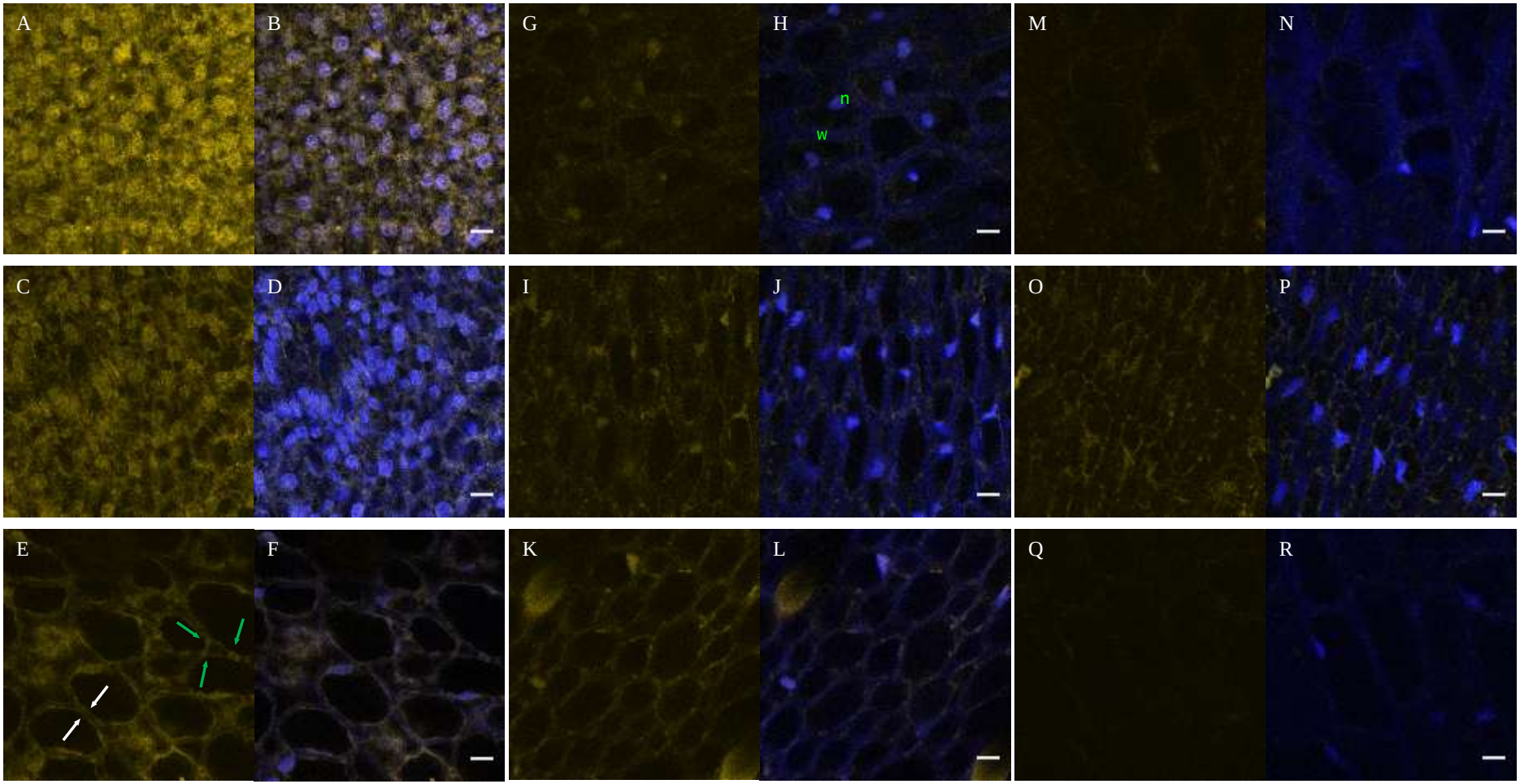

Figure 3.18. JIM7 immunohistological images show decreased signal during developmental stages. (A) 30 DAP M JIM7, and (B) 30 DAP M JIM7 and DAPI. (C) 30 DAP AZ JIM7, and (D) 30 DAP AZ JIM7 and DAPI. (E) 30 DAP P JIM7, and (F) 30 DAP P JIM7 and DAPI. (G) 120 DAP M JIM7, and (H) 120 DAP M JIM7 and DAPI. (I) 120 DAP AZ JIM7, and (J) 120 DAP AZ JIM7 and DAPI. (K) 120 DAP P JIM7, and (L) 120 DAP P JIM7 and DAPI. (M) 180 DAP M JIM7, and (N) 180 DAP M JIM7 and DAPI. (O) 180 DAP AZ JIM7, and (P) 180 DAP AZ JIM7 and DAPI. (Q) 180 DAP P JIM7, and (R) 180 DAP P JIM7 and DAPI. n = nucleus, w = cell wall. Arrows indicate signal at cell wall. Scale bar = 10 µm.

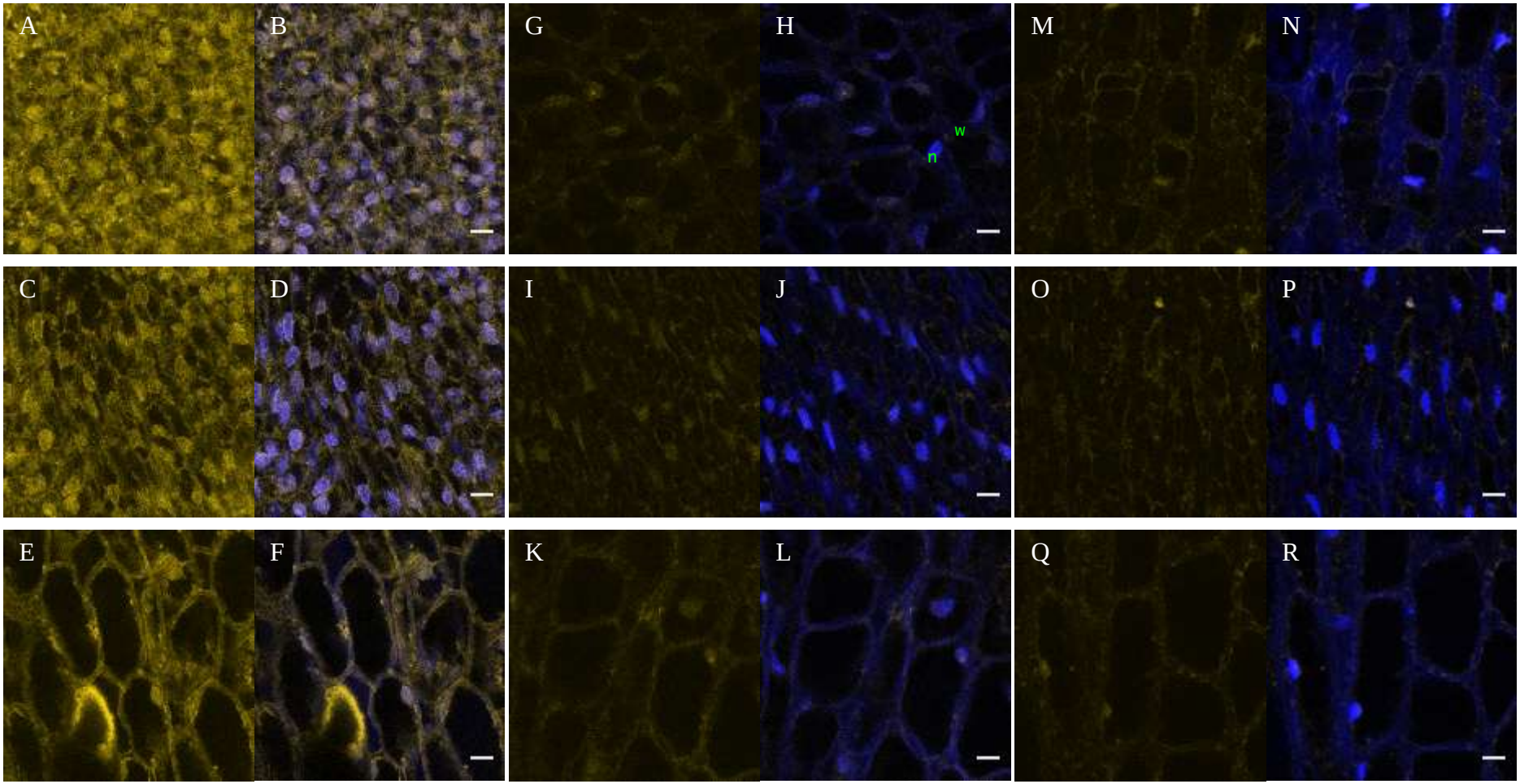

Figure 3.19. LM7 immunohistological images show decreased signal during developmental stages. (A) 30 DAP M LM7, and (B) 30 DAP M LM7 and DAPI. (C) 30 DAP AZ LM7, and (D) 30 DAP AZ LM7 and DAPI. (E) 30 DAP P LM7, and (F) 30 DAP P LM7 and DAPI. (G) 120 DAP M LM7, and (H) 120 DAP M LM7 and DAPI. (I) 120 DAP AZ LM7, and (J) 120 DAP AZ LM7 and DAPI. (K) 120 DAP P LM7, and (L) 120 DAP P LM7 and DAPI. (M) 180 DAP M LM7, and (N) 180 DAP M LM7 and DAPI. (O) 180 DAP AZ LM7, and (P) 180 DAP AZ LM7 and DAPI. (Q) 180 DAP P LM7, and (R) 180 DAP P LM7 and DAPI. n = nucleus, w = cell wall. Scale bar = 10 µm.

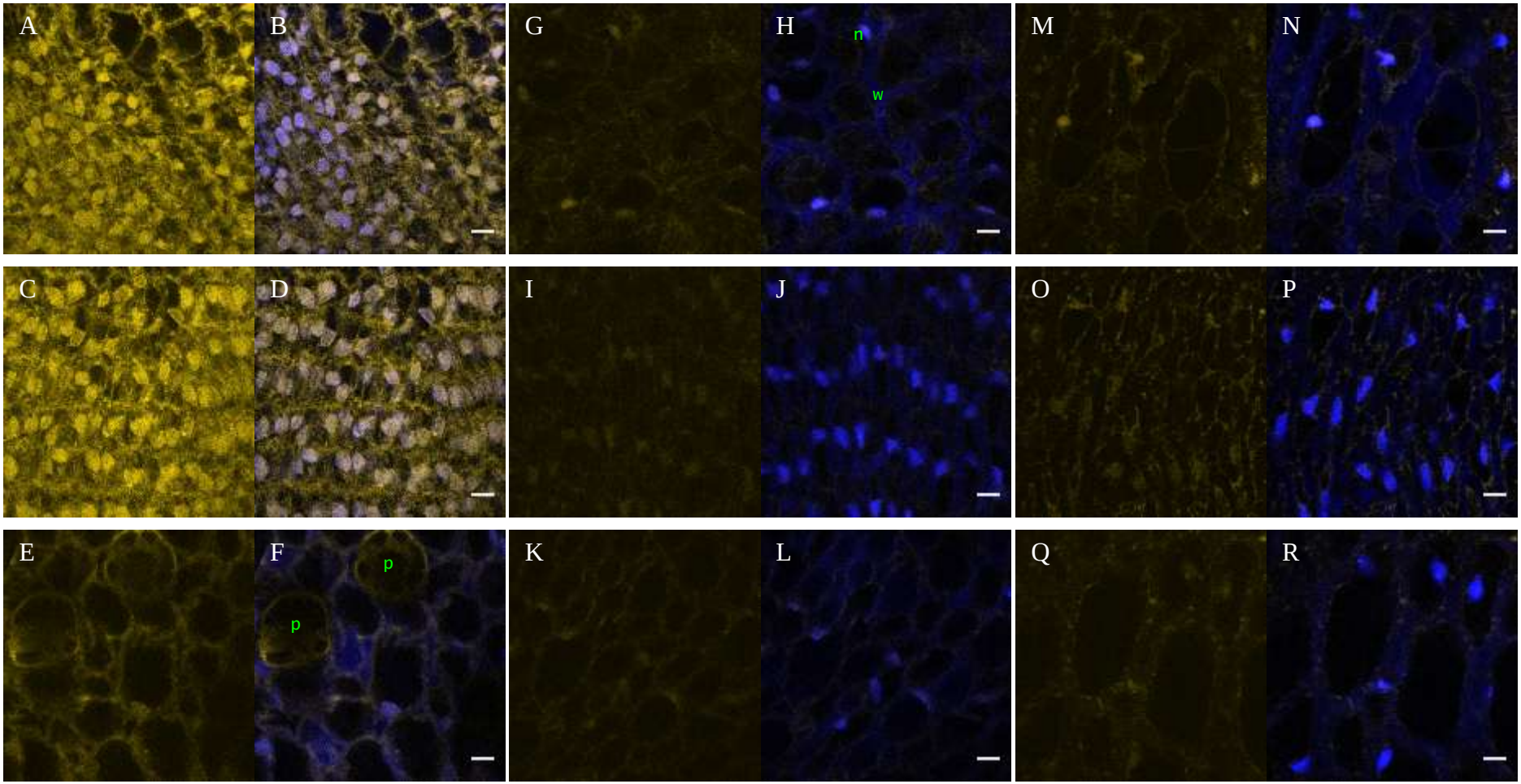

Figure 3.20. LM8 immunohistological images show decreased signal during developmental stages. (A) 30 DAP M LM8, and (B) 30 DAP M LM8 and DAPI. (C) 30 DAP AZ LM8, and (D) 30 DAP AZ LM8 and DAPI. (E) 30 DAP P LM8, and (F) 30 DAP P LM8 and DAPI. (G) 120 DAP M LM8, and (H) 120 DAP M LM8 and DAPI. (I) 120 DAP AZ LM8, and (J) 120 DAP AZ LM8 and DAPI. (K) 120 DAP P LM8, and (L) 120 DAP P LM8 and DAPI. (M) 180 DAP M LM8, and (N) 180 DAP M LM8 and DAPI. (O) 180 DAP AZ LM8, and (P) 180 DAP AZ LM8 and DAPI. (Q) 180 DAP P LM8, and (R) 180 DAP P LM8 and DAPI. n = nucleus, w = cell wall, p = polyphenolic compound. Scale bar = 10 µm.

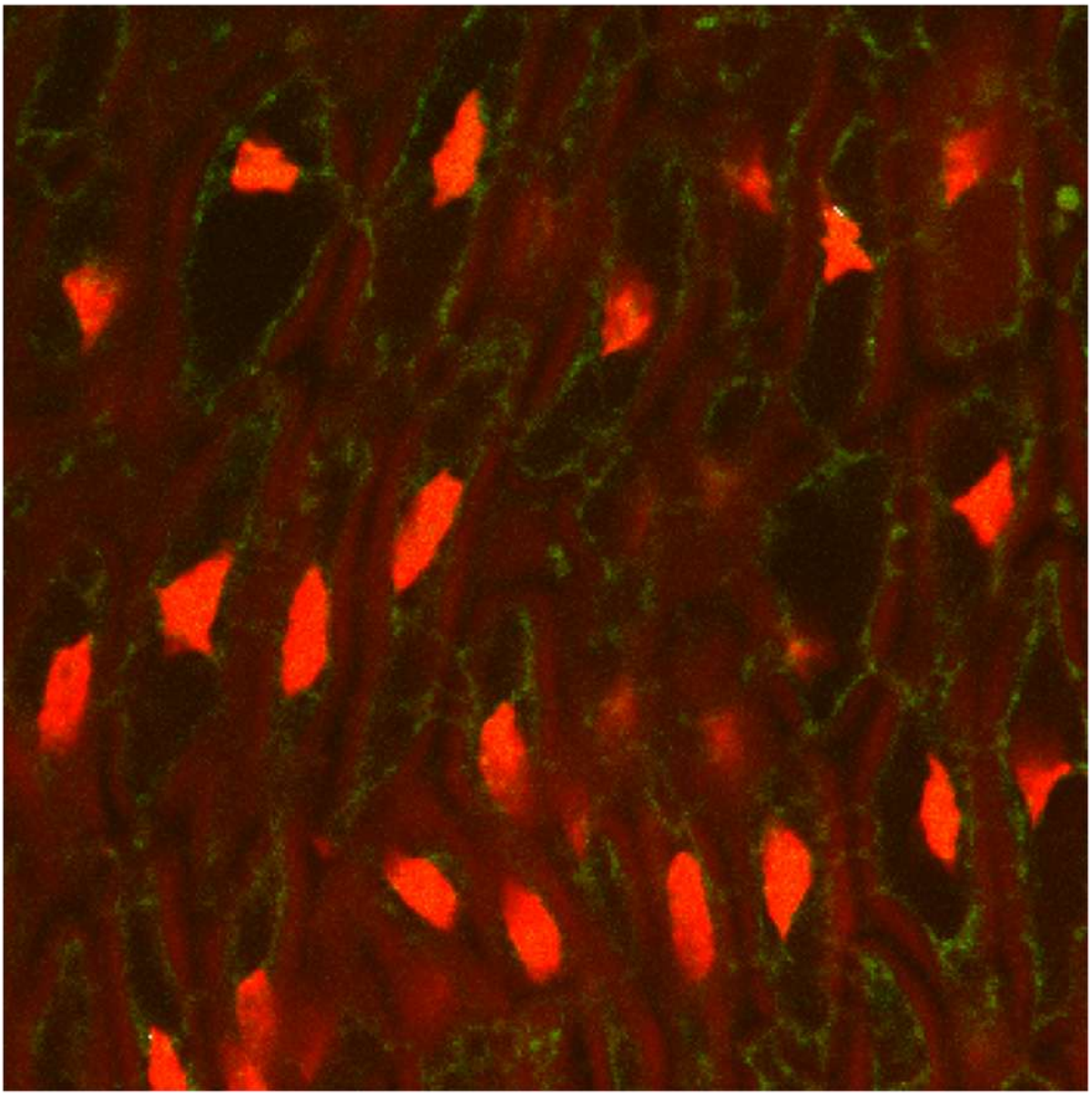

Figure 3.21. Symplastic JIM5 epitope localization shows red signal, which is the signal of DAPI autofluorescence due to ferrulic acid, and green signal that indicates the JIM5 epitope that does not co-localize with autofluorescence signal.

The signal intensity corresponding to JIM7 epitope at 30 DAP in AZ 180 DAP at 3 h without ethylene treatment and 180 DAP at 3 h and 6 h with ethylene treatment show very low immunohistological signal on the inner side of the primary cell wall. At 9 h with ethylene treatment and with separation occurring, the signal increases at the separated primary cell wall of separation layer cells in both M and P side comparing to the control (3 h without ethylene treatment). The signal on the inner side of primary cell wall and in the cytoplasm can be detected. Similar to the signal at 9 h, the signal at 12 h with ethylene treatment at the separated primary cell wall of separation layer cells in both M and P side still increases at high level. The signal inner side of primary cell wall at M side decreases but those at P side still remains. The zipper AZ at 9 h with ethylene treatment shows the signal gradually increases as separation has occurred (Figure 3.23, and Figure 3.26 E-H).

The signal in AZ of all samples (3 h without ethylene treatment, 3 h, 6 h, 9 h, 12 h with ethylene treatment) has very low signal intensity corresponding to LM7 inner side of primary cell wall (Figure 3.24).

The LM8 signal in 3 h without ethylene treatment sample is undetectable and it becomes a little bit stronger inner side of primary cell wall in 6 h and 9 h with ethylene treatment. At 9 h and 12 h with ethylene treatment and separation occurring, the signal at separation layer cells shows spotted signal and the signal shows related to vascular tissue cells (Figure 3.25, and Figure 3.26 I-L). The summary of data described above is shown in Table 3.1.

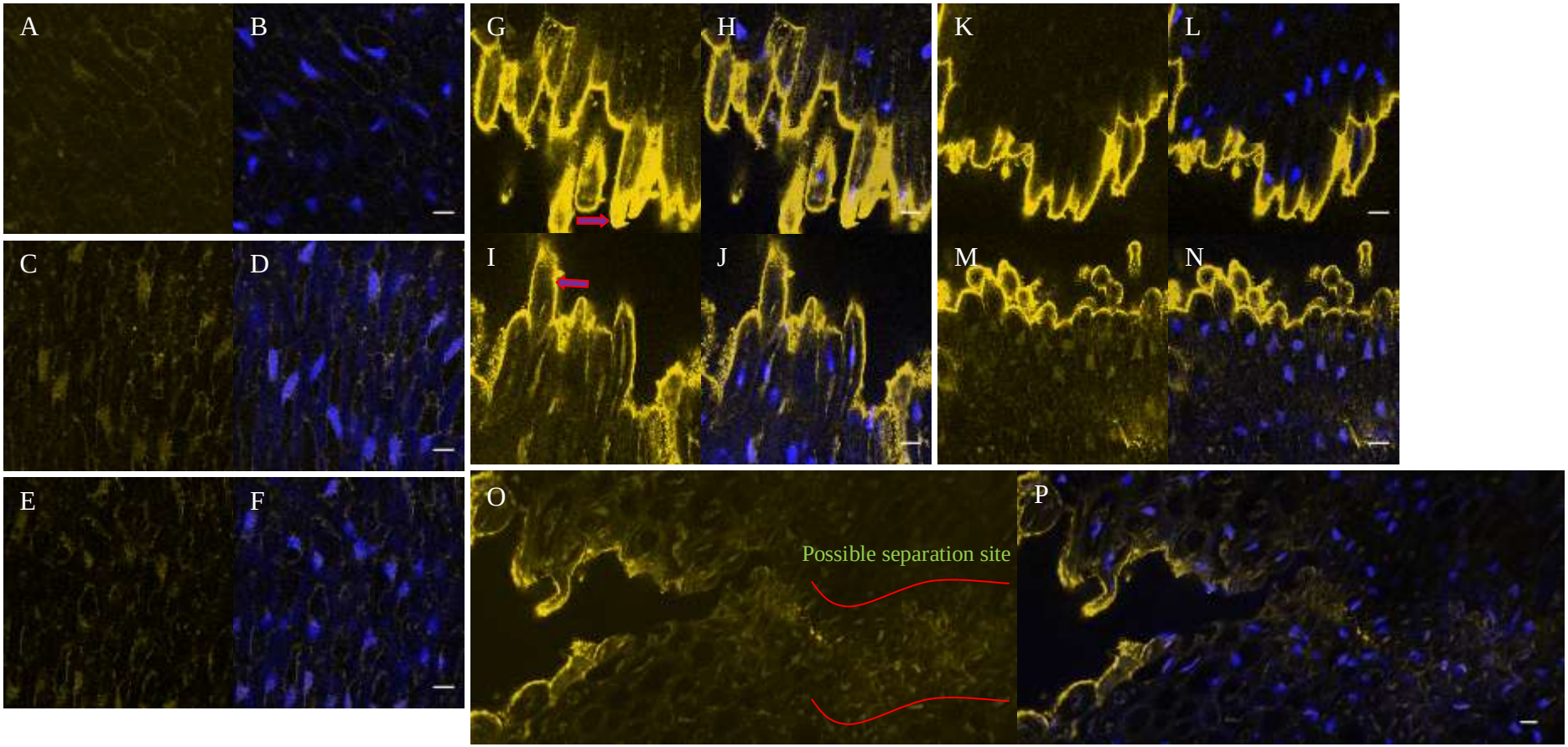

Figure 3.22. JIM5 180 DAP immunohistological images show signal changes before and after cell separation. (A) JIM5, and (B) JIM5 and DAPI AZ 3 h without ethylene treatment. (C) JIM5, and (D) JIM5 and DAPI AZ 3 h with ethylene treatment. (E) JIM5, and (F) JIM5 and DAPI AZ 6 h with ethylene treatment. (G) JIM5, and (H) JIM5 and DAPI AZ at M side at 9 h with ethylene treatment and separation occurring. (I) JIM5, and (J) JIM5 and DAPI AZ at P side at 9 h with ethylene treatment and separation occurring. (K) JIM5, and (L) JIM5 and DAPI AZ at M side at 12 h with ethylene treatment and separation occurring. (M) JIM5, and (N) JIM5 and DAPI AZ at P side at 12 h with ethylene treatment and separation occurring. (O) JIM5, and (P) JIM5 and DAPI zipper AZ at 9 h with ethylene treatment. Scale bar = 10 µm.

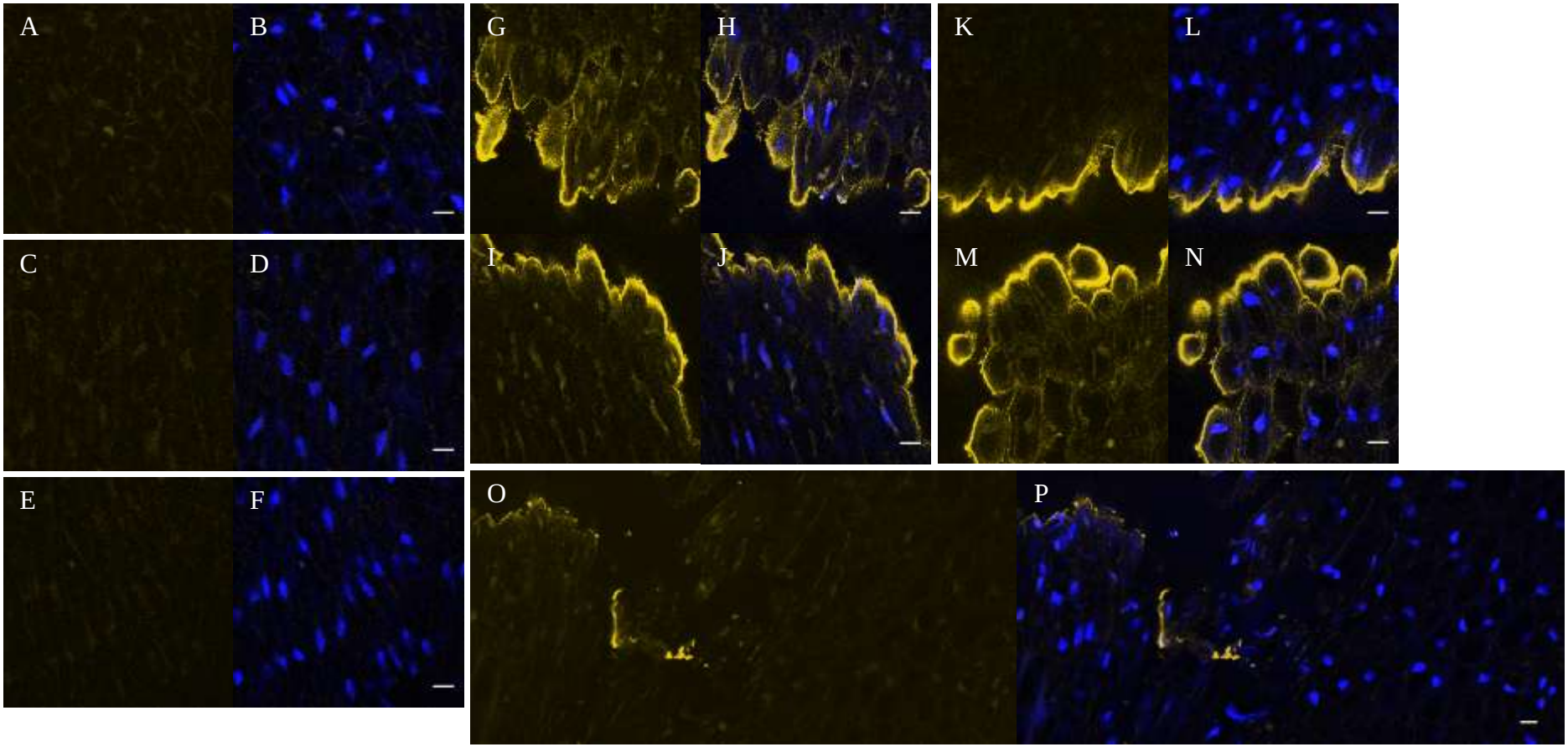

Figure 3.23. JIM7 180 DAP immunohistological images show signal changes before and after cell separation. (A) JIM7, and (B) JIM7 and DAPI AZ 3 h without ethylene treatment. (C) JIM7, and (D) JIM7 and DAPI AZ 3 h with ethylene treatment. (E) JIM7, and (F) JIM7 and DAPI AZ 6 h with ethylene treatment. (G) JIM7, and (H) JIM7 and DAPI AZ at M side at 9 h with ethylene treatment and separation occurring. (I) JIM7, and (J) JIM7 and DAPI AZ at P side at 9 h with ethylene treatment and separation occurring. (K) JIM7, and (L) JIM7 and DAPI AZ at M side at 12 h with ethylene treatment and separation occurring. (M) JIM7, and (N) JIM7 and DAPI AZ at P side at 12 h with ethylene treatment and separation occurring. (O) JIM7, and (P) JIM7 and DAPI zipper AZ at 9 h with ethylene treatment. Scale bar = 10 µm.

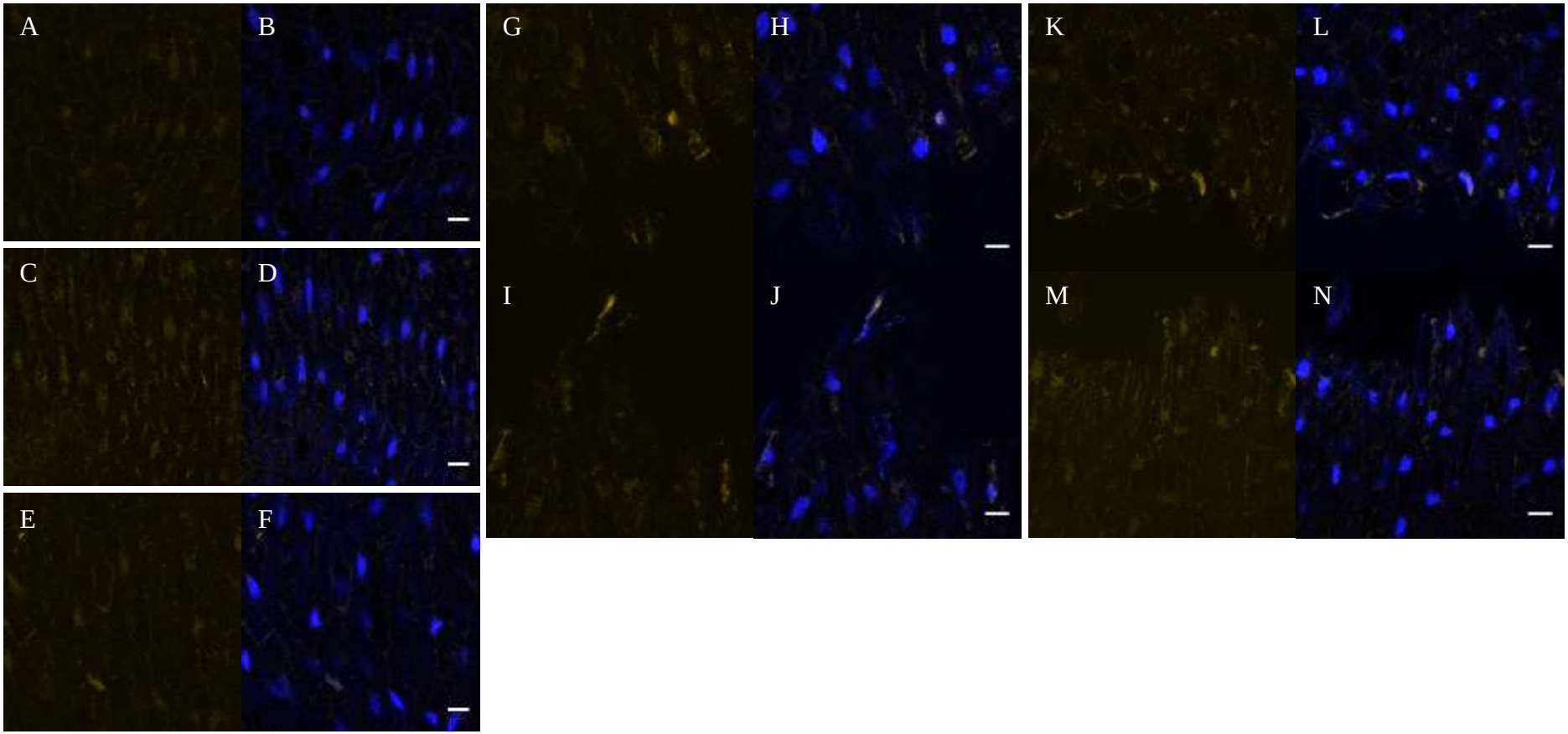

Figure 3.24. LM7 180 DAP immunohistological images show signal changes before and after cell separation. (A) LM7, and (B) LM7 and DAPI AZ 3 h without ethylene treatment. (C) LM7, and (D) LM7 and DAPI AZ 3 h with ethylene treatment. (E) LM7, and (F) LM7 and DAPI AZ 6 h with ethylene treatment. (G) LM7, and (H) LM7 and DAPI AZ at M side at 9 h with ethylene treatment and separation occurring. (I) LM7, and (J) LM7 and DAPI AZ at P side at 9 h with ethylene treatment and separation occurring. (K) LM7, and (L) LM7 and DAPI AZ at M side at 12 h with ethylene treatment and separation occurring. (M) LM7, and (N) LM7 and DAPI AZ at P side at 12 h with ethylene treatment and separation occurring. Scale bar = 10 µm.

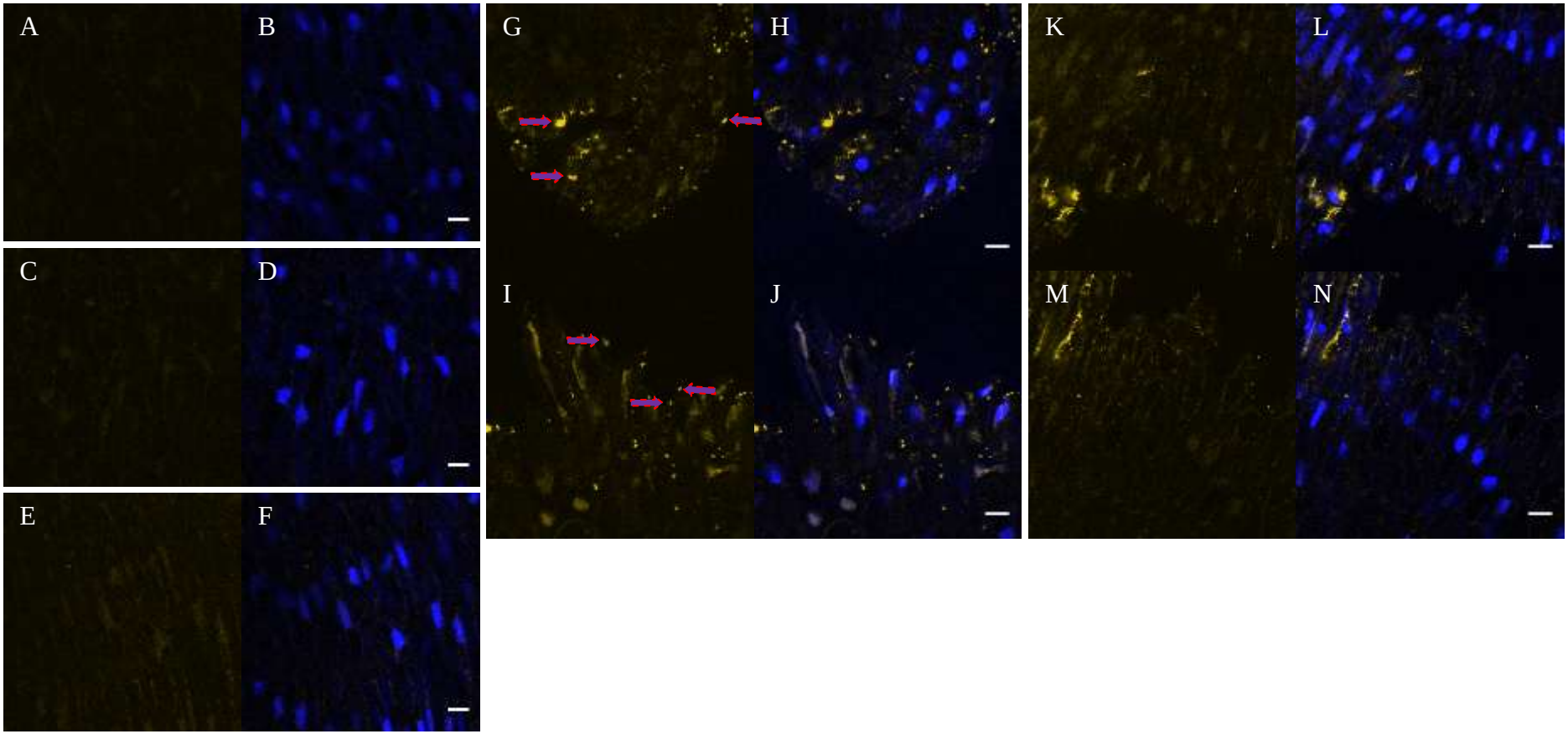

Figure 3.25. LM8 180 DAP immunohistological images show signal changes before and after cell separation. (A) LM8, and (B) LM8 and DAPI AZ 3 h without ethylene treatment. (C) LM8, and (D) LM8 and DAPI AZ 3 h with ethylene treatment. (E) LM8, and (F) LM8 and DAPI AZ 6 h with ethylene treatment. (G) LM8, and (H) LM8 and DAPI AZ at M side at 9 h with ethylene treatment and separation occurring. (I) LM8, and (J) LM8 and DAPI AZ at P side at 9 h with ethylene treatment and separation occurring. (K) LM8, and (L) LM8 and DAPI AZ at M side at 12 h with ethylene treatment and separation occurring. (M) LM8, and (N) LM8 and DAPI AZ at P side at 12 h with ethylene treatment and separation occurring. Scale bar = 10 µm.

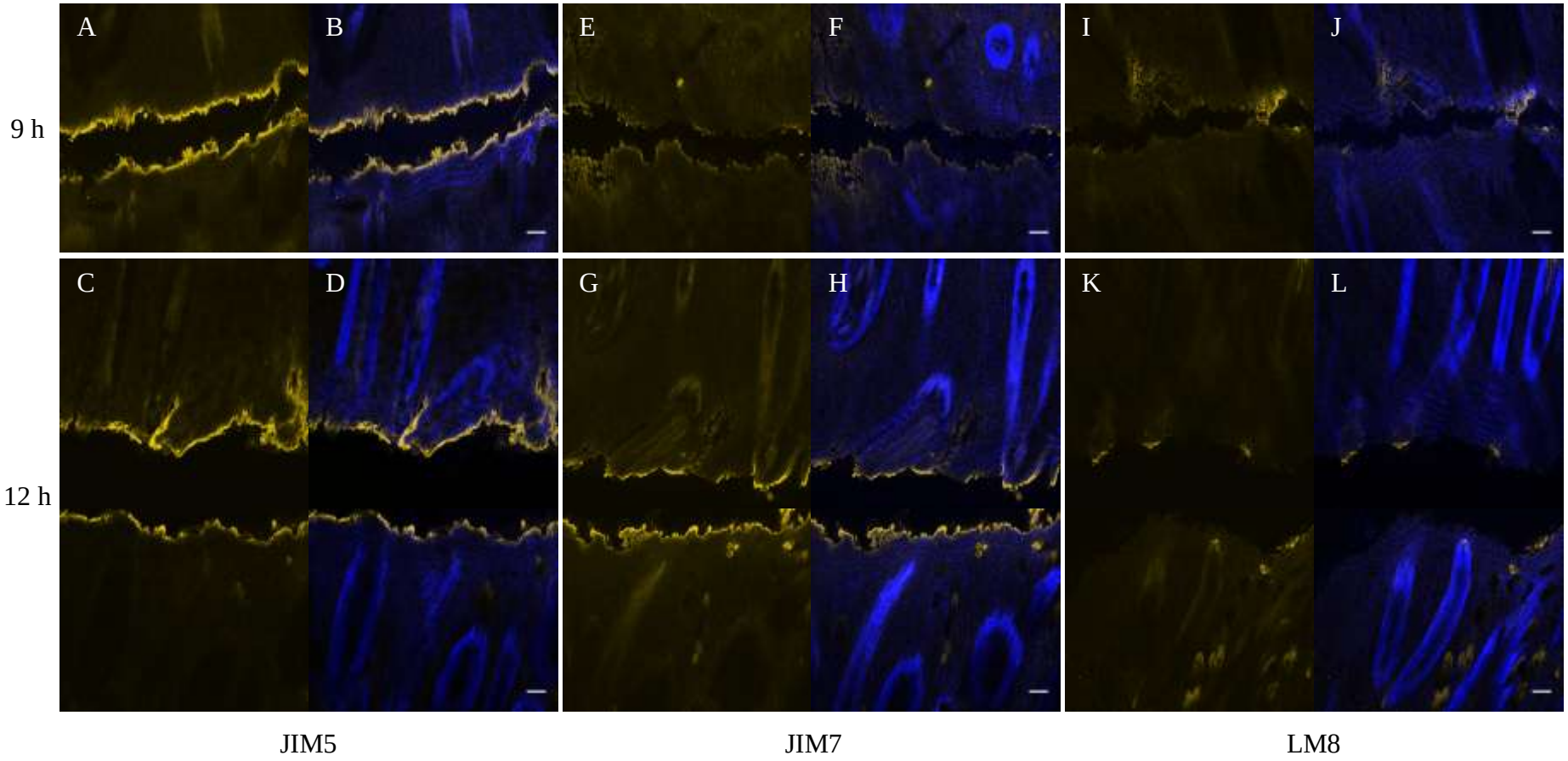

Figure 3.26. JIM5, JIM7, and LM8 180 DAP separated AZ immunohistological images show increased signal at the separation sites. (A) JIM5 separated AZ 9 h with ethylene treatment, (B) JIM5 and DAPI 9 h, (C) JIM5 separated AZ 12 h with ethylene treatment, (D) JIM7 AND DAPI 12 h, (E) JIM7 separated AZ 9 h with ethylene treatment, (F) JIM7 and DAPI 9 h, (G) JIM7 separated AZ 12 h with ethylene treatment, JIM7 and (H) DAPI 12 h, (I) LM8 separated AZ 9 h with ethylene treatment, (J) LM8 AND DAPI 9 h, (K) LM8 separated AZ 12 h with ethylene treatment, (L) LM8 and DAPI 12 h. Scale bar = 100 µm.

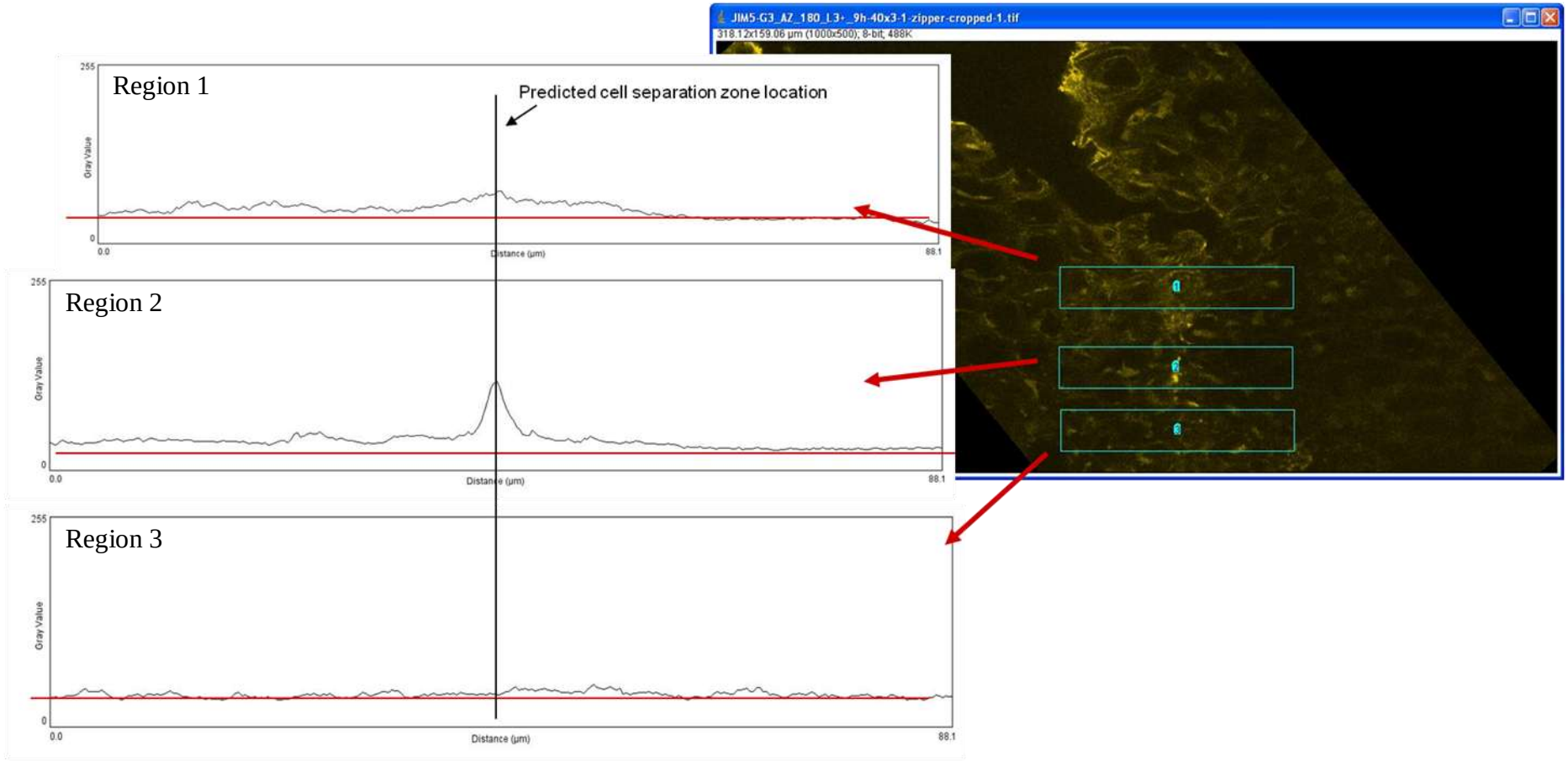

Figure 3.27. Predicted sites of separation may be associated with the JIM5 epitope. Quantification of the JIM5 grey level profile across in the AZ 180 DAP 9 h with ethylene treatment. The region 1 and 2 are the zones where separation may occur, and the region 3, which is far away from separated site, may not separate.

Antibody	Tissue	Before separation			After separation
		30 DAP	120 DAP	180 DAP	180 DAP
JIM5	Mesocarp	+++++	++	+	+
	Abscission zone	+++++	++	+	+++++ (*)
	Pedicel	+++++	++	+	+
JIM7	Mesocarp	+++++	++	+	+
	Abscission zone	+++++	++	++	+++++ (*)
	Pedicel	+++++	++	+	+
LM7	Mesocarp	+++++	++	++	++
	Abscission zone	+++++	++	++	++
	Pedicel	+++++	++	++	++
LM8	Mesocarp	+++++	+	++	+
	Abscission zone	+++++	+	++	+++ (**)
	Pedicel	++++	+	++	+

Table 3.1. Summary table of the intensity signal in different tissues at different developmental stages and after separation corresponding to JIM5, JIM7, LM7, and LM8 epitopes. * signal intensity at the separated sites, ** signal intensity of the vascular bundle tip at the separated sites. + represents signal intensity, the more +, the more signal intensity.

Discussion

Shedding of the oil palm fruit takes place after cell separation events in the AZ that consist of specialized cell layers located between the M and P. Cell separation in the AZ can be initiated by ethylene treatment, but this response depends on the developmental stage of the fruit. For example, ripe fruit at 180 DAP starts to shed within 9 h while immature fruit at 30 DAP sheds at 24 h when treated with ethylene. This study had the objective to determine whether changes in the cellular in general and in pectin portion in particular of the cell wall of AZ cells relate to functional acquisition of this zone and to cell separation events that lead to fruit shedding.

General cellular characteristics of oil palm fruit abscission zone

The combination of classical histological and electron microscopy approaches has allowed distinguishing specific cellular characteristics of oil palm fruit AZ at different stages of fruit development and by comparison with the adjacent tissues, M and P. The data revealed that AZ is differentiated early during fruit development. However at 30 DAP the AZ does not have the capacity to respond to ethylene in the same way, and does not function the same as in cells at later stages of development. Indeed, the cells of this zone show different characteristics than those observed in the functional AZ at 180 DAP. For example, at the mature stage, the observation of aligned nuclei of the AZ cells revealed in this study is the first observation found in documented plant system. The reason to explain this phenomenon is that the AZ cell division appeared at 30 DAP is periclinal, thus, at the later stages (120, and 180 DAP) the layers of the AZ prominently appear. However, the nuclear alignment can be firstly observed in vascular parenchyma tissue at 30 DAP. The observation suggests that the development in vascular parenchyma tissue starts before regular parenchyma tissue in this zone. The nuclear shape has changed during development. At 30 DAP, the shape of nucleus

is round as usually described in general cell biology books but at 120 DAP, the nuclear shape has changed to have more angles. This could be explained by the hypothesis that changes in nuclear shape affects chromatin reorganization and thereby affect gene expression (Webster *et al.* 2009). The observation also found that the nuclear shape of the parenchyma and vascular parenchyma cells within the AZ at 30 DAP are different. There is another hypothesis that could explain this phenomenon. It is proposed that changes in nuclear shape alter the rigidity of the nucleus which is beneficial for cells that need to squeeze through tight spaces (Webster *et al.* 2009).

Changing of plasmodesmata position at 120 DAP to the middle of the cell which is close to the position of nucleus might facilitate transportation of the matrix between the cell in the same layer. The other method which AZ parenchyma cells use to transport the cytoplasmic matrix is that vesicle fuses to plasmamembrane and transport to cell wall or adjoining cells (Sexton *et al.* 1977).

Incorporation of data from classical histology staining with toluidine blue and ruthenium red and electron microscopy, confirms that the fibrous matrix found by electron microscopy in AZ 120 DAP must be pectin. Moreover, the expansion of primary cell wall at the tip of the AZ 120 DAP parenchyma cell found in electron microscopy could be the dark pink staining observed with toluidine blue. However, it is unclear how the expansion of the primary cell wall at the tip of the cell has occurred, but it could be related to the accumulation of ribosome and mitochondria at the tip of the cell. Sexton *et al.* (1977) clearly showed *Impatiens* leaf AZ having the striations at the tip of the cell and plasmodesmata. They also demonstrated that *Coleus* and *Impatiens* leaf AZs increase the amount of rough endoplasmic reticulum, dictyosomes, and cytoplasmic vesicles after abscission.

In sum, the observations reveal that the AZ tissue has unique characteristics other than adjoining tissues. It has well-aligned nucleus due to periclinal division and also the nuclear

shape change during development which might involve in gene expression. Not only does the nuclear shape change, but the cell wall and cytoplasmic contents also alter. The amount of cytoplasmic vesicles increase in AZ 120 DAP, which might be involved in synthesizing substances involved in the expansion of the tip of the cell. The plasmodesmata position is changed as well which might speed up the transportation of cytoplasmic contents to neighbor cells.

Pectin fluctuation during developmental stages

Alteration of HG methylation state is important during plant development in case of cell adhesion and separation to occur (Jarvis *et al.* 2003). It is believed that pectin is synthesized in a highly methyl-esterified form in the golgi apparatus and transported to cell wall (Zhang and Staehelin 1992; Lennon and Lord 2000). After pectin deposition in the cell wall, the subsequent modification is processed by PME in order to de-methyl-esterify to form the egg-box pectin formation and to facilitate PGs hydrolysis function (Micheli 2001; Willats *et al.* 2001b). Changing in signal intensity in JIM5, JIM7, LM7, and LM8 antibodies indicates the pectin state and XGA status change during development. JIM5 binds pectin containing four contiguous unesterified GalA residues between two methyl-ester groups and also binds three unesterfied GalA residues between two methyl-ester groups. JIM7 binds three and four contiguous methyl-ester groups flanked by unesterified residues and also binds to alternating methyl-esterified and unesterified residues. LM7 binds methyl-esterified pectin containing four contiguous unesterified GalA residues between two methyl-ester groups which is one of the same methyl-esterified pectin recognized by JIM5 (Clausen *et al.* 2003) LM8 binds highly to xylose-substituted XGA (Willats *et al.* 2004) (Figure 3.1). The results confirm that methylated pectin can be found in early stage (30 DAP) in all tissues. The methylated pectin is de-methylated during maturation (120 DAP) and remains low during ripening (180 DAP).

Henderson *et al.* (2001a) demonstrated that highly unmethylated pectin could be found in ripe AZ fruit that is consistent with our data at 120 and 180 DAP. However, the previous study found more highly methylated pectin in M and P, which conflicts to our results at 120 and 180 DAP that show low signal intensity in JIM5, JIM7, and LM7. The diffused signals of JIM5, JIM7, and LM7 throughout the cell at the early stage of development are possibly due to transporting methyl-esterified pectin from golgi apparatus to be deposited in cell wall (Wolf *et al.* 2009). XGA is also found in early stage of development and decreases during the time before ripening and before cell separation occurs. This result could be explained as XGA prevents calcium-dependent interactions between HG chains (Jensen *et al.* 2008). Thus, in order to weaken the cell adhesion, XGA should be increased. In our result, it could be visualized that LM8 increases slightly at 180 DAP in all tissues compared to that of 120 DAP, and again during ethlylene induced separation.

Pectin fluctuation after cell separation

Considering the data from LM7 which has no detected signal after cell separation (Figure 3.24 G-N) and detected JIM5 signal (Figure 3.22 G-N) and also the methylated pectin patterns (Figure 3.1), it could be concluded that there is no induction of methylated pectin conformation 1 which is recognized by both JIM5 and JIM7 and the induction of methylated pectin detected by JIM5 after cell separation comes from conformation 2 (Clausen *et al.* 2003). At the present, 3 epitopes of JIM7 cannot be ruled out. The function of XGA is not well understood especially in cell detachment events; however, it might affect the physical properties of the pectic matrix. For example, the XGA will prevent calcium crosslinking of HGA chains and will also make an alteration on enzyme profiles capable of XGA modification, such that XGA is resistant to endo-PG digestion (Willats *et al.* 2004; Jensen *et al.* 2008). LM8 was found associated to cell detachment restricted to loosely attached

parenchyma cells at the inner face of the pea testa (Willats *et al.* 2004). This study supports the previous study that LM8 is associated to cell detachment by increasing the signal of LM8 epitope before and after cell separation (Figure 3.25). Moreover, an interesting feature of the oil palm fruit AZ is that the LM8 epitope is specific to separated vascular parenchyma cells (Figure 3.26 I-L).

The plant reponse to plant pathogens has been studied in several species. A high degree of pectin methylation in the middle lamella of sorghum confers plant resistant to aphids (Dreyer and Campbell 1984). The stem cell wall of potato genotype resistant to *Erwinia carotovora* subsp. *atroseptica* also shows highly methylated and branched water-soluable pectin (Marty *et al.* 1997). Thus, it could be possible that after cell separation occurs, the dramatic increase of methylated pectin along separated site might function in plant pathogen defense as a protective layer. However, it is curious that a defense layer would be synthesized as a response to pathogen attack on both the separated cell face of the P and the shed fruit M.

In this study, there are three hypotheses that could explain the occurrence of the higher JIM5 and JIM7 signal intensities observed on the separated cell faces. The first hypothesis, the "homeostasis in the wall", predicts that the activity of pectin modifying enzymes such as PME, give rise to the increase in the epitopes detected within the cell wall. After cell separation occurs, modifying enzymes within the cell wall may become active on the separated cell faces to modify pectin already present in the wall to give rise to the forms recognized by JIM5 and JIM7. Once JIM5 and JIM7 epitopes are produced through enzyme modifications of the pectin, the huge signal intensity appears (Figure 3.28 A). The second hypothesis, "separation cell layer homeostasis", is similar to the first hypothesis, except the pectin modifications are carried out by enzymes, such as PMT, within the cell (Figure 3.28 B). This hypothesis predicts that the pectin within the cell is modified by enyzmes within the

cell then secreted to the cell wall where the JIM5 and 7 epitopes accumulate to a high level. The last hypothesis, the "apoplastic transfer", predicts that pectin is transferred from other layers of AZ toward the separation layers where it accumulates. The result of immunohistology reveals that there are some line-like signals appearing within the inner side of primary walls at 9 h with ethylene treatment, and less signals at 12 h with ethylene treatment especially on M side (Figure 3.22 G-N, and Figure 3.23 G-N). This observation combined with the result of electron microscopy, which shows fewer plasmodesmata between AZ layers, suggests the lower signal at 12 h with ethylene treatment might be due to the removal of pectin from the separation layers through the apoplast, and/or channeled through the few remaining plasmodesmata between layers (Figure 3.28 C). This hypothesis is also supported by the observation that the pectin content of the AZ layers cells appears to be lost once separation has occurred. The mechanisms proposed in these hypotheses may not be mutually exclusive and may all function in combination to result in the high signal observed on the separation cell faces

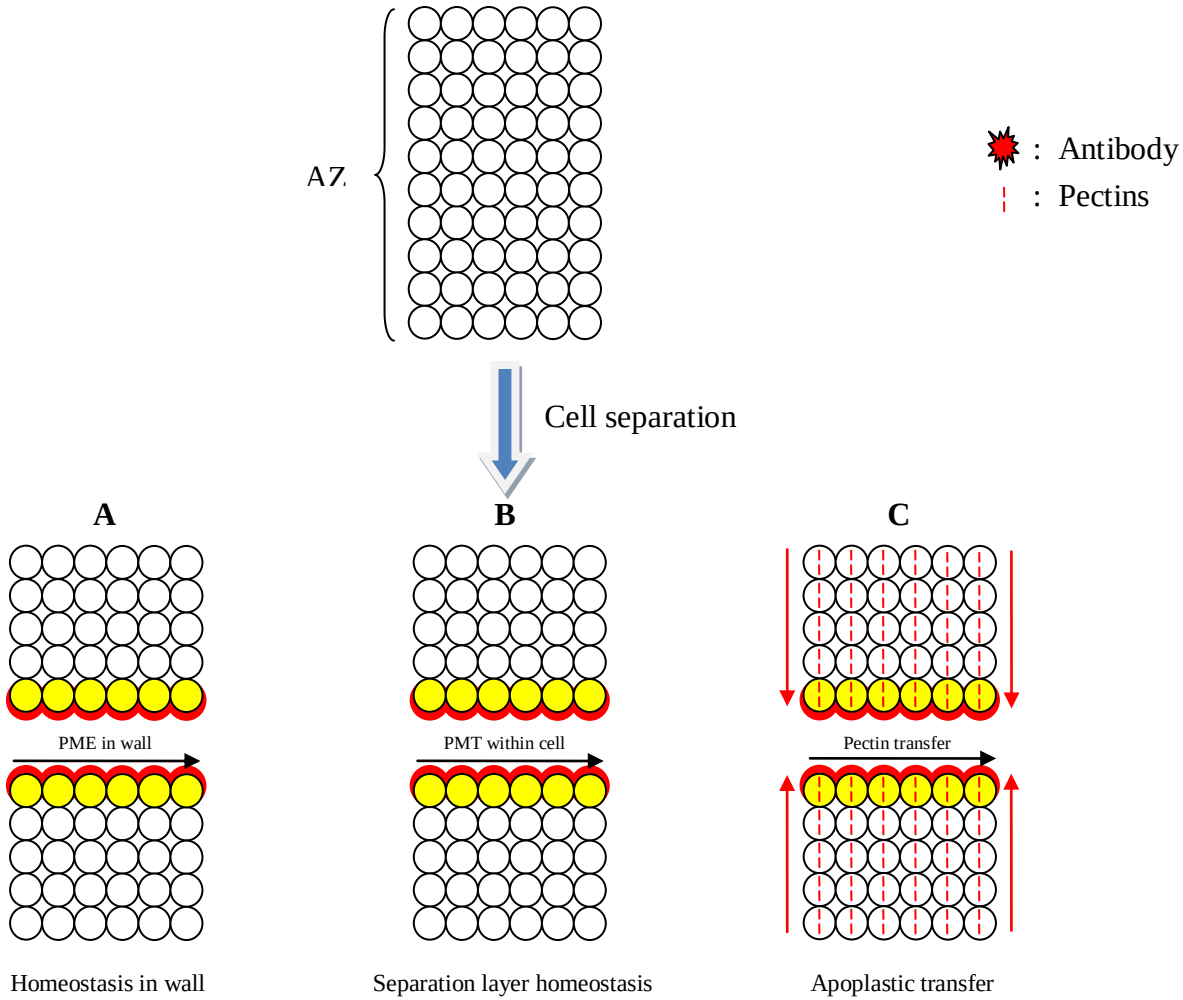

Figure 3.28. Three proposed hypotheses explain the event after cell separation occurs for JIM5 and JIM7 antibodies. (A) Homeostasis in wall hypothesis relates to PME in cell wall. (B) Separation layer homeostasis hypothesis relates to PMT within cell wall. (C) Apoplastic transfer hypothesis relates to transferring pectins from other layers of AZ to the separated layers via the apoplastic and/or plasmodesmata transfer mechanisms.

Materials and Methods

Plant Materials

Oil palm *Elaeis guineensis* fruits from CRA-PP Pobé plantation, Benin were used for classical histology experiment. Oil palm *Elaeis guineensis* variety Tenera clone C from Golden Tenera Plantation in Krabi Province, Thailand were used in the other experiments.

Oil palm fruit collection and ethylene treatment

See chapter 2

Classical histology sample preparation

Samples were fixed in 0.2 M phosphate buffer containing 2% (w/v) paraformaldehyde, 1% (w/v) caffeine, and 2% (v/v) glutaraldehyde 25% for a minimum of 2 days at 4 °C according to Buffard-Morel *et al.* (1992). Serail dehydration with ethanol from 30% to 100%, then 100% butanol/100% ethanol (v/v), and finally 100% butanol was performed for each sample and followed by impregnation and embedding in Technovit 7100 resin (Heraeus Kulzer). Semi-thin sections of 3 µm were cut using a microtome. Each section was stained with toluidine blue or ruthenium red. Microphotographs were taken with a Leica camera on a Leica LEITZ DMRB light microscope (x20/0.5; x40/0.7 and x100/1.3).

Scanning electron microscopy sample preparation

The samples were prepared as described in Verdeil *et al.* (2001).

Immunohistochemistry sample preparation

Blocking buffer (BB) : Phosphate-buffered saline (PBS) = 1:1 was prepared then add BB/PBS (500-1000 µl) mixed solution to the glass blocks. Next, add sample tissues two

pieces on each glass blocks and shake them gently on a shaker for three hours at room temperature (RT). Afterward, prepare BB : PBS : primary antibody (JIM5, JIM7, LM7, or LM8) = 9:9:2 and pipette the previous mixed solution out and add the new mixed solution containing primary antibody (500-1000 μl) to the glass blocks. Shake them gently on a shaker overnight (18 h) at 4 °C. After that, remove the mixed solution in the glass block, add PBS solution (500-1000 μl), shake them gently on a shaker for 15 min, drain out and repeat this step for two more times. From this step, do the preparation in a dark room. Prepare BB : PBS : secondary antibody (Alexa Fluor 546) = 499:499:2. Remove the mixed solution in the glass blocks and add the mixed solution with secondary antibody (500-1000 μl). Immediately, cover them with aluminum foil and shake them gently on a shaker for 1 h at RT. Add PBS solution (500-1000 μl), shake them gently on a shaker for 15 min, drain out and repeat this step for 2 more times. Prepare PBS : DAPI = 499 : 1. Cover them with aluminum foil and shake them gently on a shaker for 1 h at RT. Add PBS solution (500-1000 μl), shake them gently on a shaker for 15 min, drain out and repeat this step for 2 more times. Put the tissues on slides. Then, add a few MOWIAL droplets and cover with cover slips (No. 0). Next, leave the solution dry for a few days at RT. Finally, keep them at 4 °C with dark condition. The tissue observation was performed on Zeiss LSM 510 Meta Confocal Microscope.

Appendix

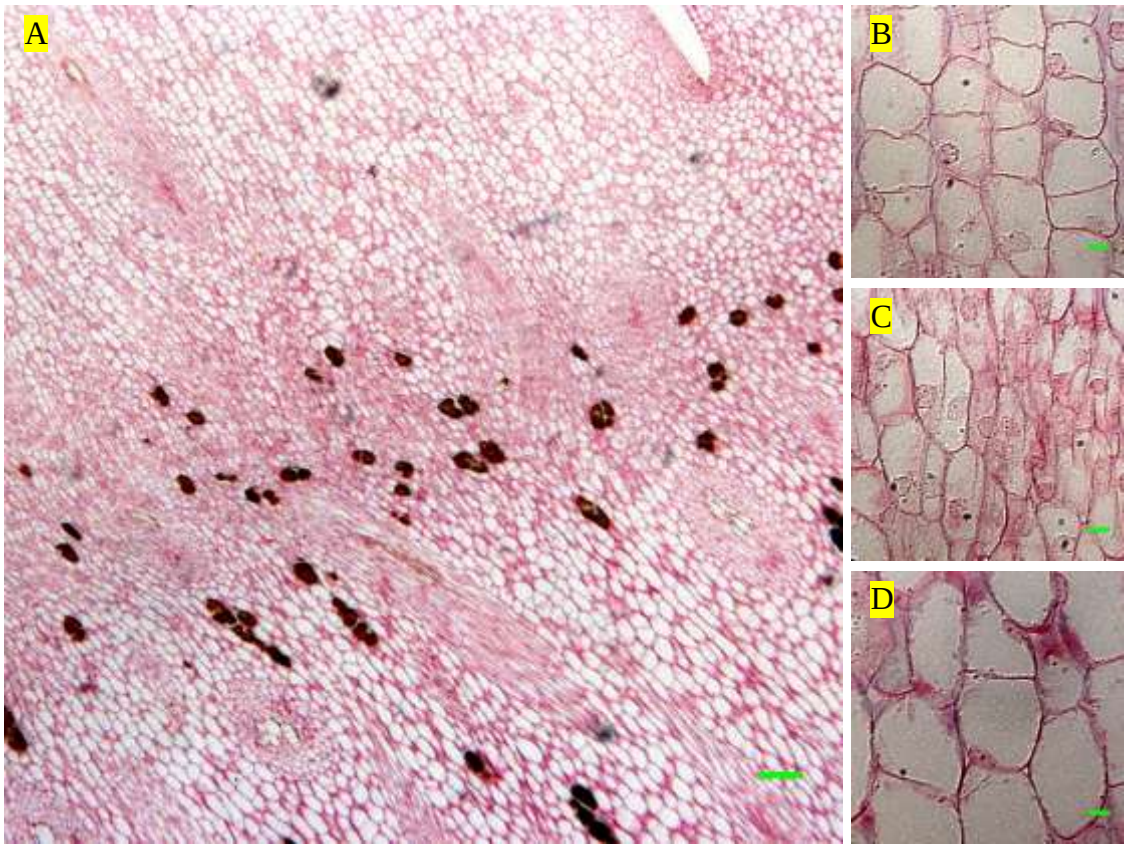

Figure S3.1. 30 DAP ruthenium red staining classical histological images show tissue overview and the details in each zones. (A) Tissue overview 5X including M, AZ, and P, (B) M 40X, (C) AZ 40X, and (D) P 40X. Scale bar = 100 µm in A, scale bar = 10 µm in B-D.

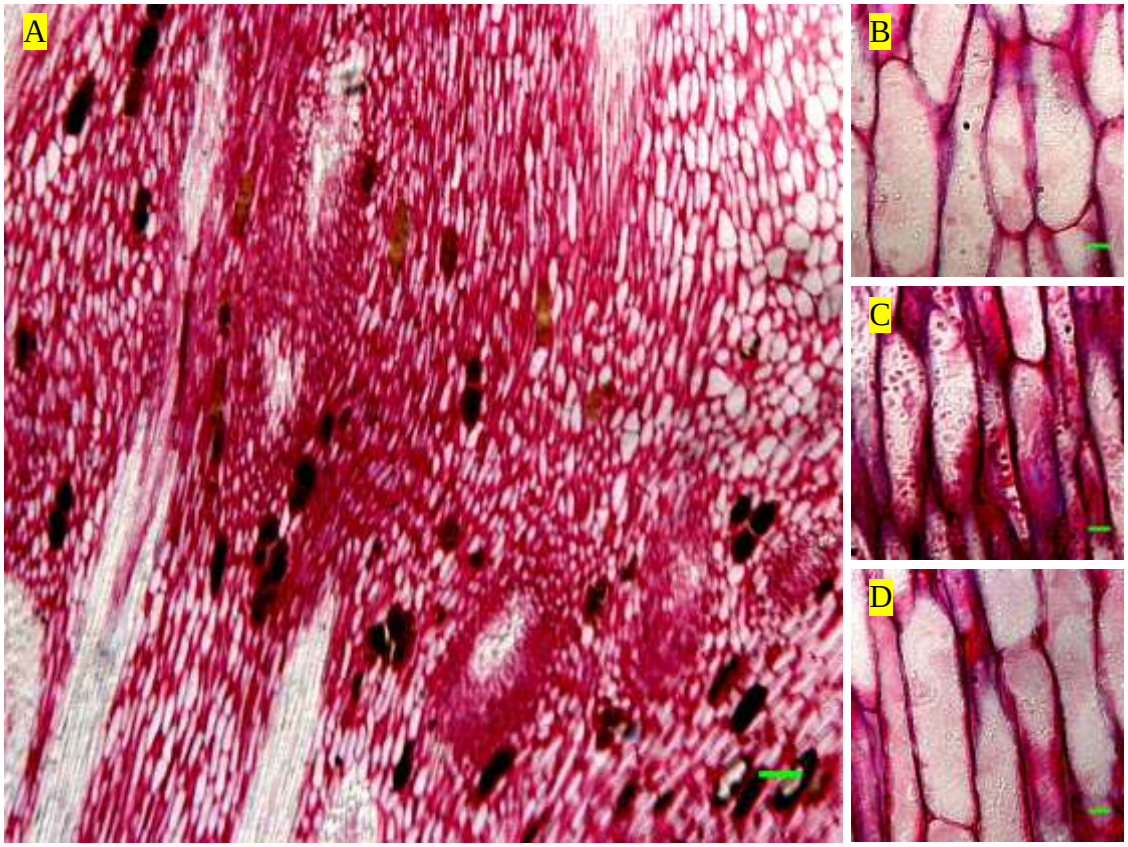

Figure S3.2. 120 DAP ruthenium red staining classical histological images show tissue overview and the details in each zones. (A) Tissue overview 5X including M, AZ, and P, (B) M 40X, (C) AZ 40X, and (D) P 40X. Scale bar = 100 µm in A, scale bar = 10 µm in B-D.

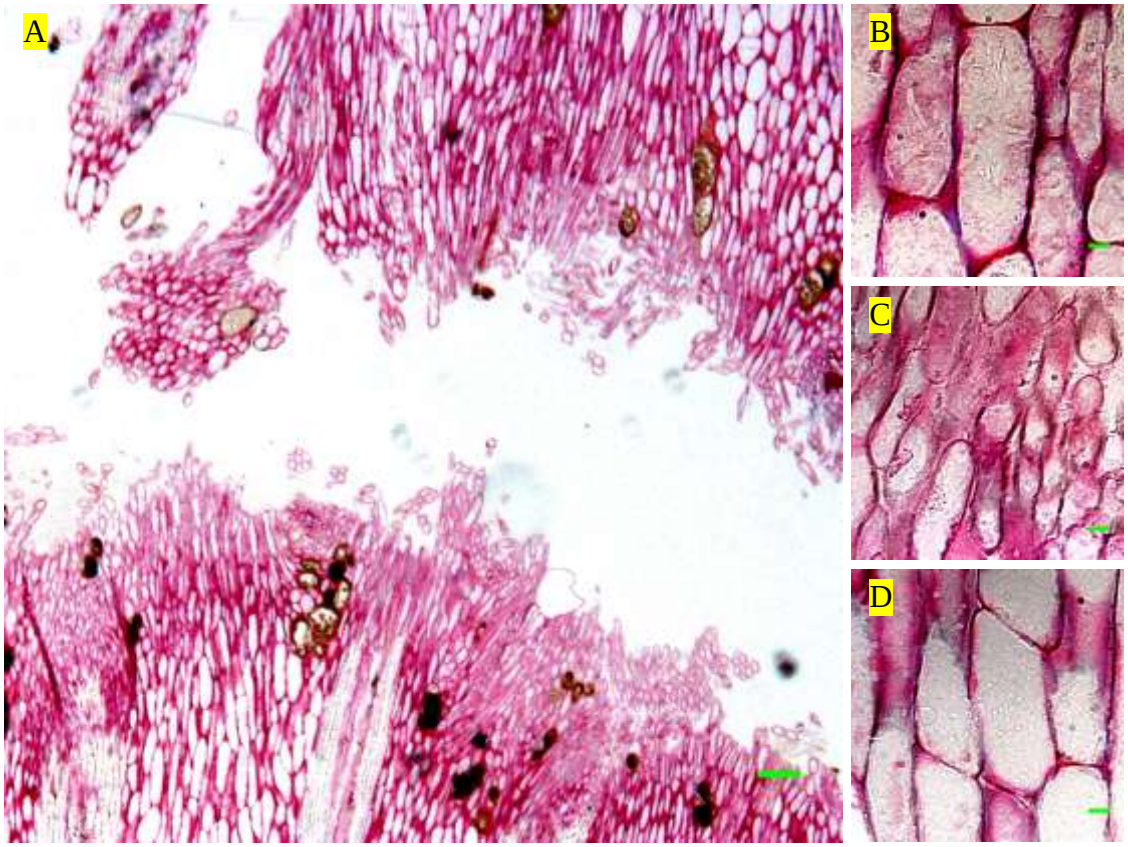

Figure S3.3. Classical histological images of 180 DAP with 9 h ethylene treatment and cell separation occurring with ruthenium red staining show tissue overview and the details in each zones. (A) Tissue overview 5X including M, AZ, and P, (B) M 40X, (C) AZ 40X, (D) P 40X. Scale bar = 100 µm in A, scale bar = 10 µm in B, C, and D.

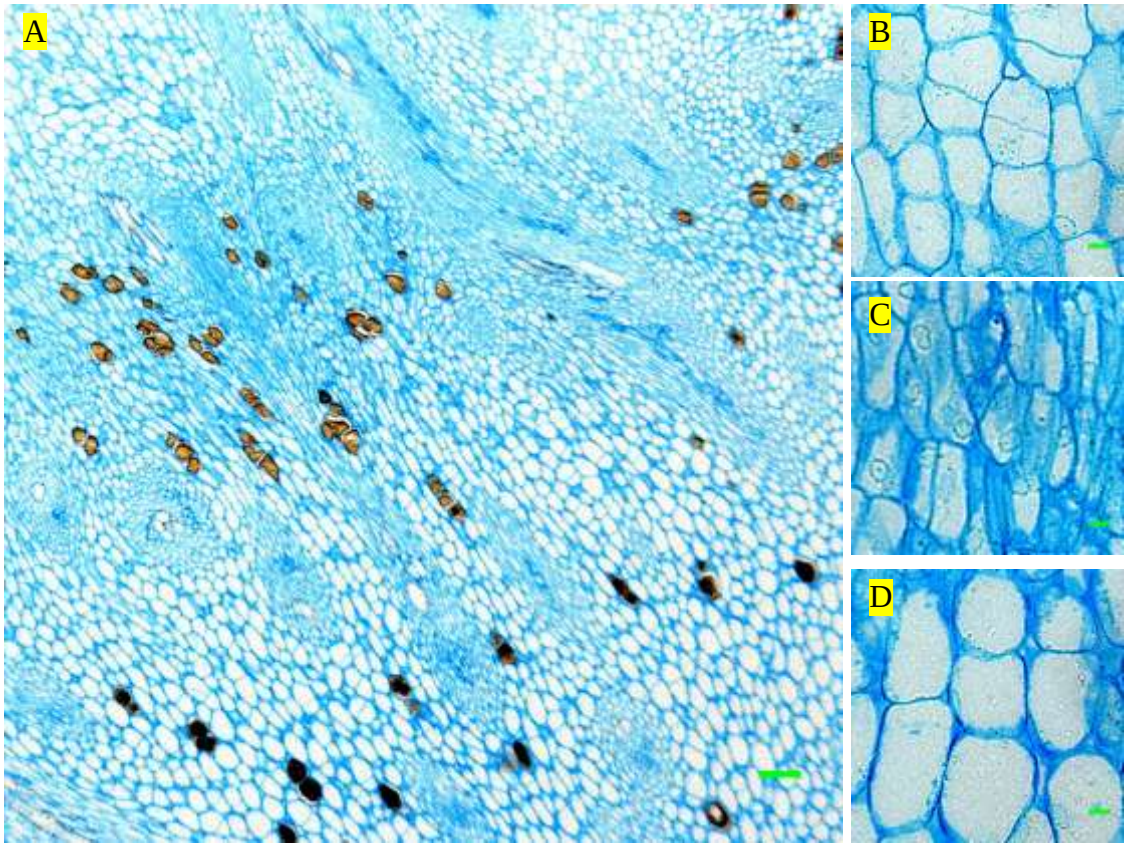

Figure S3.4. 30 DAP alcian blue staining classical histological images show tissue overview and the details in each zones. (A) Tissue overview 5X including M, AZ, and P, (B) M 40X, (C) AZ 40X, and (D) P 40X. Scale bar = 100 µm in A, scale bar = 10 µm in B-D.

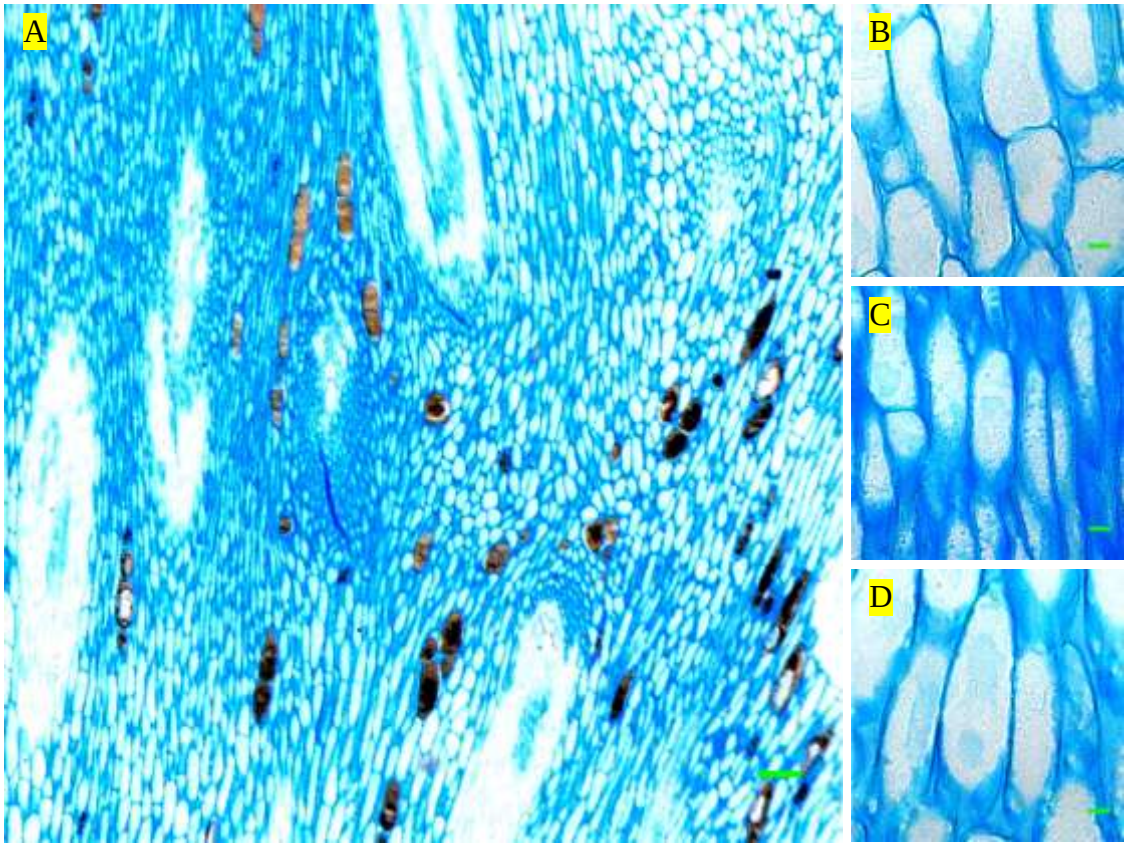

Figure S3.5. 120 DAP alcian blue staining classical histological images show tissue overview and the details in each zones. (A) Tissue overview 5X including M, AZ, and P, (B) M 40X, (C) AZ 40X, and (D) P 40X. Scale bar = 100 µm in A, scale bar = 10 µm in B-D.

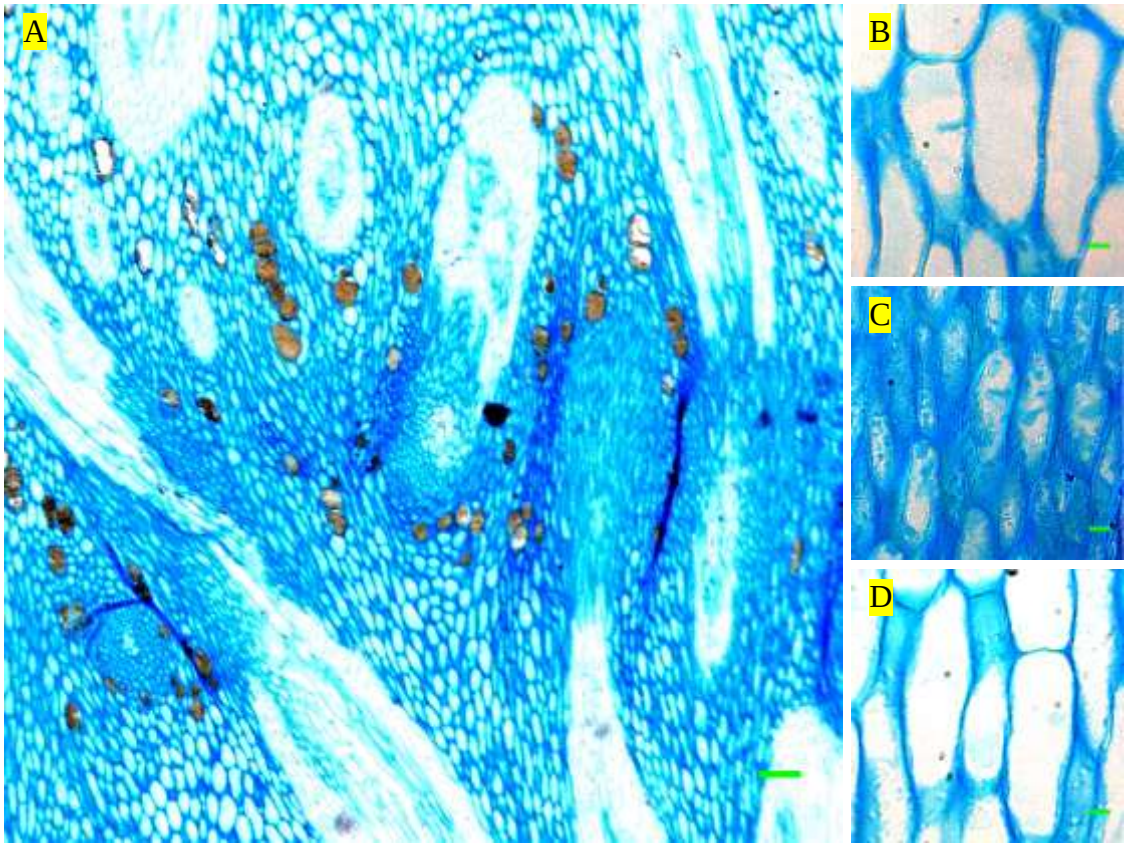

Figure S3.6. 180 DAP alcian blue staining classical histological images show tissue overview and the details in each zones. (A) Tissue overview 5X including M, AZ, and P, (B) M 40X, (C) AZ 40X, and (D) P 40X. Scale bar = 100 µm in A, scale bar = 10 µm in B-D.

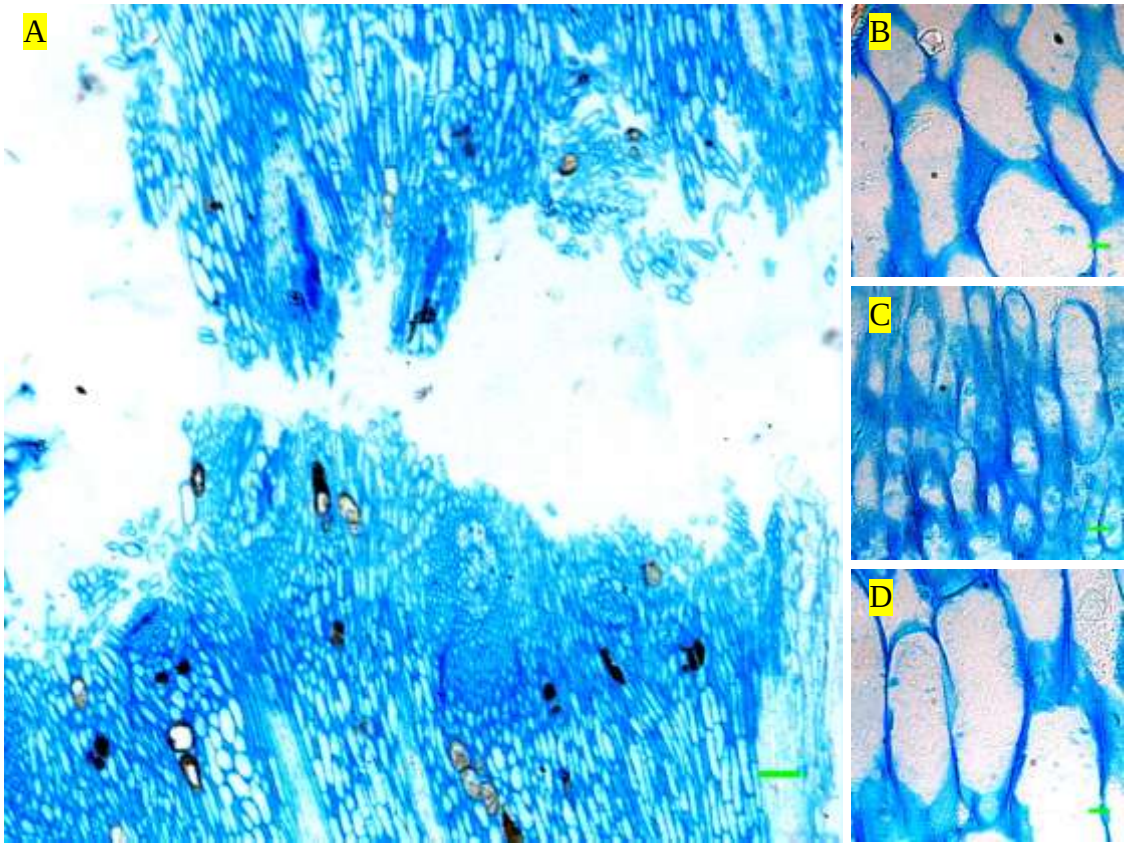

Figure S3.7. Classical histological images of 180 DAP with 9 h ethylene treatment and cell separation occurring with alcian blue staining show tissue overview and the details in each zones. (A) Tissue overview 5X including M, AZ, and P, (B) M 40X, (C) AZ 40X, (D) P 40X. Scale bar = 100 µm in A, scale bar = 10 µm in B, C, and D.

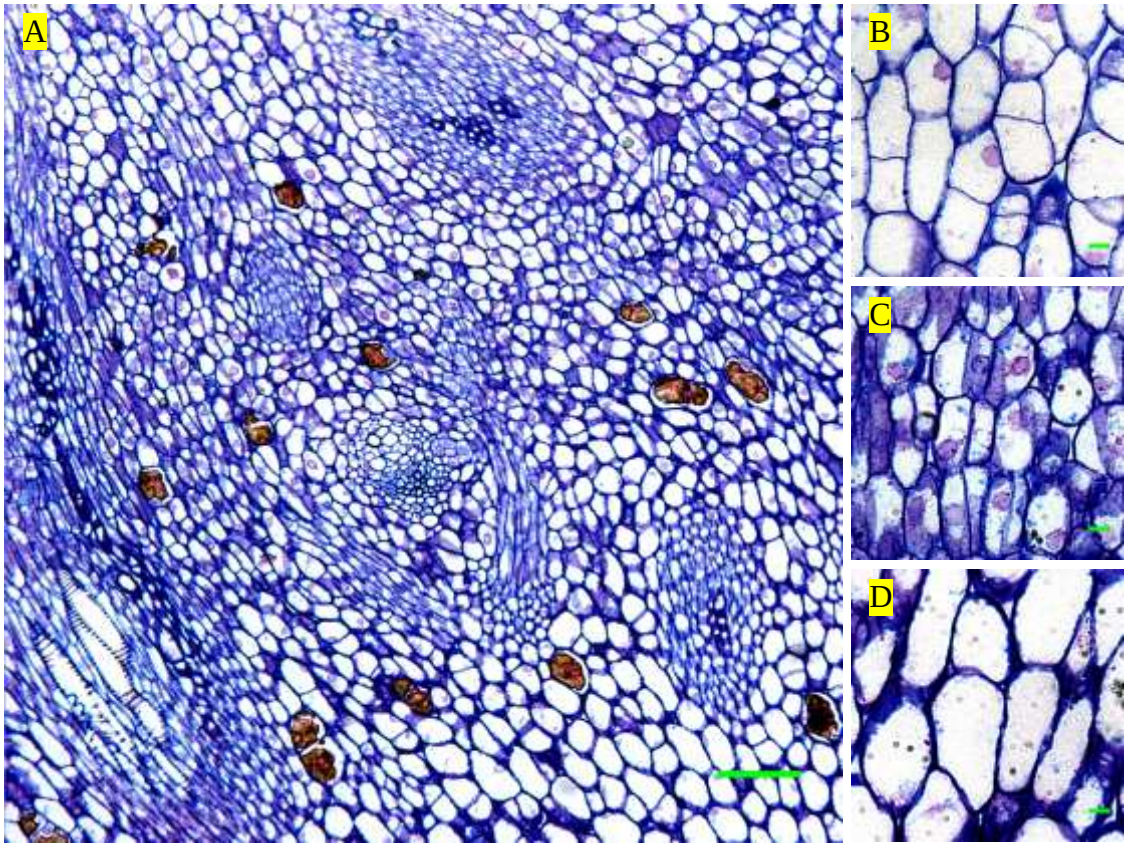

Figure S3.8. 30 DAP alcian blue and schiff's staining classical histological images show tissue overview and the details in each zones. (A) Tissue overview 10X including M, AZ, and P, (B) M 40X, (C) AZ 40X, and (D) P 40X. Scale bar = 100 µm in A, scale bar = 10 µm in B-D.

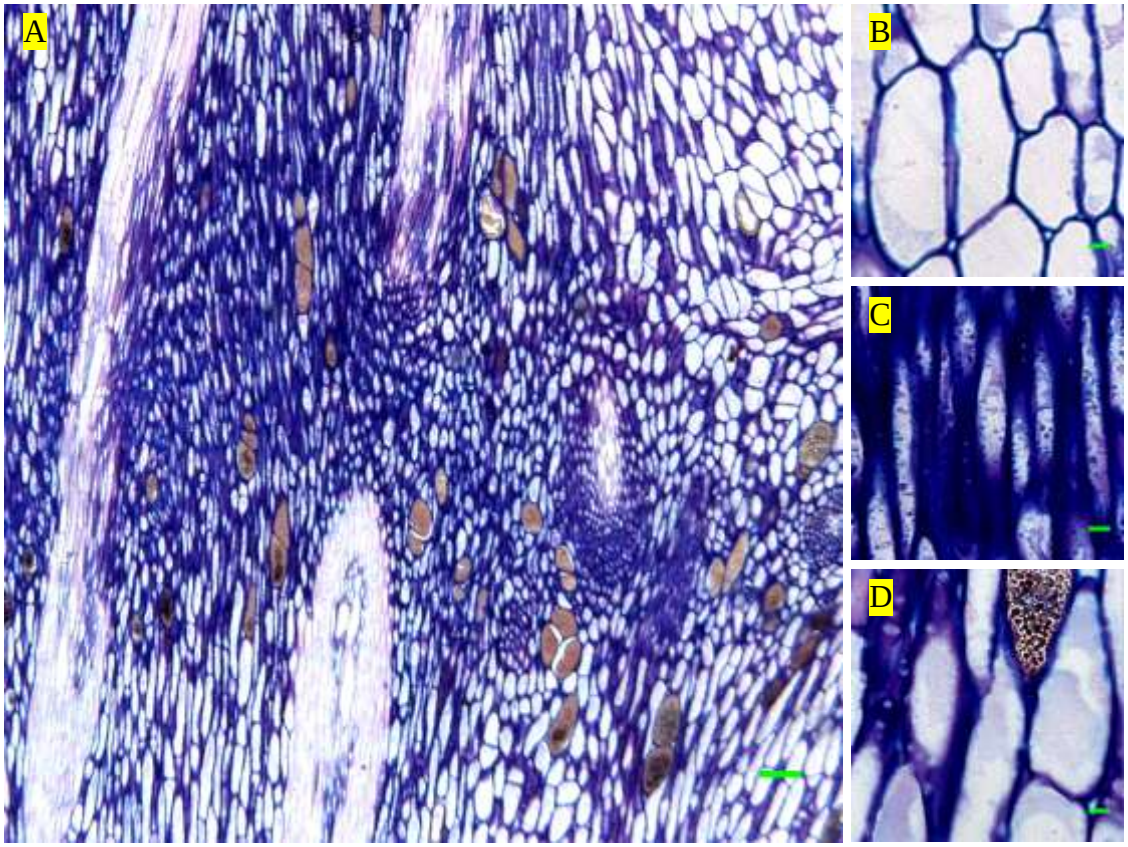

Figure S3.9. 120 DAP alcian blue and schiff's staining classical histological images show tissue overview and the details in each zones. (A) Tissue overview 5X including M, AZ, and P, (B) M 40X, (C) AZ 40X, and (D) P 40X. Scale bar = 100 µm in A, scale bar = 10 µm in B-D.

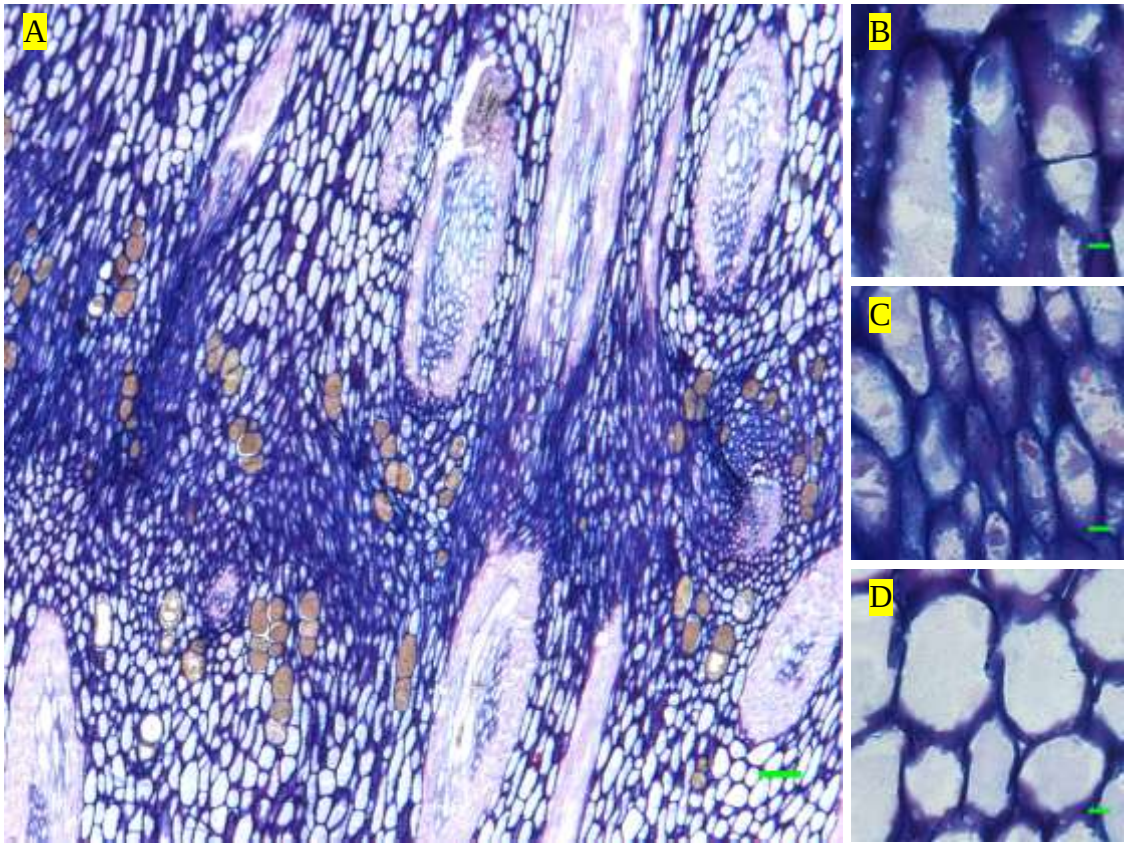

Figure S3.10. 180 DAP alcian blue and schiff's staining classical histological images show tissue overview and the details in each zones. (A) Tissue overview 5X including M, AZ, and P, (B) M 40X, (C) AZ 40X, and (D) P 40X. Scale bar = 100 µm in A, scale bar = 10 µm in B-D.

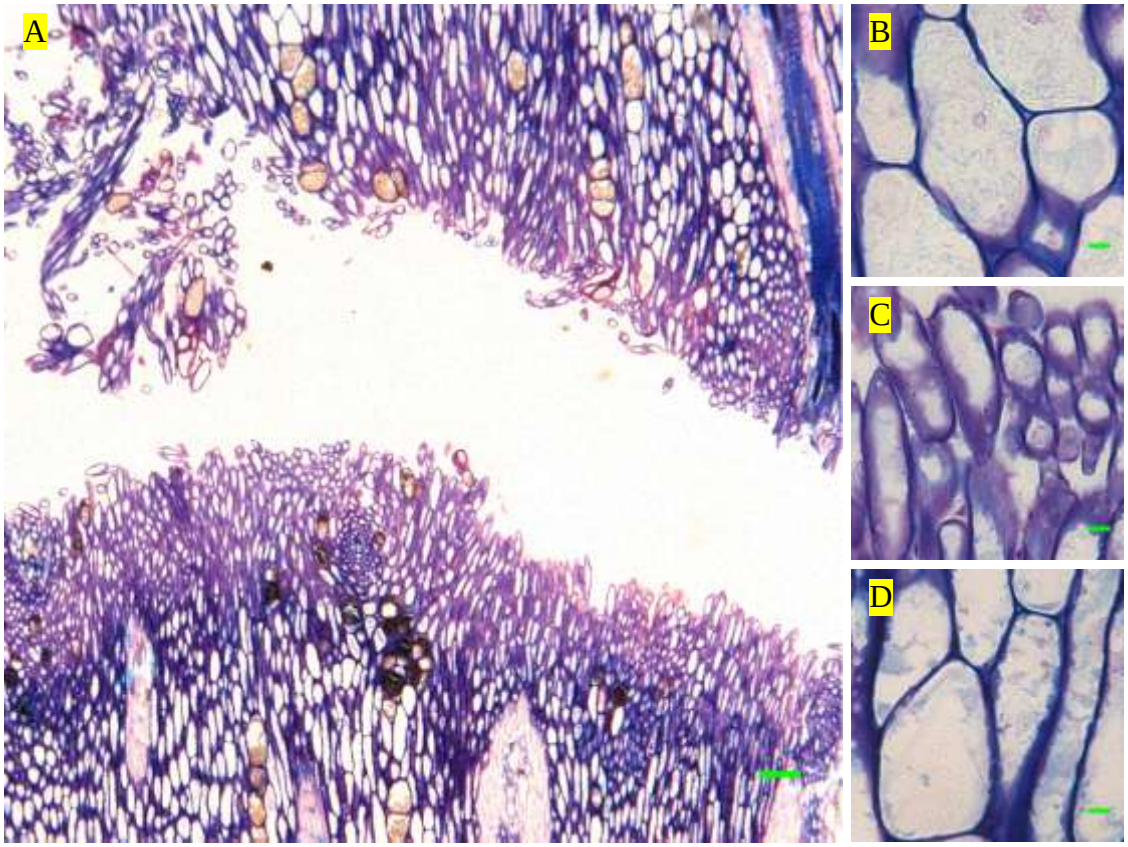

Figure S3.11. Classical histological images of 180 DAP with 9 h ethylene treatment and cell separation occurring with alcian blue and shiff's reagent staining show tissue overview and the details in each zones. (A) Tissue overview 5X including M, AZ, and P, (B) M 40X, (C) AZ 40X, (D) P 40X. Scale bar = 100 µm in A, scale bar = 10 µm in B, C, and D.

Literature Cited

Addicott, F. (1982). Abscission, University of California Press, Ltd. London.

Belfield, E. J., B. Ruperti, J. A. Roberts and S. McQueen-Mason (2005). "Changes in expansin activity and gene expression during ethylene-promoted leaflet abscission in Sambucus nigra." J Exp Bot **56**(413): 817-823.

Buffard-Morel, J., J. L. Verdeil and C. Pannetier (1992). "Embryogenèse somatique du Cocotier (*Cocos nucifera* L.) à partir de tissus foliaires : étude histologique." Can J Bot/Rev Can Bot **70**: 735-741.

Burg, S. P. (1968). "Ethylene, plant senescence and abscission." Plant Physiol **43**(9 Pt B): 1503-1511.

Cin, V. D., M. Danesin, A. Boschetti, A. Dorigoni and A. Ramina (2005). "Ethylene biosynthesis and perception in apple fruitlet abscission (Malus domestica L. Borck)." J Exp Bot **56**(421): 2995-3005.

Clausen, M. H., W. G. T. Willats and J. P. Knox (2003). "Synthetic methyl hexagalacturonate hapten inhibitors of anti-homogalacturonan monoclonal antibodies LM7, JIM5 and JIM7." Carbohydr Res **338**(17): 1797-1800.

Conrad, K. (2008). "Correlation between the distribution of lignin and pectin and distribution of sorbed metal ions (lead and zinc) on coir (Cocos nucifera L.)." Bioresour Technol **99**(17): 8476-8484.

Cosgrove, D. J. (2005). "Growth of the plant cell wall." Nat Rev Mol Cell Biol **6**(11): 850-861.

Dreyer, D. L. and B. C. Campbell (1984). "Association of the degree of methylation of intercellular pectin with plant resistance to aphids and with induction of aphid biotypes." Cell Mol Life Sci **40**(2): 224-226.

Francis, K. E., S. Y. Lam and G. P. Copenhaver (2006). "Separation of Arabidopsis Pollen Tetrads Is Regulated by QUARTET1, a Pectin Methylesterase Gene." Plant Physiol **142**(3): 1004-1013.

Gonzalez-Bosch, C., E. del Campillo and A. B. Bennett (1997). "Immunodetection and Characterization of Tomato Endo-[beta]-1,4-Glucanase Cel1 Protein in Flower Abscission Zones." Plant Physiol **114**(4): 1541-1546.

Grant, G. T., E. R. Morris, D. A. Rees, P. J. C. Smith and D. Thom (1973). "Biological interactions between polysaccharides and divalent cations: The egg-box model." FEBS Lett **32**(1): 195-198.

Hadfield, K. A. and A. B. Bennett (1998). "Polygalacturonases: Many Genes in Search of a Function." Plant Physiol **117**(2): 337-343.

Henderson, J., H. A. Davies, S. J. Heyes and D. J. Osborne (2001). "The study of a monocotyledon abscission zone using microscopic, chemical, enzymatic and solid state 13C CP/MAS NMR analyses." Phytochemistry **56**(2): 131-139.

Henderson, J. and D. J. Osborne (1994). "Inter-tissue signalling during the two-phase abscission in oil palm fruit." J Exp Bot **45**(7): 943-951.

Hou, W.-C., W.-H. Chang and C.-M. Jiang (1999). "Qualitative distinction of carboxyl group distributions in pectins with ruthenium red." Bot Bull Acad Sinica **40**: 115-119.

Jarvis, M. C., S. P. H. Briggs and J. P. Knox (2003). "Intercellular adhesion and cell separation in plants." Plant, Cell Environ **26**(7): 977-989.

Jensen, J. K., S. O. Sørensen, J. Harholt, N. Geshi, Y. Sakuragi, I. Møller, J. Zandleven, A. J. Bernal, N. B. Jensen, C. Sørensen, M. Pauly, G. Beldman, W. G. T. Willats and H. V. Scheller (2008). "Identification of a Xylogalacturonan Xylosyltransferase Involved in Pectin Biosynthesis in Arabidopsis." Plant Cell **20**(5): 1289-1302.

Kauss, H. and W. Z. Hassid (1967). "Enzymic Introduction of the Methyl Ester Groups of Pectin." J Biol Chem **242**(15): 3449-3453.

Lennon, K. and E. Lord (2000). "In vivo pollen tube cell of *Arabidopsis thaliana*; I. Tube cell cytoplasm and wall." Protoplasma **214**(1): 45-56.

Leroux, O., J. P. Knox, F. Leroux, A. Vrijdaghs, E. Bellefroid, G. Borgonie and R. L. L. Viane (2007). "Intercellular Pectic Protuberances in Asplenium: New Data on their Composition and Origin." Ann Bot **100**(6): 1165-1173.

Li, J. and R. Yuan (2008). "NAA and Ethylene Regulate Expression of Genes Related to Ethylene Biosynthesis, Perception, and Cell Wall Degradation During Fruit Abscission and Ripening in 'Delicious' Apples." J Plant Growth Regul **27**(3): 283-295.

Marty, P., B. Jouan, Y. Bertheau, B. Vian and R. Goldberg (1997). "Charge density in stem cell walls of Solanum tuberosum genotypes and susceptibility to blackleg." Phytochemistry **44**(8): 1435-1441.

Micheli, F. (2001). "Pectin methylesterases: cell wall enzymes with important roles in plant physiology." Trends Plant Sci **6**(9): 414-419.

Mohnen, D. (2008). "Pectin structure and biosynthesis." Curr Opin Plant Biol **11**(3): 266-277.

O'Neill, M. A., T. Ishii, P. Albersheim and A. G. Darvill (2004). "RHAMNOGALACTURONAN II: Structure and Function of a Borate Cross-Linked Cell Wall Pectic Polysaccharide." Annu Rev Plant Biol **55**(1): 109-139.

Osborne, D. J., J. Henderson and R. H. V. Corley (1992). "Controlling fruit-shedding in the oil palm." Endeavour **16**(4): 173-177.

Patterson, S. E. and A. B. Bleecker (2004). "Ethylene-Dependent and -Independent Processes Associated with Floral Organ Abscission in Arabidopsis." Plant Physiol **134**(1): 194-203.

Pelloux, J., C. Rustérucci and E. J. Mellerowicz (2007). "New insights into pectin methylesterase structure and function." Trends Plant Sci **12**(6): 267-277.

Roberts, J. A., K. A. Elliott and Z. H. Gonzalez-Carranza (2002). "Abscission, Dehiscence, and Other Cell Separation Processes." Annu Rev Plant Biol **53**(1): 131-158.

Sexton, R., G. G. C. Jamieson and M. H. I. L. Allan (1977). "An ultrastructural study of abscission zone cells with special reference to the mechanism of enzyme secretion." Protoplasma **91**(4): 369-387.

Sexton, R. and J. A. Roberts (1982). "Cell Biology of Abscission." Ann Rev Plant Physio **33**(1): 133-162.

Tranbarger, T. J., S. Dussert, T. Joët, X. Argout, M. Summo, A. Champion, D. Cros, A. Omore, B. Nouy and F. Morcillo (2011). "Regulatory mechanisms underlying oil palm fruit mesocarp maturation, ripening and functional specialization in lipid and carotenoid metabolism." Plant Physiol.

Usadel, B., A. M. Kuschinsky, M. G. Rosso, N. Eckermann and M. Pauly (2004). "RHM2 Is Involved in Mucilage Pectin Synthesis and Is Required for the Development of the Seed Coat in Arabidopsis." Plant Physiol **134**(1): 286-295.

Verdeil, J. L., V. Hocher, C. Huet, F. Grosdemange, J. Escoute, N. Ferrière and M. Nicole (2001). "Ultrastructural Changes in Coconut Calli Associated with the Acquisition of Embryogenic Competence." Ann Bot **88**(1): 9-18.

Watson, M. L. (1958). "Staining of Tissue Sections for Electron Microscopy with Heavy Metals." The Journal of Biophysical and Biochemical Cytology **4**(4): 475-478.

Webster, M., K. L. Witkin and O. Cohen-Fix (2009). "Sizing up the nucleus: nuclear shape, size and nuclear-envelope assembly." J Cell Sci **122**(10): 1477-1486.

Willats, W. G. T., G. Limberg, H. C. Buchholt, G.-J. van Alebeek, J. Benen, T. M. I. E. Christensen, J. Visser, A. Voragen, J. D. Mikkelsen and J. P. Knox (2000). "Analysis

of pectic epitopes recognised by hybridoma and phage display monoclonal antibodies using defined oligosaccharides, polysaccharides, and enzymatic degradation." Carbohydr Res **327**(3): 309-320.

Willats, W. G. T., L. McCartney, W. Mackie and J. P. Knox (2001a). "Pectin: cell biology and prospects for functional analysis." Plant Mol Biol **47**(1): 9-27.

Willats, W. G. T., C. Orfila, G. Limberg, H. C. Buchholt, G.-J. W. M. van Alebeek, A. G. J. Voragen, S. E. Marcus, T. M. I. E. Christensen, J. D. Mikkelsen, B. S. Murray and J. P. Knox (2001b). "Modulation of the Degree and Pattern of Methyl-esterification of Pectic Homogalacturonan in Plant Cell Walls." J Biol Chem **276**(22): 19404-19413.

Willats, W. T., L. McCartney, C. Steele-King, S. Marcus, A. Mort, M. Huisman, G.-J. Alebeek, H. Schols, A. J. Voragen, A. Goff, E. Bonnin, J.-F. Thibault and J. P. Knox (2004). "A xylogalacturonan epitope is specifically associated with plant cell detachment." Planta **218**(4): 673-681.

Wolf, S., G. Mouille and J. Pelloux (2009). "Homogalacturonan Methyl-Esterification and Plant Development." Mol Plant **2**(5): 851-860.

Zhang, G. F. and L. A. Staehelin (1992). "Functional Compartmentation of the Golgi Apparatus of Plant Cells : Immunocytochemical Analysis of High-Pressure Frozen- and Freeze-Substituted Sycamore Maple Suspension Culture Cells." Plant Physiol **99**(3): 1070-1083.

Chapter 4. Conclusion and Future Prospects

Non-synchronized ripening and subsequent shedding of the ripest fruit before harvest is an important factor that limits overall palm oil yields and increases harvest costs (Henderson and Osborne 1990). Understanding the process of oil palm fruit abscission is an important step towards providing tools for molecular breeding strategies to limit fruit shedding. In addition, a two-stage abscission process involving primary and adjacent abscission zones (AZs), plus high levels of unmethylated pectin and polygalacturonase (PG) activity reported previously in the fruit AZ, warrant further investigation to provide insights into the mechanisms of abscission in a monocot fruit species. An originality of the current study is that it is based on multi-disciplinary approaches including physiology, histology, immunolocalization, and molecular biology. The results obtained from these different approaches allow an integrated view of the fruit abscission process in oil palm and a schematic model of AZ development and function during shedding has been developed (Figure 4.1).

Briefly, the AZ arises from periclinal cell divisions early during fruit development and the capacity for the AZ to respond to ethylene increases during development and coincides with an increase in the accumulation of unmethylated pectin particles within the AZ cells. From early development, plasmodesmata (PD) are apparent between adjacent AZ cells, whereas during development, the PD become larger and less numerous between layers and remain numerous within layers. These results suggest intra-layer cell-cell communication via PD is important for the functional capacity of the AZ layers. This may be especially important for the alignment of the nuclei of the AZ cell layers that arises early during development and persists up until fruit shedding. Furthermore, AZ cells have polarized vesicle activity at the cell tips that coincides with cell elongation, which may provide inter-layer communication functions.

A major finding of these studies is the identification of *EgPG4* transcript as the best candidate for the large increase in PG activity previously observed (Henderson *et al.* 2001a). In the current study, evidence has been provided that *EgPG4* is highly induced in the AZ, but also the fact that it occurs in an exceptionally high amount in the ripening mesocarp suggests it may also function during ripening of this tissue. This contrasts with specialization of PGs that function either in ripening or abscission in tomato, and suggests differences between the associated regulatory pathways of these two divergent fruit species. Therefore, two important questions arise from these results: 1) what factors regulate the spatial expression and specificity of EgPG4 activity during abscission and during ripening in the mesocarp and 2) what is the exact function of the EgPG4 enzyme in these two distinct tissues. To address these questions is a great challenge considering the limitations to do functional studies in oil palm. Nevertheless, some available approaches have already been initiated and others can be envisaged to provide evidence for the role of EgPG4 and the regulatory factors that function during oil palm fruit shedding.

Firstly, to examine the possible factors that regulate the transcription of *EgPG4*, genomic DNA library is under construction to isolate the *EgPG4* promoter. In addition, samples collected during the ethylene time course (Figure 2.1) were collected to do both transcriptome and proteome sequencing. The proteome data is currently available and is being analyzed by the group, while the 454 pyrosequencing analysis of the abscission transcriptome is planned for the end of 2011 in Thailand. Another possible approach could be to raise antibodies to the EgPG4 protein to examine its subcellular localization in the AZ and the mesocarp. This approach could provide evidence for the role of EgPG4 in these tissues and provide additional tools for examining abscission in this species. These approaches could give insight into the regulatory pathways that function in the oil palm AZ during shedding.

The current studies also raise the question about the significance of the JIM5 and JIM7 epitopes at the separated sites, and the mechanism by which these signals increase in a polarized manner preferentially on the separated cell surface layer. Several mechanisms can be proposed to explain the phenomenon including: 1) PME activity in the separation layer cell walls acts on either pectin already present in the cell wall, or newly inserted pectin secreted during the cell separation process, 2) PMT activity within the separation layer cells methylates unmethylated pectin that is then secreted to the apoplast, 3) the transfer of pectin throughout the AZ cell layers towards the separation layer where the JIM5 and 7 pectin epitopes accumulate. These are not mutually exclusive and the increase in the JIM5 and 7 epitopes could be a combination of all these mechanisms. One important question remains to be answered is the exact subcellular localization of these epitopes and how they change during separation. In order to determine the subcellular localization, experiments have been initiated with JIM5 and JIM7 antibodies combined with electron microscopy. The results from these experiments are currently unavailable. In addition, to complete the cellular characterization of oil palm fruit AZ during development and after separation, the ultrastructure of fruit at 180 DAP and 180 DAP 9 h with ethylene treatment should be studied with electron microscopy. Together, these experiments should give a better view of cellular ultrastructure changes during development and after separation and the localization dynamics of the JIM5 and 7 epitopes during fruit shedding.

Finally, a study of the AZ using infrared spectroscopy (IRS) has been initiated and could also provide further evidence of the importance of methyl-esterification in the AZ of separated and unseparated sites comparing to mesocarp and pedicel. After the infrared spectroscopy analysis finishes, the information can be compared with the results of the immunohistochemistry of JIM5, JIM7, and LM7 given that IRS can also quantify the amount of methyl-esterification in the fruit tissues and different cell types. Moreover, it can also

quantify the amount of other compounds such as hydroxyl compounds, other polysaccharides, and lipid contents, which will also expand knowledge of the oil palm fruit AZ.

This Ph.D. work shows that the oil palm fruit AZ has many interesting characteristics. The work and results extends the oil palm fruit AZ to be used as a model to study abscission in plants, especially in fruit bearing monocots. The author also assumes that using different cellular and molecular approaches in this study and future experiments will give a better knowledge in abscission process for the ultimate goal to control the fruit shedding and to limit the loss of palm oil yield from unsynchronizing fruit shedding.

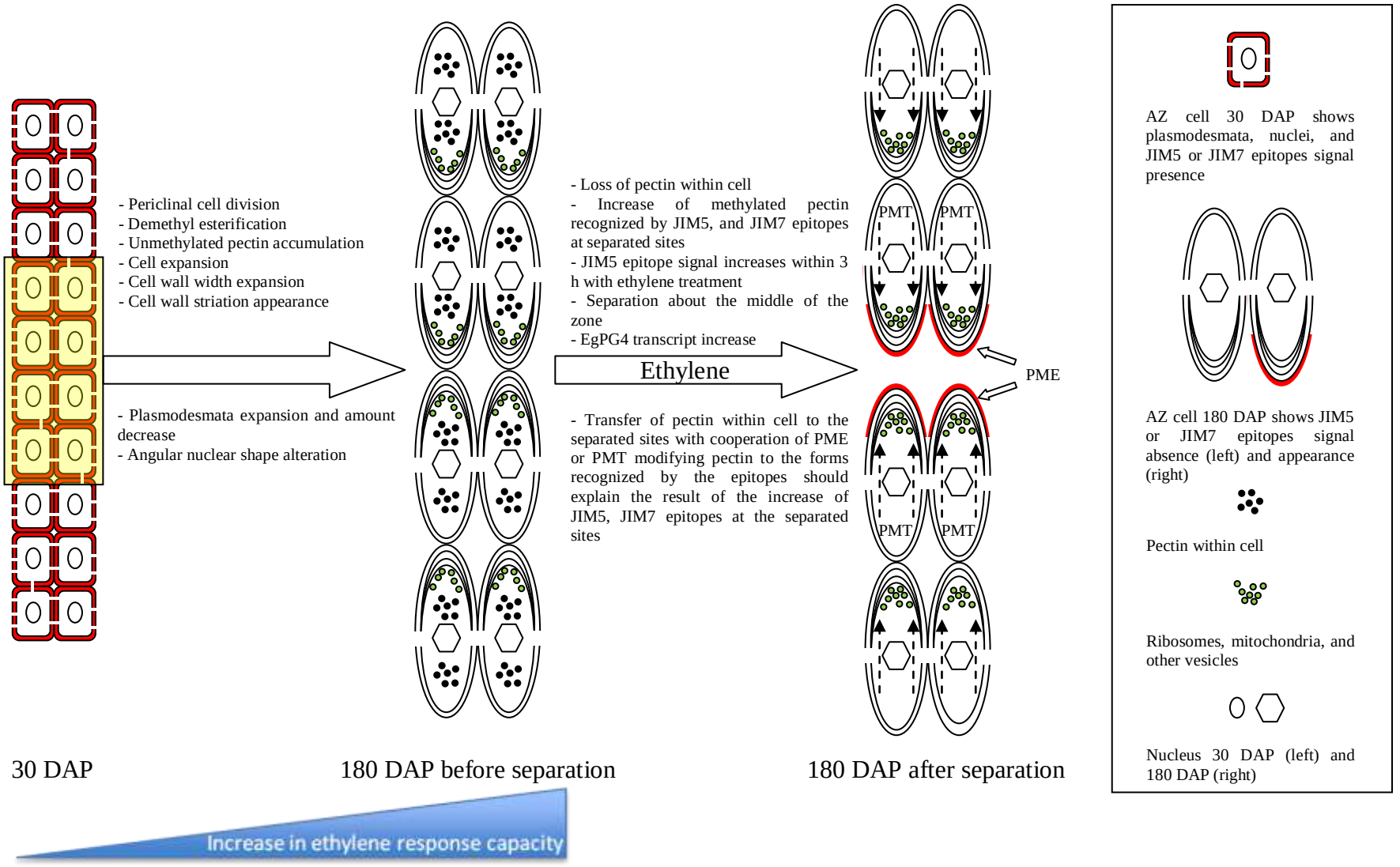

Figure 4.1. Schematic of abscission zone evolution during development until after separation corresponding to JIM5 and JIM7 epitopes.

Literature Cited

Henderson, J., H. A. Davies, S. J. Heyes and D. J. Osborne (2001). "The study of a monocotyledon abscission zone using microscopic, chemical, enzymatic and solid state 13C CP/MAS NMR analyses." Phytochemistry **56**(2): 131-139.

Henderson, J. and D. J. Osborne (1990). "Cell Separation and Anatomy of Abscission in the Oil Palm, Elaeis guineensis Jacq." J Exp Bot **41**(2): 203-210.